AN ABSTRACT OF THE THESIS OF

Richard D. Smith for the degree of Doctor of Philosophy in Geosciences presented on September 14, 1990.

Title: Streamflow and Bedload Transport in an Obstruction-affected, Gravel-bed Stream

Abstract approved: Frederick J. Swanson

Frederick J. Swanson

The mechanisms of pool maintenance were investigated in a small (width = 10 m, drainage area = 18 km^2), gravel-bed stream where pools are commonly associated with large, in-channel obstructions. Measurements of boundary shear stress, scour and fill of the stream bed, and bedload transport rate and grain-size distribution were made in a pool associated with a single, large woody debris obstruction.

Contrary to the well-known shear stress (or velocity) reversal hypothesis, which has been invoked to explain maintenance of pool-riffle structure, rate of increase with increasing discharge of the temporal-mean, near-bed velocity and boundary shear stress was the same at the pool as at pool head and pool tail locations. At a discharge 1.4 times bankfull, near-bed velocity was 102 cm/s at the pool head and tail and 82.1 cm/s at the pool center. Boundary shear stress was 25.1, 20.9, and 15.3 dynes/cm^2 at the pool head, tail, and center respectively. Furthermore, with increasing discharge no systematic spatial reversal of maximum bedload transport rate or of bedload competence, as predicted by the shear stress reversal model, was observed.

A conceptual "turbulent scour" model is presented to explain maintenance of pools associated with large, in-channel obstructions. This model relies on analogy to published descriptions of processes that maintain scour pools at bridge piers. According to this

model, temporal-mean boundary shear stress is enhanced by instantaneous turbulent velocity fluctuations created by the interaction of streamflow with the obstruction, thereby increasing instantaneous boundary shear stress in the pool. This explains the observed approximate equality of bedload transport rate and grain size distribution upstream, within, and downstream of the pool, despite lower mean shear stress in the pool.

The "turbulent scour" model accounts for the observed balance, over time periods much shorter than the duration of individual storm hydrographs, of bedload import and export for the pool, in response to apparent changes in sediment supply. This explains the approximately constant pool morphology despite bedload transport rates as large as 8300 kg/hr-m.

Streamflow and Bedload Transport in an Obstruction-affected, Gravel-bed Stream

by

Richard D. Smith

A THESIS

submitted to

Oregon State University

in partial fulfillment of
the requirements for the
degree of

Doctor of Philosophy

Completed September 14, 1990

Commencement December 1990

APPROVED:

Adjunct Professor of Geosciences in charge of major

Head of department of Geosciences

Dean of Graduate School

Date thesis is presented September 14, 1990

Typed by researcher for Richard D. Smith

ACKNOWLEDGEMENTS

I am indebted to many people who have assisted me on this project; their aid is deeply appreciated. Special thanks are extended to Fred Swanson for helpful discussions throughout the course of this project and for patiently suffering through early drafts of the manuscript. The other members of my graduate committee, in particular Bob Beschta, provided additional helpful guidance and encouragement. Tom Lisle provided valuable insights on several occasions during the study. Bill Dietrich and Paul Komar offered insightful advice on analysis techniques. Tim Max, U.S.D.A., Forest Service, Pacific Northwest Research Station, Portland, Oregon, provided advice on statistical analysis. Mary Ann Madej and Gordon Grant provided helpful review comments on the manuscript.

Several students in the Departments of Geology and Environmental Engineering, Humboldt State University, Arcata, California made this study possible by volunteering their time to assist with field work, commonly during the worst possible weather conditions. In particular, Elizabeth Cargay, Rich Chandler, Gary Palhegyi, and Debbie Thomas donated many hours of their valuable time. In addition, Arlene Doyle, U.S.D.A., Forest Service, Pacific Southwest Research Station, Arcata, California, risked life and limb to assist at night during peak flood flows and provided critical encouragement.

Scientists and technical staff at Redwood National Park, Arcata California, including Joan Florsheim, Danny Hagans, Randy Kline, Mary Ann Madej, Colleen O'Sullivan, Vicki Ozaki, Sandi Potter, Ron Sonnevil, Nick Varnum, and Bill Weaver assisted with various phases of the study and shared encouragement, advice, good times, and lasting friendship.

Principal funding for this study was received from U.S.D.I., National Park Service, Redwood National Park, Arcata, California and was coordinated by Mary Ann Madej. U.S.D.A., Forest Service, Pacific Northwest Research Station, Juneau, Alaska provided major support for data analysis and manuscript preparation. U.S.D.A., Forest Service,

Pacific Southwest Research Station, Arcata, California and the Department of Geology, Clemson University, Clemson, South Carolina provided support for laboratory analysis.

TABLE OF CONTENTS

LIST OF FIGURES

LIST OF TABLES

STREAMFLOW AND BEDLOAD TRANSPORT IN AN OBSTRUCTION-AFFECTED, GRAVEL-BED STREAM

INTRODUCTION

This study investigates the mechanisms that maintain a pool associated with a large woody debris (LWD) obstruction in a small, gravel-bed stream in a forested environment. Stream channel pools, areas of greater than average depth and typically less than average velocity, are found in nearly all perennial streams. Because of the important role of pools relative to channel morphology, fluvial sediment transport, and habitat for aquatic organisms, mechanisms by which pools are maintained are a major interest of fluvial geomorphologists and aquatic biologists.

Pools typically comprise a large portion of the channel area and persist despite the presence of a mobile bed and annual bedload yields far larger than the volume of any individual pool. This requires a mechanism to transport sediment through the low-energy pool environment, and indicates that bedload routing in these streams cannot be adequately described without an understanding of the processes that maintain pool morphology.

Interactions among these fluvial processes, channel morphology, and sediment transport provide an important link between geomorphic and biological systems. The variation in flow depth and velocity between channel units, e.g. pools and riffles, provides diversity of habitat for resident and anadromous fish (Bisson et al., 1982; Sullivan, 1986). Fluvial processes also affect the structure and textural composition of gravel stream beds, which are critical habitat for benthic organisms and fish.

Processes that affect hydraulics, sediment entrainment, transport, and deposition, and channel morphology in obstruction-affected, gravel-bed streams in forested environments are complex and difficult to model in laboratory studies or by predictive equations. Models of pool formation and maintenance, developed and quantified in pools not associated with

obstructions, are commonly applied, perhaps inappropriately, to forested streams in mountainous areas. These streams vary widely in particle-size distribution, sediment supply, character of the pavement layer, channel geometry, storm runoff response, and the extent and role of structural features, such as LWD (Klingeman and Emmett, 1982; White and Day, 1982; Beschta, 1983; Reid et al., 1985; Beschta, 1987).

In these streams, the familiar pattern of alternate bars (Leopold et al., 1964, p. 203; ASCE, 1966) and diagonal riffles (Church and Jones, 1982) is commonly disrupted by large, in-channel obstructions, including LWD, bedrock outcrops, and very large boulders. These obstructions affect the form and location of channel units such as pools and riffles (Lisle, 1986, Grant et al., 1990). Frequency of occurrence of pools in obstruction-affected streams differs substantially from frequency in streams with few obstructions (Leopold et al., 1964; Lisle, 1986; Harmon et al., 1986). Because obstruction-related pools are common in these streams (Harmon et al., 1986; Lisle, 1986; Bisson et al., 1987), processes responsible for maintenance of pool morphology and routing of sediment through pools may differ in type and/or relative importance from processes in other settings. Therefore, the extent to which familiar concepts of pool maintenance apply to obstruction-affected streams is unknown. This issue is a major focus of the present study.

Mechanisms of pool maintenance affect, and are affected by, rate and timing of bedload sediment transport. Commonly used bedload transport formulae predict transport rate based on hydraulic parameters and sediment characteristics (Vanoni, 1977, p. 190-214). This approach neglects the role of temporal changes in sediment availability (Beschta, 1987). Scour at in-channel obstructions can occur suddenly with a small increase in discharge (Beschta, 1983), supplying pulses of sediment from the stream bed. Furthermore, episodic sediment delivery from hillslopes and banks to channels is characteristic of forested, mountainous environments (Swanston and Swanson, 1976; Swanson et al., 1987), such as the present study site, indicating that sediment transport models need to address sediment supply variability.

Processes that maintain the morphology of pools unrelated to obstructions have been the subject of other studies. The well-known shear stress (or velocity) reversal hypothesis (Leopold and Wolman, 1960; Keller, 1971) attributes pool maintenance to a reversal in location of maximum boundary shear stress (or velocity) from riffles to pools as discharge increases to approximately bankfull. This results in scour and sediment transport through pools and deposition at riffles during high discharge. As discharge recedes, maximum shear stress is again present at riffles and fine sediment accumulates in the pools.

Another approach to the problem of pool maintenance includes modeling the interactive adjustments of velocity, boundary shear stress, sediment transport, and water surface and bed topography in alluvial channels (Dietrich et al., 1979; Dietrich and Smith, 1984; Dietrich and Whiting, 1989; Nelson and Smith, 1989(a); 1989(b). However, these models do not address the complex role of large, in-channel obstructions (J. Nelson and J.D. Smith, personal communication).

Studies of scour at bridge piers indicate that scour pools associated with piers are maintained by mobilization of bed material by a combination of time-averaged boundary shear stress and turbulent agitation upstream of the pier (Melville, 1975; Breusers et al., 1977). Increases in discharge result in increases in erosive force upstream of and in the scour hole (Laursen, 1962). At flows above the transport threshold, the pool undergoes cycles of scour and fill in response to sediment delivery from upstream (Chabert and Engeldinger, 1956 (reviewed by Breusers et al., 1977); Melville, 1984).

In order to investigate mechanisms of pool maintenance and dynamics of bedload transport in a LWD-related pool and to compare these mechanisms to the above models, this study addresses the following questions:

1. How does a LWD obstruction affect local streamflow hydraulics and channel morphology?
2. Can maintenance of the morphology of obstruction-related pools be explained by mechanisms commonly applied to pools without obstructions?

3. Can patterns of stream bed scour and fill and variation in bedload transport rate and grain-size distribution in this setting be explained as a function of hydraulic variables alone, or is variation in sediment supply also important?

The approach used to address these questions is to quantify variation in flow velocity, flow direction, and boundary shear stress with discharge and to associate this variation with effects of the LWD obstruction. Relationships of hydraulic characteristics to scour and fill of the bed, banks, and gravel bars are also demonstrated. Finally, effects of these hydraulic parameters on bedload transport are investigated by relating transport rate, timing, and competence to discharge, time-averaged shear stress, antecedent storm history, hydrograph characteristics, and inferred fluctuations in sediment supply.

PREVIOUS STUDIES

Flow Hydraulics in Bar-pool Sequences

Recent research has contributed to modeling flow, boundary shear stress field, water surface and bed topography, and sediment transport in bar-pool sequences in alluvial channels where large in-channel obstructions are not an important influence (Engelund, 1974; Hooke, 1975; Bathurst et al., 1979; Dietrich et al., 1979; Lisle, 1979; Leopold, 1982; Dietrich and Smith, 1983, 1984; Emmett et al., 1983; Smith and McLean, 1984; Nelson and Smith, 1989(a); 1989(b)).

In gravel-bed, sinuous alluvial channels, where large in-channel obstructions are not a common controlling influence, pool formation has been attributed to scour of diagonal bars by converging flow opposite the slip face of the bar (classification of bars follows Church and Jones, 1982). Downstream of the pool, shear stress is reduced and bedload is deposited at another bar (Shen and Komura, 1968; Gustavson, 1974; Lewin, 1976; Richards, 1976; Church and Jones, 1982). Pools have also been described, not as zones of scour, but as troughs between moving bed forms (Ackers, 1982).

Maintenance of pools has commonly been explained by the "shear stress (or velocity) reversal" hypothesis. This hypothesis states that with increasing discharge during high flow events, average velocity and shear stress increase in pools until these variables are equal to or greater than the velocity and shear stress over riffles (Leopold and Wolman, 1960; Keller, 1971; Richards, 1976; Andrews, 1979; Lisle, 1979; Emmett et al., 1983; Ashworth, 1987). This shear stress reversal causes sediment to be transported through the pool and deposited on a downstream riffle (Leopold and Wolman, 1960; Keller, 1971). Thus, pools are believed to fill during falling hydrograph limbs and during low flow and scour during high flow, while riffles do the reverse, thereby maintaining pool morphology (Andrews, 1979; Lisle, 1979; Parker and Peterson, 1980; Jackson and Beschta, 1982).

Several recent studies have supported the shear stress reversal hypothesis (Keller, 1971; Richards, 1976; Andrews, 1979; Lisle, 1979; Emmett et al., 1983; Ashworth, 1987), many of them relying on spatially averaged values of velocity and shear stress rather than local values, which directly affect bedload transport. Ashworth (1987), however, measured vertical velocity profiles and calculated shear stress from the slope of the semi-log plot of vertical distance above the bed vs velocity. This methodology resulted in a spatially localized value of boundary shear stress, more relevant to bedload transport. However, boundary shear stress calculated from velocity profiles overestimates stress (skin friction) directly responsible for bedload transport (Dietrich and Whiting, 1989).

Dietrich et al. (1979) quantified flow and sediment transport through a meander bend with well developed bar-pool topography in the sand-bed Muddy Creek channel, Wyoming. Dietrich and Whiting (1989) made similar measurements in a gravel-bed stream in New Mexico. These nonobstruction-related pools, associated with point bars in meander bends, clearly differ from the obstruction-related pool discussed in the present study, but are discussed here to describe alternate mechanisms of pool formation. In the sand-bed channel, a force balance model was compared to detailed field observations (Dietrich et al., 1979). Shoaling of flow over the point bar caused a pressure rise over the bar and a pressure drop over the pool, thus reducing the cross-stream water surface slope. As a result of this effect, centrifugal force exceeded the opposing pressure gradient force, directing flow away from the bar top and into the pool, causing a net outward flow around the bar. A zone of maximum shear stress developed, declining along the inside bank and along the bar top. This zone shifted across the channel, increasing downstream through the pool near the outside bank. Cross-stream velocities in this case were found to reach 20 % to 35 % of the average downstream velocity (Dietrich et al., 1979; Dietrich and Whiting, 1989). Cross-stream flow is normal to the general streamwise channel axis.

In the gravel-bed case, at a tributary to the Rio Grande del Ranchos, New Mexico, a data collection scheme similar to that employed in the present study was used in a

meander bend with a well-established point bar (Dietrich and Whiting, 1989). Three measurement sections were established, one roughly at the entrance to the pool, one at the deepest point, and one at the tail of the pool. Flow hydraulics were similar to the sand-bed case. Shear stress shifted from the center of the channel to the pool, along the outside bank, through the bend. Most bedload transport occurred within a narrow zone along the centerline through the bend. This limited zone of transport was attributed to boundary shear stress exceeding critical shear stress only near the center of the channel during flows at or below bankfull discharge. Shear stress reversal occurred as a result of the rapid increase of water surface slope at the pool during rising discharge (Dietrich and Whiting, 1989).

That model also predicts a reduction in cross-stream sediment delivery to pools from the adjacent bar as increasing discharge reduces shoaling-induced cross-stream flow. Pools then scour until the adjacent bar face becomes unstable, increasing sediment delivery to the pool, thereby maintaining an equilibrium (Dietrich and Whiting, 1989). As discharge recedes, shoaling-induced cross-stream flow increases bedload delivery from the bar to the pool, resulting in deposition in the pool until equilibrium is again achieved at lower flow (Dietrich and Whiting, 1989).

Few studies have directly investigated processes that maintain pools associated with naturally-occurring, in-channel obstructions. In a flume study simulating bed scour around in-channel logs, Beschta (1983) reported that obstructions created zones of exceptionally high turbulence capable of scouring and removing gravel, even though temporal-mean, near-bed velocities indicated otherwise. This observation indicated that entrainment with rising discharge may be caused by an increase in obstruction-related turbulence rather than increased average shear stress; therefore the shear stress reversal mechanism may not be required to maintain pools formed by scour at obstructions.

In laboratory studies simulating fluvial scour around piers, large-scale vortices were the primary mechanism of local scour (Breusers et al., 1977). Downward flow in front of the

pier induced a "horseshoe vortex" that wrapped around the pier near the bed (Tison, 1961). Vortices with low-pressure centers were cast off from the pier, lifting mobile sediment from the bed with the generation of each vortex (Breusers et al., 1977).

In laboratory simulations of pier-related scour holes, bed material was mobilized by a combination of time-averaged boundary shear stress and turbulent agitation both ahead of the pier and in the lower portion of the scour hole (Melville, 1975; Breusers et al., 1977). Downward flow and scouring vortices created pools at average shear stresses less than those required in the absence of obstruction-related scour (Tison, 1961; Carstens, 1966; Breusers et al., 1977). Turbulent velocity fluctuations near the bed in the scour hole had greater energy in the 1 Hz to 10 Hz range relative to the approaching flow (Melville, 1975). Bed scour near a pier may begin at velocities as low as 42 percent of the critical average velocity for material transport in the undisturbed part of the stream (Carstens, 1966; Breusers et al., 1977). Melville (1984) reported that scour depth around bridge piers in laboratory, gravel-bed channels was greatest at the nonobstruction-affected entrainment threshold, then started to decrease with stage in response to increased sediment delivery (Breusers et al. 1977; Melville, 1984).

In laboratory studies Melville (1975) found that size and velocity of near-bed vortices increased rapidly as a new scour hole enlarged. The magnitude of combined temporal-mean bed shear stress and turbulent fluctuations at the bed decreased as the scour hole enlarged until an equilibrium form was reached (Melville, 1975). As flow continued to increase, depth of scour could increase again if scouring action in the pool exceeded the rate of input of sediment (Melville, 1984; Melville and Sutherland, 1988). Field studies by Lisle (1986) suggested that maximum scour in pools occurred at flood peaks. Laursen (1962) described equilibrium scour conditions in pier-related scour holes as a balance of sediment discharge into and out of the scour hole. Increases in discharge resulted in increases in erosive force upstream of and in the scour hole, maintaining depth of scour (Laursen, 1962).

Flume studies by Chabert and Engeldinger (1956) indicated that below the transport threshold of the upstream bed, scour depth remained stable. Above the transport threshold, depth underwent approximately hourly cycles of scour and fill in response to sediment delivery from upstream (Chabert and Engeldinger, 1956). Melville and Sutherland (1988) reported that scour depth was a function of stream depth, mean velocity, bed grain size and size distribution, diameter and shape of the pier, alignment with the flow, and sediment supply.

Sediment Entrainment

Miller et al. (1977) reviewed relationships between critical values of entrainment parameters and entrainment of bed material. A parameter commonly used is the average boundary shear stress (τ_b), which, by definition, is directly proportional to the velocity gradient (Middleton and Southard, 1984, p. 5). Average boundary shear stress may be expressed by the Duboys' relationship $\tau_b = \delta RS$, where δ is the specific weight of water, R is the hydraulic radius (approximated by the mean depth in wide streams), and S is the energy gradient (approximated by the water surface slope) (Leopold et al., 1964, p. 157).

Flow velocity is also used as an entrainment parameter. Velocity does not directly determine applied stress; however both are dependent on depth and slope (Vanoni, 1977, p. 96), making velocity a useful measure of the ability of flow to transport sediment (Keller, 1971; Andrews, 1979). Depth must also be specified for mean velocity to be meaningful as an entrainment parameter (Vanoni, 1977, pp.102).

Velocity varies with vertical location in the water column. Fluid velocity near the bed is believed to have the greatest importance in bedload transport (Bagnold, 1954), and relatively accurate estimates of boundary shear stress can be determined from near-bed velocity (Dietrich and Whiting, 1989). Velocity and shear stress also vary across the channel width, therefore scour and sediment transport is unlikely to be uniform across the

channel.

Total boundary shear stress required for initial motion of grains in natural stream beds varies in part because of lift forces that tend to reduce the mean boundary shear stress entrainment threshold (Baker and Ritter, 1975; Carling, 1983). Lift force is created by flow-induced pressure differences between the top and bottom of a grain, and is approximately proportional to the square of the velocity (Vanoni, 1977, p. 103). The average lift force to boundary shear stress ratio can be as large as 2.5 (Vanoni, 1977, p.104). Instantaneous drag and lift forces may be two to nine times the mean, implying that turbulent velocity fluctuations may be largely responsible for sediment transport (Sutherland, 1967; Vanoni, 1977, pp.96; Richards, 1982, pp. 84). Cheetham (1979) experimentally determined the competence of braided rivers by introducing spherical particles, and found instantaneous shear stresses caused by instantaneous turbulent velocity fluctuations to be ten times the mean.

Lift and drag forces at a grain boundary in fully turbulent flow depend, in part, on the relative roughness, i.e. the ratio of size of the grain (D) to water depth (d) (Fenton and Abbott, 1977; Carling, 1983). Characteristics of the pavement layer such as imbrication and shielding of small particles tend to increase the entrainment threshold (Klingeman and Emmett, 1982; Parker et al., 1982; Andrews, 1983; Reid et al., 1985). Conversely, projection of relatively large particles into the flow tends to reduce their entrainment threshold relative to a bed of uniform grain size (Parker et al., 1982; Andrews, 1983). Strict dependence of entrainment threshold on clast size is complicated by these effects of variable exposure of grains to the flow, creating a tendency toward equal mobility (Fenton and Abbott, 1977; Parker et al., 1982; Andrews, 1983; Andrews and Parker, 1987; Komar, 1987; Wilcock, 1988; Wilcock and Southard, 1988; Ashworth and Ferguson, 1989). This issue has important implications for prediction of bedload transport rate, for the effects of pavement on sediment transport, and for downstream fining of stream beds.

Several studies show an increase in sampled bedload clast size with increasing shear stress (Milhous, 1973; Baker and Ritter, 1975; Carling, 1983; Ashworth and Ferguson, 1989). However, Wilcock (1988) calls attention to scaling problems in quantifying the variation of competence with shear stress on the basis of the largest sampled clast size. The probability of sampling a relatively rare, coarse fragment increases with increased sample size, commonly associated with increased shear stress (Wilcock, 1988). This implies that correlation of clast size with shear stress may simply be a function of sample size (Wilcock, 1988). Conversely, Komar and Shih (1988) argue that the grain-size distribution of bedload collected by Milhous (1973) in Oak Creek, Oregon changes systematically with increasing discharge as a function of increasing shear stress (Komar and Shih, 1988; Komar, 1989).

In order to relate fluid shear stress on a stream bed to sediment entrainment, Shields (1936) combined the parameters sediment density (p_s), median grain diameter (D_{50}), fluid density (p), kinematic fluid viscosity (v), fluid shear stress (τ_b), and gravitational acceleration (g) into an entrainment function (τ_b^*) such that $\tau_b^* = \tau_{bc}/(p_s\text{-}p)gD_{50}$, where τ_{bc} is the critical boundary shear stress or the stress at initiation of transport. τ_{bc} is a function of U^*D/v, the dimensionless grain Reynolds number, denoted Re^*. U^* (shear velocity), equal to $(\tau_b/p)^{1/2}$, is a convenient expression of boundary shear stress with the dimensions of velocity. Re^* can be interpreted as an indicator of the degree to which grains project into the turbulent zone of the boundary layer, thereby indicating the drag and lift on the grain (Middleton and Southard, 1984).

Data for this empirical relationship were obtained by Shields and several other workers using laboratory flumes with artificially flattened beds of noncohesive sediment and fully-developed, turbulent flow. Shields found that at high values of Re^*, such as are typical of gravel bed streams, τ_b^* can be regarded as a constant equal to 0.06 (Middleton and Southard, 1984). In order to solve for a value of τ_{bc} or D, τ_b^* is commonly assumed to be 0.06 for flow conditions found in gravel-bed streams (large Re^*). Other values for τ_b^* have

been suggested (Miller et al., 1977; Vanoni, 1977, pp. 94-101). Miller et al. (1977) use $\tau_b^* = 0.045$ based on an extension of Shields' data from flume experiments. Church and Jones (1982), using D_{90}, calculated a range of values from 0.05 to 0.1 depending on sediment fabric. Parker and Klingeman (1982) suggested a value of $\tau_b^* = 0.035$ for gravel-bed streams with pavement based on field data published by Milhous (1973) for Oak Creek, Oregon.

The variety of values suggested for τ_b^* at high Re^* is partly caused by differing definitions of how much motion constitutes initiation of transport (Vanoni, 1977, pp.94; Andrews, 1983). Flume experiments investigating the threshold of initiation of motion for particles subjected to fluid shear stress suggest that initial motion is statistical in nature and that near critical conditions bedload transport occurs in gusts distributed randomly in time and space (Shields, 1936; Vanoni, 1977, pp. 94).

Local, rather than average, boundary shear stress may be derived from a measured velocity gradient using a form of the "law of the wall" equation $\tau_b = p[((u_2-u_1)K)/\ln(z_2/z_1)]^2$, where τ_b is the boundary shear stress at a point, p is the density of the fluid, u_2 and u_1 are the point mean velocities at distances z_2 and z_1 measured from and normal to the boundary, and K is the von Karman constant, usually taken to be 0.4 (Middleton and Southard, 1984, p. 123-155; Dietrich and Whiting, 1989). K reflects the vertical turbulent transport of streamwise fluid momentum (Middleton and Southard, 1984, p. 123-155). The above equation can be written as $u^* = Uk/(\ln z/z_o)$, where u is the velocity at height z above the bed, z_o, the roughness length, is a constant for fully rough flows equal to approximately $K_s/30$ for close-packed, uniform sand-grain roughness. K_s, the effective roughness height, can be approximated by 3.5 D_{84} (Hey, 1979; Prestegaard, 1983; Dietrich and Whiting, 1989). The equation then reduces to:

$$u^* = 0.4u/[\ln(z/0.12D_{84})] \qquad (1).$$

This equation gives satisfactorily accurate results for gravel-bed streams in a field situation (Dietrich and Whiting, 1989).

Bedload Transport in Bar-pool Sequences

Bedload sediment transport relationships may be stated in terms of discharge, shear stress, or stream power. Total stream power (Ω) is the time rate of energy expenditure or the time rate of doing work, defined as $\Omega = \delta QS$, where δ = specific weight of water, Q = discharge, and S = water surface slope (Dingman, 1984, p.131-2). Stream power per unit bed area (W) is a useful concept because it can be viewed as the power available to transport sediment load (Bagnold 1973, 1977). $W = \Omega/w$, where w is the channel width. W is equivalent to $\tau_b U$, where τ_b is the boundary shear stress and U is the average water velocity (Bagnold, 1954; Middleton and Southard, 1984, p. 284). Bagnold (1954) stated that the appropriate velocity for this relationship is the velocity at the effective distance from the bed at which fluid pushes bedload along. In this study, near-bed velocity measurements, taken 4.6 cm above the bed, are used for this purpose. The effective stream power expenditure of the flow is WE_b, where E_b is the efficiency with which available power is converted to work in moving the bedload. E_b is affected by form roughness, is 0 below the transport threshold, and increases rapidly when transport begins (Richards, 1982, p. 114-115).

Other field studies have examined flow and bedload transport through bar-pool sequences in gravel-bed streams where pools were not linked to scour at obstructions. Jackson and Beschta (1982) presented a two-phase model of bedload transport. Phase 1 occurs at relatively low discharge and consists of the transport of relatively fine (sand-size) material out of bars and into pools. Phase 2 begins when increasing discharge and shear stress disrupt the riffle pavement layer as particles larger than sand-size are entrained. This phase of bedload transport begins at flows near bankfull, and is highly unsteady and non-uniform. Jackson and Beschta (1982) found that at peak discharge the maximum pool velocity lowered to 10 to 12 cm above the bed. This resulted in an increase in boundary shear stress that caused bed material to be routed through the pool. The pool thalweg

scoured prior to the hydrograph peak, then filled on the recession limb (Jackson and Beschta, 1982).

In a southeast Alaska bar-pool sequence that was only slightly affected by large woody debris, Estep (1982) reported that sediment was transported past the upstream riffle and deposited in the pool during small storm events. During large events, sediment was transported past the lower riffle, suggesting that sediment was stored in the pool prior to being scoured during high flow. Once the pavement layer was dislodged, transport was accomplished by lesser magnitude events until pavement developed again.

In a bar-pool sequence in a second-order southeast Alaska stream, Campbell and Sidle (1985) and Sidle (1988) reported that competence reversal occurred at about bankfull stage. During moderate flows sediment was imported into the pool. During flows greater than bankfull there was a net filling of the riffle and a net scour of the pool. Fine (<1 mm) sediment was transported more frequently than coarse (>8 mm) sediment, which was scoured only by flows with a return period greater than five years (Sidle, 1988). Sediment transport was partly determined by antecedent storm history and cumulative antecedent discharge greater than the threshold for bedload transport (Campbell and Sidle, 1985; Sidle, 1988).

At several gravel-bed streams, scour, fill, and bedload transport have been observed to be localized rather than to occur uniformly across the channel width (Jackson and Beschta, 1982; Reid et al., 1985; Klingeman and Emmett, 1982; Thompson, 1985; Carson and Griffiths, 1987, p.55). Dietrich and Whiting (1989) attributed this to a tendency for gravel-bed channels to have low excess shear stress, i.e. a maximum shear stress only slightly larger than the critical shear stress for the bed material. This tends to confine the zone of significant bedload transport to a narrow band of high shear stress flow (Dietrich and Whiting, 1989).

High variability in bedload transport rate at a station is common and is attributed to the variability of sediment supply, pavement effects, clustering of coarse clasts, changes in

form roughness, effects of large woody debris or other obstructions, time of sampling relative to the storm hydrograph, and antecedent storm history (Vanoni, 1977, pp.94; Klingeman and Emmett, 1982; Richards, 1982, pp. 111-112; White and Day, 1982; Beschta, 1983; Reid et al., 1985; Beschta, 1987; Kuhnle and Southard, 1988; Sidle, 1988).

Geomorphic Effects of Large Woody Debris

LWD has important effects on stream hydraulics, sediment transport, channel morphology, and lotic ecosystems (Swanson et al., 1976; Swanson and Lienkaemper, 1978; Harmon et al., 1986; Bisson et al., 1987). Pools are commonly associated spatially with LWD, implying that the pools are caused by scour at these obstructions (Swanson et al., 1976; Keller and Swanson, 1979; Keller and Tally, 1979; Lisle and Kelsey, 1982; Hogan, 1985; Lisle, 1986). These pools provide important cover and rearing habitat for fish (Everest et al.,1987). Pool tails can provide important spawning habitat (Sedell et al., 1982)

In many gravel-bed streams in forested environments, the pattern of alternate or diagonal bars (Leopold et al., 1964, p. 203; ASCE, 1966; Church and Jones, 1982) is disrupted by large in-channel obstructions, such as LWD, which may affect the pattern (temporal and spatial) of scour and fill. Lisle (1986), for example, found that in Jacoby Creek, a northwest California stream with average active channel width of 12 m, eighty-five percent of the pools were formed by scour at obstructions and ninety-two percent of the obstructions formed pools (Lisle, 1986). Obstructions also strongly influence the size and distribution of gravel bars (Lisle, 1986). Bedload transport rate can be strongly affected when high streamflow causes LWD to shift, releasing stored sediment (Lisle, 1986).

METHODS

Study Area

Tom McDonald Creek is a fourth-order (Strahler, 1957) tributary to Redwood Creek, within Redwood National Park, Humboldt County, California (Fig. 1). Redwood Creek drainage basin is underlain by sheared, highly erodible rocks of the Jura-Cretaceous Franciscan assemblage. The basin is approximately bisected by the Grogan Fault, which separates sandstone on the eastern side from low-grade metamorphic rocks on the west (Harden, et al., 1981).

In Redwood Creek basin, highly erodible landscapes, intense storms, and land use have combined in recent years to accelerate erosion processes (Harden et al., 1978; Janda, 1978; Kelsey, 1980), adversely affecting aquatic habitat (Hofstra, 1981; Ozaki, 1988). The interaction of LWD and sediment supply, both affected by forest management, probably influences the type and extent of habitat alteration.

The basin receives an estimated mean annual precipitation of 203 cm, primarily between October and April. Rainfall occurs infrequently during the summer months (Harden et al., 1978). Five major storms have occurred in the past 25 years (Harden et al., 1978). The 1964-65 storm caused severe alteration of the watershed, especially in the southern, inland portion. Effects of the storm included extensive streamside landsliding and channel aggradation. Storms in 1972 and 1975 significantly impacted the northern, coastal portion of the basin, including Tom McDonald Creek basin (Kelsey et al., 1981). These infrequent, high magnitude floods were major sediment producing and transporting events.

Inventories of fish species in Redwood Creek basin verified the presence of steelhead trout (Salmo gairdneri), coho salmon (Oncorhynchus kisutch), and chinook salmon (O. tshawytscha) (Anderson and Brown, 1980; Hofstra, 1981).

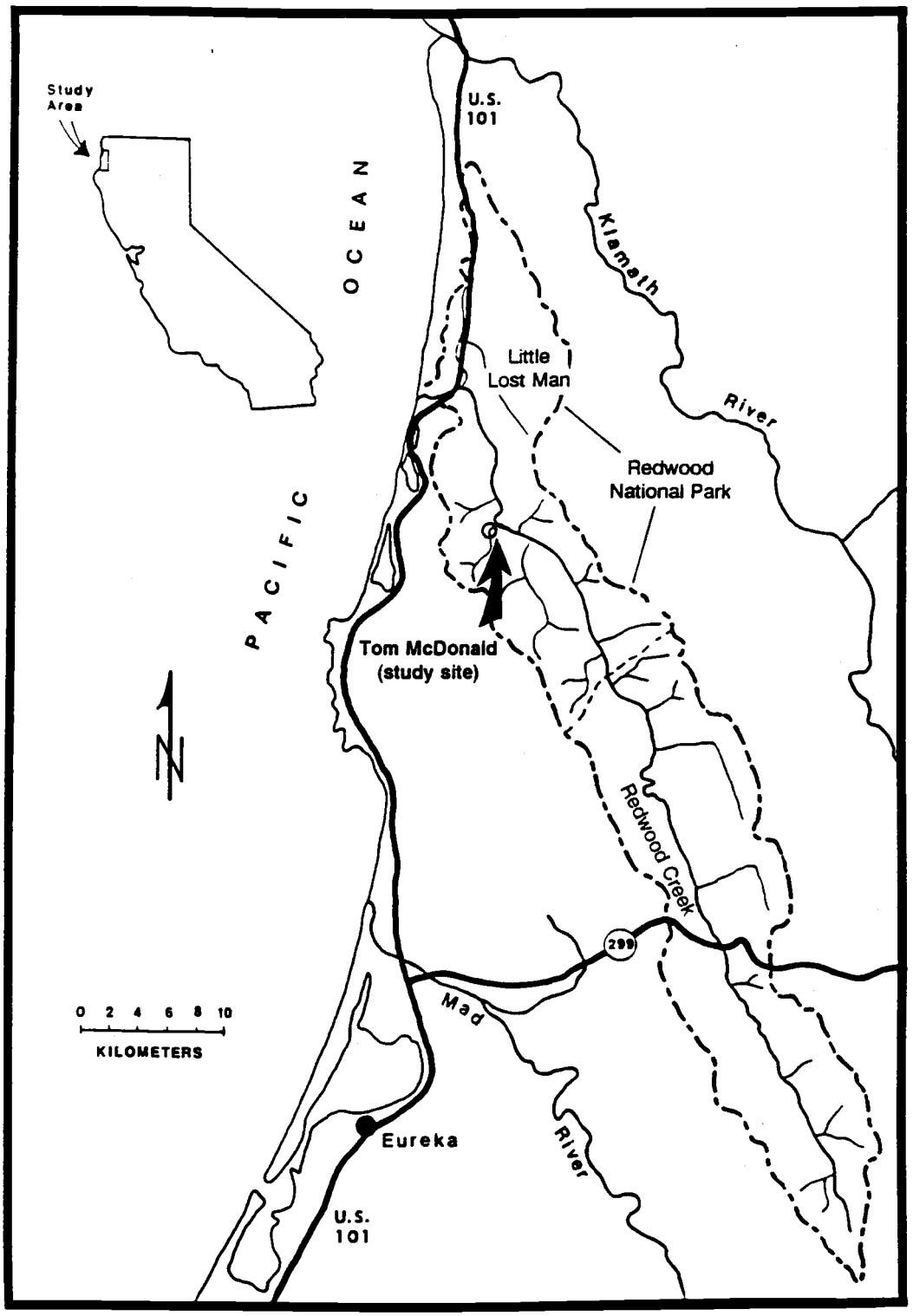

Figure 1. Location map of study area (after Pitlick, 1982).

Tom McDonald Creek drainage basin is underlain by schist and covers an area of 18.0 km^2 above the study site. Soil in the basin is dominantly brown acidic loam exhibiting good to excessive drainage and moderate to very high erosion hazard (Iwatsubo et al., 1976, p. 24-31). Average channel gradient for Tom McDonald Creek is 0.07 (Pitlick, 1982). The gradient through the study reach is 0.006. Active channel width, defined as the unvegetated portion of the channel bed, averages 10 m at the study site. Grain size of the channel bed ranges from cobble to fine sand. The bed is used for spawning by salmonids. The general streamwise bearing is N45E.

Bankfull discharge (Q_{bf}), based on field observations of discharge when flow reached the prominent convex-upward break in the channel bank, is 3.64 m^3/s at the study reach. Thalweg depth at bankfull discharge is 0.71 m, 1.46 m, and 0.59 m at the pool head, pool center, and pool tail respectively. The study reach includes a pool associated with a LWD, in-channel obstruction (Fig. 2).

Selection of the study site was based on the following characteristics: 1) it is a channel reach containing a distinct pool associated with a large woody debris obstruction, 2) channel morphology is simple, consisting of a pool with a distinct pool head (tail of the upstream riffle) and pool tail (crest of the downstream riffle), 3) sediment supply does not appear to be limiting; no bedrock outcrops occur within several hundred meters of the study reach, 4) the channel gradient and grain size of the bed are suitable for spawning by anadromous salmonids, i.e. the bed is predominantly composed of sand, pebbles, and cobbles, therefore geomorphic processes at the site have direct implications for fish habitat, and 5) channel width is small enough to be spanned by a simple foot bridge.

The drainage basin supports mixed stands of redwood (Sequoia sempervirens) and Douglas fir (Pseudotsuga menziesii) forests. Eighty-six percent of Tom McDonald Creek basin has been logged (Iwatsubo et al., 1976, p. 31), however much of the land adjacent to the lower portion of the channel, where the study site is located, has not been logged and retains old-growth redwood forest.

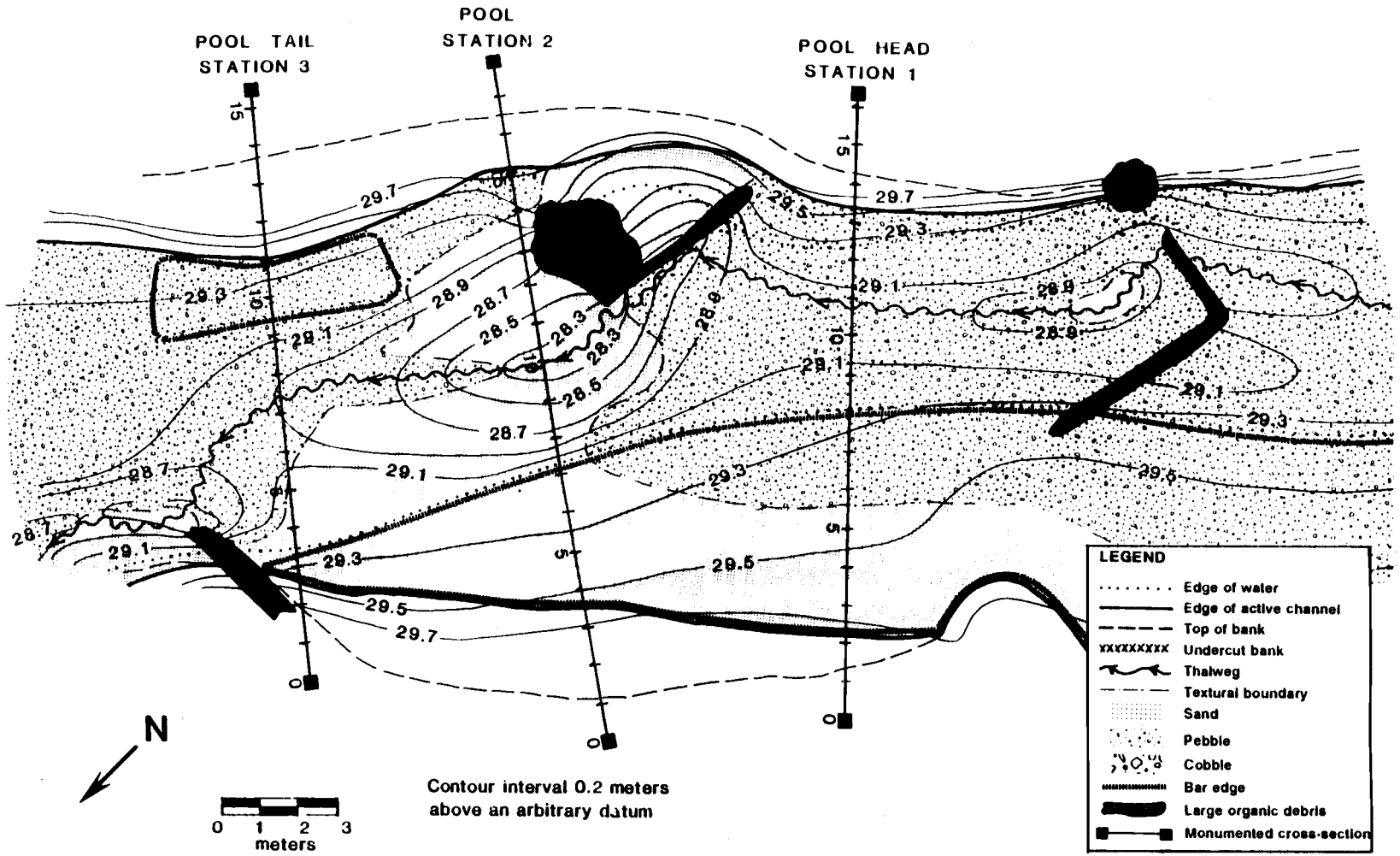

Figure 2. Study site. Mapping was done on September 7, 1984 at summer low flow. Flow direction is indicated by the thalweg symbol.

Study Design

Field Setting

Detailed sampling of flow and sediment transport was done from three foot bridges oriented perpendicular to the thalweg. One bridge was located over the head of the pool, one over the deepest part of the pool, seven meters downstream of the pool-head bridge, and the third was over the tail of the pool, six meters downstream of the pool bridge (Fig. 2). These three sampling locations are referred to in this paper as stations 1, 2, and 3 respectively. Bridges were constructed following a design developed by Hawks et al. (1987). This configuration permitted detailed measurements of flow and bedload transport into and out of the scour pool at high discharge (exceeding bankfull) without disturbing the flow or stream bed.

Site Characterization

To characterize the study site, topography and surface features were mapped at a scale of 1:60 using a plane table and alidade (Fig. 2). The channel longitudinal profile was surveyed over approximately twelve channel widths centered on the scour pool (Fig. 3). Channel cross-sections were monumented and surveyed along the upstream edges of the three bridges (Fig. 2).

Rainfall data were collected at a continuous recording rain gage 3.5 km from the study site maintained by Redwood National Park at 290 m elevation, approximately the median elevation of Tom McDonald Creek drainage basin.

In order to determine the grain-size distribution of material available for transport, bed material was sampled using the "freeze-core" technique with a tri-tube, cryogenic gravel

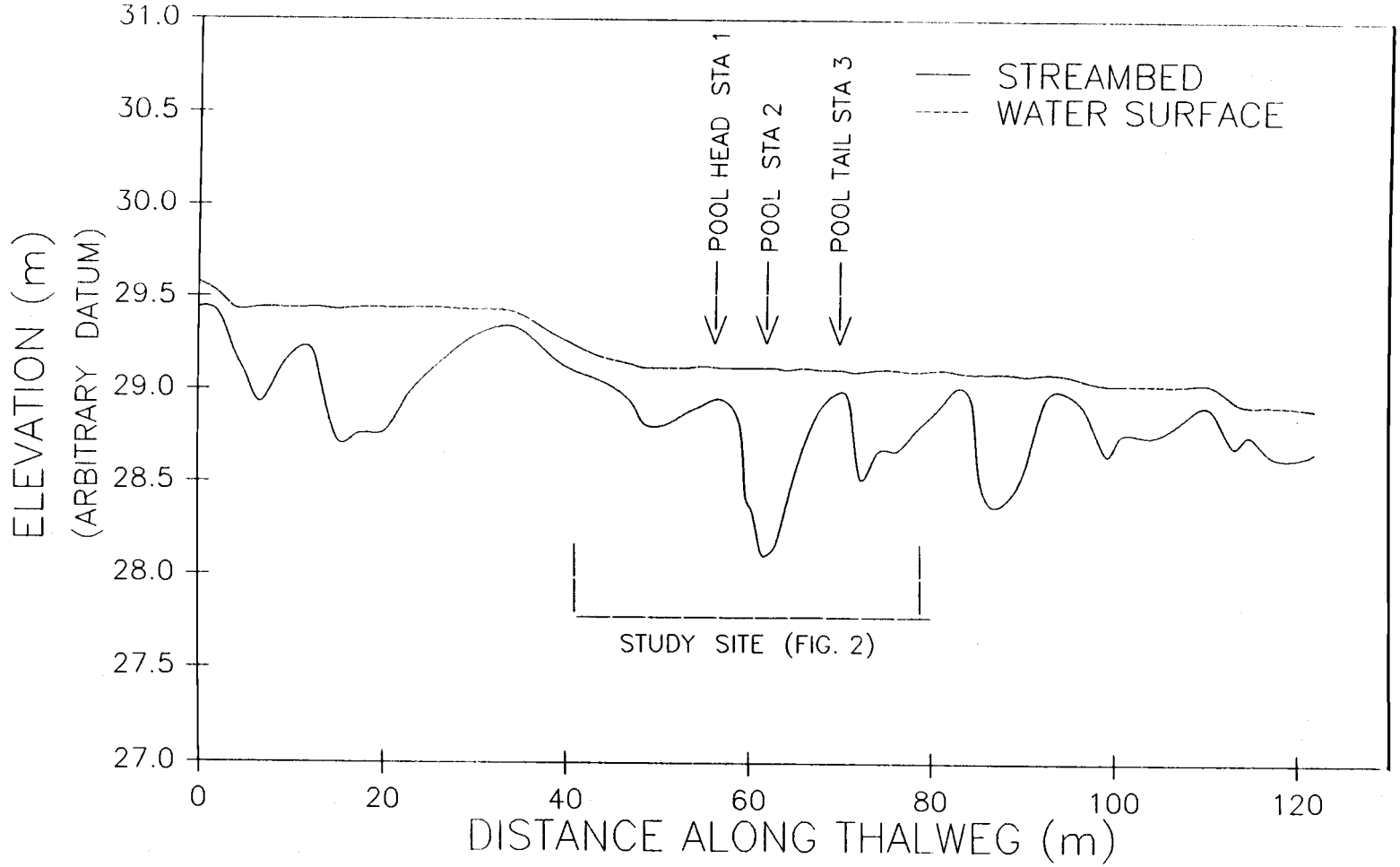

Figure 3. Longitudinal profile of the study site.

sampler (Walkotten, 1976; Everest et al., 1981). Samples were taken to a depth of 40 cm at the crest of a riffle 20 m downstream of the study reach. This location was chosen to avoid impacting the study site. A riffle crest was of interest, because such sites are favored by salmonids for spawning. Samples were located randomly across the riffle, with the limitation that no two samples be closer together than 30 cm.

The freeze-core technique can sample boulders, which have only a small portion of their volume within the diameter of the core. Because of the ambiguity involved in including these clasts, analyses were limited to grain sizes with intermediate diameter 45 mm and smaller. Four sets of three freeze-core samples each were taken during the study. Grain-size analysis techniques were the same as those used for bedload samples described below. Pebble counts (Wolman, 1954) were done over a 3 m x 3 m area centered on each cross section at the center of the low-flow channel to characterize the grain-size distribution of the bed surface.

Measurement of Hydraulic Variables

Shear stress on a stream bed is a function of the energy gradient, approximated by the water surface slope (Leopold et al., 1964, p.157). In order to measure slope over a range of discharge, an array of staff gages was installed along the study reach approximately every 3.5 m among the bridges and 17 m and 29 m upstream of the upstream bridge and downstream of the downstream bridge. Staff gages were located away from sites of strong turbulent fluctuations. Measurements of water surface slope at a point were based on water surface elevations upstream and downstream of the point of interest.

The stage-discharge relationship, developed using standard techniques (Leopold et al., 1964, p. 167) with a Price current meter, showed the least variation at the upstream bridge, so this cross section was used to develop a rating curve for the stream. A

continuous record of stage height was provided by a water level recorder in a stilling well 25 m downstream of the pool bridge. Gage heights at the continuous gage and upstream bridge gage were related using linear regression analysis.

An array of vertical velocity profiles distributed across the channel can be used to determine the characteristics of flow and the boundary shear stress derived from the near-bed velocity gradient using the "law of the wall" relationship (Middleton and Southard, 1984, p. 123-155). Velocity and direction of streamflow were measured over a range of flows along profiles spaced at 30 cm or larger intervals across the channel at each of the stations. Velocity measurements were averaged over one minute, yielding a temporal-mean value. Measurements were taken as close to the bed as possible without interfering with the mechanical current meter (4.6 cm for the standard Price meter). Vertical measurement intervals were commonly 2.5 cm at the pool head and pool tail stations and 15 cm at the pool, but larger spacing was sometimes required to finish profiles quickly in changing flow conditions.

Measurement of the direction of flow was made possible by attaching the current meter to a free-moving insert in a hand-held pole. A high-quality bearing at the insert-pole contact allowed the current meter to adjust freely to flow direction even at low discharge. Azimuth of the flow was determined from a compass attached to the top of the insert. Measurement of flow direction allowed magnitude and direction of cross-stream flow to be determined. Cross-stream flow magnitude gives an indication of the degree of flow modification by features such as the LWD obstruction. Direct measurements of turbulence were not made, because, to the author's knowledge, instrumentation has not been developed that is small enough to measure turbulence on the spatial scale of interest without being subject to interference from moving bedload.

In addition to the vertical velocity profiles, several measurements of only the near-bed velocity were taken at 30 cm or larger horizontal intervals along the three stations. Boundary shear stress was calculated from these temporal-mean velocity data using

equation (1) above. The design of the velocity meter caused z to be fixed at 4.6 cm. D_{84} of the bed surface was calculated from pebble counts and assumed to remain constant. This allowed z and D_{84} in equation (1) to be held constant for each cross-section, and the shear velocity was calculated as the bottom velocity times a numerical constant. This method of shear stress computation provided more consistent results than methodology such as that presented in Middleton and Southard (1984, p. 385-386), which requires artificial vertical adjustment of the zero-velocity point of the velocity profile to achieve the straightest possible semi-log plot of velocity vs distance from the bed. This adjustment had a large effect on the computed shear stress for these data, introducing an undesirable degree of subjectivity into the computation. Furthermore, shear stress derived from velocity profiles includes a component of stress attributable to form drag from bed forms and very large clasts in addition to skin friction, which is the component directly related to bedload transport (Dietrich and Whiting, 1989).

Considering the ambiguity involved in determining the slope of the vertical velocity profile and the difficulty of obtaining an accurate measurement of water surface slope in a situation of complex flow patterns (Ackers, 1982; Carling, 1983), those methodologies were not pursued herein. The near-bed velocity methodology, used in the present study, provided more objective and consistent results, and measured only skin friction, the component of total boundary shear stress responsible for bedload transport.

A pygmy-Price current meter was used in a attempt to collect flow data as close to the bed as possible. At high discharge, organic material traveling near the bed became entangled in the meter, interfering with measurements; therefore only data obtained using the standard Price meter are presented here.

At this study reach, as at other locations, bedload transport was observed to be localized over a small portion of the channel width, rather than occurring uniformly across the channel (Jackson and Beschta, 1982; Reid et al., 1985; Klingeman and Emmett, 1982; Thompson, 1985; Carson and Griffiths, 1987, p.55; Dietrich and Whiting, 1989). Therefore,

in order to relate changes in discharge to changes in shear stress and to bedload transport rate, measurements of near-bed velocity, from which shear stress was calculated, were averaged over 2.5 m of channel width, spanning the zone of shear stress maximum. A small portion of the channel width was of interest because localized shear stress may promote bedload transport, even though shear stress averaged over the entire channel width is less than the transport threshold. Averaging shear stress over the entire channel width can obscure the shear stress-bedload transport relationship when transport occurs over a limited portion of the channel. Averaging shear stress over this portion also allowed comparisons of the three cross sections independent of the channel width.

Scour and Fill

Extent of scour and fill of the channel bed by streamflow was computed from repeat surveys of the bed elevation along the three cross sections. Soundings at one or more of the stations were done on 38 occasions throughout the course of the study. Nineteen of these were of particular interest, because they documented important changes in the bed profile. Accordingly, these were selected for further analyses. The soundings done on May 14, 1985 had a large number of closely spaced data points and were completed early in the study. They were, therefore, selected as a datum for the purpose of comparison with other soundings.

Sounding data were supplemented by an array of scour chains (Leopold et al., 1964, p. 235-236). Scour chains were used to measure net change in bed elevation during the 1985-86 storm season, the period of highest flows in this study. Scour chains can indicate that the bed has either scoured, scoured then filled, or simply filled, however sediment deposited prior to scouring may be eroded, altering the record of its original thickness.

Chains were evenly spaced along seven lines located at three to four meter intervals up and downstream of the pool station (Fig. 4). Scour chain lines consisted of either three

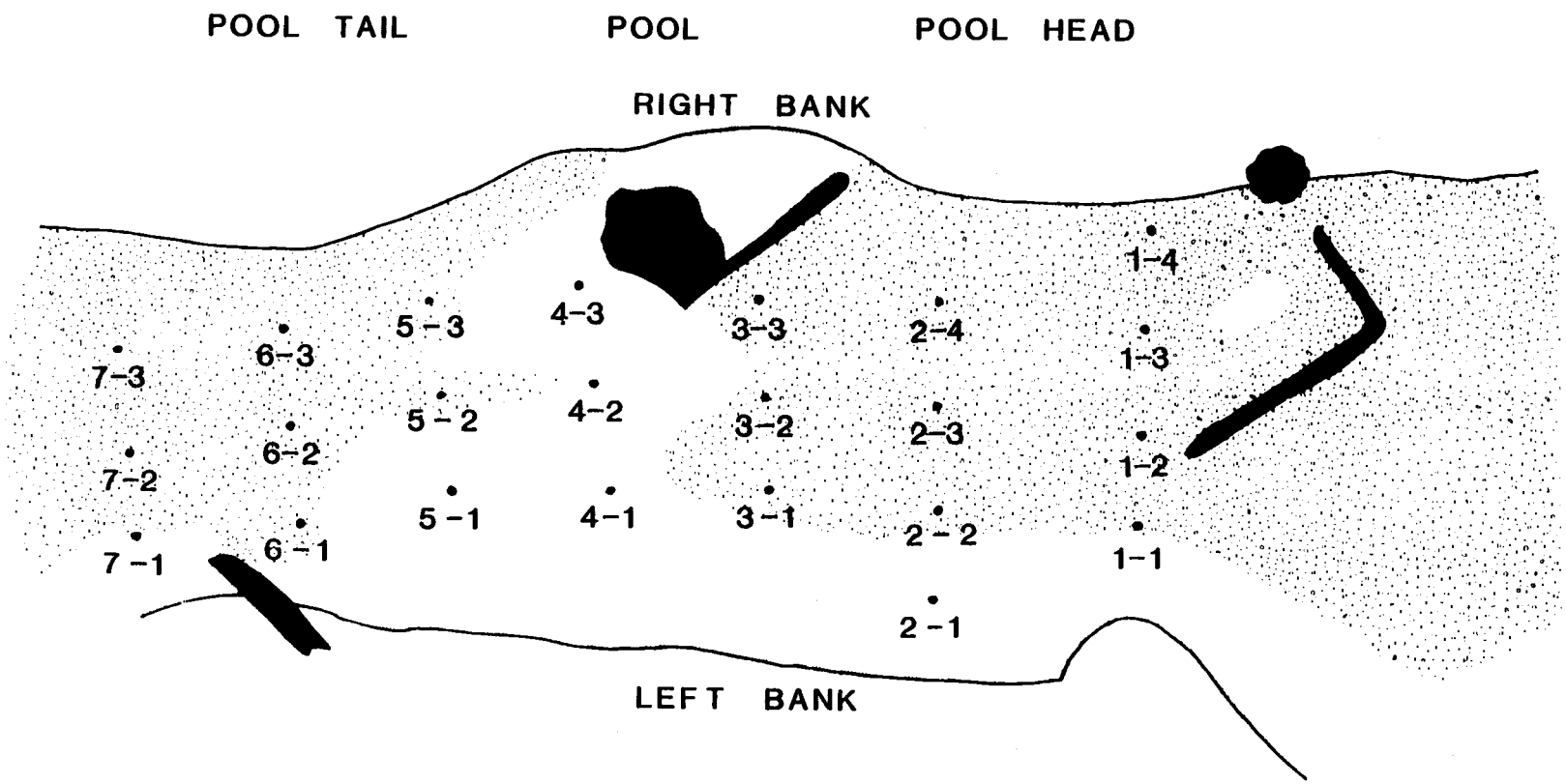

Figure 4. Scour chain locations. Direction of flow is from right to left.

or four chains, depending upon local channel width, with two meter spacing between chains (Fig. 4). Twenty-three scour chains were installed in July 1985 during low-flow conditions by driving a 26 mm diameter hollow pipe into the bed. The pipe was withdrawn, leaving the scour chain in place. This procedure disturbed only an area slightly larger than the pipe diameter at each chain location; therefore scour of the bed was unaffected.

Scour chains were excavated and a single remeasurement was made in September 1986 during a low-flow period at the end of the study after all other data had been collected. Chain 3-3 was never recovered and may have been scoured out of the bed (Fig. 4).

Bedload Transport

Bedload transport rates were measured using a hand-held Helley-Smith bedload sampler (Helley and Smith, 1971) with an enlarged bag, which has been shown to better maintain sampling efficiency than the smaller, standard bag (Beschta, 1981). Bedload transport was measured at discharges ranging from the beginning of significant transport to flows exceeding bankfull.

The initiation of bedload transport is difficult to define objectively, because entrainment is a stochastic process and some sediment is in motion at virtually all discharges (Vanoni, 1977, pp. 94). In this study, trial bedload sampling was done from the three bridges at low flow to determine the lower limit of discharge for sampling. The lowest discharge at which a sample weighing at least several grams was collected in two minutes was 1.26 m^3/s or 0.07 $m^3/s\text{-}km^2$. This was selected as the minimum discharge for bedload sampling. For comparison, Sidle (1988) reported that the bedload entrainment threshold in Bambi Creek, a small, gravel-bed stream in southeast Alaska, was 0.16 $m^3/s\text{-}km^2$. Entrainment threshold for Flynn Creek in the Oregon Coast Range was 0.2 $m^3/s\text{-}km^2$ (Beschta et al., 1981).

Bedload samples were dried at 100°C, weighed, ashed at 500°C for eight hours to remove organic material, reweighed to determine the proportion of organic material, then sieved to determine the inorganic grain-size distribution by weight following well established procedures (Folk, 1968, p. 34-36).

During high-flow events, measurements of discharge, water surface and bed elevation, vertical velocity profiles, near-bed velocity, flow azimuth, and bedload transport rate were made. All measurements were taken as frequently as possible by a two- to five-person crew throughout each storm hydrograph.

During very high storm flows on February 17, 1986, rising flow reached the bottom of the pool sampling bridge and measurements could no longer be made safely. The study site was abandoned later that night. Many details of the hydrograph between February 17 and 21 were inferred from the precipitation record, because high water necessitated removing the stage height recorder during this period. Measurements from the pool bridge resumed on February 24 after flood damage to the bridge was repaired.

Competence

Competence is a measure of the ability of streamflow to move sediment of a given size. This is commonly expressed as the largest grain size a given flow can transport. Maximum grain size in flood deposits has been used as a measure of storm flow competence (Baker and Ritter, 1975; Costa, 1983; Komar, 1987). In this study, the mean length of the intermediate axes of the five largest clasts in each bedload sample was computed. These means were related to the calculated boundary shear stress to determine the relationship between shear stress and maximum particle size entrained (Baker and Ritter, 1975; Carling, 1983). An abundant supply of clasts with diameter up to and exceeding the capacity of the bedload sampler was available in the channel bed, indicating that the maximum size of sampled material was not supply limited.

Analysis of the correlation of boundary shear stress with competence was complicated by the correlation of competence with sample weight, which resulted from increased probability of sampling a less abundant, large clast as sample size increased (Wilcock, 1988). Effect of sample weight on the competence vs shear stress relationship was examined by using partial sums of squares regression techniques to determine the associated partial regression coefficients (Neter et al., 1983, p. 286-9; SAS Inst., Inc., 1987, p. 584-588; T. Max, personal communication).

This procedure involved partitioning the total sum of squares for a multiple regression model into Type I and Type II sums of squares. Type I sum of squares indicated the contribution of the first independent variable to the total sum of squares. The remaining portion of the total was attributed to the second dependent variable. Type II sum of squares indicated the contribution of the first independent variable to the total sum of squares after all other independent variables were accounted for. The significance of the partial regression coefficient was tested by comparing the tabular critical F value to the ratio of the Type II mean square over the mean square error for the full model. In this way, the correlation of competence with shear stress, disregarding effects of the sample weight, was examined (Neter et al., 1983, p. 286-9; SAS Inst., Inc., 1987, p. 584-588; T. Max, personal communication).

Analysis of Covariance

Analysis of covariance techniques (Snedecor and Cochran, 1980, p. 385-388) were used several times during the data analysis to test the appropriateness of using a common regression equation for each of the three sampling stations. This analysis was done using SAS statistical software (SAS Inst., Inc., 1987, p. 584-640).

The procedure partitioned the model sum of squares into the components attributable to a class variable, a continuous variable, and an interaction variable. The sum of squares

for the interaction variable was the reduction in sum of squares due to fitting separate slopes beyond that due to fitting a common slope (Souter, 1987). This was reported in the SAS output as the Type I sum of squares (sequential sum of squares) for the interaction variable (SAS Inst., Inc., 1987, p.584-640). The calculated F value was the ratio of this reduction in sum of squares to the mean square error for the full model. The probability of a greater value of F was given by the program output. If this probability was greater than the critical probability level (0.05 unless otherwise specified), the null hypothesis was accepted.

The procedure for testing for a common intercept was analogous to that for slope. The reduction in sum of squares due to fitting separate intercepts was given, in the SAS output, by the Type III sum of squares (partial sum of squares) for the class variable (SAS Inst., Inc., 1987, p.584-640; Souter, 1987). In all of these analyses, the assumption of homogeneity of variance between stations was tested at the 0.05 probability level. If variance was not homogeneous, further analysis was not pursued.

RESULTS AND DISCUSSION

Hydrologic Conditions

The time period of this study included a series of large-magnitude storms beginning on February 12, 1986 (day 773, Fig. 5) that produced flows exceeding bankfull discharge (Fig. 5). Gaging records on Tom McDonald Creek were insufficient to determine the return interval of this sequence of large storms. However, gaging records were available for two nearby streams, Redwood Creek (drainage area 720 km^2) and Little Lost Man Creek (drainage area 8.96 km^2), which is located 12 km north of the study site (Fig. 1). Both gaging stations were operated by the U. S. Geological Survey, Water Resources Division, Eureka, CA. As an indication of the regional magnitude of peak flows during this time period, Figure 5 shows the concurrent hydrograph for Little Lost Man Creek

The annual maximum return interval for the February 17 peak, the largest flow of the study period, was 4.6 years and 5.5 years for Redwood Creek and Little Lost Man Creek respectively (U.S.G.S., Water Resources Division, Sacramento, CA, records on file). The February 17 peak flow was the second largest in 10 years of record for Little Lost Man Creek (Fig. 6). The return interval for Tom McDonald Creek was probably similar to that for Little Lost Man Creek, because the two streams are located close to one another, are approximately the same distance from the coast, and are similar in size (Fig. 1).

Magnitude of the largest gaged discharge during this study was 13.0 m^3/s (3.57 Q_{bf}), measured on February 19, 1986. Higher discharge values shown on Figure 5 (broken line) were estimates based on extrapolation of the rating curve. Estimated discharges were shown for interest only and were not used in further analyses. Peak flow on February 17 (day 778) may have been as high as 26.3 m^3/s (7.2 Q_{bf}) based on trimlines measured the following day. Comparison with the discharge record for Little Lost Man Creek (Fig. 5) indicated that this estimate was reasonable.

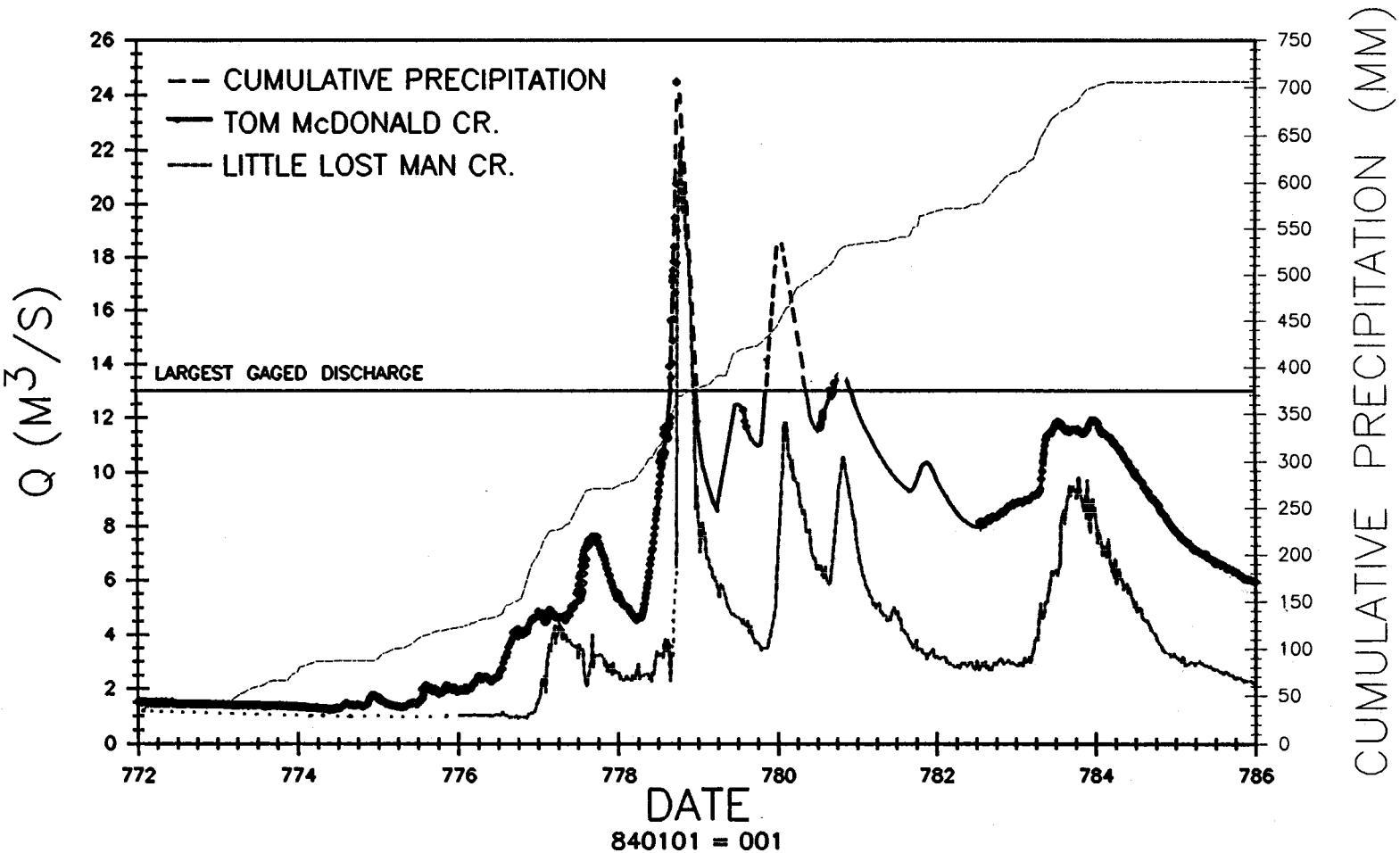

Figure 5. Instantaneous discharge (Q) and cumulative precipitation at Tom McDonald Creek. Discharge data for Little Lost Man Creek are shown for comparison. Dates are shown as sequential numbers beginning with January 1, 1984 as day 1.

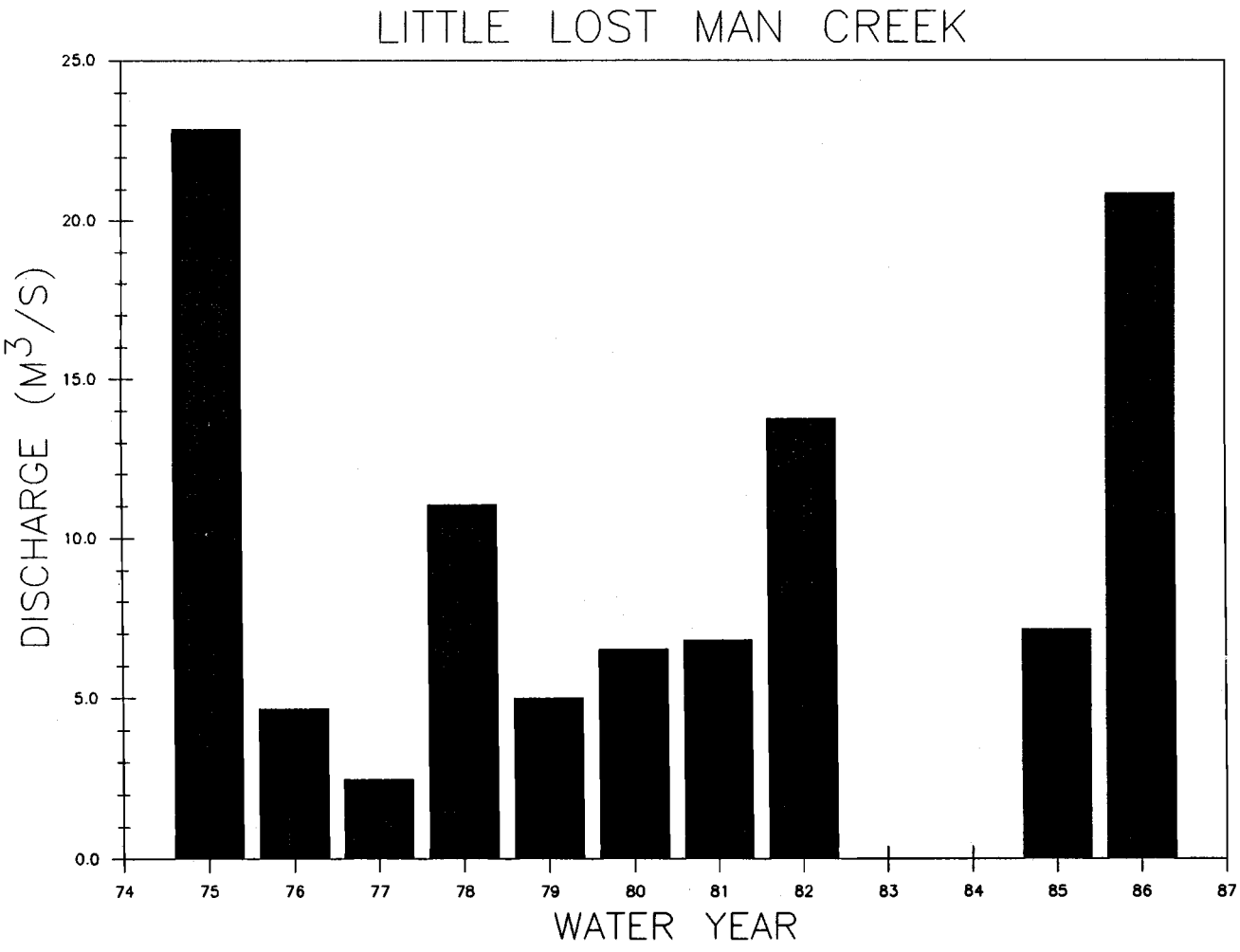

Figure 6. Annual peak flow record for Little Lost Man Creek. No data were collected during 1983 and 1984.

Stream Bed Grain-size Distribution

Values of D_{84} for the stream bed surface at the pool head, pool, and pool tail were 75 mm, 45 mm, and 54 mm respectively. D_{50} of the surface was 39 mm, 4.4 mm, and 16 mm respectively. D_{84} is a measure of the grain-size distribution of a sample. D_x indicates that x percent of the sample is finer than D_x.

Weighted mean values of D_{84} of the stream bed from 0 cm to 40 cm below the bed surface ranged from 31 mm to 34 mm, with an overall mean of 32 mm (App. A). D_{84} of the subsurface between 10 cm and 40 cm below the bed surface ranged from 30 mm to 33 mm, with a weighted mean of 32 mm (App. A). The ratio of the mean surface D_{84} at the two riffles in the study reach to the mean subsurface D_{84} was 2.02, clearly indicating that a pavement layer was present. Pavement is the coarse surface layer of clasts commonly present on gravel stream beds, generally believed to result from scouring of fine clasts by receding flows following hydrograph peaks (Andrews and Parker, 1987).

Obstruction Characteristics

The LWD obstruction in the study reach was a redwood rootwad lying on the channel bed, allowing very little flow to pass underneath. At low discharge the effective width of the obstruction perpendicular to the channel axis was 3.6 m (0.36 times the average active channel width). This included a small gravel bar between the right edge of the obstruction and the right edge of the channel (Fig. 2). The directions left and right are always used in this paper from the perspective of looking downstream. The obstruction surface was irregular, and extended above the level of bankfull discharge. Discharge at the time of submergence was somewhat ambiguous, however the obstruction was almost totally submerged at a discharge of 8.2 m^3/s (2.3 Q_{bf}). Immediately upstream of the obstruction, a smaller piece of LWD, which was mostly elevated above the channel bed, caused scour at

higher flows, adding to the pool length in the upstream direction (Fig. 2).

Lisle (1986) presented a general model for the stabilization of bars in gravel-bed streams by large obstructions and non-alluvial bends based on studies in Jacoby Creek, a gravel-bed stream with bankfull discharge of 19.6 m^3/s, located approximately 40 km south of the Tom McDonald Creek study site. Minimum width of an obstruction in Jacoby Creek causing scour of a pool and termination of an upstream bar was shown by Lisle (1986) to be $B = W_b - W_s \sec \beta - L_s \sin \beta$, where B = obstruction width perpendicular to the bank, W_b = stream bed width of the approach channel, W_s is the width of the scour hole measured perpendicular to the axis of the scour hole at the widest point of the obstruction, L_s = length of the scour hole measured from the widest point of the obstruction to the downstream lip of the scour hole and β = deflection angle, i.e. the angle between the axis of the scour pool and the approaching flow direction. Values of these variables for the Tom McDonald Creek study site were as follows: B = 3.6 m, W_b = 9.72 m, W_s = 2.52 m, β = 19°, and L_s = 9.3 m. The approach angle, i.e. the angle between the obstruction face and the approaching channel center line was α = 47°. The width of this bar-terminating obstruction (3.6 m) was somewhat smaller than predicted by the above equation (4.59 m).

Lisle (1986) plotted dimensionless characteristics of sampled obstructions, W_s/W_b, L_s/W_b, and $\sin \beta / \sin \alpha$ as a function of dimensionless obstruction width β/W_b. Sample sizes ranged from 11 to 16 obstructions for these relationships. For all three of these characteristics, the obstruction in the present study plotted together with those that form bar-terminating pools sampled by Lisle. However, the Tom McDonald Creek obstruction plotted close to the transition between pool-forming obstructions and those which do not form pools and terminate bars.

Lisle (1986) plotted $\sin \alpha$ as a function of B/W_b, which successfully discriminated scour holes from pools for his study reaches on Jacoby Creek Scour holes, unlike pools, do not span the entire channel and do not terminate upstream bars. The obstruction in Tom McDonald Creek plotted very close to the discriminating function in the zone characterizing

obstructions that form scour holes, not bar-terminating pools (Fig. 7). This was in agreement with field observations in Tom McDonald Creek that the upstream bar nearly continued past the pool, and might have done so except for the channel constriction just downstream of the pool (Fig. 2). These findings indicated that characteristics of pool-forming obstructions may be quite variable, and are dependent on other channel characteristics such as neighboring constrictions. Therefore, intentional manipulation of channel morphology through the introduction of obstructions must be carefully planned.

Streamflow Patterns

One of the questions addressed in this study was how a LWD obstruction affects local streamflow hydraulics and channel morphology. In the following section, streamflow patterns (direction and velocity) and their change with discharge are related to effects of the LWD obstruction. Obstruction-related effects on channel morphology are then discussed.

Deflection by the LWD obstruction created cross-stream flow with velocities as large as 29% of the total flow velocity (Table 1). Sufficiently large total-flow shear stresses were created so that sediment accumulating at the base of the slip face of the upstream, left-bank lateral bar (Fig. 2) was removed, halting downstream migration of the bar. In addition, location of the right-bank lateral bar was determined by deposition in a low-shear stress environment in the lee of the obstruction. In this way, the obstruction anchored the location of these gravel bars, thus stabilizing channel morphology. The bars further modified streamflow patterns, as discussed below, particularly at moderate and high discharge.

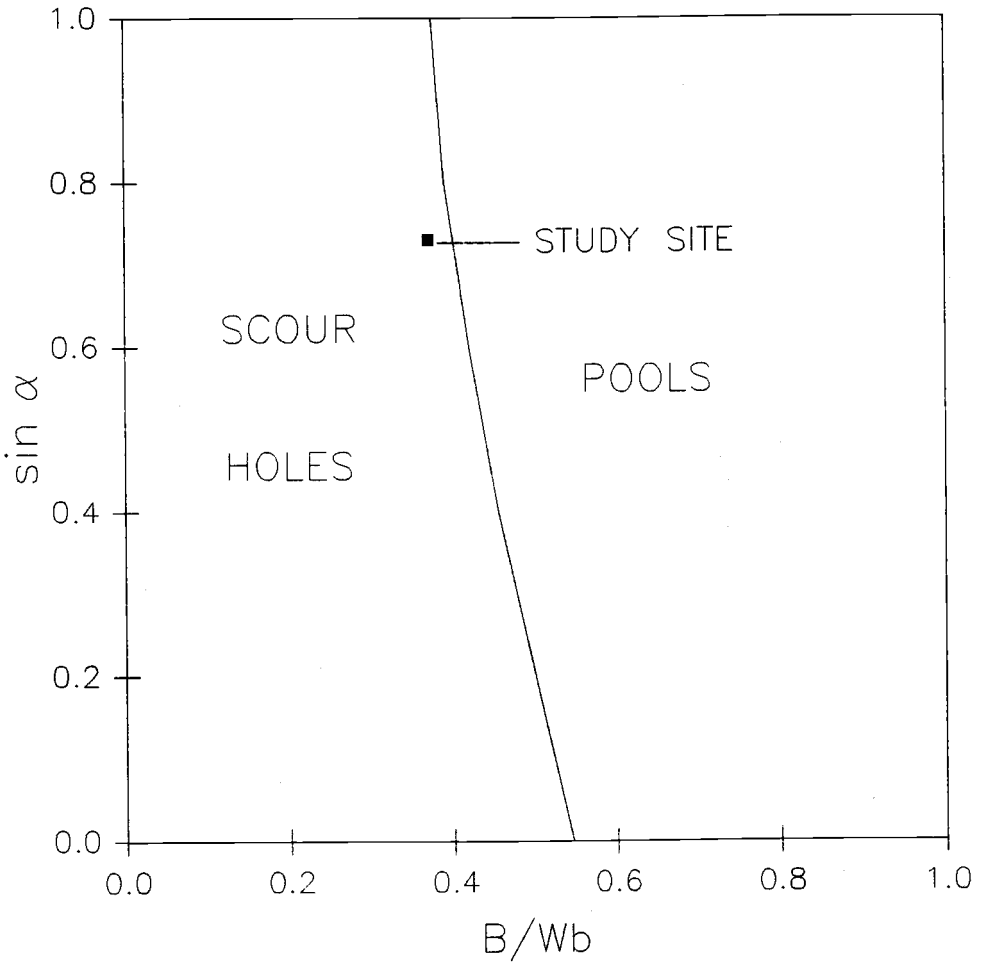

Figure 7. Obstruction size classification of Lisle (1986). See text for explanation.

TABLE 1. MAXIMUM NET (U_n) AND CROSS-STREAM (U_s) VELOCITIES. Q = instantaneous discharge; Q_{bf} = bankfull discharge (3.64 m^3/s). Cross-stream velocities were not measured at low flow.

STATION	Q/Q_{bf}	MAX U_n (cm/s)	MAX U_s (cm/s)	MAX U_s/ MAX U_n
1	0.12	63	---	---
1	0.52	161	31	.19
1	0.90	226	28	.12
2	0.10	55	---	---
2	0.54	133	39	.29
2	1.23	209	55	.26
3	0.15	45	---	---
3	0.56	107	21	.24
3	0.89	150	21	.14

Pool Head Cross Section

At low discharge, effects of the LWD obstruction on streamflow patterns were minimal at the pool head. Velocity distribution at a discharge of 0.12 Q_{bf} was approximately logarithmic (Fig. 8A). The location of maximum velocity was depressed below the water surface, because of a reduction of surface velocity (Fig. 8A). This is common in small channels (Leopold et al., 1964, p. 166), and is attributed to secondary currents resulting from flow interacting with the channel banks (Richards, 1982, p. 71-72). Additional selected velocity profiles for the three sampling stations, taken at low, moderate, and high discharge are presented in Appendix B.

At a discharge of 0.52 Q_{bf}, flow approaching the pool head was deflected toward the right by a left-bank lateral bar (Fig. 2). This deflection created right-directed cross-stream flow in the upper part of the water column (Fig. 9A). Additional selected cross-stream flow distributions for the three sampling stations, taken at moderate and high discharges are presented in Appendix C. Cross-stream flow may have caused the increase in velocity gradient near the stream surface relative to the low flow case (Fig. 8B).

As discharge increased above 0.52 Q_{bf}, backwater effects of the LWD obstruction caused super elevation of the water surface on the right side of the channel (Fig. 2, 10) This was particularly evident at flows greater than bankfull (Fig. 10), becoming less pronounced, but still apparent, at very high discharge (3.49 Q_{bf}) when the large obstruction was submerged by about 30 cm (Fig. 10). Backwater effects depressed velocities in the upper part of the water column (Fig. 8C) and countered right-directed cross-stream flow (Fig. 9B). This caused cross-stream flow to become less important at high discharge (0.90 Q_{bf}) than at moderate discharge (0.52 Q_{bf}) relative to net downstream velocity (Table 1).

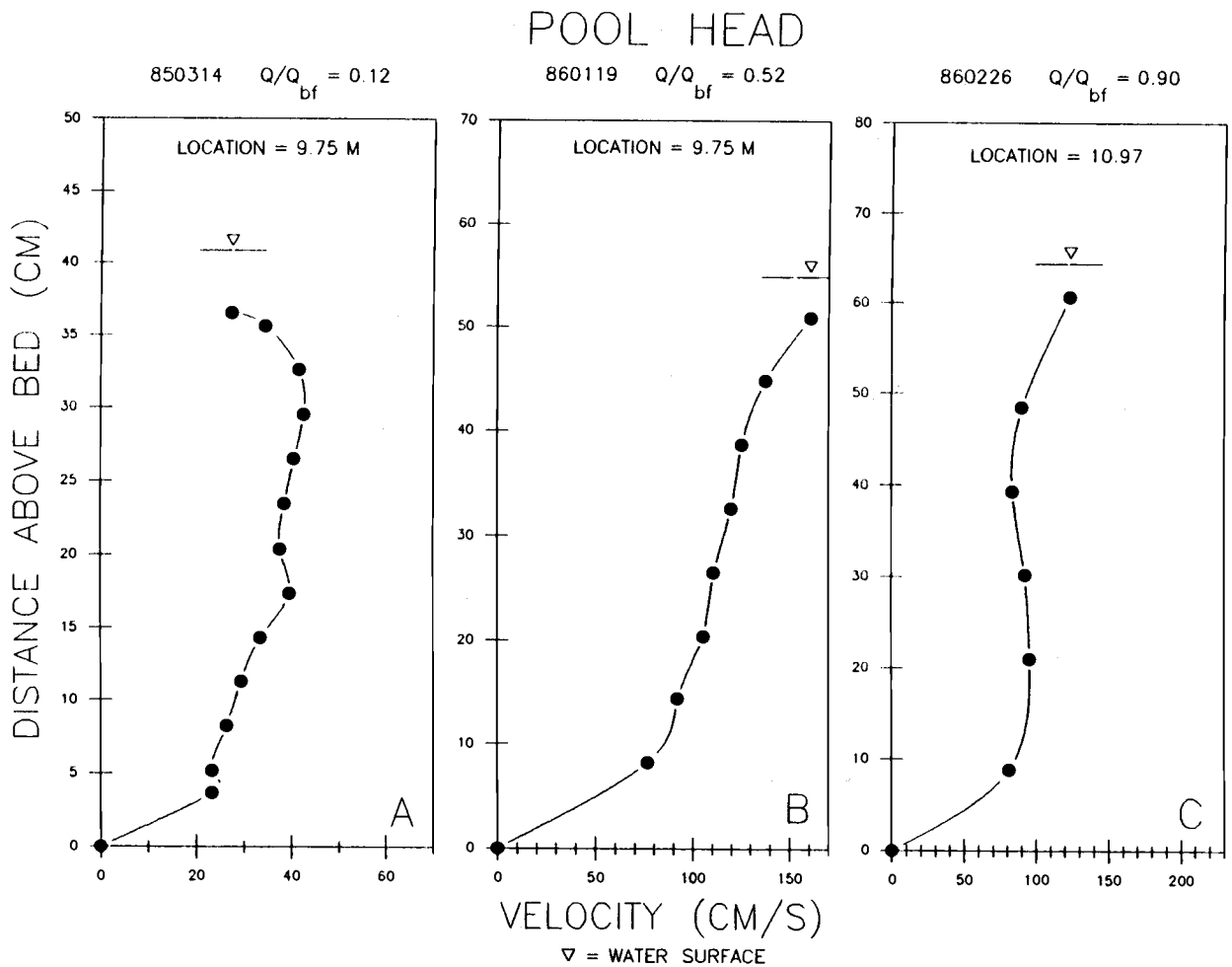

Figure 8. Velocity profiles. Locations are the distance from the left survey monument (Fig. 2). Q is water discharge. Q_{bf} is bankfull discharge. Note scale differences.

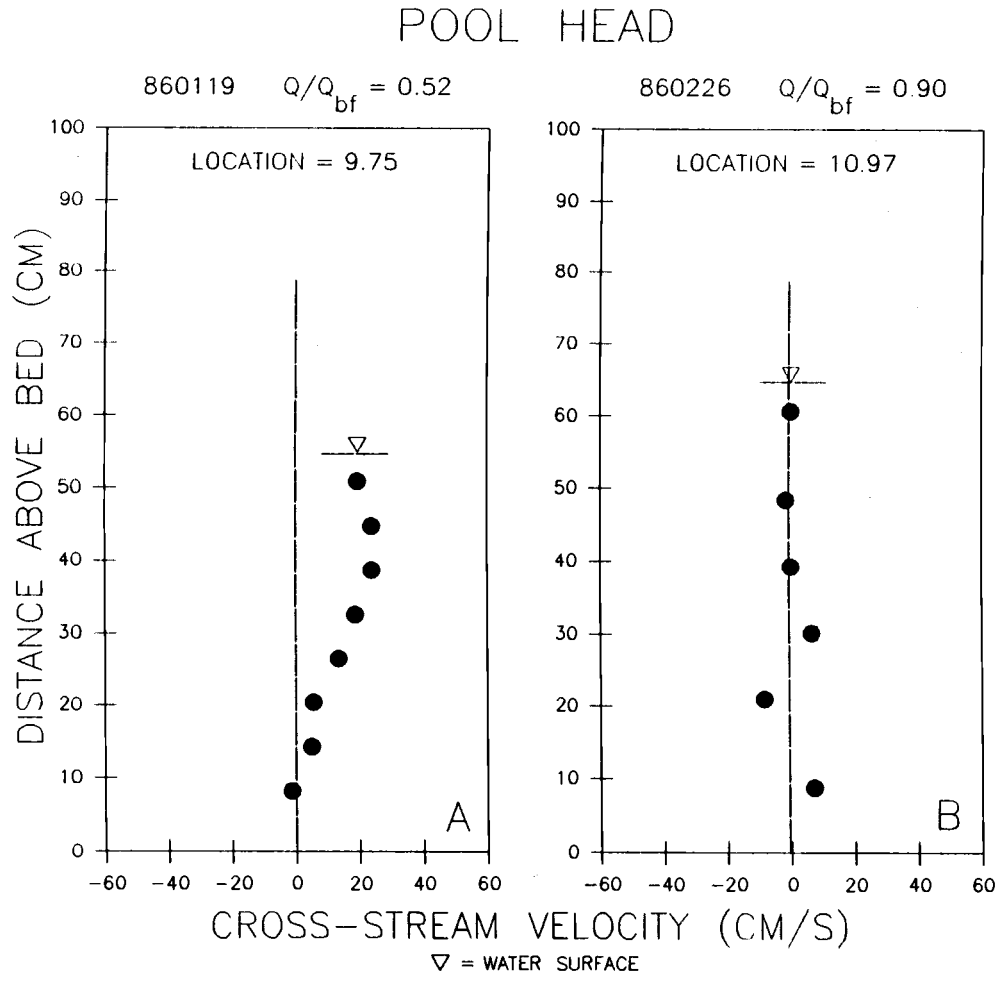

Figure 9. Cross-stream velocity distribution. Locations are the distance from the left survey monument (Fig. 2). Q is water discharge. Q_{bf} is bankfull discharge.

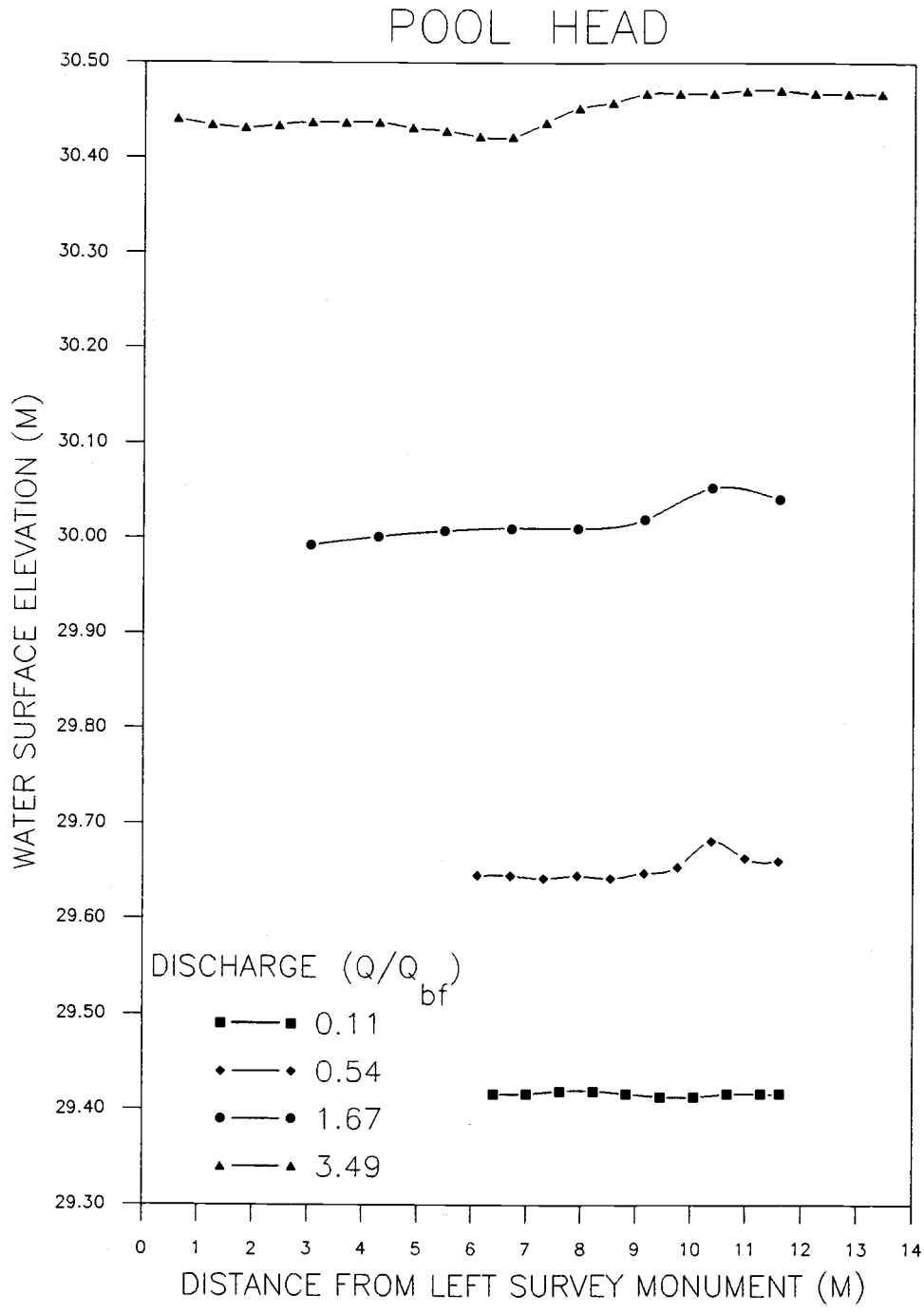

Figure 10. Variation in water surface elevation with discharge. Perspective is looking downstream. Elevation is relative to an arbitrary datum.

Pool Cross Section

Effects of the LWD obstruction on streamflow patterns were most pronounced at the pool cross-section, and were evident even at low discharge. The most striking effects included the creation of highly turbulent eddies and vortices and strong deflection of the flow. In addition, a large area of low-velocity, eddying current was created in the lee of the obstruction.

At low discharge (0.10 Q_{bf}) vertical velocity distribution was approximately logarithmic (Fig. 11A). As discharge increased to 0.54 Q_{bf}, flow deflected toward the left bank by the obstruction created backwater effects that raised the water surface on the left side of the channel (Fig. 12). The resulting pressure gradient induced cross-stream flow toward the right that strongly modified the general pattern of left-directed cross-stream flow (Fig. 13A) and reduced net velocity in the central part of the water column (Fig. 11B).

At 1.23 Q_{bf} these effects were still apparent but less pronounced (Fig. 11C, 12, 13B). Close to the obstruction (location 9.45 m), velocity in the upper half of the flow was strongly depressed (Fig. 11D) by interaction of the dominant flow with a large eddy downstream of the obstruction (Fig. 2). Maximum cross-stream velocities increased with discharge, and changed little relative to maximum net velocities (Table 1).

The velocity profile at this high discharge (1.23 Q_{bf}) clearly differed from profiles at lower discharge and from profiles measured in pools without obstructions (Fig. 14). The profile in Figure 14A was derived from an isovel diagram of cross section 20, a representative pool cross section, in Muddy Creek, Wyoming at a discharge of 0.80 Q_{bf} (Dietrich et al., 1979). The profile in Figure 14 B was based on flume data of Beschta (1983; personal communication) for an obstruction-related pool at maximum discharge for the apparatus. The laboratory and field profiles for obstruction-related pools were quite similar (Fig. 14). This may have been largely coincidence; however both illustrate the magnitude of flow distortion produced by obstructions. Given this distortion, it is

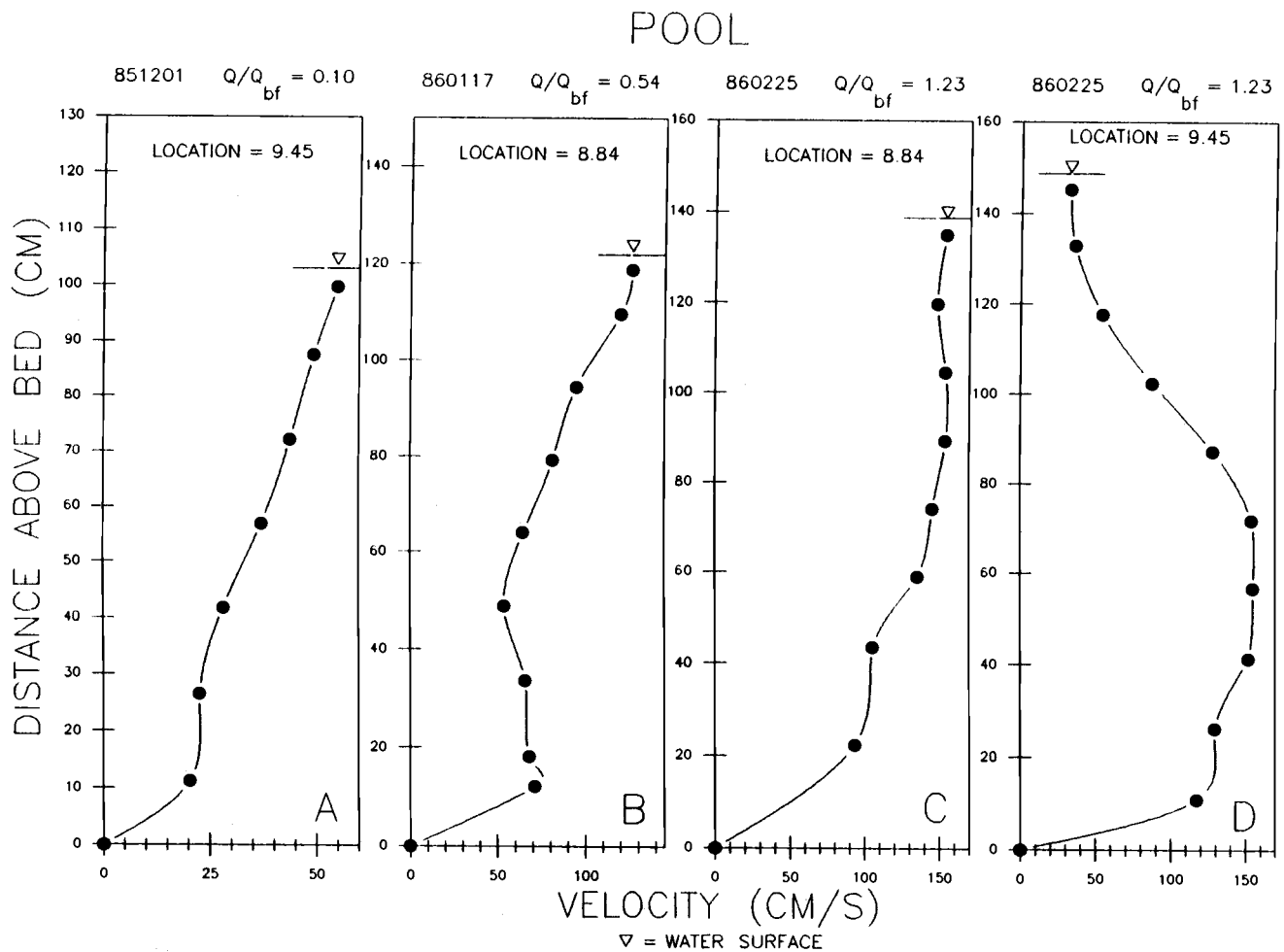

Figure 11. Velocity profiles. Locations are the distance from the left survey monument (Fig. 2). Q is water discharge. Q_{bf} is bankfull discharge. Note scale differences.

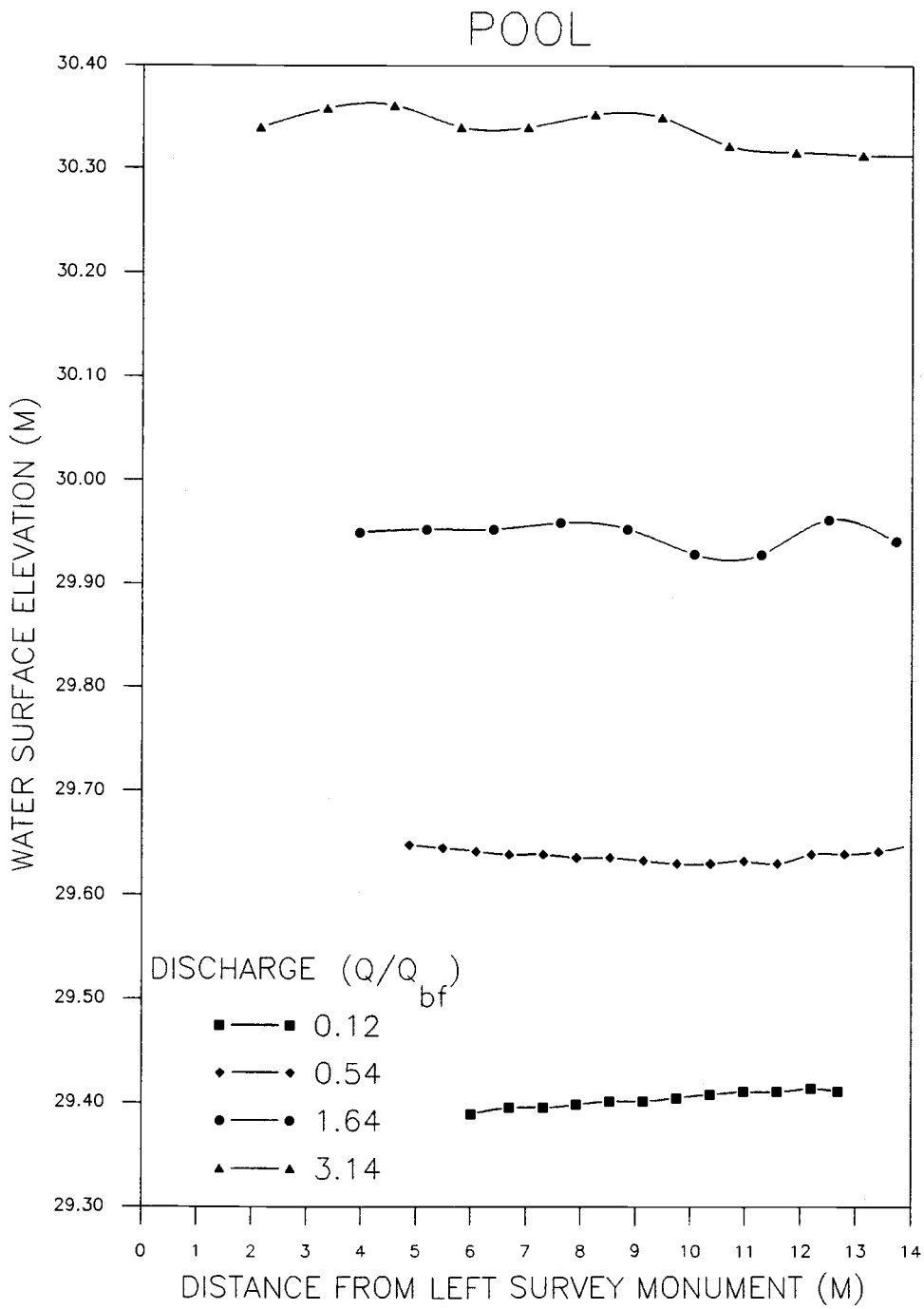

Figure 12. Variation in water surface elevation with discharge. Perspective is looking downstream. Elevation is relative to an arbitrary datum.

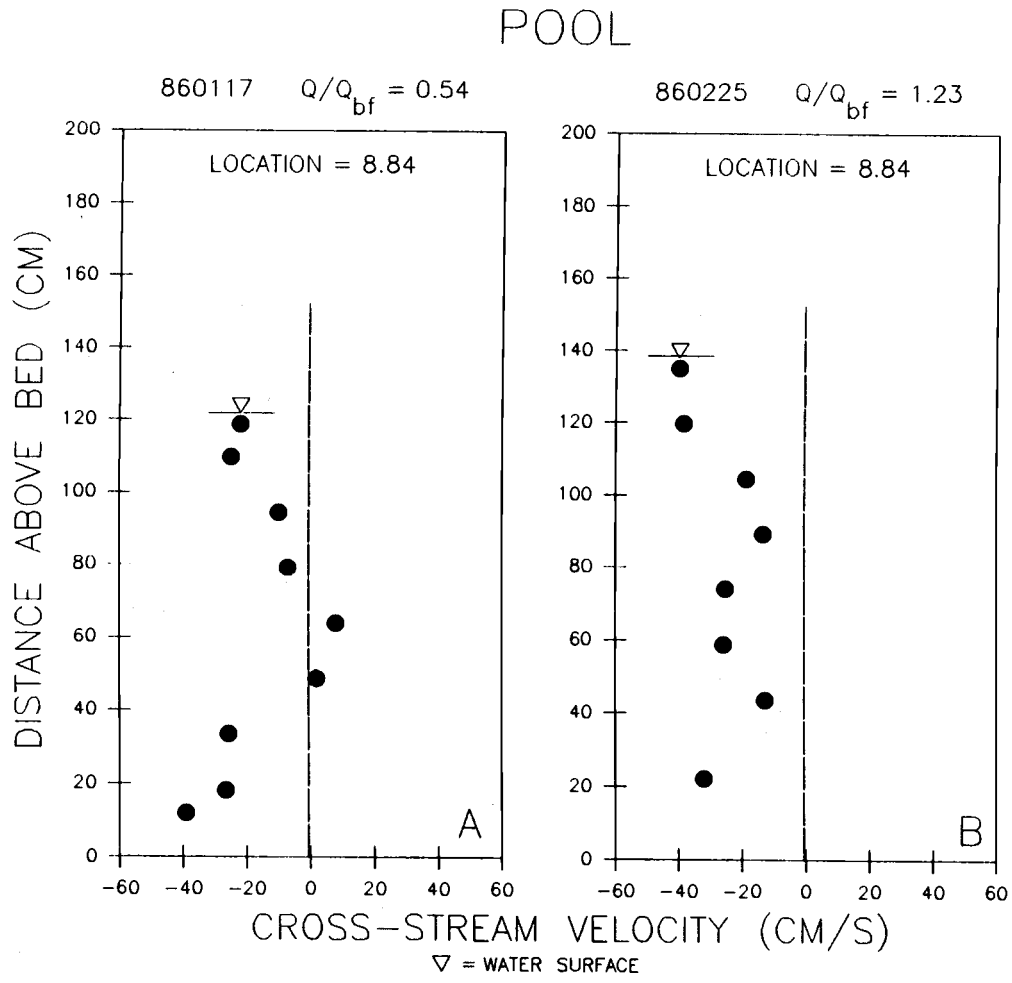

Figure 13. Cross-stream velocity distribution. Locations are the distance from the left survey monument (Fig. 2). Q is water discharge. Q_{bf} is bankfull discharge.

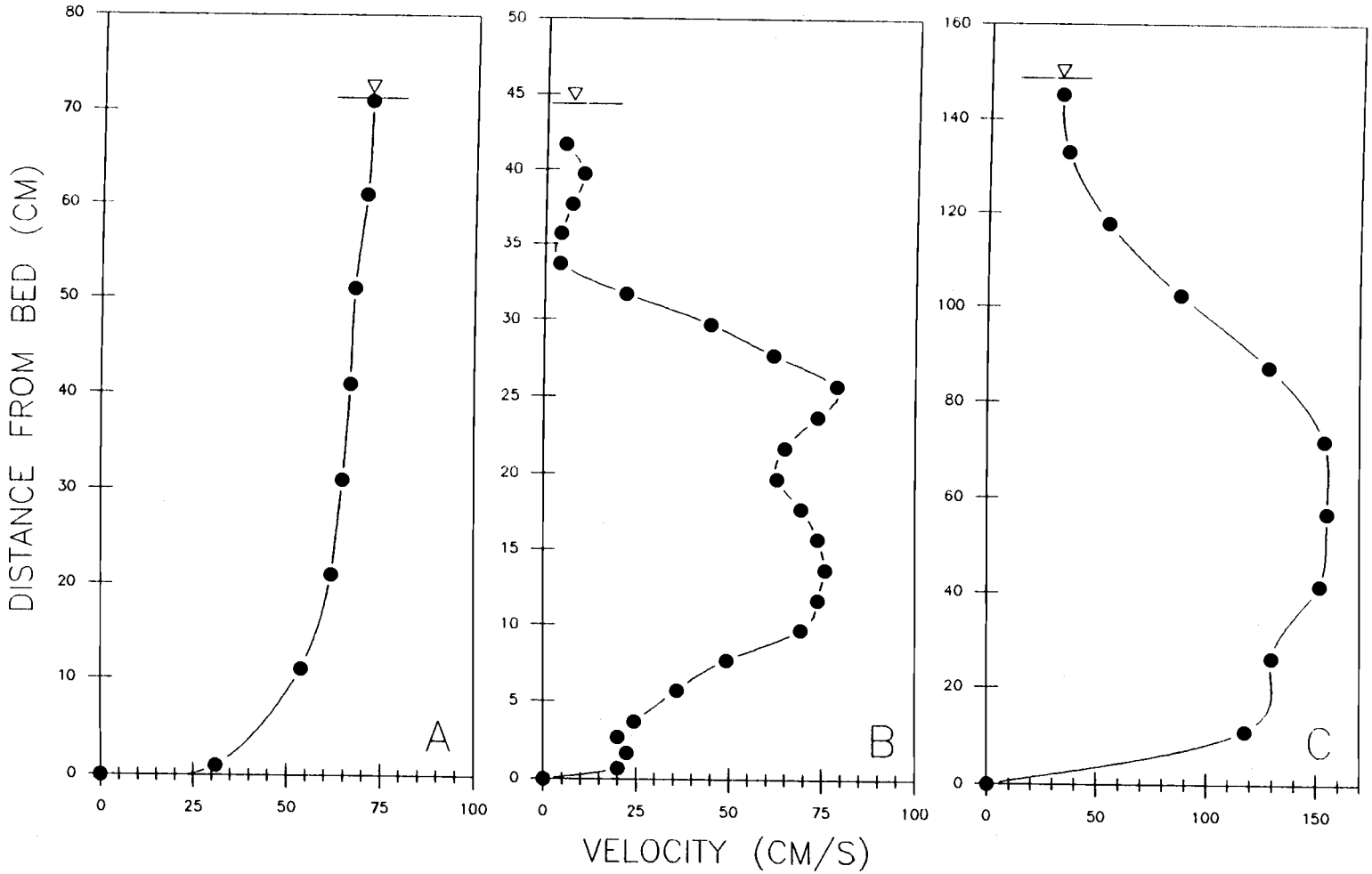

Figure 14. Comparison of velocity profiles in pools. Profile A is from Muddy Creek, Wyo. (Dietrich et al., 1979). Profile B is from a flume study (Beschta, 1983). Profile C is from Tom McDonald Creek

reasonable to expect increased turbulent velocity fluctuations to affect sediment entrainment in obstruction-related pools. In addition, depressed velocities near the surface (Fig. 14 B, C) may provide low-energy habitat for fish during high flow.

The general streamflow pattern was altered only slightly when the large obstruction was overtopped at a discharge greater than 2.3 Q_{bf}. Local surface turbulent eddies were created and eddying current downstream of the obstruction was modified, but, in general, subsurface flow was not greatly changed. Superelevation on the left side persisted as discharge increased up to flows at least as large as 3.14 Q_{bf} (Fig. 12).

Pool Tail Cross Section

At the pool tail, streamflow was modified by strong leftward deflection of flow by the obstruction and by deflection around the upstream left-bank lateral bar and the right-bank lateral bar in the lee of the obstruction (Fig. 2). At low discharge (0.15 Q_{bf}), velocity profiles were generally logarithmic (Fig. 15A). As discharge increased, super elevation of the water surface on the left side of the channel (Fig. 16) was caused by backwater upstream of a piece of LWD at the left bank (Fig. 2).

At moderate discharge (0.56 Q_{bf}), this backwater and deflection of flow toward the right by the upstream, left-bank lateral bar created cross-stream flow toward the right (Fig. 17A). Velocity profiles continued to be approximately logarithmic, with quite steep gradients near the bed (Fig. 14B).

At high discharge (0.89 Q_{bf}), cross-stream flow at the surface was directed toward the left (Fig. 17B) by the lateral bar in the lee of the obstruction. This cross-stream flow appeared to increase net velocity near the water surface (Fig. 15C). Opposing right- and left-directed cross-stream currents caused a decrease in the ratio of maximum cross-stream velocity to maximum net velocity with an increase from moderate to high discharge, (Table 1).

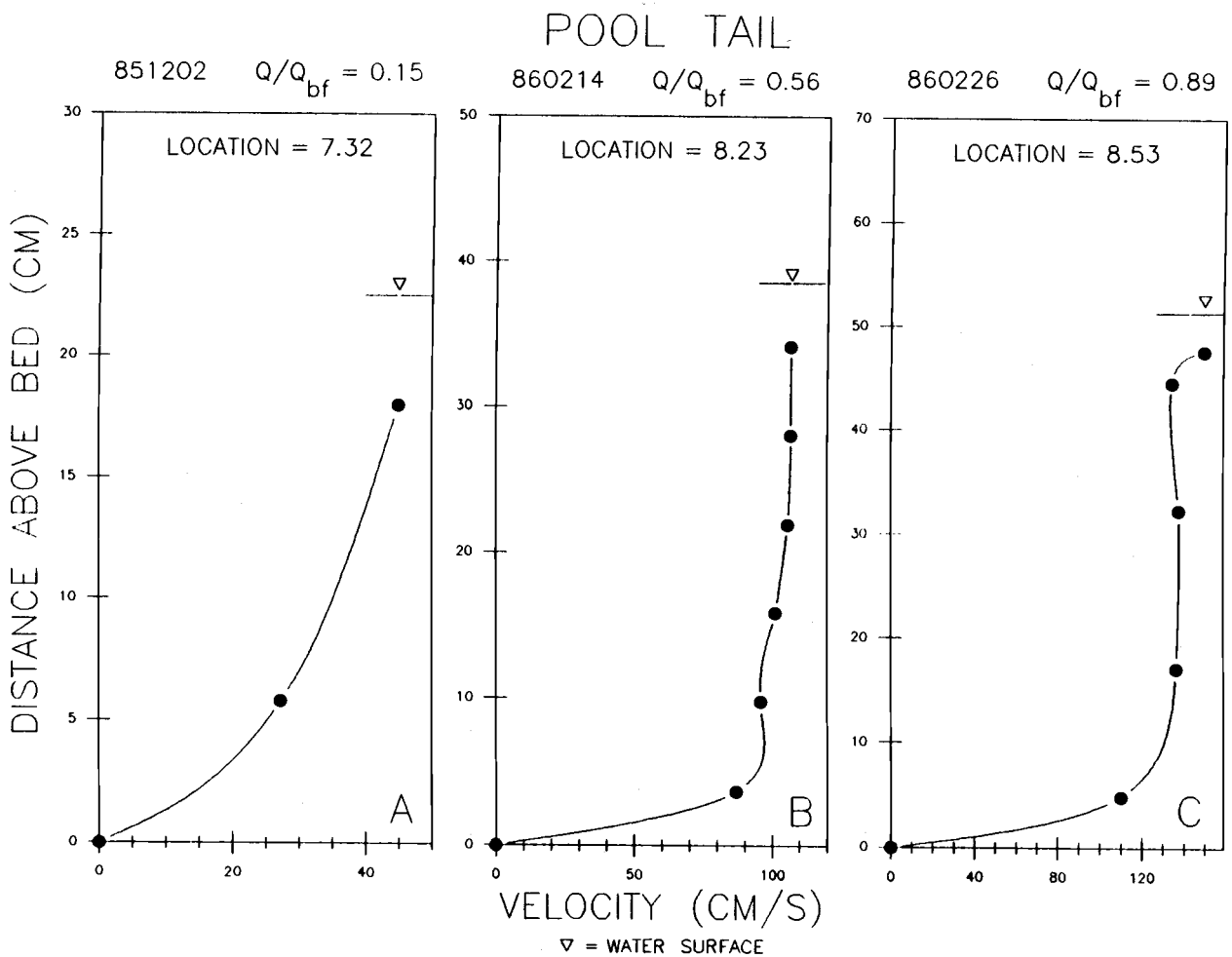

Figure 15. Velocity profiles. Locations are the distance from the left survey monument (Fig. 2). Q is water discharge. Q_{bf} is bankfull discharge. Note scale differences.

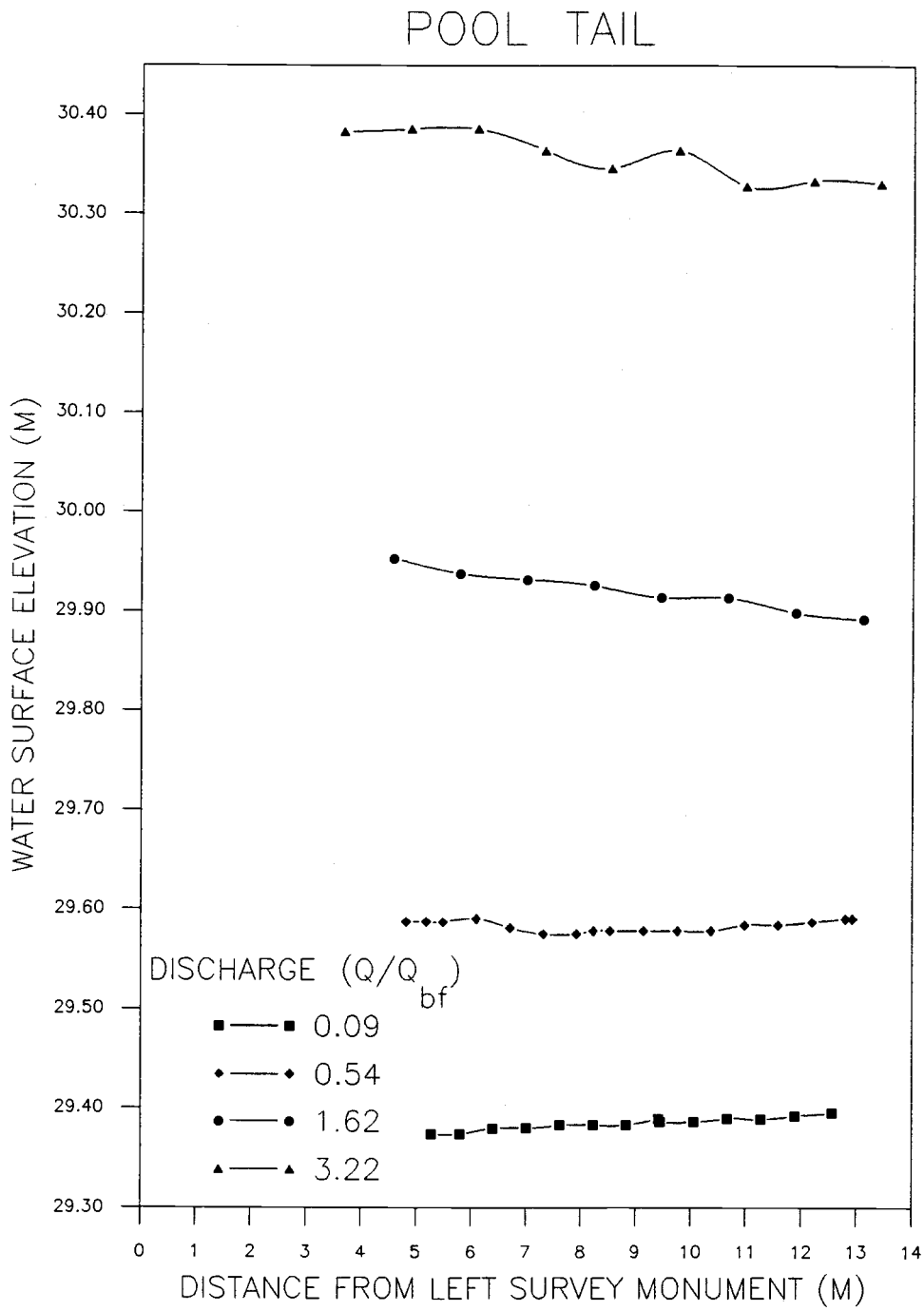

Figure 16. Variation in water surface elevation with discharge. Perspective is looking downstream. Elevation is relative to an arbitrary datum.

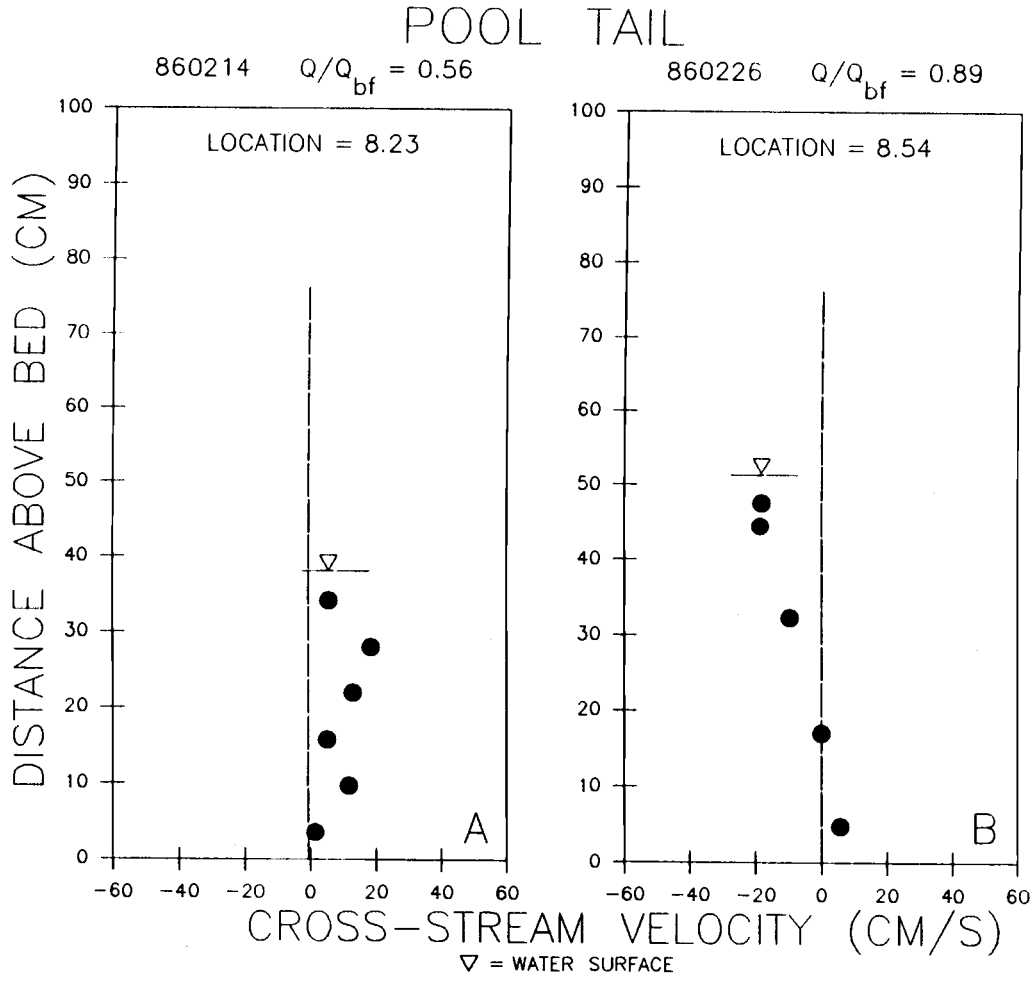

Figure 17. Cross-stream velocity distribution. Locations are the distance from the left survey monument (Fig. 2). Q is water discharge. Q_{bf} is bankfull discharge.

Effects of the obstruction included modifying cross-stream flow and creation of backwater effects. These effects modified net velocity magnitude and direction. In some cases, these effects created localized sites of low velocity that may have provided refuge for fish during high-flow conditions. The largest and most persistent potential refuge was the zone of eddying current in the lee of the LWD obstruction.

Boundary Shear Stress

Cross-channel Location of Shear Stress Maximum

In sinuous stream reaches containing pools where large obstructions are not an important influence, the trace of boundary shear stress maximum crosses from one side of the channel to the other in response to forces exerted by channel curvature and bed topography (Dietrich et al., 1979; Dietrich and Whiting, 1989). In this study, where a large, in-channel obstruction was a major influence, location of the boundary shear stress maximum was strongly dependent on the path of flow deflected by the obstruction.

At the pool head, location of boundary shear stress maximum changed with increasing discharge (Fig. 18). Upstream bed configuration directed flow toward the left side of the channel at low discharge. As discharge increased to 0.50 Q_{bf}, location of the boundary shear stress maximum shifted 2 m toward the right in response to right-directed cross-stream flow (Fig. 9A). At high discharge (1.27 Q_{bf}), this maximum shifted back 1 m toward the left as cross-stream flow became redirected in a more streamwise direction (Fig. 9B) as a result of increased deflection of flow by a zone of backwater upstream of the large obstruction (Fig. 2).

In the pool, maximum boundary shear stress was distinctly lower than at the pool head, even at discharges well in excess of bankfull (Fig. 18, 19). Statistical evaluation of this difference is presented below. At moderate discharge (0.50 Q_{bf}), high shear stress

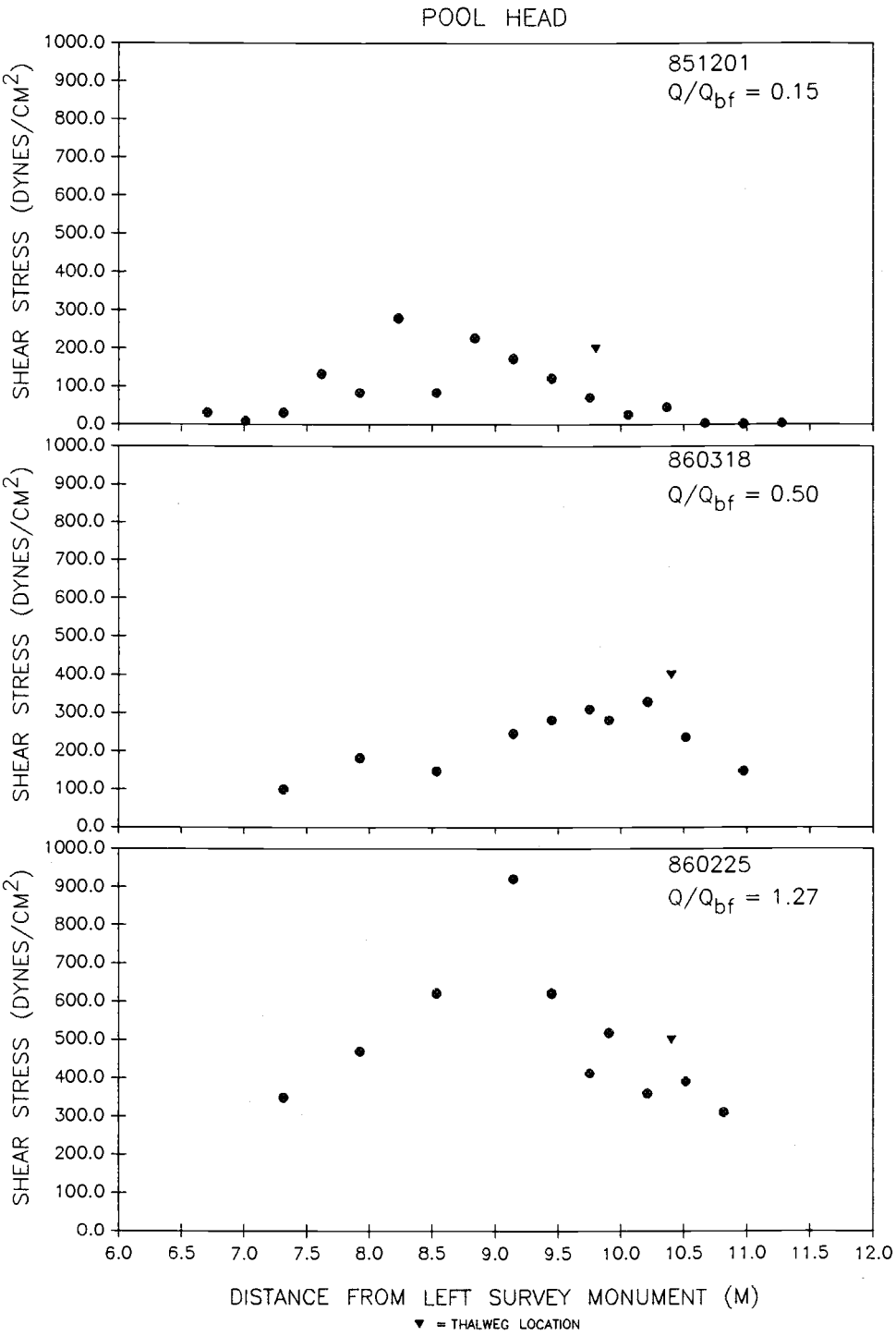

Figure 18. Cross-channel variation in shear stress.

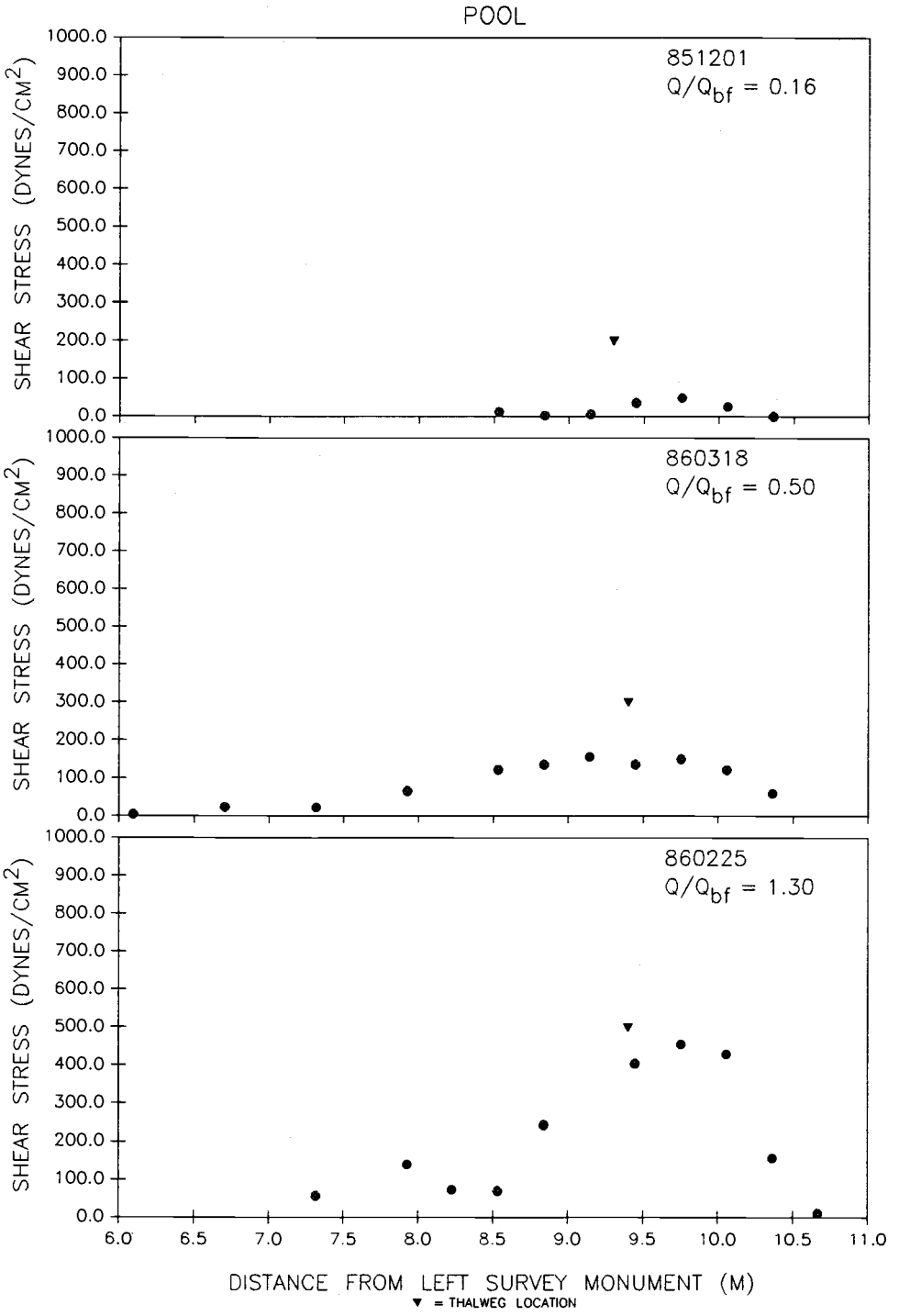

Figure 19. Cross-channel variation in shear stress.

occurred over a broader zone than at higher or lower discharge, spanning approximately 1 m of the channel width (Fig. 19). General location of maximum shear stress remained quite stable with changing discharge (Fig. 19). Deflection of flow by the large obstruction spatially anchored the path of high-velocity flow and shear stress maximum. This temporal-mean (averaged over one minute) shear stress, in addition to turbulent velocity fluctuations caused by the obstruction, tended to maintain pool morphology and stabilize the location of the deepest part of the pool through a wide range of discharge.

At the pool tail, high boundary shear stress occurred along several meters of the channel width, but became more focused as discharge increased (Fig. 20). The wide span of boundary shear stress maxima was not surprising considering the wide, relatively uniform elevation and grain-size distribution of the bed at this cross section. Shear stress magnitude was generally greater than in the pool but less than at the pool head (Fig. 18, 19, 20). These differences are discussed in more detail below.

At all three stations, the shear stress maximum was commonly not located at the thalweg (Fig. 18, 19, 20). Increases in shear stress can be accommodated by scour, coarsening of the bed, or concentration of sediment transport (Dietrich and Whiting, 1989). The location of the thalweg was displaced at the pool head and tail by deposition of bedload, which tended to be transported along the trace of shear stress maximum.

Boundary Shear Stress Magnitude

At all three stations, near-bed velocity, averaged over 1 min and over 2.5 m of channel width, increased linearly with discharge up to flows of at least 1.4 Q_{bf} (Fig. 21(a)). At discharges higher than 1.4 Q_{bf}, data were very scattered and the relationship was poorly defined. This may have been caused by flow encountering complex roughness outside the banks. Overbank flows encountered additional obstructions, adding to the complexity of large scale turbulence and cross-stream currents. This added roughness also changed

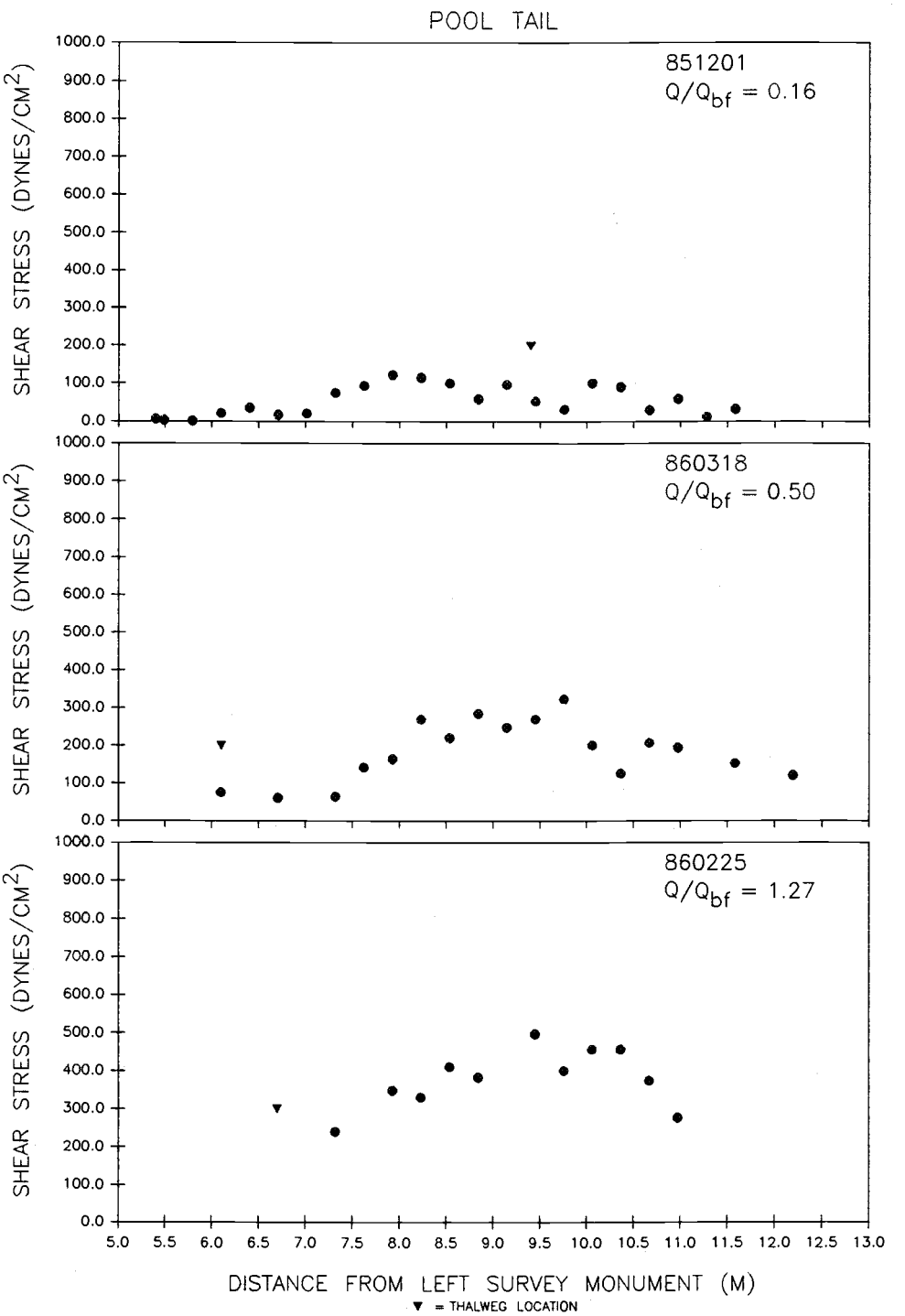

Figure 20. Cross-channel variation in shear stress.

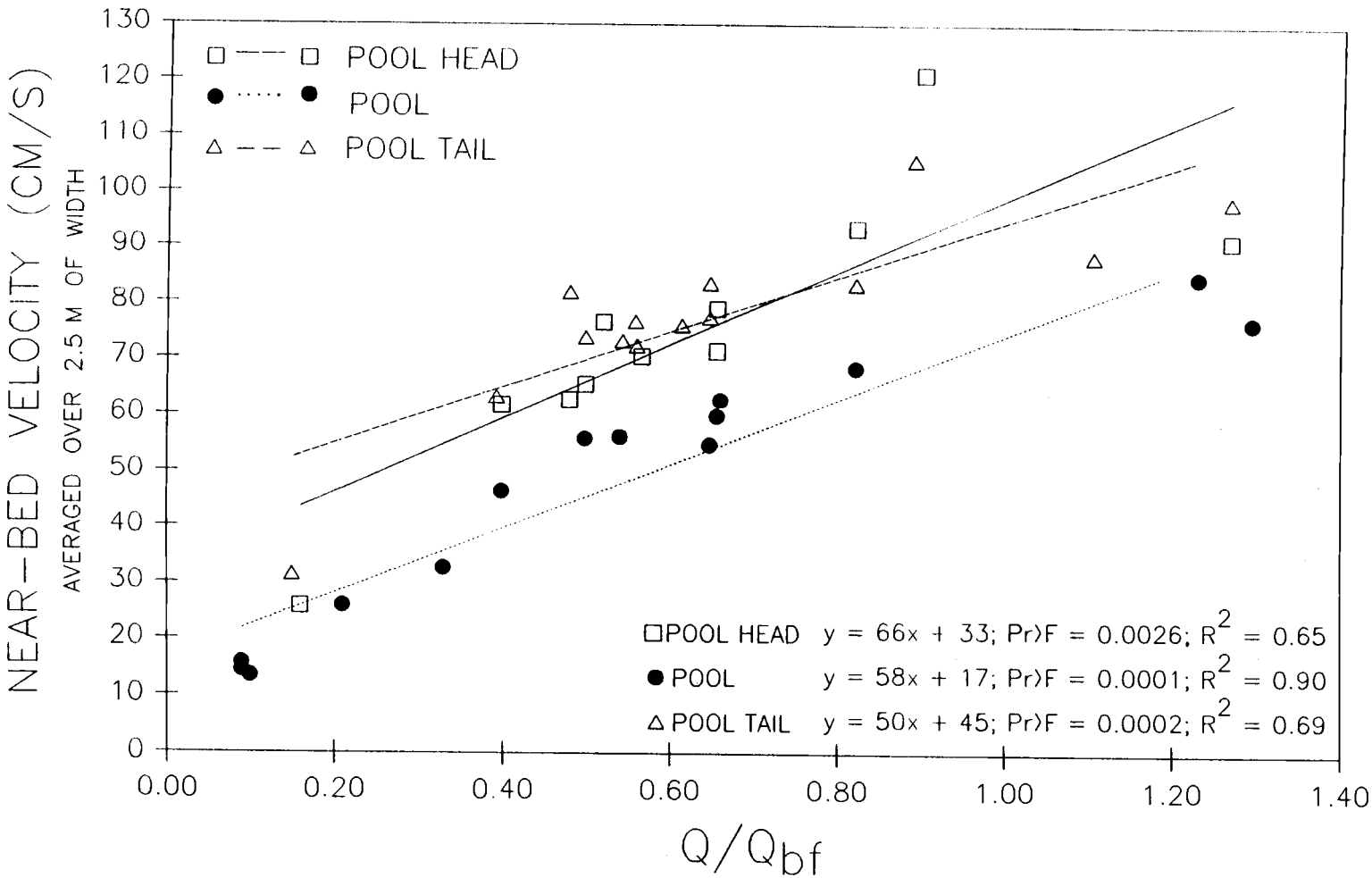

Figure 21(a). Variation in near-bed velocity with dimensionless discharge. Q is water discharge. Q_{bf} is bankfull discharge.

the proportion of boundary (stream bed) roughness to effective form roughness, thus altering the shear stress distribution (Bathurst, 1982; Bray, 1982). Interference of bedload with the velocity meter at higher discharge may have also contributed to this data scatter, although significant interference was not noticeable.

Analysis of covariance techniques (Snedecor and Cochran, 1980, p. 385-388), using SAS statistical software (SAS Inst., Inc., 1987; Souter, 1987), were used to test the appropriateness of a common regression of near-bed velocity on discharge for the three stations. An analysis summary is presented in Appendix D-1.

The rate of increase in near-bed velocity, i.e. slope of the regression equations, was not statistically different at any of the three stations; however magnitude of near-bed velocity (indicated by the intercept in the regression equation) at the pool was significantly lower than that at the pool head or tail (Fig. 21(a), App. D-1).

Scatter in Figure 21(a) resulted, in part, from unevenness of the coarse stream bed, which caused undesirable variation in the distance between the bed and the velocity meter. The same conclusions regarding relative magnitude and rate of increase of near-bed velocity were found for a subset of these data, measured with an apparatus fitted with an enlarged base, which minimized variation in distance from the bed (Fig. 21(b), App. D-2). These data were less scattered, and were used for all further analyses in the present study.

Magnitude of local shear stress, expressed for convenience as shear velocity (U^*), was determined from near-bed velocity measurements at a range of flows. Shear velocity magnitude increased linearly with discharge up to flows at least as large as 1.4 Q_{bf} at the three sampling stations (Fig. 22). The relationships illustrated in Figure 22 were tested to determine the appropriateness of a common regression, using analysis of covariance techniques. Results are summarized in Appendix E. The magnitude of shear velocity, averaged over 1 min and over 2.5 m of channel width, was significantly different at the three sampling stations, although rate of increase was not significantly different (Fig. 22,

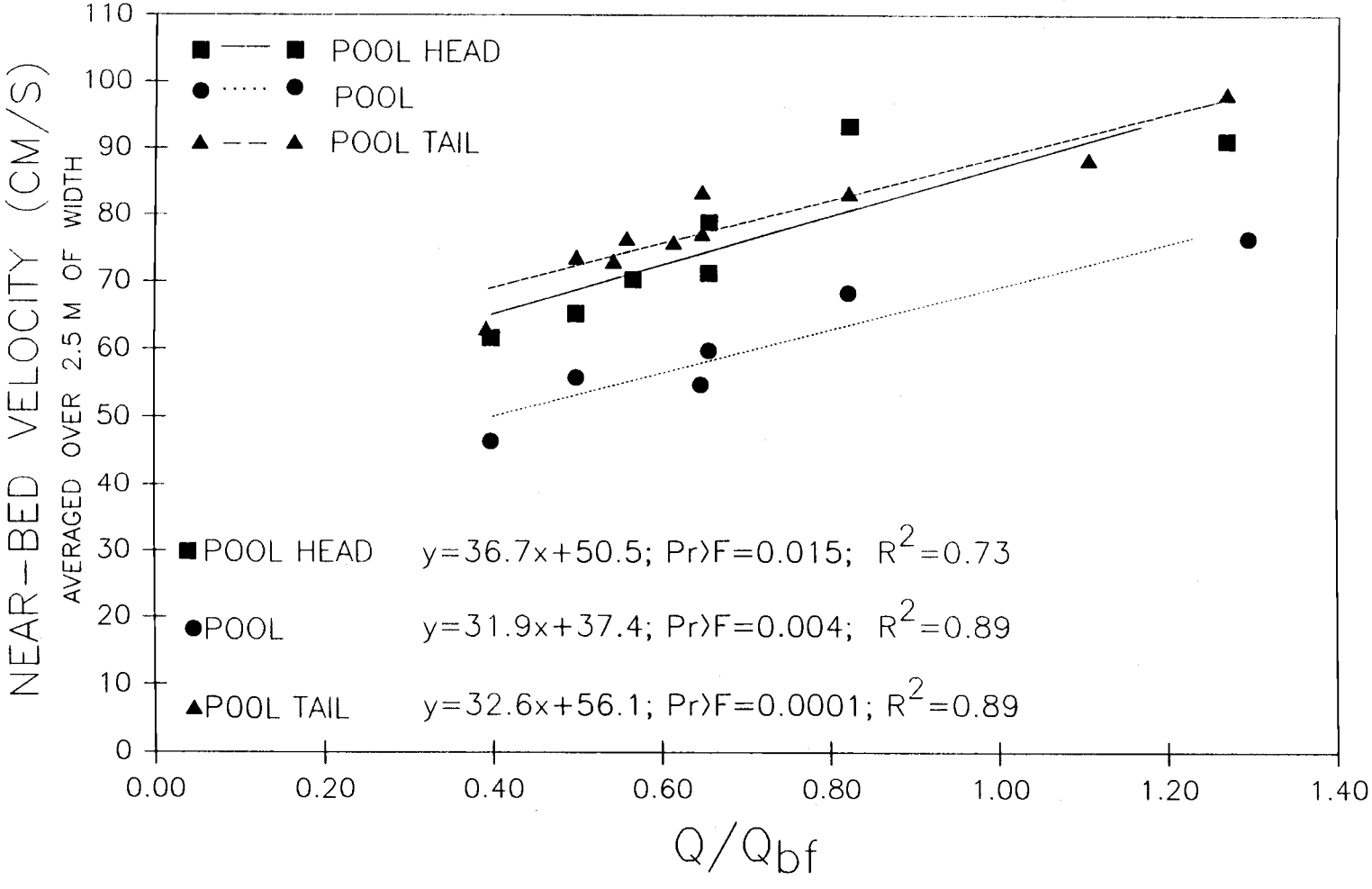

Figure 21(b). Variation in near-bed velocity with dimensionless discharge for a subset of the data. See text for explanation. Q is water discharge. Q_{bf} is bankfull discharge.

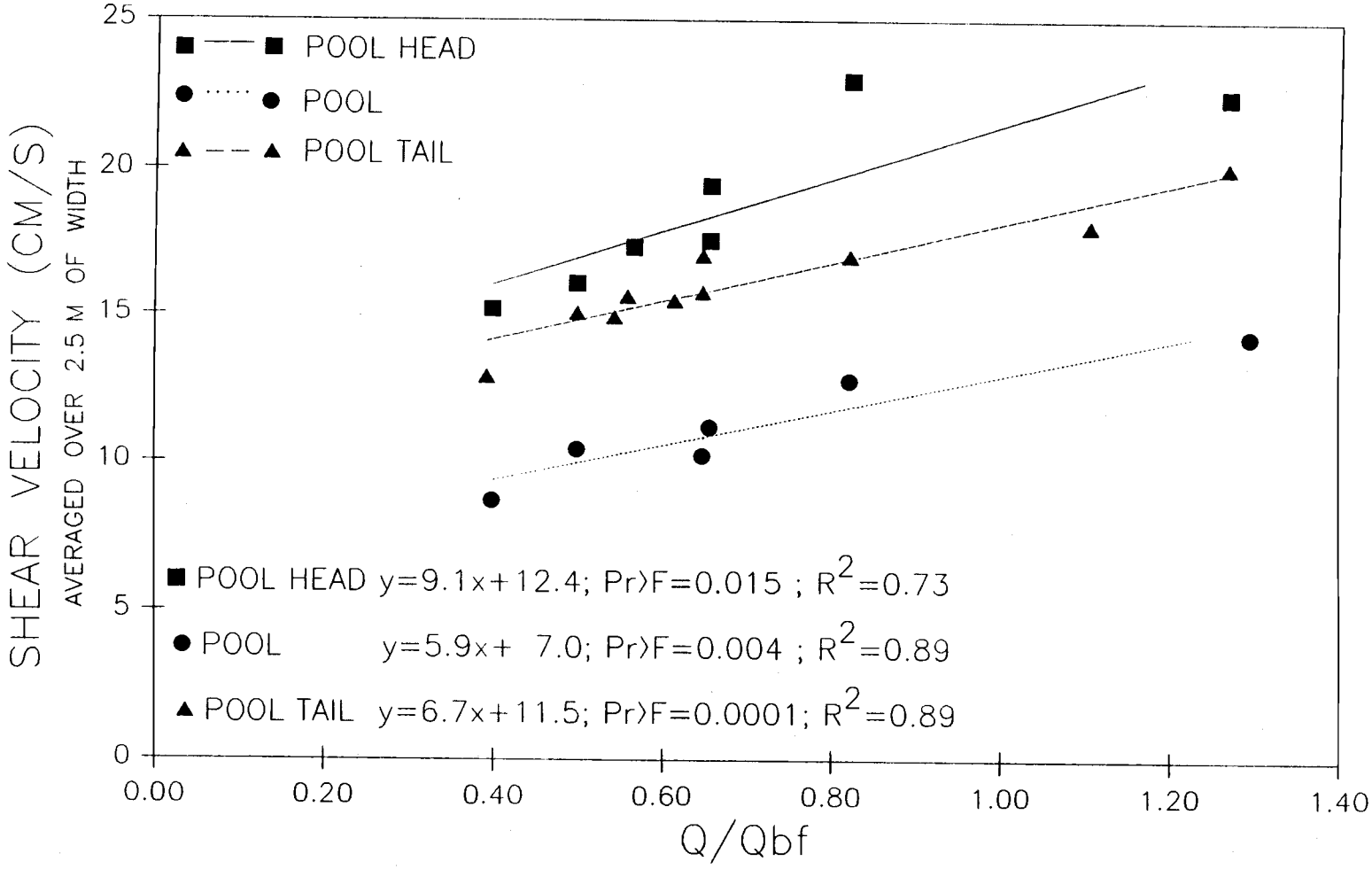

Figure 22. Variation in boundary shear velocity with dimensionless discharge. Q is water discharge. Q_{bf} is bankfull discharge.

App. E).

Thus, measurements of near-bed velocity, from which shear stress was derived, over a range of discharge demonstrated that the concept of velocity or shear stress reversal did not apply in the case examined here. Maintenance of the pool, formed by scour around a large in-channel obstruction, was attributable to processes other than shifting of the location of maximum time-averaged velocity or shear stress to pools at high discharge. Clearly, competence in the pool must at times be sufficient to transport material delivered from upstream in order to maintain pool depth. Therefore, supplemental erosive force, in addition to temporal-mean shear stress, must be accounted for in order to explain maintenance of pool morphology in this case. The only apparent source of this instantaneous lift and drag force was turbulence created by interaction of streamflow with the large obstruction.

Analogous hydraulic conditions have been described for fluvial scour around bridge piers (Melville, 1975; Breusers et al., 1977; Lisle, 1986). In pier-related scour holes, bed material is mobilized by a combination of time-averaged boundary shear stress and turbulent agitation in the scour hole (Melville, 1975; Breusers et al., 1977). Bed scour near a pier starts at average shear stresses less than those present in the absence of piers. Scouring may begin at average velocities as low as 42 percent of the non-obstruction threshold (Tison, 1961; Carstens, 1966; Breusers et al., 1977). This difference in magnitude of scouring threshold could easily compensate for the differences in velocity and shear stress between the pool and the other two stations at the present study site (Fig. 21, 22). Therefore, with the addition of instantaneous turbulent forces induced by the obstruction, sediment transporting ability in the pool could be expected to equal or exceed that at the pool head or tail. This would allow pool morphology to be formed initially and maintained thereafter. The idea of a total erosive force composed of a combination of temporal-mean shear stress and obstruction-enhanced instantaneous turbulent velocity fluctuations in the pool is a major component of the "turbulent scour" model of pool

maintenance developed in this study.

Stream Bed Scour and Fill

Scour and fill of the channel bed were measured to identify changes in channel morphology attributable to the LWD obstruction. Scour and fill also have important implications for the routing of bedload. Areas of scour provide sources of bedload, and areas of fill are storage sites. If the volume of bedload exported from a pool during a storm flow is much greater than the volume scoured, then other, upstream sites of sediment storage or delivery are required to explain the high level of responsiveness of sediment transport rate to discharge. Furthermore, magnitude of scour and fill determine the stability of the bed, which is critical to successful spawning by anadromous salmonids. Excavation of spawning sites or burial by fine sediment can decrease spawning success (Everest et al., 1987).

The maximum recorded flow during the 1984-85 storm season (September 1984 through May 1985) and until February 12 of the 1985-86 storm season, was 3.37 m3/s (0.93 Q_{bf}) on February 3, 1986 (Fig. 23, day 764). Dates in Figures 23, 25, and 34 are listed, for convenience, as sequential numbers beginning with January 1, 1984 as day 1. All occurrences of discharge exceeding 0.5 Q_{bf} during this study are listed in Appendix F. Detailed soundings of the central portion of the channel at the three sampling stations are presented in Appendix G.

Pool Cross Section

The most striking morphologic characteristic of the pool was the lack of major scour or fill in spite of the magnitude of sediment-transporting flows during the study. Minor scour and fill did occur however. Fine-grained sediment (sand-size and smaller) and

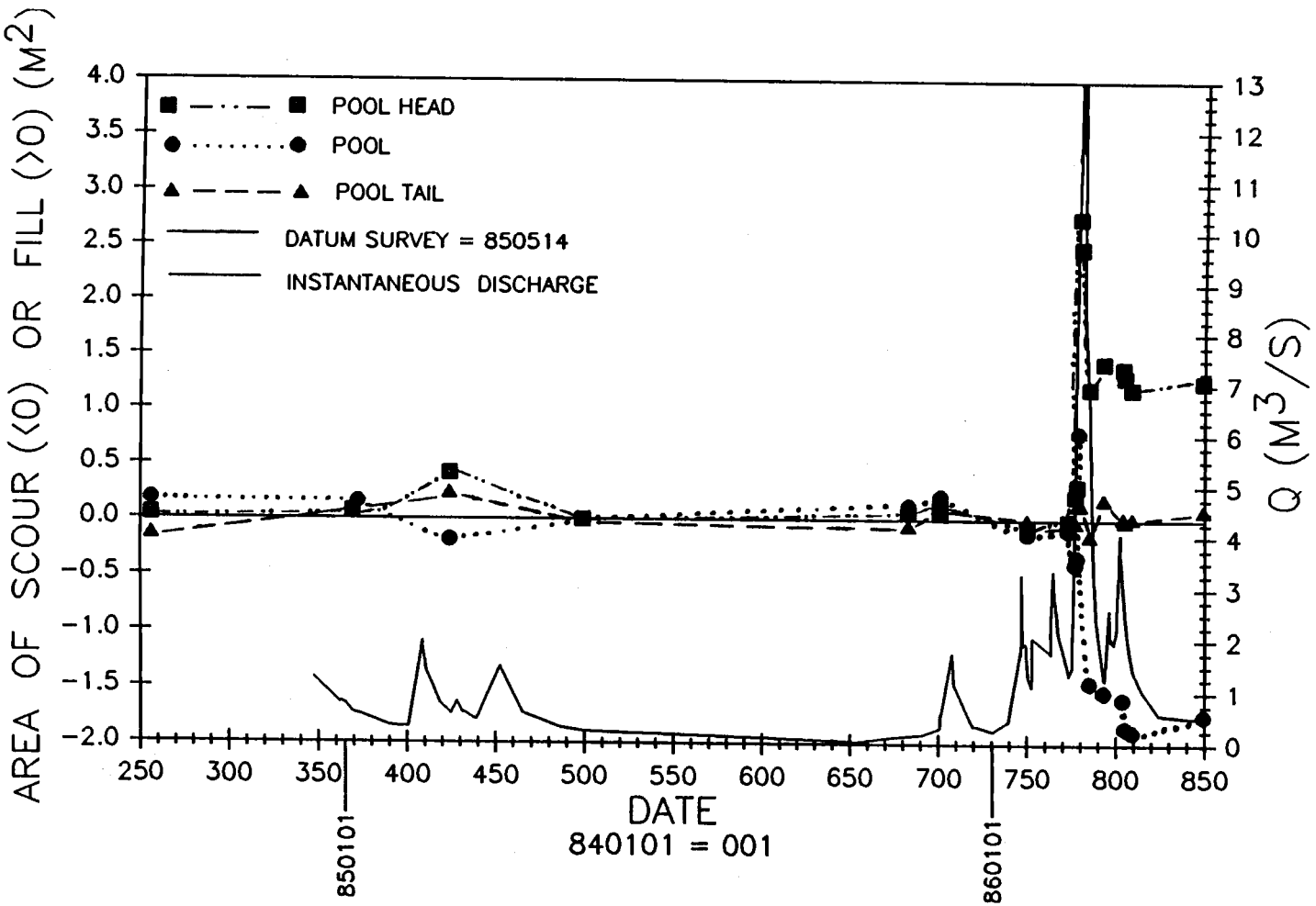

Figure 23. Cross-sectional area of stream bed scour (-) and fill (+). Discharge (Q) is also shown. Datum (0.0) is the 850514 survey. Dates are shown as sequential numbers beginning with January 1, 1984 as day 1.

organic material accumulated on the left side of the pool, away from the obstruction, during periods of low flow and scoured readily during moderate-magnitude storms.

For example, on September 13, 1984 (day 256) volume of fill was 108% of the 850514 datum total pool volume (14.5 m^3) (Fig. 23). Estimates of change in pool volume were made with the assumption that the percentage change in cross-sectional area shown in Figure 23 was constant for the total pool length. By February 28 (day 424), scour on the left side of the pool removed this fill plus an additional 8% of the datum fill volume (Fig. 23, App. G). The largest storm recorded during this period of scour peaked on February 12 (day 408) at 0.55 Q_{bf} (Fig. 23), resulting in a sharp increase in boundary shear stress on the left side of the pool (Fig. 19). Between February 28 and May 14 (day 499), as discharge returned to a low level, the pool filled to the datum volume (Fig. 23).

This scour at the pool contrasted with the pool head and tail, which filled slightly during the period that included the small storm on February 12 then scoured during later receding flows following the February 12 and March 28 (day 452) storms (Fig. 23). Scouring of fines from the pool was noted again during the December 8, 1985 (day 707) storm, which had a discharge of 0.50 Q_{bf} (Fig. 23). Inspection of the scour chains indicated that no observable scour or fill occurred beyond this area of fines at the left side of the pool.

During the 1985-86 storm season, maximum scour for the reach was on the left side of the pool. Scour chain 4-1 indicated an initial scour of 25 cm (Fig. 4, Table 2), deep enough to destroy salmonid redds (Everest et al., 1981). This scour was followed by 32 cm of fill at the downstream end of a left-bank lateral bar, leaving a net fill of 7 cm for the season (Fig. 4, Table 2). Cross-channel means of scour chain data were not particularly meaningful, because sample size was small and variance was large. In most cases these means were not significantly different from 0. These data are useful, however, as an indication of local maximum scour and net fill over the 1985-86 storm season.

TABLE 2. SCOUR CHAIN DATA. Chains were installed in July 1985 and recovered in September 1986.

CHAIN NUMBER	SCOUR (cm)	FILL (cm)	NET CHANGE (cm)
1-1	15	37	+22
1-2	2	14	+12
1-3	0	6	+6
1-4	0	21	+21
2-1	2	30	+28
2-2	0	11	+11
2-3	0	10	+10
2-4	7	14	+7
3-1	0	7	+7
3-2	8	6	-2
3-3		NOT RECOVERED	
4-1	25	32	+7
4-2	8	9	+1
4-3	23	15	-8
5-1	2	6	+4
5-2	0	31	+31
5-3	8	18	+10
6-1	25	8	-17
6-2	0	19	+19
6-3	0	18	+18
7-1	1	18	+17
7-2	16	1	-15
7-3	4	15	+11

Through the entire study reach, minor changes during the early part of the 1985-86 storm season (Fig. 24) were overwhelmed by changes resulting from a series of high flow events beginning on February 15 (day 776, Fig. 23, 25). A series of large-magnitude rain storms during this time period began on February 12 (day 773, Fig. 5). Flow exceeded bankfull discharge at 1530 hours on February 15 (day 776) and remained above bankfull until February 26 (day 787) in response to 589 mm of rain during the 12 day period (Fig. 5, 25).

The series of high-flow events beginning on February 15 resulted in obvious changes in the bed profile at the pool cross section (Fig. 25, 26). Maximum scour, disregarding severe bank erosion between days 780 and 785, was 17% of the pool volume relative to the 850514 datum. This was measured on February 16 (day 777). By February 18, growth of the downstream end of the left-bank lateral bar was apparent on the left side of the pool (Fig. 25, 26). This was the maximum fill measured during the study, equivalent to 35% of the pool volume. Other changes were relatively minor (Fig. 26).

Between February 18 (day 779) and March 4 (day 793), on the left side of the channel, as much as 35 cm of the newly-deposited sediment was scoured (Fig. 25, 26, 27). Receding flows on the right side of the channel were deflected toward the right by the large obstruction, causing dramatic lateral erosion of nearly 2 m of the right bank between February 18 and March 4 (Fig. 25, 26, 27). By March 4, the bed profile in the center portion of the channel returned to nearly the May 1985 level (Fig. 27).

Pool Head and Pool Tail Cross Sections

By far the largest-magnitude scour and fill events at the pool head and pool tail resulted from growth and scour of two lateral bars during the series of large storms in February 1986. Deposition was localized at the bars rather than distributed uniformly across the channel. Location of these bars was fixed by hydraulic conditions strongly

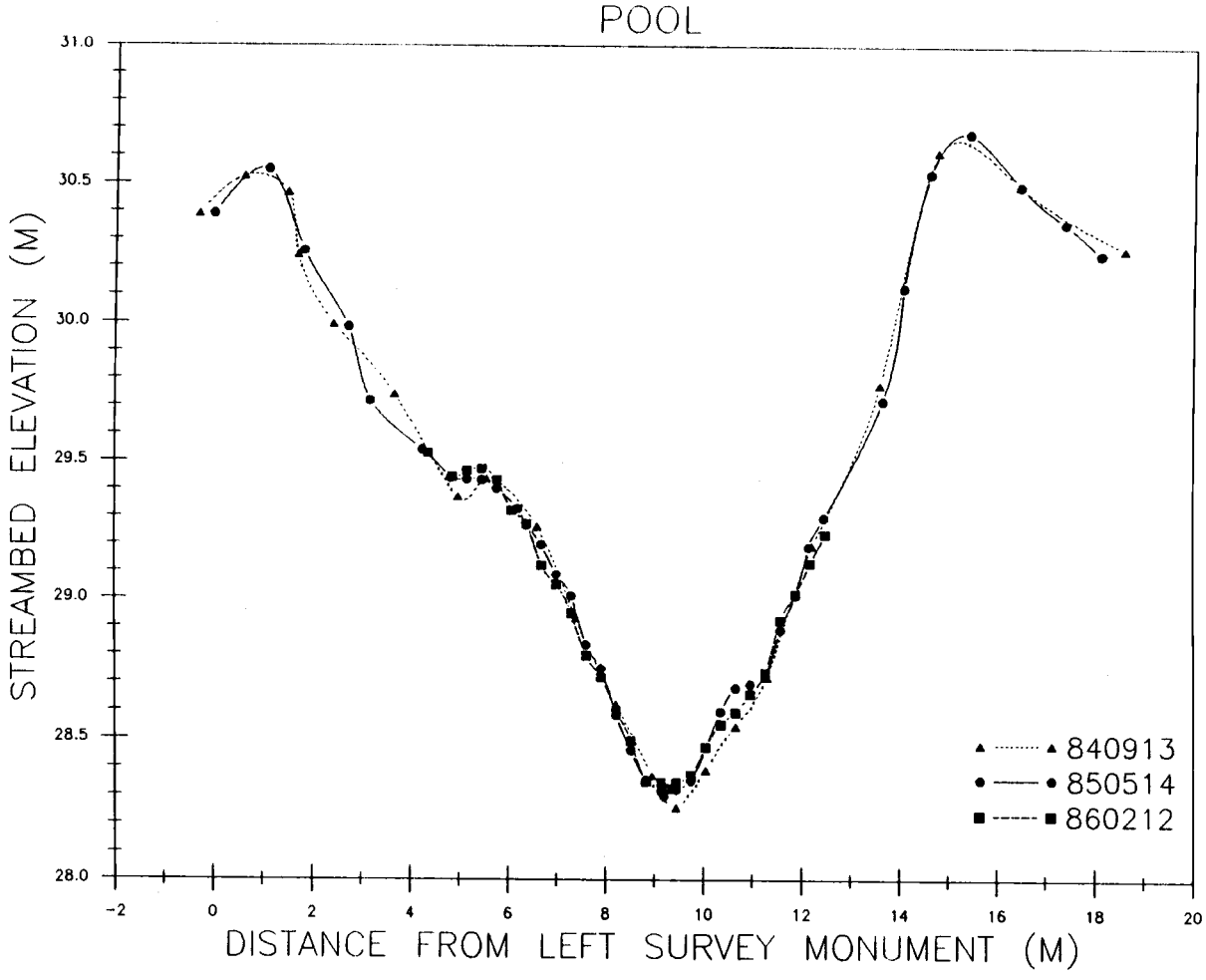

Figure 24. Cross-sectional soundings. Elevation is relative to an arbitrary datum.

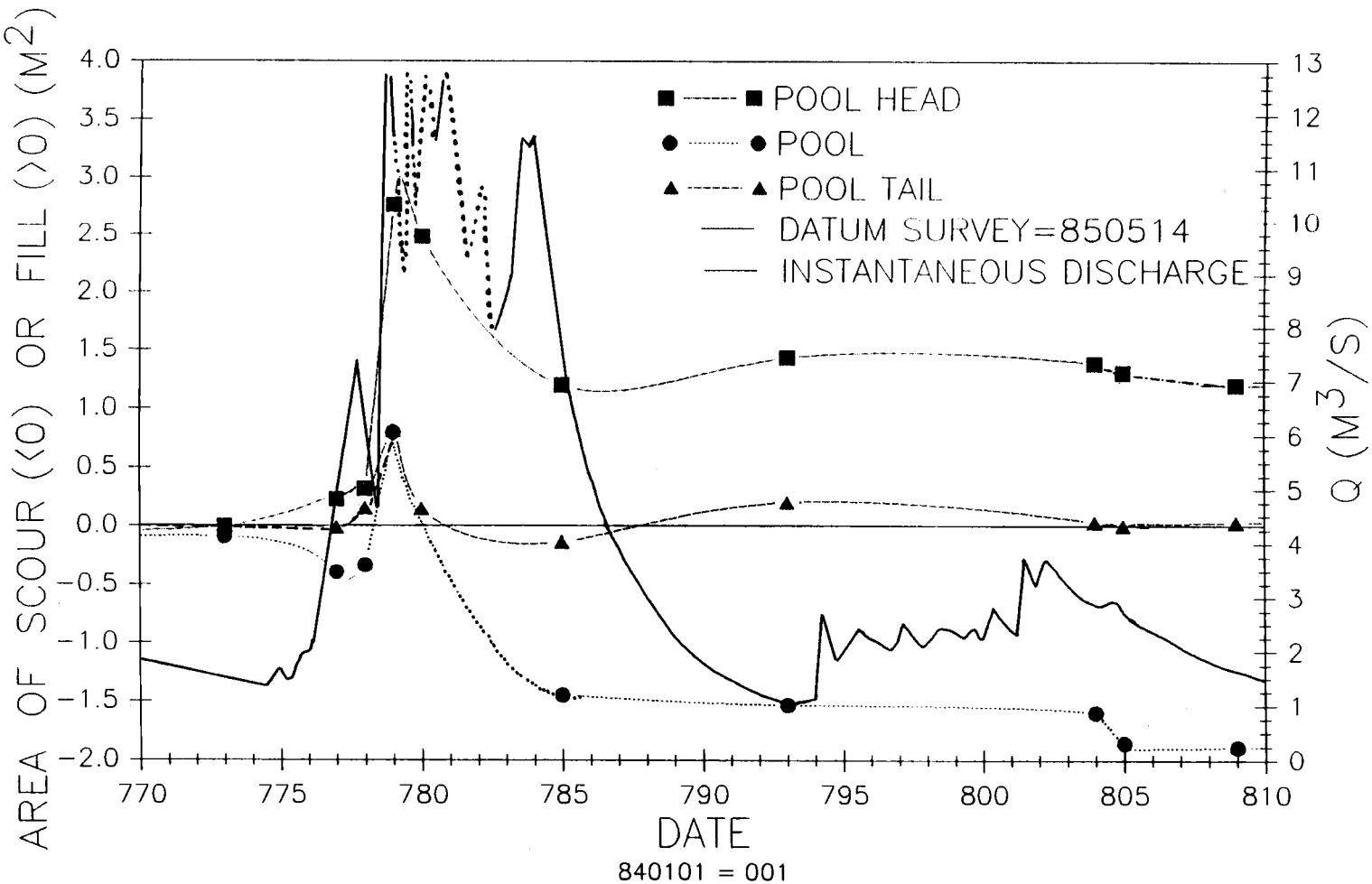

Figure 25. Cross-sectional area of stream bed scour (-) and fill (+). Discharge (Q) is also shown. Dates are shown as sequential numbers beginning with January 1, 1984 as day 1. Datum (0.0) is the 850514 survey.

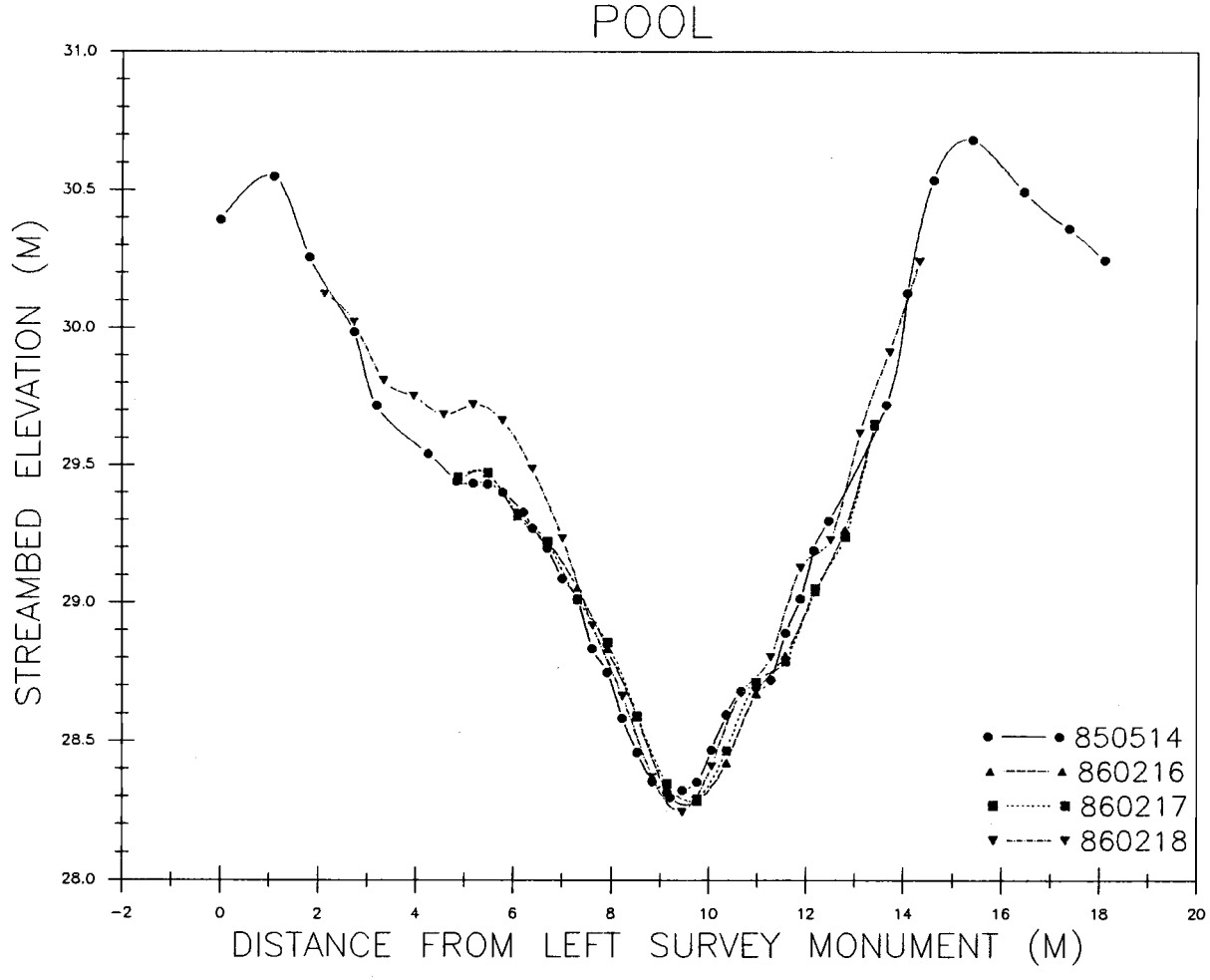

Figure 26. Cross-sectional soundings. Elevation is relative to an arbitrary datum.

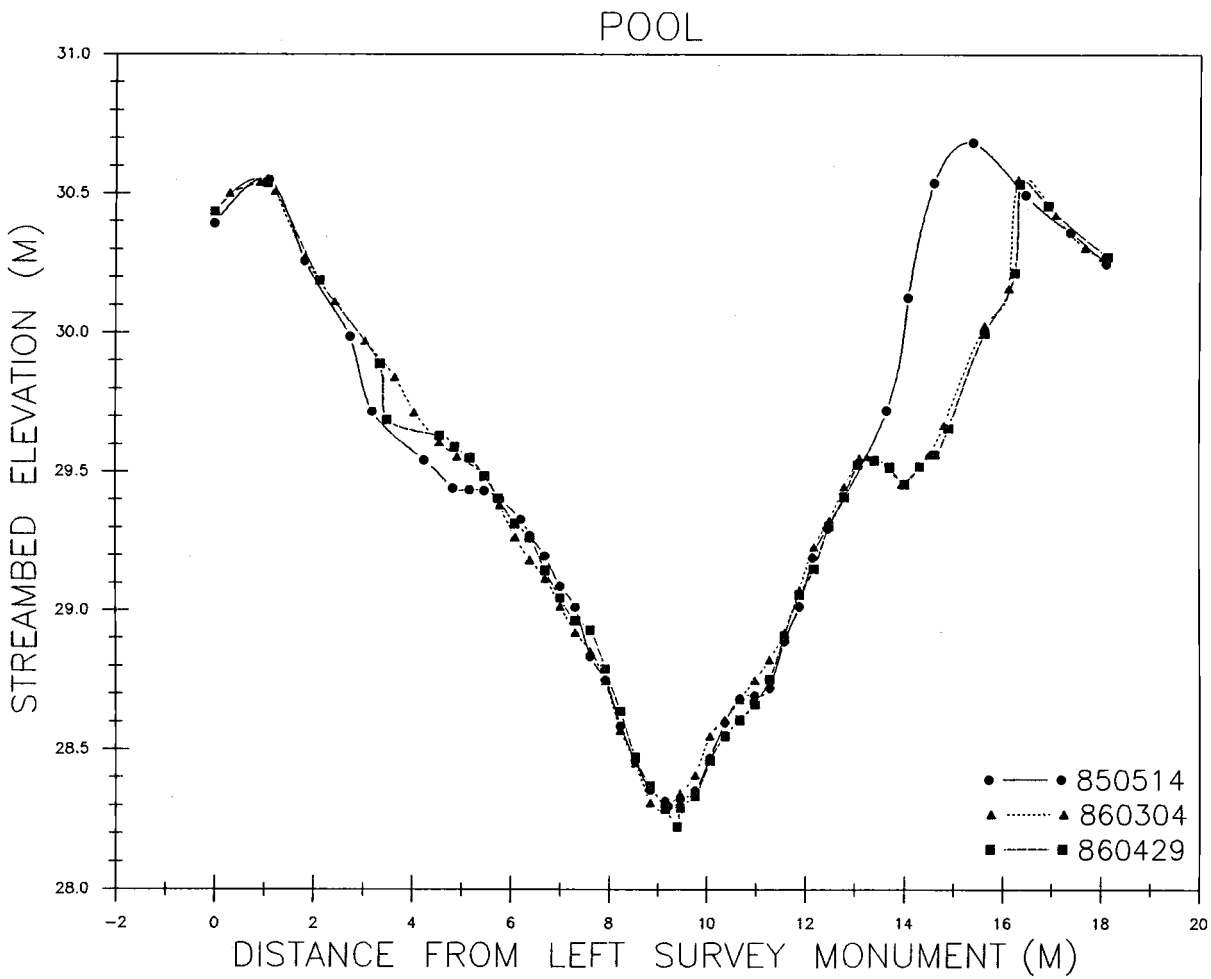

Figure 27. Cross-sectional soundings. Elevation is relative to an arbitrary datum.

influenced by the LWD obstruction.

During the period preceding February 13, 1986 (day 774), scour and fill was relatively minor in spite of the occurrence, on two occasions, of flows in excess of 0.90 Q_{bf}. Scour and fill occurred at various places along the cross sections, but changes in the bed surface elevation were limited to less than 10 cm vertically over less than 2 m of channel width (Fig. 23, 28, 29).

At the pool head, response to the large February storms was relatively minor through February 17 (day 778), reflecting some enlargement of the left-bank lateral bar (Fig. 25, 30). By February 18 (day 779), following the storm peak, dramatic enlargement of this bar was evident. As much as 60 cm of fill occurred over a 10 m span on the left side and center of the channel (Fig. 25, 30). Bar growth displaced the thalweg 30 cm to the right and 20 cm higher than its former location and refilled previous scour on the right side of the channel (Fig. 30). By the next day, receding flows scoured up to 15 cm of the new fill across most of the channel, while up to 28 cm of sediment were deposited on the extreme left side (Fig. 25, 30). Scour chain 1-1 recorded 37 cm of fill in the area of the bar. This fill followed 15 cm of scour, leaving a net fill of 22 cm for the season (Table 2, Fig. 4). Growth of the bar at the left side and center of the channel directed flow against the right bank, causing as much as 28 cm of lateral erosion and displacing the thalweg more than 1 m to the right by February 19 (Fig. 30).

Between February 19 and March 4 (day 793), a period dominated by receding flows, maximum thickness of the newly-deposited bar was markedly reduced (Fig. 25, 30, 31). The left side of the channel was degrading and the right side aggrading toward the May 1985 level, however bar deposition at the far left remained largely unchanged (Fig. 25, 30, 31). Between March 4 and March 15 (day 804), as much as 6 cm of scour and 15 cm of fill occurred locally, but little net change occurred for the remainder of the storm season (Fig. 25, 31).

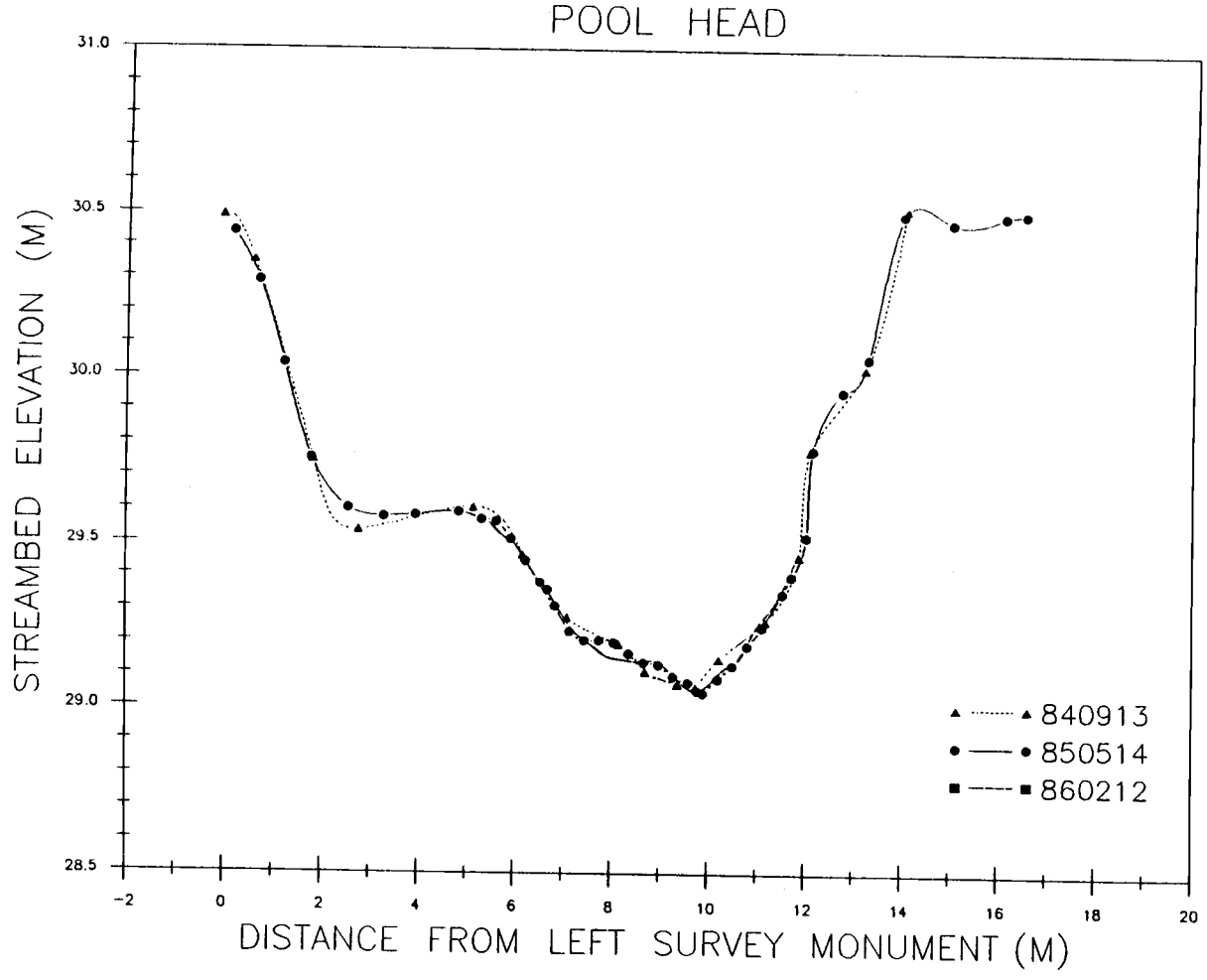

Figure 28. Cross-sectional soundings. Elevation is relative to an arbitrary datum.

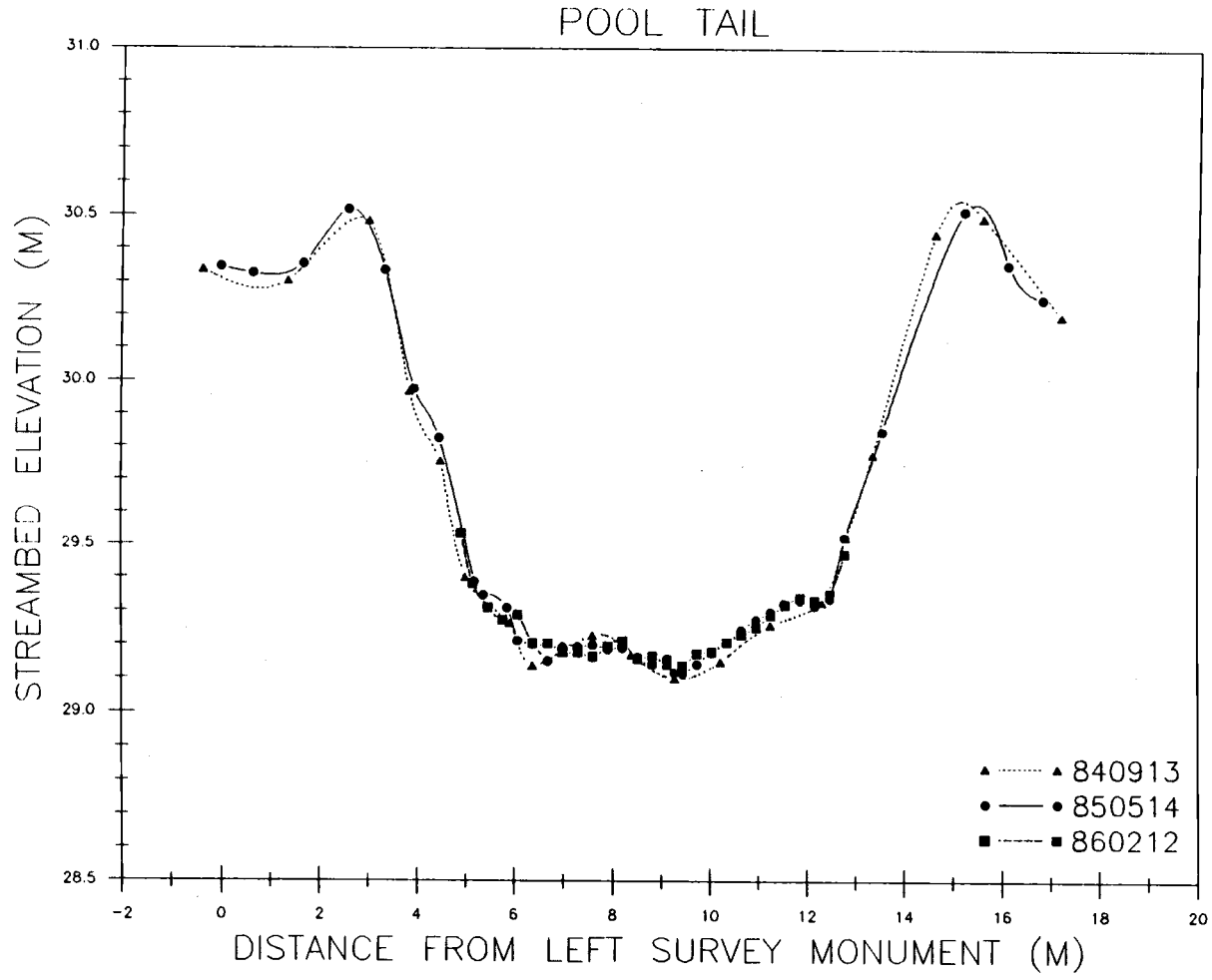

Figure 29. Cross-sectional soundings. Elevation is relative to an arbitrary datum.

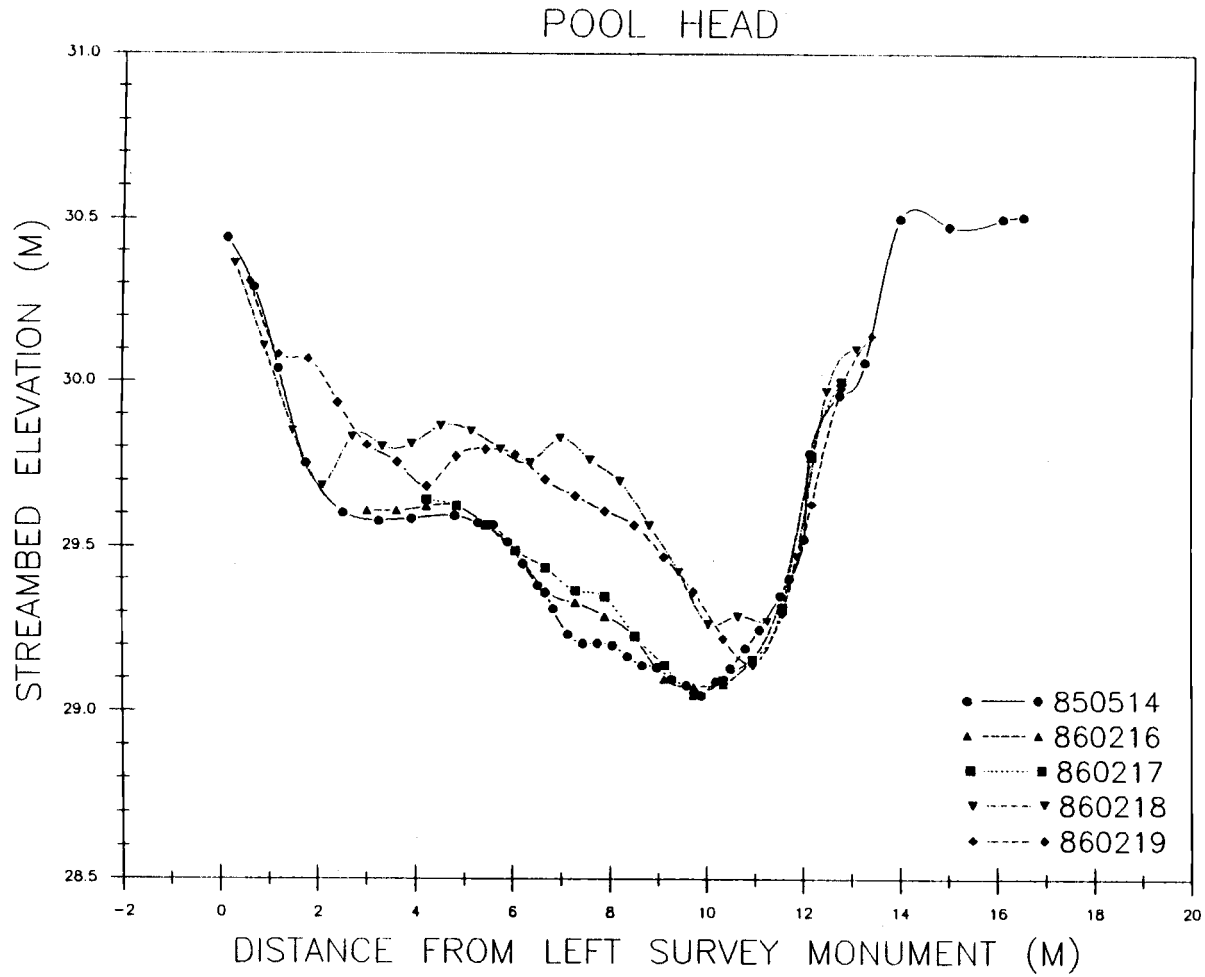

Figure 30. Cross-sectional soundings. Elevation is relative to an arbitrary datum.

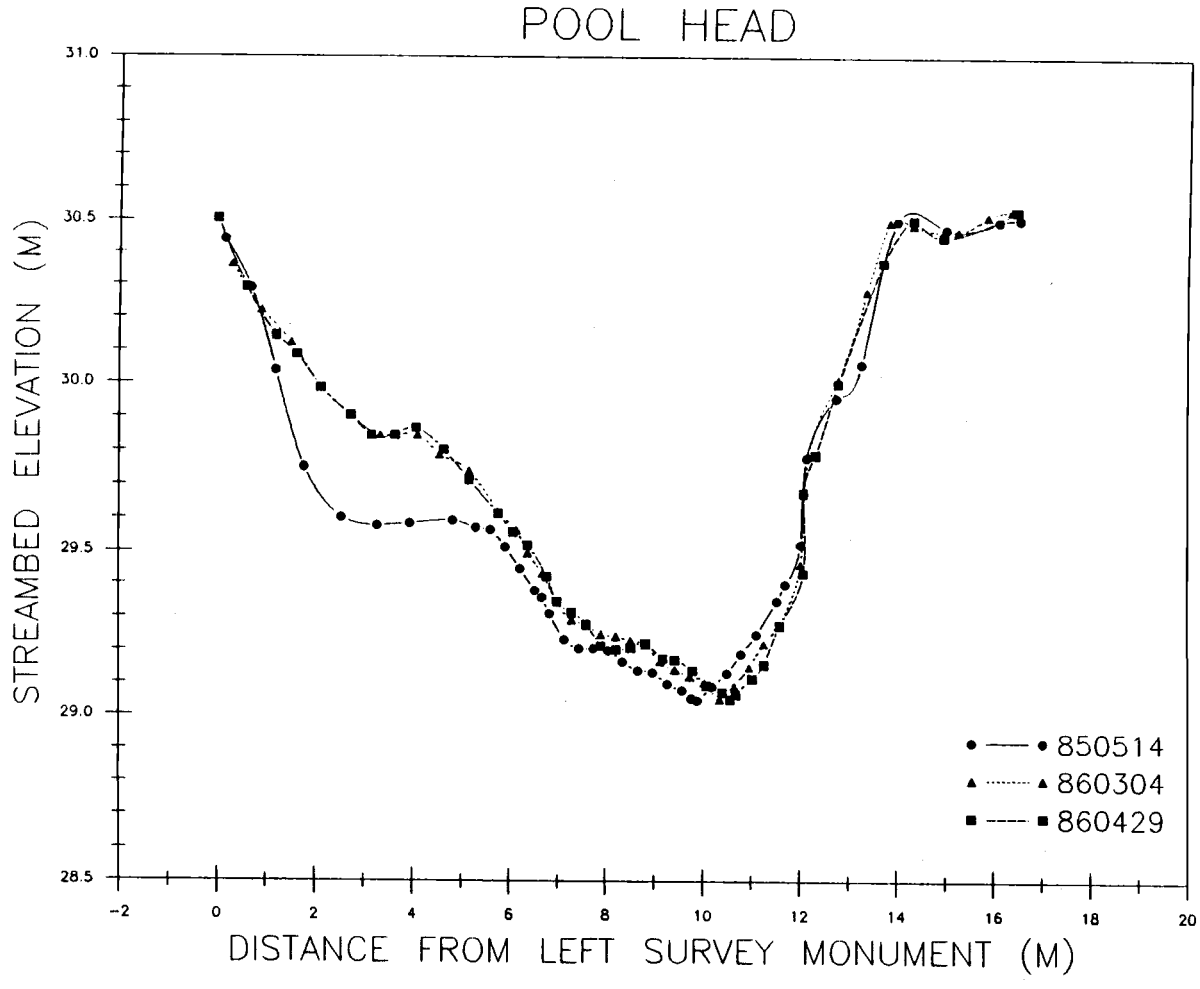

Figure 31. Cross-sectional soundings. Elevation is relative to an arbitrary datum.

At the pool tail, growth of the right-bank lateral bar in the lee of the obstruction was apparent in the February 17 survey (Fig. 32). By February 18, as much as an additional 26 cm had been deposited (Fig. 25, 32). Approximately one-half of this fill was scoured by the time of the February 19 survey (Fig. 25, 32). Flow deflected by the enlarged right-bank lateral bar scoured a new thalweg to a depth 12 cm below the May 14, 1985 level on the far left side of the channel (Fig. 32).

Major bed morphology changes occurred during receding flows between February 19 and March 4 (day 793). Growth of the right-bank lateral bar was evident between 8.5 m and 11.5 m on the cross section (Fig. 32, 33). Major scouring occurred immediately to the left of the new bar, across 3.4 m of channel, centered on the new location of the thalweg. This scour deepened the channel by more than 20 cm relative to the May 1985 level (Fig. 25, 32, 33). Only slight change occurred for the remainder of the storm season (Fig. 23, 33).

Scour chain 6-1 indicated a net scour of 17 cm for the season in the area where flow was constricted by the enlarged right-bank lateral bar in the lee of the obstruction (Table 2, Fig. 4). Chains 5-2, 5-3, 6-2, 6-3, and 7-3 all showed large amounts of fill, indicating growth of this bar (Table 2, Fig. 4).

Patterns of scour and fill through the study reach did not always conform with the shear stress reversal model, which calls for systematic filling of pools at discharge less than bankfull and scour at higher flows. Likewise, the pool head and tail did not necessarily fill at discharges above bankfull and scour at lower flow as predicted by the shear stress reversal model. Sand-size and smaller sediment did accumulate in the pool during low-flow periods, but this was scoured by moderate-discharge flows and commonly accounted for less than 5% of the pool cross-sectional area (App G). Maximum scour and fill in the pool were 17% and 35% respectively of the datum pool volume, disregarding severe bank erosion between days 780 and 785. This maximum scour and fill reflected the effects of a storm of approximately 5-year return interval.

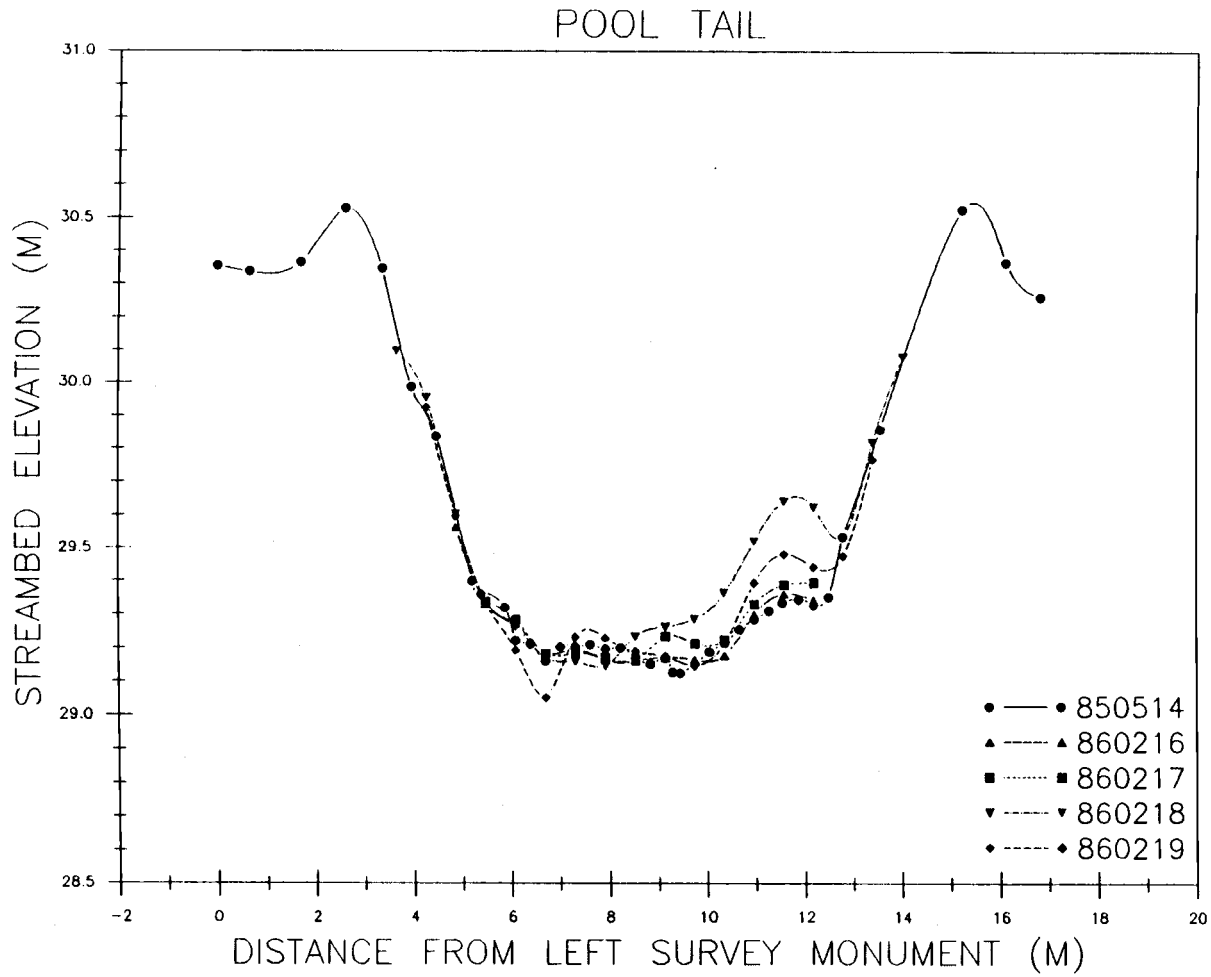

Figure 32. Cross-sectional soundings. Elevation is relative to an arbitrary datum.

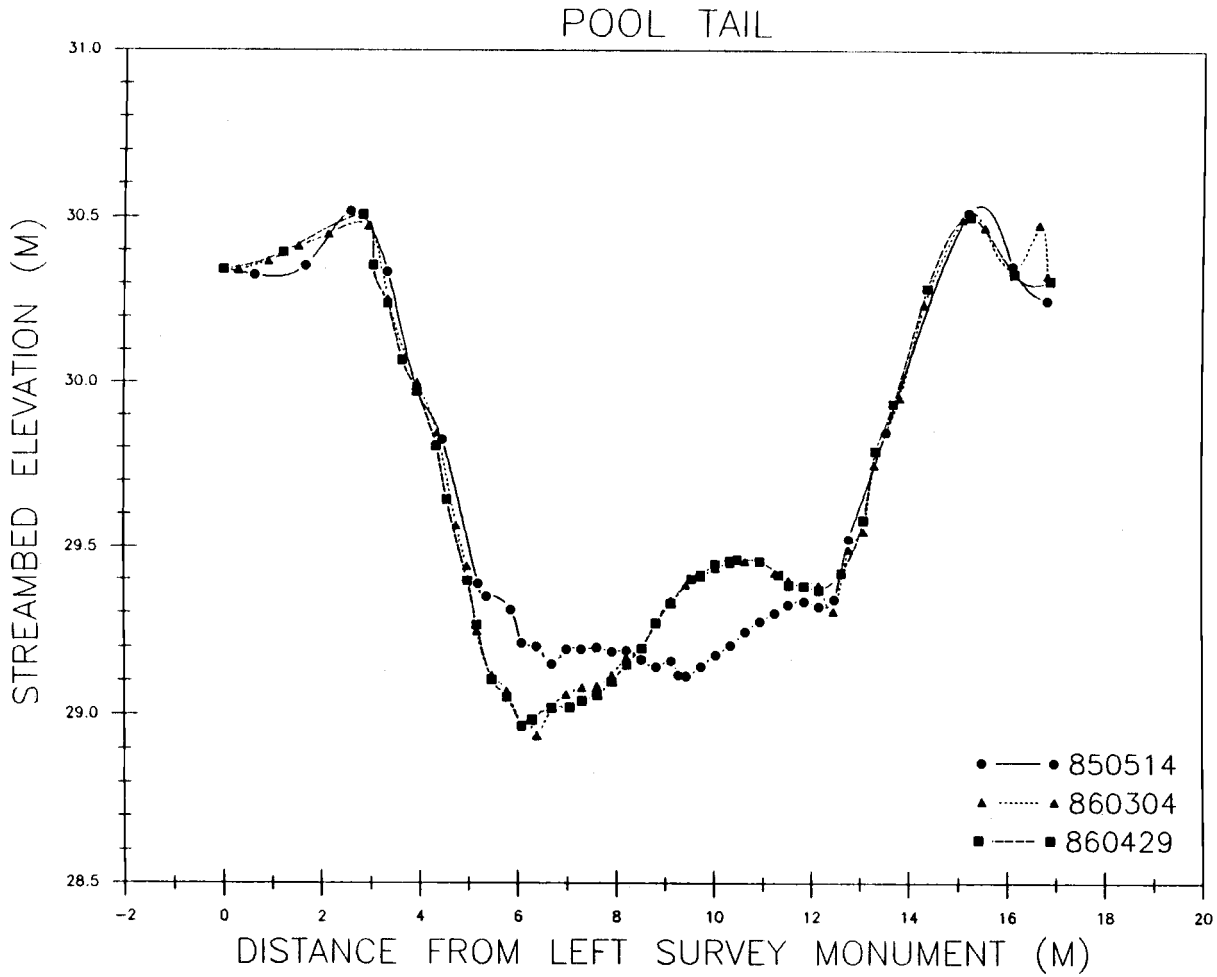

Figure 33. Cross-sectional soundings. Elevation is relative to an arbitrary datum.

A large increase in sediment supply during the first of a series of large storms appeared to dominate scour and fill throughout the study reach. The rapid growth of two lateral bars in response to increased sediment availability caused the largest-magnitude deposition at each of the three sampling stations. Much of this sediment later scoured during lower-magnitude flows, including flows well above bankfull.

Pool cross-sectional area changed remarkably little, considering the magnitude of the February 1986 storms. The combination of temporal-mean shear stress and instantaneous turbulent forces in the pool was clearly capable of transporting sediment delivered from upstream throughout the range of measured flows. The notable exception to this was deposition at the edge of the pool, opposite the LWD obstruction at the downstream end of the left-bank lateral bar, following the storm peak on February 17.

Bedload Transport

Transport rate of bedload was measured in order to investigate effects of the LWD obstruction on relative rate and timing of transport at the three sampling stations. Data are summarized in Appendix H. No bedload transport events were measured during the 1984-85 storm season because of the absence of moderate- to large-magnitude storms. During a high flow event on January 16, 1986 (day 746, Fig. 34), organic and fine inorganic material (sand-size and smaller), which had accumulated during low-flow periods, was scoured out of the left edge of the pool, exposing coarser sediment to the flow. The portion of the bedload finer than 1 mm decreased from 62% to 14% at the pool between the first (day 746) and second (day 749) sampling periods in spite of very similar discharge, reflecting removal of stored fines (Fig. 34, App. I). Breakup of fine-grained pavement by this first storm of the season may explain the sharply higher transport rate at the pool shortly after the January 16 storm (Fig. 34).

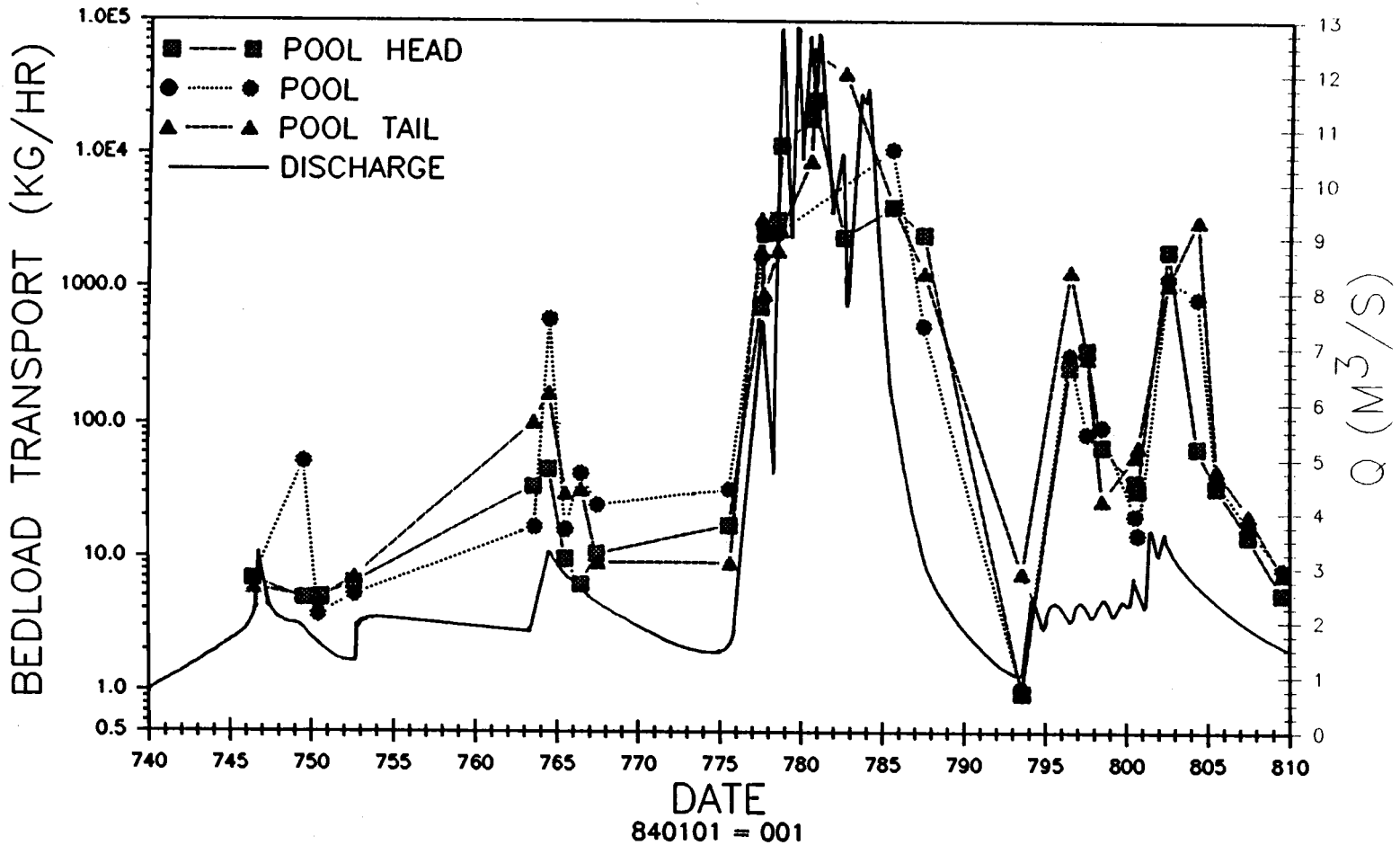

Figure 34. Variation in bedload transport rate with time and discharge (Q). Dates are shown as sequential numbers beginning with January 1, 1984 as day 1.

Transport rate at the pool occasionally exceeded the rate at the pool head and tail (for example, day 764, Fig. 34), indicating that sediment redistribution within the pool exceeded import or export. Net import or export of bedload was indicated by the ratio of transport rate at the pool tail ($Q_{bl\text{-}tail}$) to rate at the pool head ($Q_{bl\text{-}head}$). Patterns of change in this ratio were quite complex, and could not be explained simply by variation of discharge (Table 3).

Net scour of the pool ($Q_{bl\text{-}tail}/Q_{bl\text{-}head} > 1$) occurred at discharges ranging from 1.26 m^3/s to 12.93 m^3/s (0.35 Q_{bf} to 3.55 Q_{bf}), nearly the full range over which bedload was sampled (Table 3). On February 16 (day 777, Fig. 34), during rising discharge between 1.45 Q_{bf} and 1.53 Q_{bf}, bedload export out of the pool exceeded import by a factor or 4.5 (Table 3). Five hours later, following the hydrograph peak at 2.10 Q_{bf}, import exceeded export by a factor of 2.8 at a discharge of 2.03 Q_{bf} (Table 3). On February 19 (day 780) during rising discharge of approximately 3.32 Q_{bf}, rate of bedload transport into the pool was about double the rate exiting the pool (Table 3). With a small increase in discharge to 3.55 Q_{bf} 3.5 hours later, bedload transport rate increased by 37% at the pool head, but increased more than six fold at the pool tail to more than double the rate at the pool head (Table 3). As these examples illustrate, scouring or filling of the pool, as measured by bedload transport, had little relationship to timing of the storm hydrograph (Table 3). That is, scour and fill occurred during both rising and falling hydrograph limbs over the entire range of discharge sampled.

This complexity in the relationship of pool scour to discharge is contrary to the shear stress or velocity reversal hypothesis, which calls for a predictable pattern of pool scour at a threshold discharge near bankfull. $Q_{bl\text{-}tail}/Q_{bl\text{-}head}$ ratios as large as 48 clearly indicated scour of the pool on several occasions at discharges less than bankfull (Table 3). Variation in upstream sediment supply was apparently responsible for much of the variation in bedload transport rate. Incidence of mass erosion events increases during high-intensity storms, and these events are an important source of sediment to some streams (Swanston

TABLE 3. BEDLOAD FLUX. All data are for the pool tail. Q is water discharge. Q_{bf} is bankfull discharge. Q_{bl} is bedload transport rate. Subscripts t and h indicate pool tail and head respectively. Rows are arranged in order of increasing bedload export from the pool (increasing Q_{blt}/Q_{blh} ratio).

Q_{blt}/Q_{blh}	Q_{bl} (kg/hr)	Q (m^3/s)	Q/Q_{bf}	HYDROGRAPH LIMB	DATE	TIME
0.4	890	7.41	2.03	FALLING	860216	1806
0.4	27	1.98	0.54	RISING	860309	1235
0.5	8900	12.1	3.32	RISING	860219	1400
0.5	1300	3.29	0.90	FALLING	860226	1324
0.5	9.1	2.06	0.57	RISING	860214	1545
0.6	1100	3.99	1.10	FALLING	860313	1329
0.6	1900	10.6	2.93	RISING	860217	1329
0.9	5.9	1.78	0.49	RISING	860116	1221
0.9	9.2	2.18	0.60	FALLING	860206	1250
0.9	310	2.06	0.57	FALLING	860308	1411
0.9	4.8	1.32	0.36	FALLING	860120	1340
1.0	4100	5.86	1.61	FALLING	860224	1513
1.1	7.1	1.82	0.50	RISING	860122	1655
1.4	46	2.39	0.66	FALLING	860316	1253
1.4	7.5	1.45	0.40	FALLING	860320	1329
1.4	21	1.83	0.50	FALLING	860318	1205
1.6	58	2.21	0.61	FALLING	860311	1301
2.1	69	2.48	0.68	FALLING	860311	1729
2.2	56000	12.9	3.55	RISING	860219	1717
3.0	100	2.43	0.67	RISING	860202	1435
3.1	30	2.85	0.78	FALLING	860204	1335
3.6	170	3.23	0.89	PEAK	860203	1256
4.5	3200	5.56	1.53	RISING	860216	1320
5.1	1300	2.49	0.68	FALLING	860307	1241
5.2	32	2.60	0.71	FALLING	860205	1245
7.9	7.7	1.26	0.35	FALLING	860304	1402
17.4	41000	7.78	2.14	RISING	860221	1452
47.7	3200	2.88	0.79	FALLING	860315	0855

and Swanson, 1976; Swanson et al., 1987). In addition, new sediment sources are accessed by the stream as the wetted channel area increases during storms (Beschta, 1987).

The pool did not store important volumes of sediment relative to the volume transported as bedload. Estimated volume of the pool was 14.5 m^3, providing a potential storage site for a maximum of 34,000 kg of bedload, assuming a maximum dry density for closely-packed silty sand and gravel of 2,360 kg/m^3 (Holtz and Kovacs, 1981, p. 105). The maximum fill in the pool, in excess of the 850514 arbitrary datum, was 35% of the pool volume, deposited during 16 hours on February 17 and 18 (days 778 and 779; Fig. 23, 25). During this same period, 84,000 kg of bedload, the equivalent of 250% of the pool volume and 700% of the volume of fill, was exported from the pool. Even this maximum volume of fill did not significantly change pool depth. Deposition occurred on the left edge of the pool, away from the obstruction and the thalweg.

Maximum scour, disregarding severe bank erosion between days 780 and 785, occurred between February 12 and 16 (days 773 and 777) and was 17% of the pool volume. During this same period, 38,000 kg of bedload was exported from the pool, equivalent to 110% of the pool volume and 660% of the volume of scour. Clearly, upstream sources supplied much more bedload than was stored in the pool during low-flow periods.

Following the series of very high flows from February 16 (day 777) through 23 (day 784), bedload transport rate appeared to be more responsive to changes in discharge than prior to the storms (Fig. 34). A rapid increase in discharge on March 4 (day 793) followed by several small discharge peaks between March 4 and 7 (day 796) resulted in a sharp increase in bedload transport rate at all three stations (Fig. 34). On March 7 at a discharge of 2.6 m^3/s, bedload transport rate had increased above March 4 rates by orders of magnitude (Fig. 34). A similar response occurred following two discharge peaks slightly exceeding bankfull on March 12 (day 801) and March 13 (day 802). Bedload transport rate increased more than an order of magnitude over the preceding rate on March 11 (Fig. 34).

Rapid decreases in transport rate in the absence of large changes in discharge were also noted, again indicating that sediment supply was an important variable influencing transport rate. Bedload transport rate fell sharply between days 796 and 798 in spite of fairly constant discharge through the period.

The apparent increased responsiveness of transport rate to small changes in discharge may have been caused by deposition of a large quantity of easily mobilized sediment by rapidly receding flows between days 784 and 793 (Fig. 34). The previous, large-magnitude storms disrupted the pavement layer of the channel bed and deposited gravel with poorly-developed pavement as discharge fell. These recent deposits were easily mobilized by subsequent storm flows on days 794 and 795 (Fig. 34). After the most readily-mobilized material was removed, transport rates fell even though discharge remained fairly constant. Subsequent increases in discharge on days 800 and 801 accessed additional new deposits and transport rate increased sharply again (Fig. 34).

Response of Bedload Transport Rate to Hydraulic Variables

Total bedload transport rate increased with increasing discharge at all stations (Fig. 35). Analysis of covariance indicated that this relation was not significantly different for any of the stations (App. J). Steep, obstruction-affected, gravel-bed streams vary widely in particle size distribution, sediment supply, character of the pavement layer, channel geometry, storm runoff response, and role of structural features such as LWD (Vanoni, 1977, pp.94; Klingeman and Emmett, 1982; Richards, 1982, pp. 111-112; White and Day, 1982; Beschta, 1983; Reid et al., 1985; Beschta, 1987; Kuhnle and Southard, 1988; Sidle, 1988). Therefore, the large amount of data scatter shown in Figure 35 is to be expected in bedload transport relationships.

Bedload transport rate was high relative to rates reported for other small, gravel-bed streams in the Oregon Coast Range and in southeast Alaska (Fig. 36, Table 4). This was

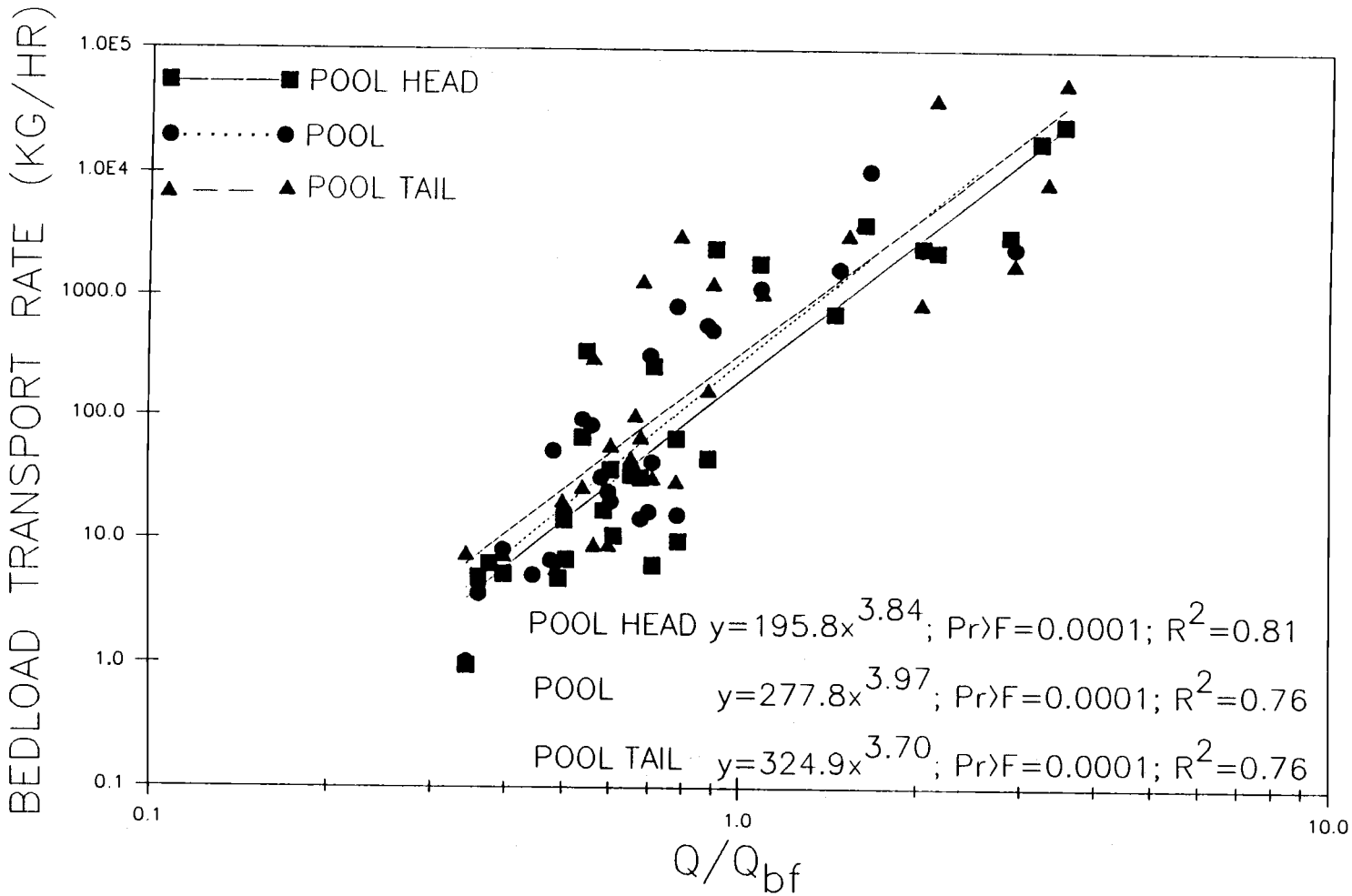

Figure 35. Variation in bedload transport rate with dimensionless discharge. Q_{bf} is bankfull discharge.

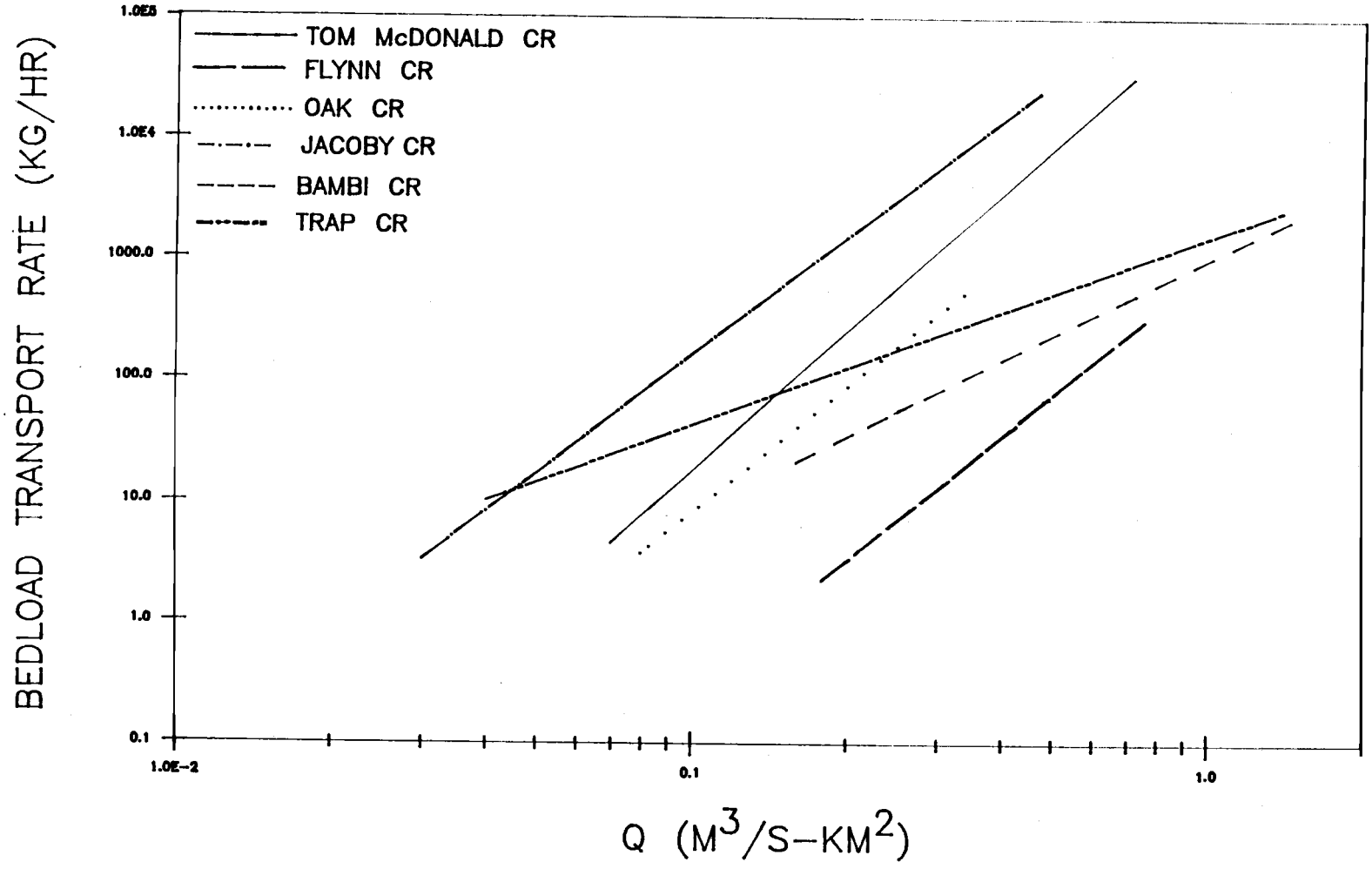

Figure 36. Comparison of the bedload transport rate-discharge (Q) relationship for six small, gravel-bed streams in forested environments.

TABLE 4. CHARACTERISTICS OF SITES FOR COMPARISON OF BEDLOAD TRANSPORT RATE FOR DATA SHOWN IN FIGURE 36.

STREAM	LOCATION	DRAINAGE AREA (km^2)	DATA SOURCE
Tom McDonald Creek	North-coastal California	18.0	This report
Jacoby Creek	North-coastal California	36	Lisle, personal communication
Flynn Creek	Oregon Coast Range	2.2	Beschta et al., 1981
Oak Creek	Oregon Coast Range	7.5	Beschta et al., 1981
Bambi Creek	Southeast Alaska	1.5	Sidle, 1988
Trap Creek	Southeast Alaska	14	Estep and Beschta, 1985

consistent with regionally high erosion rates in north-coastal California (Judson and Ritter, 1964; Madej and Kelsey, 1981; Nolan and Janda, 1981).

Bedload transport rate clearly increased as a function of the temporal-mean boundary shear stress (Fig. 37). Rate of increase in transport rate with shear stress was not significantly different at any of the three stations; however intercepts, and therefore magnitudes, were all significantly different from the other stations (App. K).

Bedload transport relationships are commonly stated in terms of stream power. Stream power per unit bed area (W) is the power available to transport sediment load and is equivalent to $\tau_b U$, where τ_b is the temporal-mean boundary shear stress and U is the average water velocity (Bagnold, 1954, 1973, 1977; Middleton and Southard, 1984, p. 284). Average values of stream power were calculated for 2.5 m of the channel width, spanning the zone of shear stress maximum.

The relationship of bedload transport rate to stream power was similar to the relationship to shear stress (Fig. 38). Rate of increase of bedload transport rate with increasing stream power was not significantly different for the three stations, although magnitude was different (App. L).

In spite of significantly lower boundary shear stress and stream power in the pool, the range of bedload transport rate in the pool was similar to the range at the pool head and tail (Fig. 35). This indicated that the instantaneous turbulent forces in the pool were supplementing time-averaged shear stress and stream power to drive bedload transport rate.

In general, high discharge was associated with high bedload transport rates (Fig. 34, 35); instantaneous rates were commonly more complex however. Peaks in bedload rate tended to occur after streamflow had peaked, and bedload transport commonly was greater on the falling limb of a storm hydrograph than at the same discharge on the rising limb (Fig. 34).

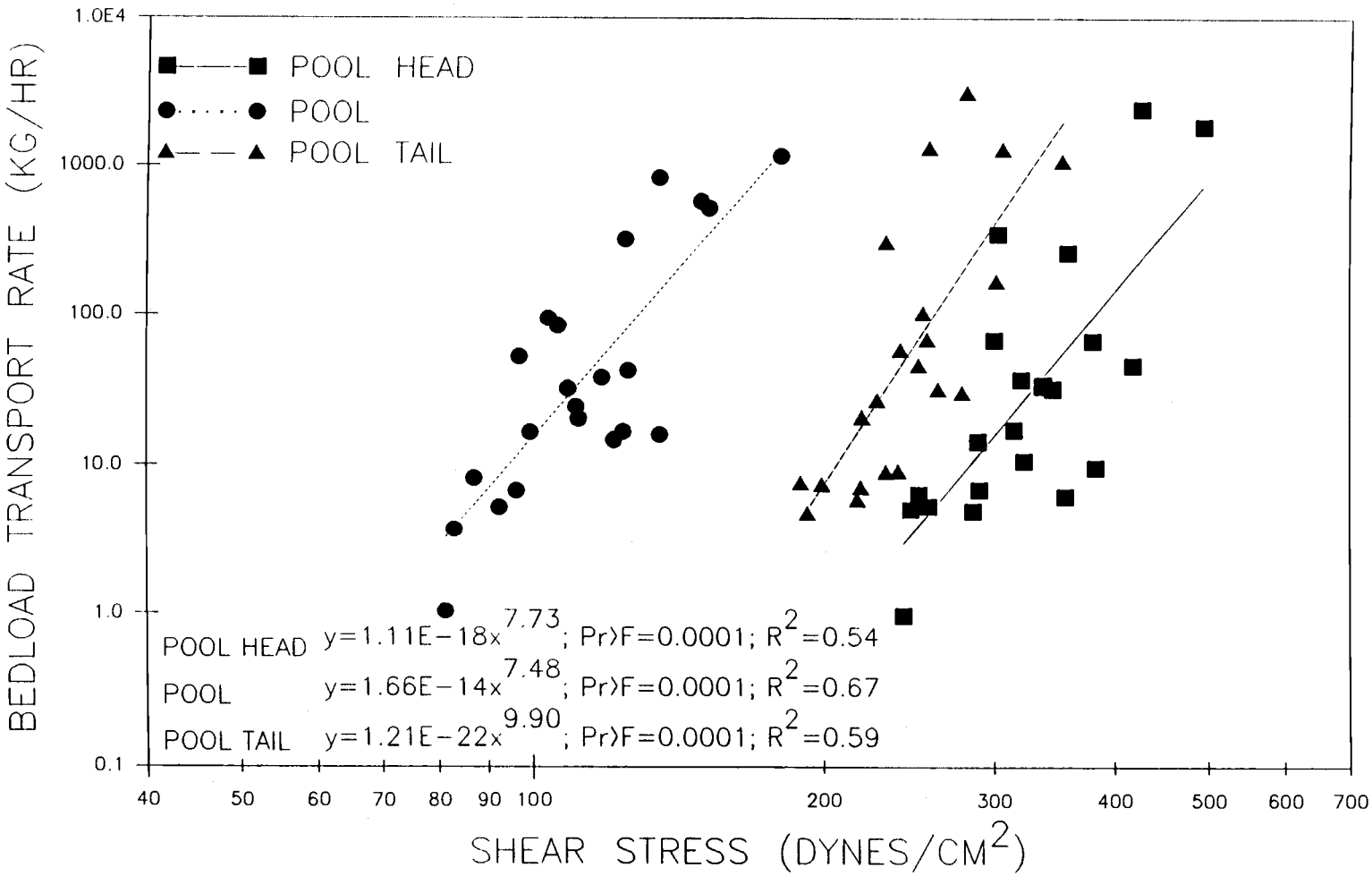

Figure 37. Variation in bedload transport rate with temporal-mean boundary shear stress.

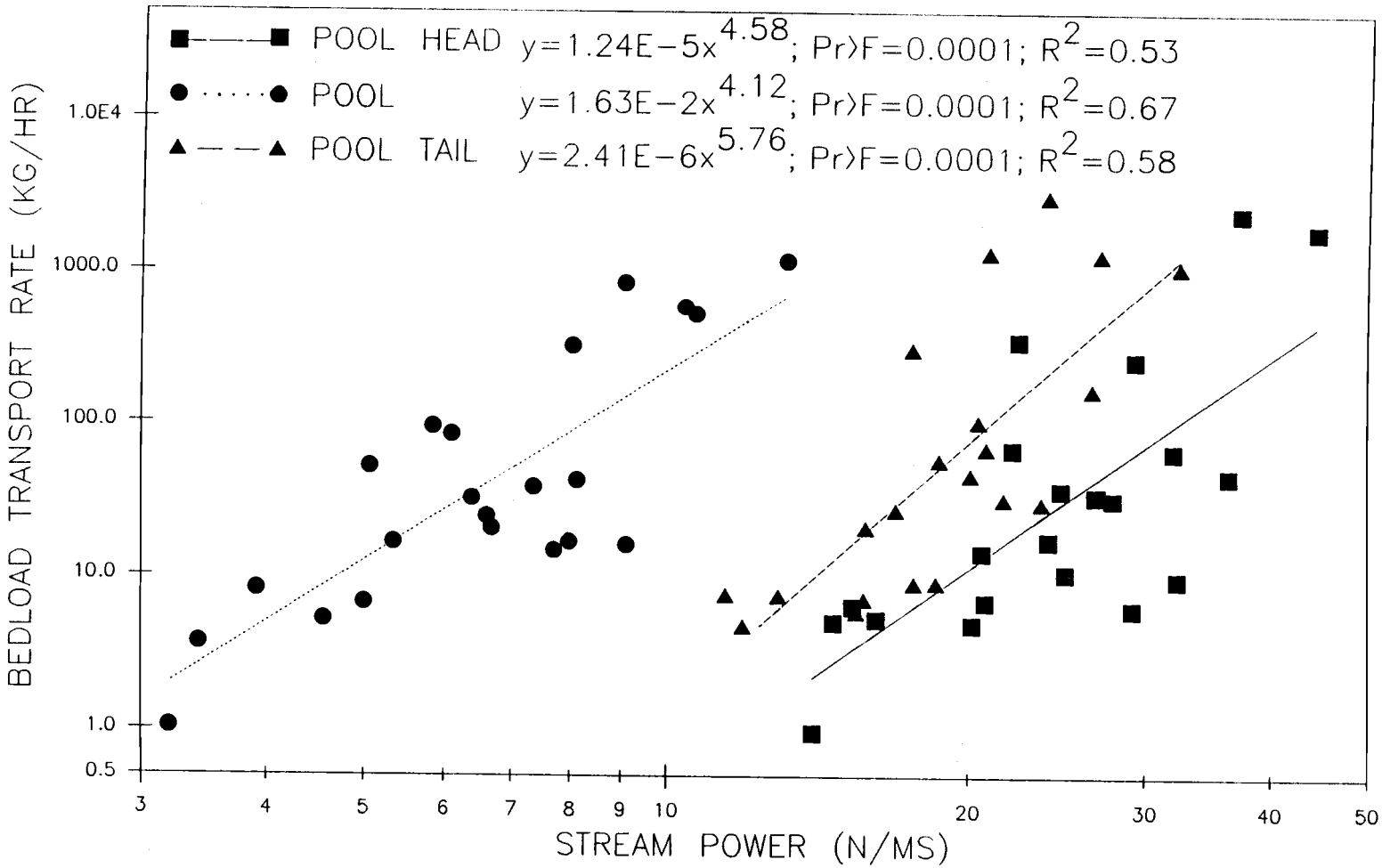

Figure 38. Variation in bedload transport rate with temporal-mean stream power per unit bed area.

Other research has also documented hysteresis in bedload transport rates during individual storm hydrographs (Jackson and Beschta, 1982; Klingeman and Emmett, 1982; Sidle, 1988). This trend may result from a peak in sediment supply at the storm hydrograph peak. Episodic delivery of sediment from upstream occurs as a result of bank collapse or sediment input from landslides, and probability of these events may reach a maximum at the storm peak. In addition, the maximum sediment source area is reached at peak discharge, thus more sediment is available to the stream on receding than rising flows (Beschta, 1987).

When data from all storms were combined, rates measured during rising hydrograph limbs appeared to be lower and increase less rapidly than rates during falling limbs at all three stations (Fig. 39). Only at the pool were the two relationships significantly different, however (App. M). At the pool, rate of increase was the same for rising and falling limbs, but intercepts were different at the 0.05 probability level (App. M). At the pool head, the bedload rate vs discharge relationship for the rising limb had remarkably low variance (R^2 = 0.98). This resulted in a significant difference in variance for the rising limb vs falling limb relationships, therefore the analysis of covariance techniques were not valid (App. M).

Antecedent storm history affected the rate of bedload transport in that recently mobilized beds were prone to higher rates. Analysis of covariance indicated that the magnitude of bedload transport rate, as a function of discharge, became significantly higher at the pool head and pool tail following the large storms in February 1986 (Fig. 40, App. N). Magnitude in the pool appeared to follow the same trend, although the relationship of transport magnitude to discharge was not significantly different before vs after the February storms (Fig. 40, App. N). In contrast to magnitude, rate of increase in bedload transport rate with discharge was not statistically different before vs after the series of large storms for any of the stations (Fig. 40, App. N). Data for these relationships were limited to discharge less than bankfull, because no larger flows occurred prior to the series of large February storms during this study.

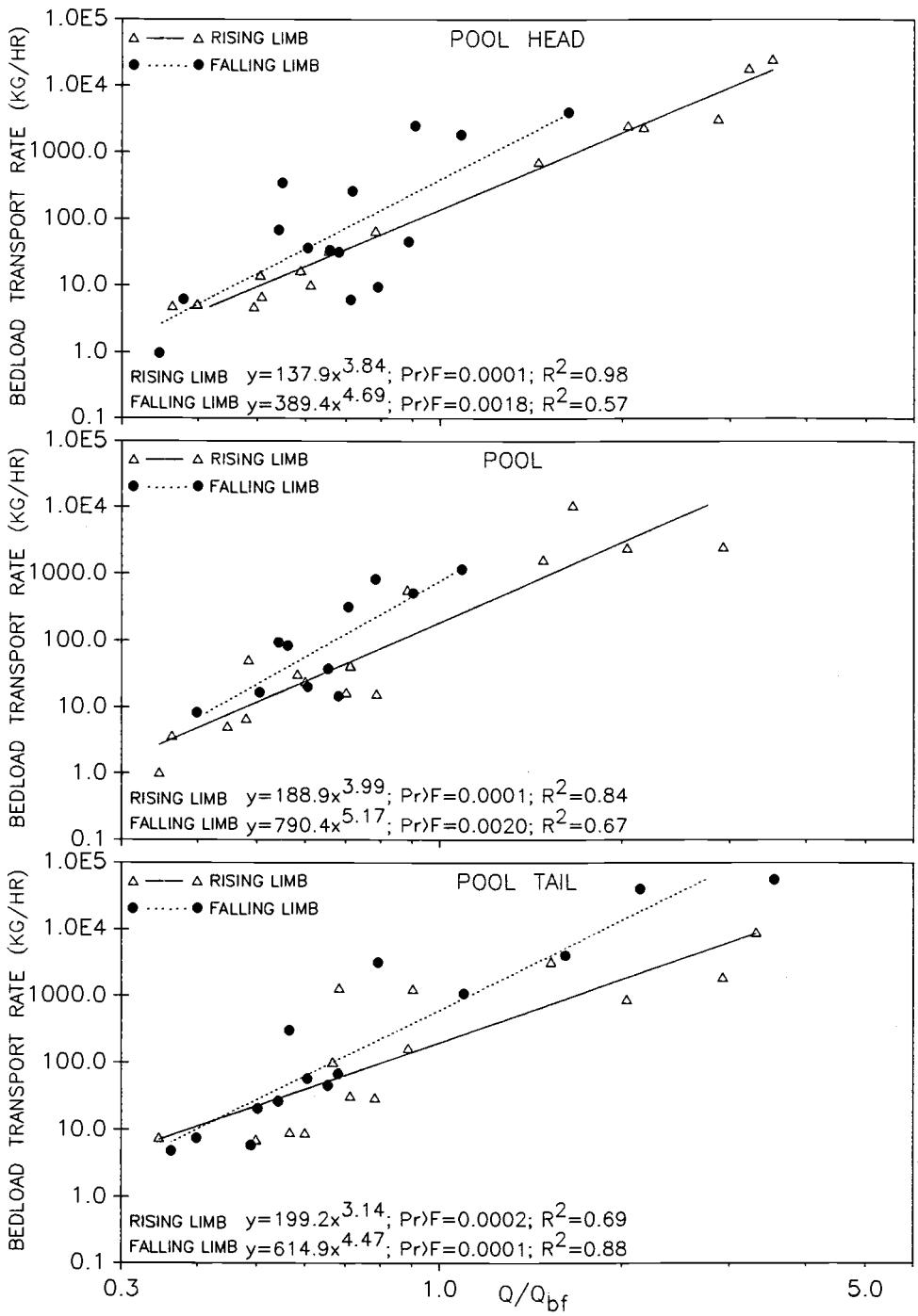

Figure 39. Variation in bedload transport rate with dimensionless discharge on rising and falling hydrograph limbs. Q is water discharge. Q_{bf} is bankfull discharge.

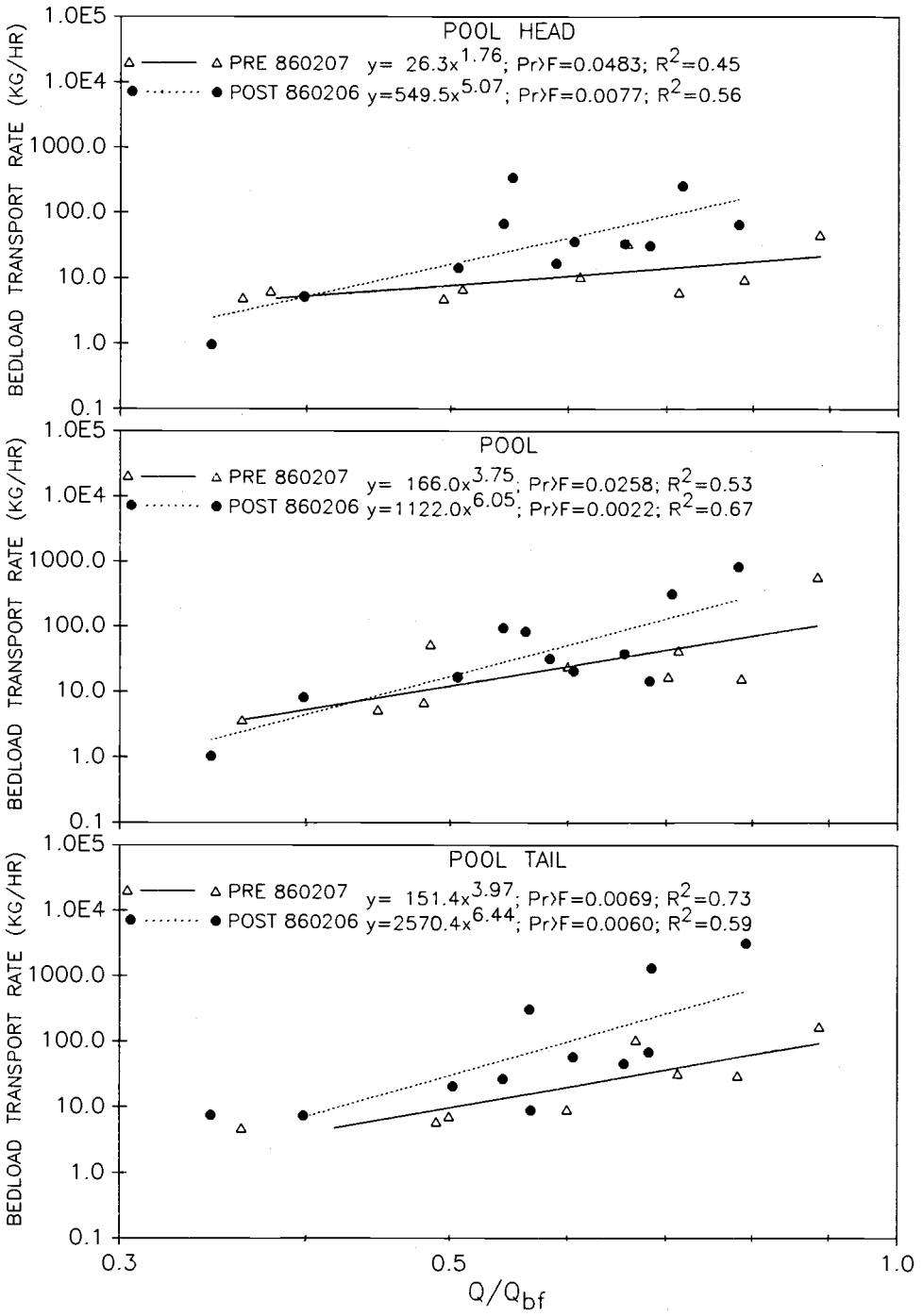

Figure 40. Variation in bedload transport rate with dimensionless discharge before and after a series of major storm flows. Q is water discharge. Q_{bf} is bankfull discharge.

Large variability in bedload transport rates present in this study, owing to variables such as sediment supply, antecedent storm history, and obstruction-related turbulence imply that commonly used predictive equations for bedload transport rate may not be valid in similar streams if applied to brief time periods. These equations typically express transport rate as a function of mean hydraulic variables and of grain-size distribution of the bed (Vanoni, 1977, p. 190-214). Most of the variation in bedload transport rate shown in the present study could be explained by variation in discharge (Fig. 35) or shear stress (Fig. 37) if all data were combined. These hydraulically-based relations would clearly be less appropriate, however, if applied to a instantaneous transport rates.

Bedload transport patterns were similar to those described in laboratory studies of scour holes associated with bridge piers, and are incorporated into the "turbulent scour model" presented herein. Patterns of net bedload export as well as stability of the pool cross-section, in spite of bedload flux much larger than the volume of the pool, indicated that of major scour and fill did not coincide predictably with storm hydrographs. Large temporal variability of bedload transport rate with respect to discharge implied that sediment supply was an important influence on bedload export from the pool. Furthermore, in spite of significantly lower temporal-mean boundary shear stress and stream power in the pool, magnitude and variation of bedload transport rate with discharge was similar to that at the pool head and tail throughout the range of discharge sampled (Fig. 35). This indicated that the pool was not systematically filling at low discharge and scouring at high discharge. Rather, bedload was transported through the study site, at all measured discharges, without marked changes in pool storage.

Stream Competence

Bedload transport rates at the pool were shown above to be similar to rates at the pool head and tail in spite of lower time-averaged boundary shear stress and stream power

in the pool. This apparent contradiction is attributed to drag and lift forces generated by instantaneous turbulent velocity fluctuations created by interaction of streamflow with the LWD obstruction. In the following section a similar argument is presented to demonstrate that effects of the large obstruction on turbulence also account for very similar competence vs shear stress relationships at the three sampling stations. These effects contribute to the maintenance of pool form.

Stream competence, the ability to transport sediment of a given size, is a function of boundary shear stress but also varies with grain exposure, fabric of the pavement layer, and lift forces determined by instantaneous turbulent velocity fluctuations (Miller et al., 1977; Richards, 1982, pp. 84; Carling, 1983; Reid et al., 1985; Andrews and Parker, 1987). In addition to these variables, the size of sediment transported by a stream varies with the grain-size distribution of the sediment supply, which can vary with time (Beschta, 1987).

Grain-size analyses of bedload samples indicated that, in general, bedload was dominated by sand-size material at lower values of discharge and by gravel-size material at discharge greater than 0.5 Qbf (Fig. 41). At all three stations, bedload samples with D84 less than 4.0 mm were limited to discharges less than about 0.7 Q_{bf} (Fig. 42). At the pool head and pool tail, one fine-grained bedload sample was collected at a discharge greater than 13.0 m^3/s, but not shown in Fig. 41 or Fig. 42, because the magnitude of discharge was not well defined. These samples had a D50 less than 2.0 mm and a D_{84} smaller than 4.0 mm. This unusually small grain-size distribution may indicate passage of a fine-grained bed form, or a sudden input of fine sediment from a bank collapse or other upstream event.

The mean size of the five largest clasts in a bedload sample can serve as an estimate of the competence of flow (Andrews, 1983; Carling, 1983). In this study the mean intermediate diameter of the five largest clasts in each bedload sample at each sampling station was correlated with discharge and boundary shear stress, estimated from the regression of shear velocity on discharge. At all stations, competence increased linearly

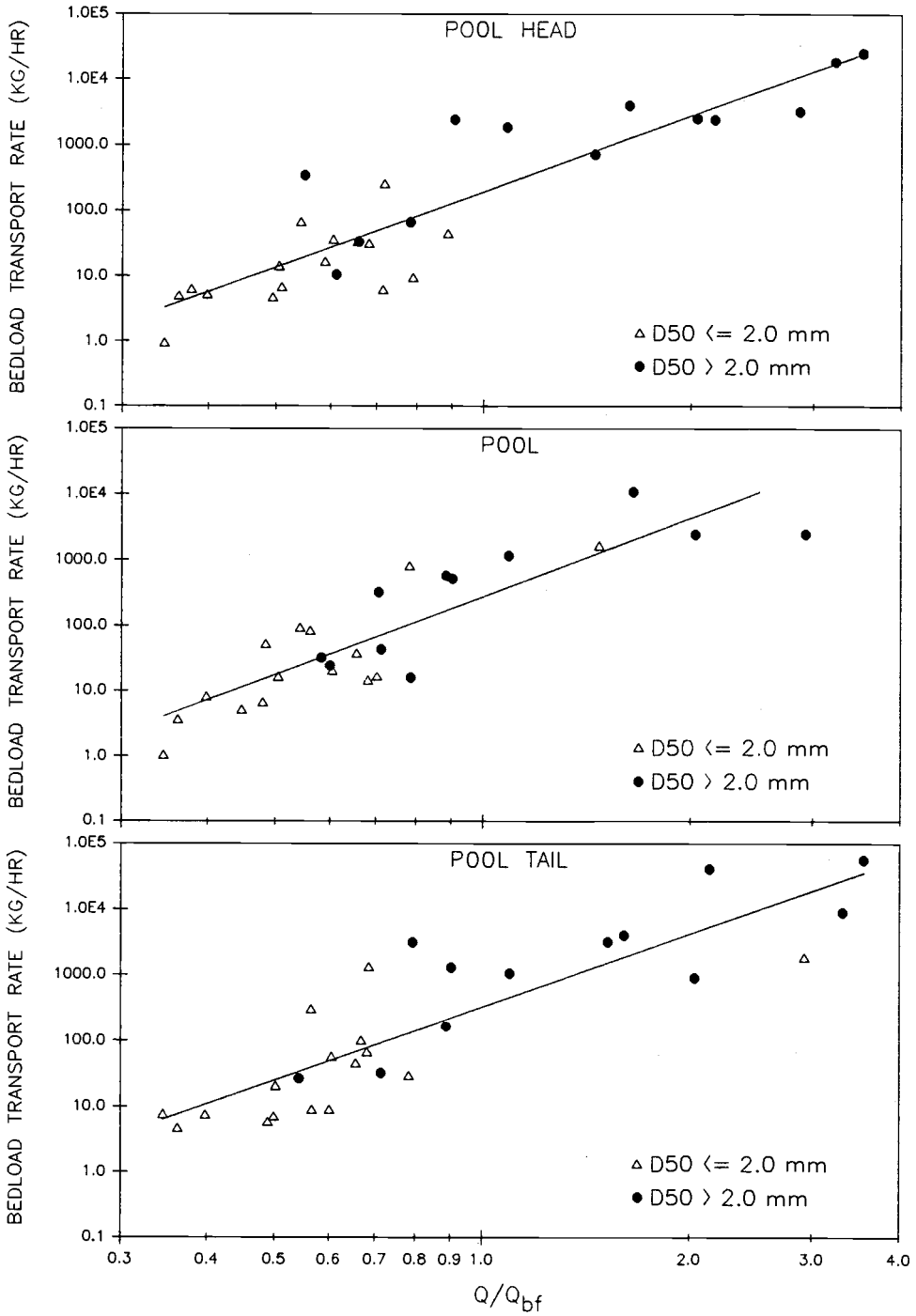

Figure 41. Variation in grain-size distribution (D_{50}) of bedload samples with dimensionless discharge. Q is water discharge. Q_{bf} is bankfull discharge.

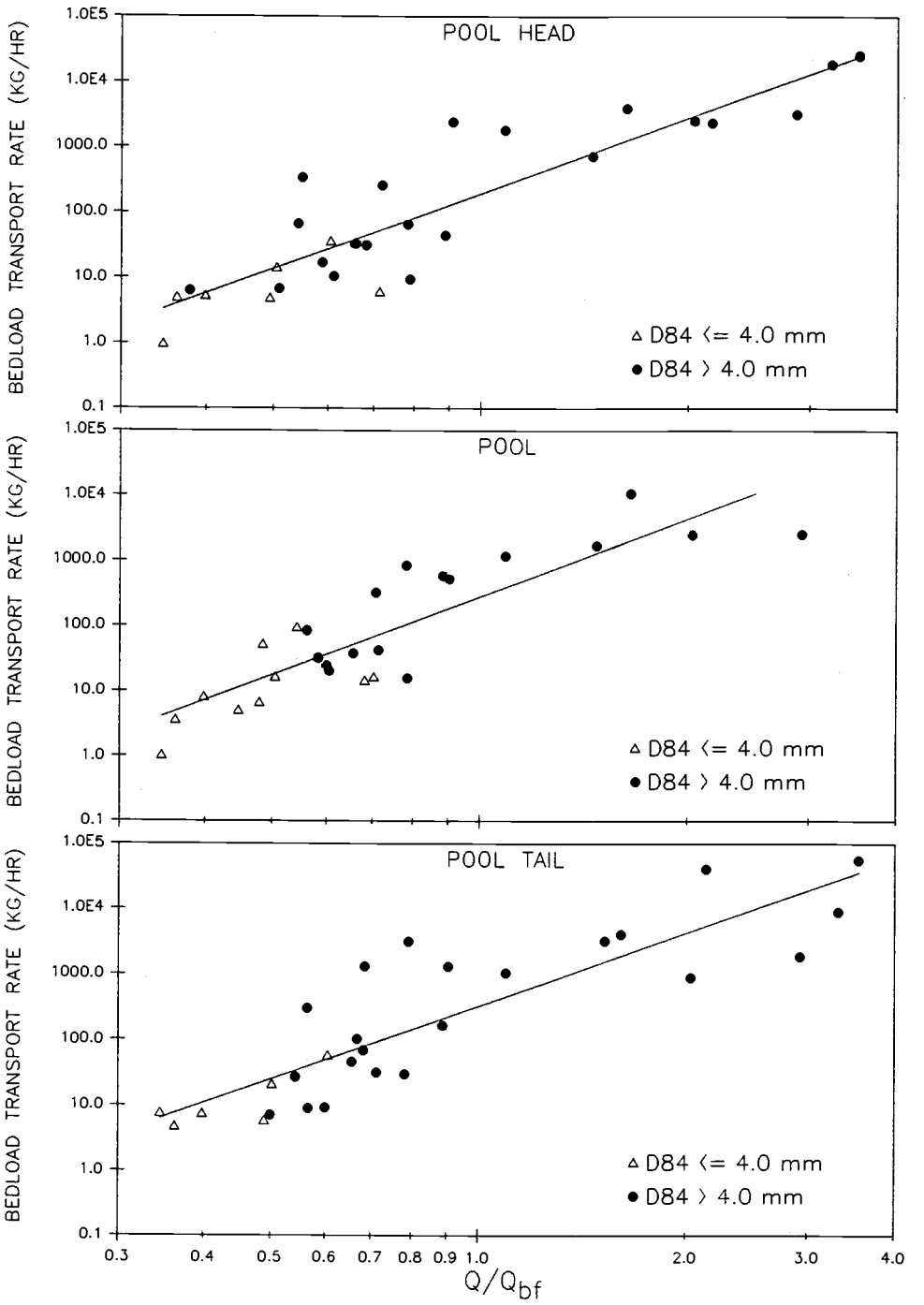

Figure 42. Variation in grain-size distribution (D_{84}) of bedload samples with dimensionless discharge. Q is water discharge. Q_{bf} is bankfull discharge.

with the log of the dimensionless discharge (Fig. 43). Analysis of covariance indicated that competence did not increase faster at the pool than at the pool head or tail (Fig. 43, App. O).

Three fine-grained outliers are apparent at high discharge in Figure 43. These samples were all collected within a single hour on February 17, 1986, one at each station. These samples apparently reflected an input of fine sediment from upstream, possibly resulting from bank collapse, or the passage of a fine-grained bed form. The competence vs discharge regression analysis was repeated for discharge less than 1.4 Q_{bf} to test for a trend toward competence reversal without the large variation at higher discharge indicated in Figure 43. These analyses confirmed that there was no significant difference in rate of competence increase between any of the three stations. Therefore no competence reversal was indicated.

In studies of initial motion of bedload, shear stress is commonly plotted as a function of the diameter of the largest clast or clasts in an associated bedload sample. In recent published analyses, these values of stress are treated as a dependent variable, and can be interpreted as the threshold shear stress for the associated grain size, provided that larger grains are available for transport (Andrews 1983; Carling, 1983).

Data from this study indicated an increase in threshold shear stress with increasing grain size (Fig. 44). Regression equations shown in Figure 44 for the three sampling stations yielded exponents similar to, although somewhat lower than, those for the data sets of Milhous for Oak Creek, Oregon (Milhous, 1973) and Carling for Great Eggleshope Beck, U.K. (Carling, 1983), 0.57 and 0.38 respectively as presented by Komar (1987). Larger exponents reflect greater tendency toward selective entrainment (Komar, 1987).

The rate of increase in threshold shear stress with grain size was less at all three stations than predicted by the Shields equation for dimensionless critical shear stress, where T* is taken as 0.06 (Fig. 44). Shear stress required for entrainment was larger than predicted by the Shields equation for nearly all samples collected at the pool head and tail

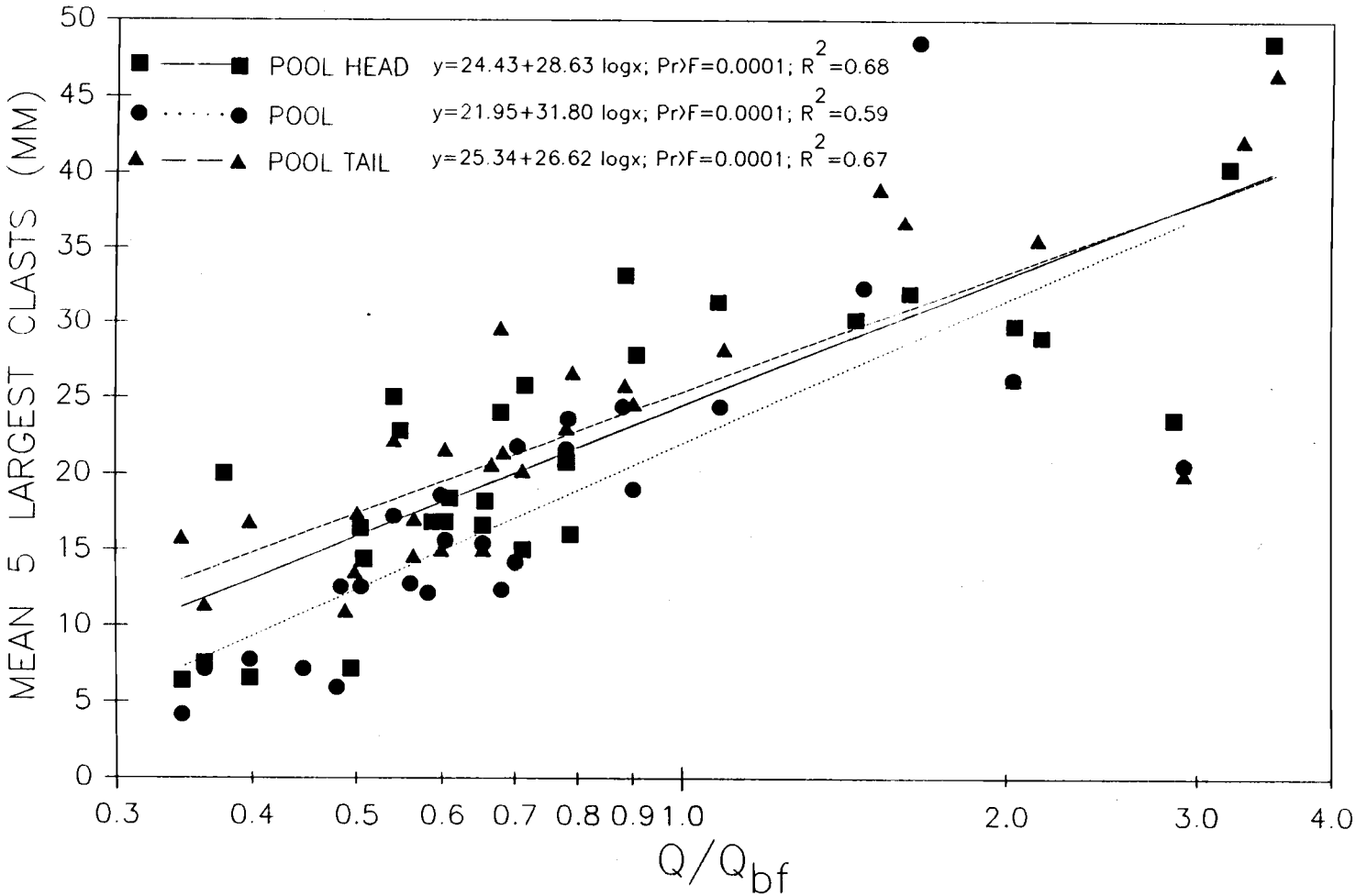

Figure 43. Variation in streamflow competence with dimensionless discharge. Competence was measured as the mean of the five largest clasts in each bedload sample. Q is water discharge. Q_{bf} is bankfull discharge.

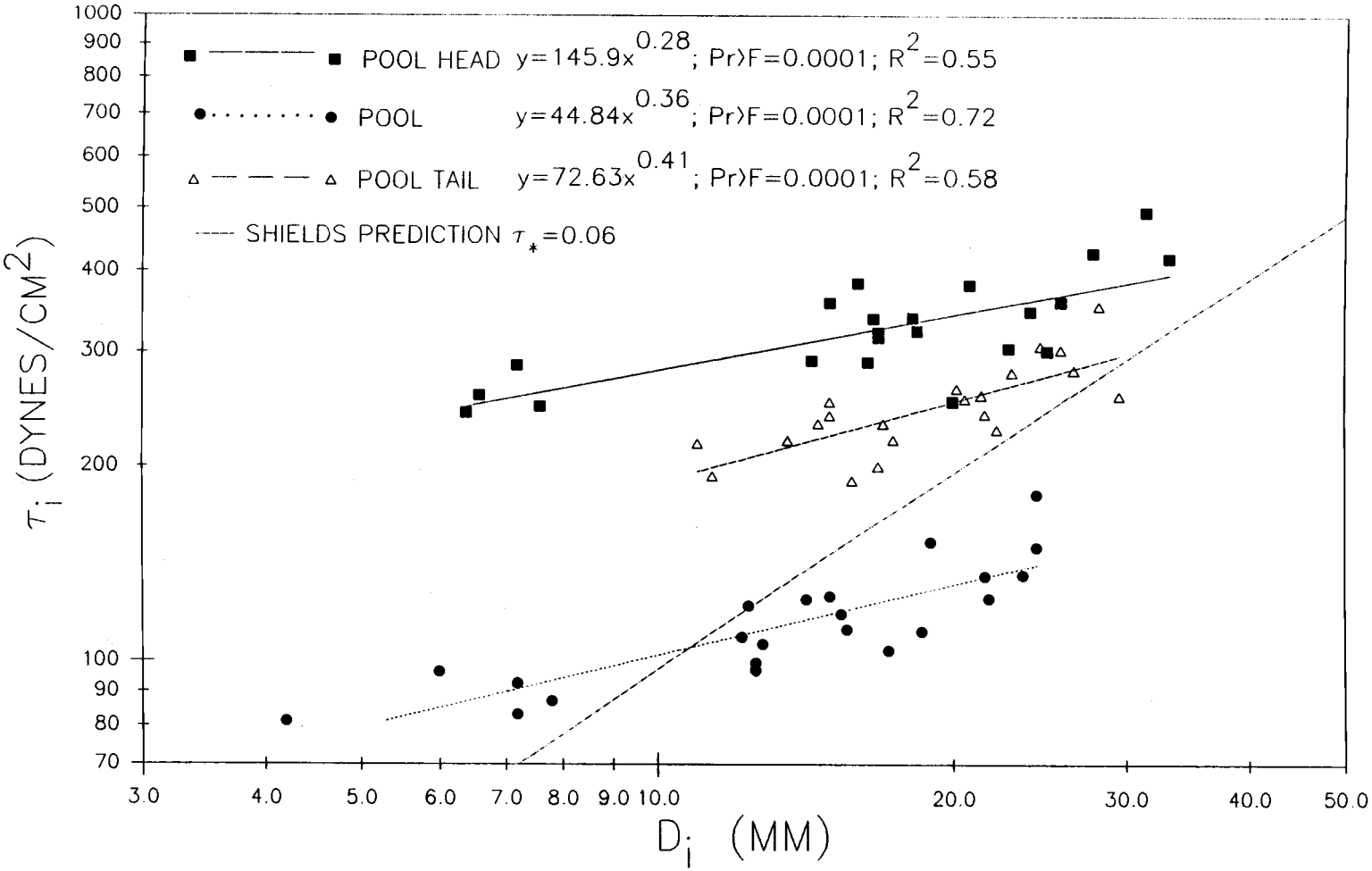

Figure 44. Variation in temporal-mean boundary shear stress entrainment threshold (τ_i) with bedload grain size (D_i).

at discharges as large as 1.4 Q_{bf} (Fig. 44). However, the trend of the data suggested that for grain sizes larger than about 40 mm at the pool head and 30 mm at the pool tail, threshold shear stress would be smaller than predicted by the Shields equation (Fig. 44). At the pool, this appeared to happen for grain sizes larger than about 10 mm (Fig. 44).

Increase in the entrainment threshold above levels predicted by the Shields equation can be explained as the result of two processes related to pavement effects. Imbrication in the pavement layer interlocks grains, making them more difficult to entrain than more loosely packed clasts, thus a greater shear stress is required to initiate motion. In addition, shielding of small grains by larger ones results in small grains requiring a larger shear stress to become entrained (Parker et al, 1982; Andrews, 1983; Andrews and Parker, 1987).

Increasing shear stress will eventually overcome the effects of interlocking of grains, and entrainment will then depend on grain size, weight, shape, and exposure to the flow as well as hydraulic variables. Greater exposure of larger grains will tend to counteract the increased resistance of these heavier grains to entrainment (Parker et al, 1982; Andrews, 1983; Andrews and Parker, 1987), resulting in entrainment threshold being less than the Shields prediction (Fig. 44).

Entrainment of similar grain sizes at the three sampling stations, while temporal-mean boundary shear stress remained significantly lower in the pool than at either of the other stations (Fig. 22, 44, App. E) indicated that total entrainment force on the grains in the pool was underestimated by time-averaged shear stress measurements presented in Fig. 44. Entrainment of grains in the pool resulted, in part, from drag and lift forces created by instantaneous turbulent velocity fluctuations created by interaction of flow with the LWD obstruction.

Analyzing grain-size distribution of the bedload in terms of the few largest grains accounts for only a small portion of the distribution. For this reason, D_{84} and D_{50}, which reflect the entire grain-size distribution of the bedload were also related to boundary shear stress. D_{84} increased approximately with the square of the shear stress at the three

sampling stations, from the beginning of significant transport to discharges exceeding bankfull (Fig. 45). A similar analysis of D_{50} for the bedload samples indicated the same trends with somewhat lower exponents (Fig. 46).

All three of the above measures of competence, including largest sizes in transport, D_{84}, and D_{50} demonstrated an increase in competence with increasing boundary shear stress. This indicated that the tendency toward equal mobility of various grain sizes in gravel-bed streams with pavement (Parker et al., 1982; Andrews, 1983; Andrews and Parker, 1987; Wilcock, 1988; Ashworth and Ferguson, 1989) does not completely overcome selective entrainment as a function of shear stress (Komar, 1987). Similar conclusions have been reached for data sets from other gravel-bed streams (Komar, 1987; Komar and Shih, 1988; Ashworth and Ferguson, 1989; Komar, 1989).

Wilcock (1988) suggested that, in field studies, correlation of competence with shear stress is affected by sample size, because at higher discharge, samples are commonly larger, increasing the probability of collecting a relatively rare, coarse fragment. Multiple regression analyses of the data presented here were done to test the effect of sample weight on the shear stress vs competence relationship. There was a highly significant logarithmic relationship between shear stress and competence at all stations (Fig. 44, Table 5). Shear stress and sample weight were highly correlated at the pool head and pool tail (Table 5). Correlation of competence and sample weight, as predicted by Wilcock (1988), occurred at the pool head and tail (Table 5).

Use of D_{84} or D_{50}, rather than the largest grains, to describe grain-size distribution reduces potential problems in sampling uncertainty described by Wilcock (1988), because D_{84} and D_{50} reflect the grain-size distribution of the entire bedload sample rather than only a few of the largest grains (Komar, personal communication). For this reason, variation of D_{84} and D_{50} with shear stress was analyzed.

Regression of D_{84} as a function of shear stress indicated a highly significant relationship at all three stations. In the case of D_{84}, there was no significant relationship

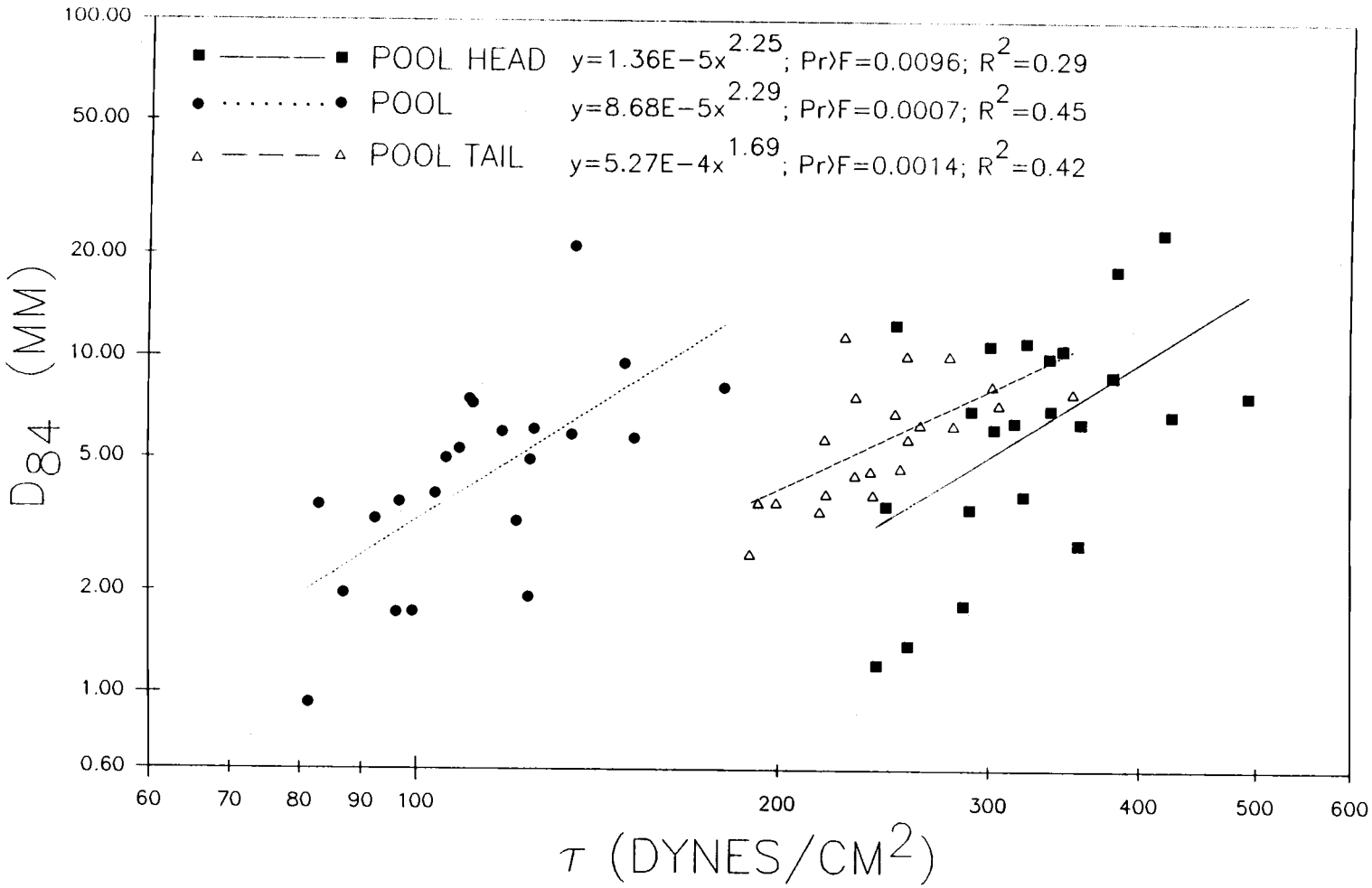

Figure 45. Variation in bedload D_{84} with temporal-mean boundary shear stress (τ). D_{84} is the size for which 84% of the bedload sample is finer.

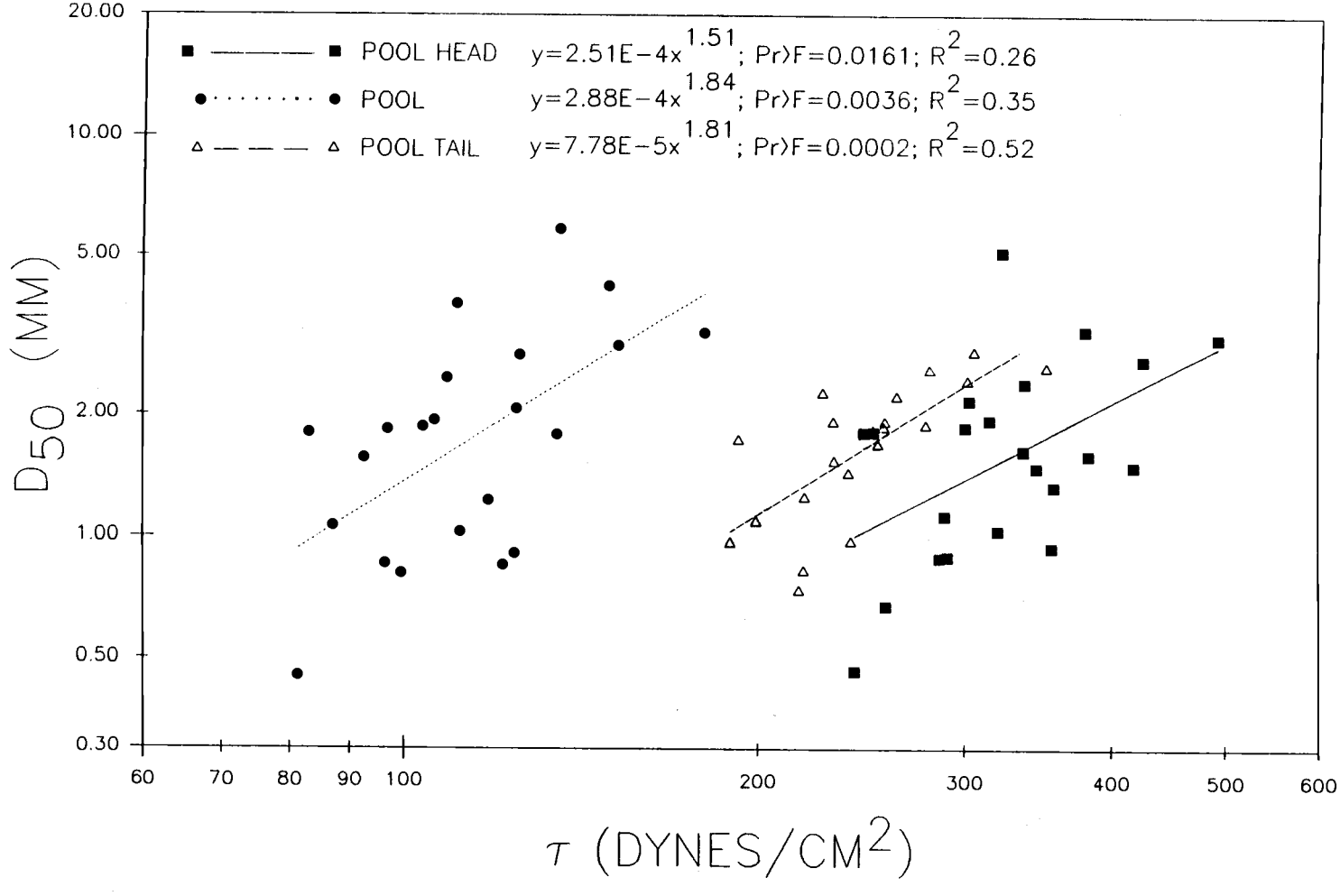

Figure 46. Variation in bedload D_{50} with temporal-mean boundary shear stress (τ). D_{50} is the size for which 50% of the bedload sample is finer.

TABLE 5. SHEAR STRESS, COMPETENCE, AND SAMPLE WEIGHT REGRESSION RELATIONSHIPS.

LOG SHEAR STRESS VS LOG COMPETENCE		
STATION	SIGNIFICANCE	R^2
1	**	0.55
2	**	0.72
3	**	0.58

LOG SHEAR STRESS VS SAMPLE WEIGHT		
STATION	SIGNIFICANCE	R^2
1	**	0.42
2	---	---
3	**	0.41

LOG COMPETENCE VS SAMPLE WEIGHT		
STATION	SIGNIFICANCE	R^2
1	**	0.30
2	---	---
3	**	0.30

LOG D_{84} VS LOG SHEAR STRESS		
STATION	SIGNIFICANCE	R^2
1	**	0.29
2	**	0.45
3	**	0.42

LOG D_{84} VS SAMPLE WEIGHT		
STATION	SIGNIFICANCE	R^2
1	---	---
2	---	---
3	---	---

LOG D_{50} VS LOG SHEAR STRESS		
STATION	SIGNIFICANCE	R^2
1	*	0.26
2	**	0.35
3	**	0.52

LOG D_{50} VS SAMPLE WEIGHT		
STATION	SIGNIFICANCE	R^2
1	*	0.19
2	---	---
3	**	0.34

Pr > F: ** <0.01; * < 0.05; --- >0.05

with sample weight (Table 5). Regression of D_{50} on shear stress and sample weight indicated a correlation with sample weight at two of the stations (Table 5).

Correlation of boundary shear stress with competence was analyzed despite the correlation of competence with sample weight by using partial sums of squares regression techniques to determine the associated partial regression coefficients (Neter et al., 1983, p. 286-9; SAS Inst. Inc., 1987, p. 584-588; T. Max, personal communication).

At the pool head, competence was highly significant after correlation with sample weight was accounted for in the regression model (Table 6). Sample weight was barely significant at the 0.05 probability level ($p \approx 0.045$) after competence was accounted for in the model. At the pool and pool tail, competence was highly significant, while sample weight was not significant after competence was accounted for (Table 6).

A similar analysis of the regression of D_{84} on shear stress and sample weight indicated that shear stress was highly significant at all stations after the correlation with sample weight was accounted for (Table 7). As noted above, there was no significant relationship between D_{84} and sample weight even at the first and third stations, where shear stress and sample weight were correlated (Table 5, 7).

Because of high variability in the regression of D_{50} on shear stress and sample weight, neither independent variable was significant at the pool head after correlation with the other was accounted for (Table 8). At the remaining two stations however, results were similar to those for D_{84}. Shear stress was significant after correlation with sample weight was accounted for, while sample weight was not significant after correlation with shear stress was accounted for in the model (Table 8).

These partial regression analyses demonstrated that there was a highly significant logarithmic relationship between competence and shear stress and between D_{84} and shear stress at all sampling stations in this study (Table 5). These relationships remained highly significant after correlation of competence or D_{84} with sample weight was accounted for in the regression model (Tables 6, 7). In only one case was sample weight barely significant

TABLE 6. PARTIAL SUMS OF SQUARES ANALYSIS OF LOG SHEAR STRESS VS LOG COMPETENCE (LGCP) AND SAMPLE WEIGHT (SPWT).

INDEPENDENT VARIABLES	Pr	R^2	T II SS	F	Fcr	T II Pr
POOL HEAD						
LGCP & SPWT	**	0.63				
LGCP			0.029	10.95	8.18	**
SPWT			0.012	4.45	4.38	*
POOL						
LGCP & SPWT	**	0.74				
LGCP			0.116	52.55	8.18	**
SPWT			0.003	1.57	4.38	---
POOL TAIL						
LGCP & SPWT	**	0.65				
LGCP			0.022	12.50	8.28	**
SPWT			0.006	3.61	4.41	---

Pr > F: ** <0.01; * < 0.05; --- >0.05

TABLE 7. PARTIAL SUMS OF SQUARES ANALYSIS OF LOG D_{84} VS LOG SHEAR STRESS (τ_b) AND SAMPLE WEIGHT (SPWT).

DEPENDENT VARIABLES	Pr	R2	T II SS	F	Fcr	T II Pr
POOL HEAD						
LG τ_b & SPWT	*	0.35				
LG τ_b			0.776	9.52	8.18	**
SPWT			0.145	1.78	4.38	___
POOL						
LG τ_b & SPWT	**	0.45				
LG τ_b			0.811	14.55	8.18	**
SPWT			0.002	0.03	4.38	___
POOL TAIL						
LG τ_b & SPWT	**	0.48				
LG τ_b			0.263	14.71	8.28	**
SPWT			0.034	1.92	4.41	---

Pr > F: ** <0.01; * < 0.05; --- >0.05

TABLE 8. PARTIAL SUMS OF SQUARES ANALYSIS OF LOG D_{50} VS LOG SHEAR STRESS (τ_b) AND SAMPLE WEIGHT (SPWT).

DEPENDENT VARIABLES	Pr	R2	T II SS	F	Fcr	T II Pr
POOL HEAD						
LG τ_b & SPWT	*	0.28				
LG τ_b			0.105	2.25	4.38	---
SPWT			0.024	0.53	4.38	___
POOL						
LG τ_b & SPWT	**	0.37				
LG τ_b			0.489	9.29	8.18	**
SPWT			0.024	0.45	4.38	___
POOL TAIL						
LG τ_b & SPWT	**	0.55				
LG τ_b			0.119	8.09	4.41	*
SPWT			0.015	1.05	4.41	---

Pr > F: ** <0.01; * < 0.05; --- >0.05

at the 0.05 probability level after correlation with competence or D_{84} was accounted for (Table 6, 7).

Although results were less clear using D_{50} as an indicator of grain-size distribution of the bedload, at all three stations, shear stress was significantly related to D_{50} at the 0.01 or 0.02 probability level (Table 5, Fig. 46). This relationship held at two of the three sampling stations at the 0.01 or 0.02 probability level after correlation with sample weight was accounted for (Table 8). In no case was there a significant relationship between D_{50} and sample weight after shear stress was accounted for in the model (Table 8).

These analyses indicated that the grain size-shear stress relationships presented in Figures 44-46 remained statistically significant after bias introduced by variable sample weight was accounted for in the models. The only exception to this was for the D_{50} vs shear stress relationship at the pool head, which had very large variability, causing neither independent variable to be significant after the other was included in the model.

SUMMARY

This study investigated the mechanisms of pool maintenance and the dynamics of associated bedload transport in a small gravel-bed stream in a forested environment. A conceptual "turbulent scour" model of pool maintenance was presented, which agreed well with measurements of stream hydraulics, scour and fill of the stream bed, and bedload sediment transport rate and grain-size distribution.

Streamflow Patterns

The LWD obstruction at this site affected hydraulic conditions by deflecting and constricting flow, causing backwater effects, creating turbulence, and by creating a large area of low-velocity, eddying current in the lee of the obstruction. Deflected flow scoured sediment from the downstream end of a gravel bar on the opposite side of the channel, thereby fixing the location of the bar. Flow constriction at the obstruction increased velocity and shear stress on the bed, enhancing the scouring ability of flow near the obstruction. Entrainment forces at the bed were further enhanced by instantaneous turbulent velocity fluctuations and scouring vortices associated with the LWD obstruction.

Shear stress on the bed was sufficient to scour the stream bed and transport bedload, creating a scour pool downstream of and beside the obstruction. Downstream of the obstruction, flow expanded laterally, shear stress was reduced, and bedload was deposited on a lateral bar in the lee of the obstruction. The locations of both lateral bars in the study reach were determined by effects of the LWD obstruction on streamflow hydraulics. Once the bars were in place, they deflected streamflow and enhanced cross-stream flow generated primarily by the interaction of streamflow with the obstruction.

Velocity of cross-stream flow was as large as 29% of the net velocity. Cross-stream currents created complex hydraulic conditions that may provide low-velocity refuge for fish

during high discharge. Areas of eddying current in the lee of obstructions appeared to provide the most important potential high-flow refuge at this site.

Boundary Shear Stress Patterns

The pool, associated with the LWD obstruction, maintained its depth by scour and bedload transport resulting from a combination of temporal-mean boundary shear stress and instantaneous shear stress and lift force generated by instantaneous turbulent velocity fluctuations and vortices associated with the large obstruction. Near-bed velocity and boundary shear stress, averaged over 2.5 m of the channel width and over 1 min time periods, were higher at the head and tail of the pool than at the pool center. This was true for all measured discharges at least as large as 1.4 Q_{bf}. In this respect, the pool differed from non-obstruction related pools, where the location of maximum velocity and shear stress has been reported to shift from the riffles to the pools at high discharge (Leopold and Wolman, 1960; Keller, 1971; Richards, 1976; Andrews, 1979; Lisle, 1979; Emmett et al., 1983; Ashworth, 1987).

Clearly, competence in pools must at times equal or exceed competence at upstream sediment source areas, otherwise pools would fill over time or never form initially. Therefore, variation in time-averaged shear stress alone did not account for maintenance of the pool morphology. A component of total force acting to entrain and transport sediment must have been added by turbulent effects generated by interaction of streamflow with the large obstruction. This combination of temporal mean shear stress and instantaneous turbulent forces created and maintained the pool at a site where a pool may not have occurred in the absence of an obstruction. These hydraulic conditions are characteristic of the conceptual "turbulent scour" model developed in the present report.

Scour and Fill

Patterns of stream bed scour and fill were more complex in this setting than in previously described pool-riffle sequences, and were strongly influenced by the large obstruction. At the pool head and tail, during small or moderate-magnitude storms there was a general tendency for fill to occur during rising hydrograph limbs and scour to occur on falling limbs. However, at all three sampling stations scour and fill cycles occurred during individual rising and falling limbs. Measurements of bedload import and export during storms verified this tendency for the pool. At all three sampling stations, scour and fill were dominated by the growth and scour of lateral bars during and after a period of sustained, very high flow.

At the pool, cross-sectional area was remarkably constant except for bank erosion, in spite of the occurrence of very high flow events. This pattern differed from previous descriptions of scour and fill in riffle-pool sequences. Previous work identified a reversal of maximum competence, changing from riffles to pools as discharge increased above bankfull. This reversal is believed to cause pools to scour at high flow, thereby maintaining their depth. Maintenance of pool morphology, in the case presented here, was accountable to scour and bedload transport resulting from a combination of temporal mean shear stress and turbulent forces associated with the LWD obstruction. Predictable patterns of scour during rising discharge and fill during falling discharge were demonstrated only for low- or moderate-magnitude storm events when sand-size and smaller sediment and organic material was scoured from the pool. Fine sediment did accumulate during low-flow periods, at the edge of the pool, away from the obstruction, but did not cause marked changes in maximum depth. The large obstruction anchored the location of scouring vortices and turbulent velocity fluctuations and constricted the channel, creating a more stable pool morphology than in non-obstruction related pools.

Bedload Transport

Variation in bedload transport rate, as a function of discharge, was not significantly different in the pool than at the pool head or tail. However, variability in rate at a station and relative rates between stations was high. There was a significant linear relationship between bedload rate and temporal mean boundary shear stress and stream power up to a discharge at least as large as 1.4 Q_{bf}. Bedload rates tended to peak after the hydrograph peak of large storm events, and high rates were easily induced following large storms, at least for high flows occurring within a period of several days.

Stream Competence

Competence, as measured by the mean of the five largest clasts sampled in the bedload, increased linearly with maximum shear stress at all stations at least up to a discharge of 1.4 Q_{bf}, in spite of the recognized tendency toward equal mobility of all grain sizes in gravel-bed streams. This dependence of competence on shear stress was statistically significant even after bias introduced by variable sample weight was accounted for in a regression model.

This measure of competence indicated that small grain sizes became mobile at shear stresses larger than predicted by the Shields equation for dimensionless critical shear stress. Conversely, the data trend suggested that very large grain sizes would become entrained at lower values of shear stress than predicted for uniform grain size conditions. These patterns resulted from shielding of small grains and greater exposure of large grains, creating a tendency toward equal mobility of various grain sizes.

In spite of consistently lower time-averaged, near-bed velocity and shear stress in the pool, the rate of increase of competence with discharge was not significantly different from that at the pool head or tail. Previous research on pool-riffle sequences suggests a

competence reversal at approximately bankfull flow (Leopold and Wolman, 1960; Keller, 1971; Lisle, 1979; Ashworth, 1987). In this case, no evidence for such a competence reversal was found.

Similarity of transport rate and competence at the three cross-sections implied that total entrainment force at the pool was underestimated by time-averaged shear stress alone. Average stress must have been enhanced by instantaneous turbulent velocity fluctuations and vortices associated with the LWD obstruction.

Maintenance of Pool Morphology

The analyses presented above indicated that maintenance of pool morphology in this case, where the pool was formed by scour around a LWD obstruction, could not be explained by the familiar shear stress reversal hypothesis. There was no tendency for temporal mean, near-bed velocity or shear stress in the pool to exceed that at the pool head or tail, at least for flows as large as 1.4 Q_{bf}.

Scour and fill at this site did not follow a systematic trend of pool filling at discharges below bankfull and scour at higher flows. Scour pool morphology changed little in spite of large, sediment-transporting storms with an associated bedload flux much larger than the volume of the pool. Sounding measurements indicated that both scour and fill in the pool occurred well above and well below bankfull discharge and on rising as well as falling hydrograph limbs. Pool scour and fill, calculated from import and export of bedload, likewise did not follow the pattern predicted by the shear stress reversal hypothesis. Measured differences between bedload import and export at the pool indicated that sediment was stored, then scoured from the pool in cycles varying in time from several minutes to several hours. Scour and fill occurred at each of the sampling stations, most notably in response to inferred changes in sediment supply, throughout a wide range of discharge.

Increase in bedload transport rate with discharge at the pool was not statistically different from increase at the pool head and pool tail. Furthermore, bedload transport rate spanned the same range of magnitude in the pool as at the pool head and tail, in spite of lower temporal mean shear stress and stream power in the pool. In addition, grain-size distribution of the bedload at the pool was similar to that at the pool head and tail.

Similarity of bedload transport rate and of bedload grain-size distribution between the three sampling stations required that mean stress in the pool be supplemented by additional tractive or lift forces. These additional forces were inferred to result from instantaneous turbulent velocity fluctuations created by interaction of the flow with the LWD obstruction.

Lisle (1986) proposed that scour at naturally-occurring obstructions was analogous to fluvial scour at bridge piers. His idea was extended in the present study by quantification of boundary shear stress, scour and fill of the stream bed, and bedload transport in a setting where a pool was formed by scour at a large, in-channel obstruction. The resulting "turbulent scour" conceptual model, describing the maintenance of obstruction-related pool morphology, offers an alternative to the shear stress reversal concept, which is not consistent with data presented herein.

The elements of the "turbulent scour" model are as follows:

1. The total erosive force that maintains obstruction-related pool morphology is a combination of temporal-mean bed shear stress and instantaneous lift and drag forces created by turbulent velocity fluctuations, caused by interaction of streamflow with the obstruction.

2. In spite of significantly lower temporal-mean boundary shear stress and stream power in the pool, magnitude and variation of bedload transport rate and grain-size distribution with discharge are similar to that at the pool head and tail when significant amounts of bedload are being transported. This indicates that, through a wide range of discharge, total erosive force in the pool is similar to that at the pool head (upstream

sediment supply section) and pool tail and that bedload is transported without discharge-dependent changes in pool storage.

3. Major scour and fill in the pool do not occur in a consistent pattern associated with rising and falling storm hydrograph limbs.

4. Fluctuations in sediment supply from upstream result in cycles of scour and fill at time intervals much shorter than the duration of individual storm hydrographs and involving much less than the total pool volume.

The "turbulent scour" conceptual model for the maintenance of obstruction-related scour pool morphology and transport of bedload through these pools is supported by measurements and observations reported in the present study. The turbulence-dependent mechanism is suggested as an explanation for the maintenance of pools formed by scour at LWD obstructions in small, gravel-bed streams.

Application of the "turbulent scour" model to alluvial, gravel-bed streams in forested environments suggests that random input of exogenous LWD can be a dominant mechanism, perhaps as important as temporal-mean hydraulic variables and sediment grain-size characteristics, controlling local channel morphology and local bedload transport dynamics. However, size and shape of LWD pieces and clusters in streams vary widely, as do geometric relationships of obstructions to scour pools. Extrapolation of results of this study to other obstruction-pool geometries is untested.

Results of this study are of interest not only to geomorphologists studying channel morphology and sediment transport, but also to engineers and land managers involved with aquatic habitat restoration through manipulation of channel morphology. These results provide insight into the mechanisms responsible for scour and maintenance of pools associated with either naturally-occurring or artificially-placed obstructions. Large, in-channel obstructions can modify streamflow in a way that creates an equilibrium between local hydraulics, channel morphology, and sediment transport such that the associated pool morphology is maintained through a wide range of discharge. This stable pool

environment may provide critical habitat for aquatic organisms, particularly in heavily management-impacted streams. In addition to stable pool habitat, obstructions can also modify local hydraulics to create habitats with a wide variety of depth and velocity conditions. Such a diversity of habitats can meet the varying requirements of a number of organisms.

BIBLIOGRAPHY

A.S.C.E., Task Force on Bed Forms in Alluvial Channels, 1966, Nomenclature for bed forms in alluvial channels: Journal of the Hydraulics Division, Amer. Soc. of Civil Engineers, V. 92, p. 51-64.

Ackers, P., 1982, Meandering channels and the influence of bed material, in Hey, R.D., Bathurst, J.C., and Thorne, C.R., eds., Gravel-bed rivers: New York, John Wiley & Sons Ltd., p. 389-422.

Anderson, D., and Brown, R., 1980, Preliminary report, survey of salmonid nursery areas, Redwood Creek basin, Humboldt County, California: Arcata CA, on file at Redwood National Park, 2 p.

Andrews, E.D., 1979, Scour and fill in a stream channel, East Fork River, western Wyoming: U.S. Geol. Surv. Prof. Paper 1117, 49 p.

Andrews, E.D., 1983, Entrainment of gravel from naturally sorted river bed material: Geol. Soc. Am. Bull., V. 94, p. 1225-1231.

Andrews, E.D., and Parker, G., 1987, Formation of a coarse surface layer as the response to gravel mobility, in Thorne, C.R., Bathurst, J.C., and Hey, R.D., eds., Sediment transport in gravel-bed rivers: New York, John Wiley & Sons Ltd., p. 269-325.

Ashworth, P.J., 1987, Bedload transport and channel change in gravel-bed rivers, Ph.D. thesis: Stirling, Scotland, Univ. of Stirling.

Ashworth, P.J., and Ferguson, R.I., 1989, Size-selective entrainment of bed load in gravel-bed streams: Water Resour. Res., V. 25, p. 627-634.

Bagnold, R.A., 1954, Experiments on a gravity-free dispersion of large solid spheres in a Newtonian fluid under shear: Proc. Roy. Soc. London, V. A225, 49-63.

Bagnold, R.A., 1973, The nature of saltation and of "bed load" transport in water: Proc. Roy. Soc. London, V. A332, 473-504.

Bagnold, R.A., 1977, Bedload transport by natural rivers: Water Resour. Res., V. 13, 303-312.

Baker, V.R., and Ritter, C.F., 1975, Competence of rivers to transport coarse bedload material: Geol. Soc. Am. Bull., V.86., p.975-978.

Bathurst, J.C., 1982, Theoretical aspects of flow resistance, in Hey, R.D., Bathurst, J.C., and Thorne, C.R., eds., Gravel-bed rivers: New York, John Wiley & Sons Ltd., p. 83-108.

Bathurst, J.C., Thorne, C.R., and Hey, R.D., 1979, Secondary flow and shear stress at river bends: J. Hydraul. Div., Amer. Soc. Civ. Eng., V. 105, p.1277-1295.

Beschta, R.L., 1981, Increased bag size improves Helley-Smith bedload sampler for use in streams with high sand and organic matter transport, in Erosion and sediment transport measurement, Internat. Assoc. of Hydrological Sciences, Pub. No. 133, p. 17-25.

Beschta, R.L. 1982. Comment on "Stream system evaluation with emphasis on spawning

habitat for salmonids" by Mastafa A. Shirazi and Wayne K. Seim., Water Resources Research, V. 18, p. 1292-1295.

Beschta, R.L., 1983, Effects of large organic debris on channel morphology, Proc. D.B. Simons Symposium on Erosion and Sedimentation: Fort Collins, Colorado, Simons, Li, & Assoc., p. 8.63-8.78.

Beschta, R.L., 1987, Conceptual models of sediment transport in streams, in Thorne, C.R., Bathurst, J.C., and Hey, R.D., eds., Sediment transport in gravel-bed rivers: New York, John Wiley & Sons Ltd., p. 387-419.

Beschta, R.L., O'Leary, S.J., Edwards, R.E., and Koop, K.D., 1981, Sediment Transport in Oregon Coast Range Streams, WRRI-70: Corvallis, OR, Oregon St. Univ., Water Resources Research Institute, 67 p.

Bisson, P.A., Nielsen, J.L., Palmason, R.A., and Grove, L.E., 1982, A system of naming habitat types in small streams with examples of habitat utilization by salmonids during low streamflow, in: Armantrout, N.B., ed., Acquisition and utilization of aquatic habitat inventory information, Proc. of a symposium held 28-30 October, 1981, Portland, OR, U.S.A.: Western Division, Amer. Fisheries Soc., pp.62-73.

Bisson, P.A., Bilby, R.E., Bryant, M.D., Dolloff, C.A., Grette, G.B., House, R.A., Murphy, M.L., Koski, K.V., and Sedell, J.A., 1987, Large woody debris in forested streams in the Pacific Northwest: past, present, and future, in Salo, E.O., and Cundy, T.W., eds., Streamside management: forestry and fisheries interactions, Contribution no. 57: Seattle, WA, College of Forest Resources, Univ. of Washington, p.143-190.

Bray, D.I., 1982, Flow resistance in gravel-bed rivers, in Hey, R.D., Bathurst, J.C., and Thorne, C.R., eds., Gravel-bed rivers: New York, John Wiley & Sons Ltd., p. 109-137.

Breusers, H.N.C., Nicollet, G., and Shen, H.W., 1977, Local scour around cylindrical piers. J. of Hydraul. Res., V. 15, p. 211-252.

Campbell, A.J., and Sidle, R.C., 1985, Bedload transport in a pool-riffle sequence of a coastal Alaska stream: Water Res. Bull., V. 21, p. 579-590.

Carling, P.A., 1983, Threshold of coarse sediment transport in broad and narrow natural streams: Earth Surface Processes and Landforms, V. 8, p. 1-18.

Carson, M.A., and Griffiths, G.A., 1987, Bedload transport in gravel channels: J. Hydrology, N.Z., V. 26, 151 p.

Carstens, M.R., 1966, Similarity laws for localized scour: J. Hydraul. Div., Am. Soc. Civ. Eng., V. 92, p. 13-16.

Chabert, J., and Engeldinger, P., 1956, Etude des affouillements autour des piles des ponts: Chatou, France (in French), Laboratoire National d'Hydraulique.

Cheetham, G.H., 1979, Flow competence in relation to stream channel form and braiding: Geol. Soc. Am. Bull., V. 90, p. 877-886.

Church, M., and Jones, D., 1982, Channel bars in gravel-bed rivers, in Hey, R.D., Bathurst, J.C., and Thorne, C.R., eds., Gravel-bed rivers: New York, John Wiley & Sons Ltd., p. 291-

338.

Costa, J.E., 1983, Paleohydraulic reconstruction of flash-flood peaks from boulder deposits in the Colorado Front Range: Geol. Soc. Am. Bull., V. 94, p. 986-1004.

Dietrich, W.E., Smith, J.D., and Dunne, T., 1979, Flow and sediment transport in a sand bedded meander: J. Geol., V. 87, p. 305-315.

Dietrich, W.E., and Smith, J.D., 1983, Influence of the point bar on flow through curved channels: Wat. Res. Res., V. 19, p. 1173-1192.

Dietrich, W.E., and Smith, J.D., 1984, Bedload transport in a river meander: Wat. Res. Res. V. 20, p. 1355-1380.

Dietrich, W.E., and Whiting, P., 1989, Boundary shear stress and sediment transport in river meanders of sand and gravel, in Ikeda, S., and Parker, G., eds., River meandering: Washington, D.C., Amer. Geophysical Union, p. 1-50.

Dingman, S.L., 1984, Fluvial Hydrology: New York, Freeman, 383 p.

Emmett, W.W, Leopold, L.B., and Myrick, R.M., 1983, Some characteristics of fluvial processes in rivers, Proc. second international symposium on river sedimentation: Water Resources, and Electric Power Press, China, p. 730-754.

Engelund, F., 1974, Flow and bed topography in channel bends: J. Hydraul. Div., Am. Soc. Civ. Eng., V. 100, p. 1631-1648.

Estep, M.A., 1982, Bedload sediment transport and channel morphology of a southeast Alaskan stream, M.S. thesis, Corvallis, OR, Oregon St. Univ., 144 p.

Everest, F.H., and Meehan, W.R., 1981, Forest management and anadromous fish habitat productivity, Transactions of the 46th North American Wildlife and Natural Resources Conf.: Washington, D.C., Wildlife Management Institute, p. 521-530.

Everest, F.H., Lotspeich, F.B., and Meehan, W.R., 1981, New perspectives on sampling, analysis, and interpretation of spawning gravel quality, in Armantrout, N.B., ed., Acquisition and utilization of aquatic habitat inventory information, Western Division, American Fisheries Society, Portland, OR, p. 325-333.

Everest, F.H., Beschta, R.L., Schrivener, J.C., Koski, K.V., Sedell, J.R., and Cederholm, C.J., 1987, Fine sediment and salmonid production: a paradox, in Salo, E.O., and Cundy, T.W., eds., Streamside management: forestry and fisheries interactions, Contribution no. 57: Seattle, WA, College of Forest Resources, Univ. of Washington, p.98-142.

Fenton, J.D., and Abbott, J.E., 1977, Initial movement of grains on a stream bed: the effect of relative protrusion: Proc. Royal Soc. London, V. 352, p. 523-537.

Folk, R.L., 1968, Petrology of Sedimentary Rocks: Austin, Texas, Hemphill's, 170 p.

Grant, G.E., Swanson, F.J., and Wolman, M.G., 1990, Pattern and origin of stepped-bed morphology in high-gradient streams, Western Cascades, Oregon: Geol. Soc. Am. Bull., V. 102, p. 340-352.

Gustavson, T.C., 1974, Sedimentation of gravel outwash fans, Malaspina Glacier foreland, Alaska: J. of Sedimentary Petrology, V. 44, p. 374-389.

Harden, D.R., Kelsey, H.M., Morrison, S., and Stephens, T., 1981, Geology of the Redwood Creek Basin, Humboldt County, California, Open-file Report 81-143: Menlo Park, CA, U.S. Geol. Surv., one sheet.

Harden, D.R., Janda, R.J., and Nolan, K.M., 1978, Mass movements and storms in the drainage basin of Redwood Creek, Humboldt County, California - a progress report, Open-file report 78-486: Menlo Park, CA, U.S. Geological Survey, 161 p.

Harmon, M.E., Franklin, J.F., Swanson, F.J., Sollins, P., Gregory, S.V., Lattin, J.D., Anderson, N.H., Cline, S.P., Aumen, N.G., Sedell, J.R., Lienkaemper, G.W., Cromack, K., Jr., and Cummins, K.W., 1986, Ecology of coarse woody debris in temperate ecosystems: Adv. Ecol. Res., V. 15, p. 133-302.

Hawks, A., Beschta, R.L., and Jackson, W.L., 1987, A lightweight, inexpensive footbridge for stream sampling, Tech. Bull. No. 36, Shorter Technical Methods (VI), British Geomorphological Research Group: Norwich, UK, Geo Books, p. 8-12.

Helley, E.J., and Smith, W., 1971, Development and calibration of a pressure difference bedload sampler, Open File Report: Menlo Park, CA, Water Res. Divis., U.S. Geol. Surv., 18 p.

Hey, R.D., 1979, Flow resistance in gravel-bed rivers: J. Hydraul. Div., Am. Soc. Civ. Eng., V. 107, p.365-379.

Hofstra, T., 1981, Aquatic resources rehabilitation program, Redwood national Park, in Coats, R.N. ed., Watershed Rehabilitation in Redwood National Park and Other Pacific Coastal Areas: Berkeley, CA, Center of Natural Resource Studies, John Muir Inst. Inc., p. 230-235.

Hogan, D., 1985, The influence of large organic debris on channel morphology in Queen Charlotte Island streams, Proc. West. Assoc. Fish and Wildlife Agen., p. 263-273.

Holtz, R.D., and Kovacs, W.D., 1981, An Introduction to Geotechnical Engineering, Englewood Cliffs, N.J., Prentice-Hall, 733 p.

Hooke, R.L., 1975, Distribution of sediment transport and shear stress in a meander bend: J. Geol., V. 83, p. 543-565.

Iwatsubo, R.T., Nolan, K.M., Harden, D.R., Glysson, G.D., 1976., Redwood National Park Studies, data release number 2, Redwood Creek, Humboldt County and Mill Creek, Del Norte County, California, Open File Report 76-678: Menlo Park, CA, U.S. Geol. Survey, 247 p.

Jackson, W.L., and Beschta, R.L., 1982, A model of two-phase bedload transport in an Oregon Coast Range stream: Earth Surface Processes and Landforms, V. 7, p. 517-527.

Janda, R.J., 1978, Summary of watershed conditions in the vicinity of Redwood National Park, California, Open File Report 78-25: Menlo Park, CA, U.S. Geol. Survey, 82 p.

Judson, S., and Ritter, D.F., 1964, Rates of regional denudation in the United States: J.

Geophys. Res., V. 69, p. 3395-3401.

Keller, E.A., 1971, Areal sorting of bed load material: The hypothesis of velocity reversal: Geol. Soc. of Amer. Bull., V. 82, p. 753-756.

Keller, E.A., and Swanson, F.J., 1979, Effects of large organic material on channel form and fluvial process: Earth Surface Processes, V. 4, p. 361-380.

Keller, E.A., and Tally, T., 1979, Effects of large organic debris on channel form and fluvial processes in the coastal redwood environment, in Rhodes, D., and Williams, G.P., eds., Adjustments of the fluvial system, Proceedings, Tenth annual geomorphology symposium, State University of New York, Binghamton: Dubuque, Iowa, Kendall/Hunt Publishing Co., p. 169-197.

Kelsey, H.M., 1980, A sediment budget and an analysis of geomorphic process in the Van Duzen River basin, north-coastal California, 1941-1975: Geol. Soc. Am. Bull., V. 91, p. 1119-1216.

Kelsey, H., Madej, M.A., Pitlick, J., Coghlan, M., Best, D., Belding, R., Stroud, P., 1981, Sediment sources and sediment transport in the Redwood Creek basin: a progress report, Tech. Report 3: Arcata, CA, Redwood National Park, 114 p.

Klingeman, P.C., and Emmett, W.W., 1982, Gravel bedload transport processes, in Hey, R.D., Bathurst, J.C., and Thorne, C.R., eds., Gravel-bed rivers: New York, John Wiley & Sons Ltd., p. 141-179.

Komar, P.D., 1987, Selective grain entrainment by a current from a bed of mixed sizes: a reanalysis: J. Sedimentary Petrology, V. 57, p. 203-211.

Komar, P.D., and Shih, S., 1988, Grain-size variations during transport and the equal mobility of gravels in Oak Creek, Oregon, Eos, Transactions, Am. Geophys. Union, V. 69, p. 1217-1218.

Komar, P.D., 1989, Flow-competence evaluations and the non-equal mobility of gravels in Oak Creek, Oregon, Eos, Transactions, Am. Geophys. Union, V. 69, p. 320.

Kuhnle, R.A., and Southard, J.B., 1988. Bed load transport fluctuations in a gravel bed laboratory channel: Water Resources Research, V. 24, p. 247-260.

Laursen, E.M., 1962, Scour at bridge crossings, Trans, Am. Soc. Civ. Eng., 127, Pt. 1, p. 116-179.

Leopold, L.B., 1982, Water surface topography in river channels and implications for meander development, in Hey, R.D., Bathurst, J.C., and Thorne, C.R., eds., Gravel-bed rivers: New York, John Wiley & Sons Ltd., p. 359-388.

Leopold, L.B., and Wolman, M.G., 1960, River Meanders, Geol. Soc. Am. Bull., V. 71, p. 769-794.

Leopold, L.B., Wolman, M.G., and Miller, J.P., 1964, Fluvial processes in geomorphology: San Francisco, W.H. Freeman and Co., 522 p.

Lewin, J., 1976, Initiation of bed forms and meanders in coarse-grained sediment: Geol.

Soc. Am. Bull., V. 87, p. 281-285.

Lisle, T.E., 1979, A sorting mechanism for a riffle-pool sequence: Geol. Soc. Am. Bull., V. 90, p.1142-1157.

Lisle, T.E., 1986, Stabilization of a gravel channel by large streamside obstructions and bedrock bends, Jacoby Creek, northwestern California: Geol. Soc. Am. Bull., vol. 97, p. 999-1011.

Lisle, T.E. and Kelsey, H.M., 1982, Effects of large roughness elements on the thalweg course and pool spacing, in Leopold, L.B., ed., Am. Geomorphological Field Group field trip guidebook, 1982 conference, Pinedale Wyo.: Berkeley, CA, Am. Geophys. Union, p. 134-135.

Madej, M.A., and Kelsey, H., 1981, Sediment routing in stream channels: its implications for watershed rehabilitation, in Coats, R.N. ed., Watershed rehabilitation in Redwood National Park and other Pacific coastal areas: Berkeley, CA, Center for Natural Resource Studies, John Muir Institute Inc., p. 17-25.

Max, T., 1989, mathematical statistician, personal communication: Portland, OR, U.S.D.A., Forest Service, Pacific Northwest Research Station

Melville, B.W., 1975, Local scour at bridge sites, Ph.D. thesis: Auckland, N.Z., Univ. of Auckland.

Melville, B.W., 1984, Live-bed scour at bridge piers: J. Hydraul. Eng., V. 110, p. 1234-1247.

Melville, B.W., and Sutherland, A.J., 1988, Design method for local scour at bridge piers: J. Hydraul. Eng., V. 114, p. 1210-1226.

Middleton, G.V., and Southard, J.B., 1984, Mechanics of sediment movement, short course no. 3: Tulsa, OK, Soc. Econ. Paleontologists and Mineralogists, 401 p.

Milhous, R.T., 1973, Sediment transport in a gravel-bottomed stream, Ph.D. thesis: Corvallis, OR, Oregon St. Univ., 232 p.

Miller, M.C., McCave, O.N., and Komar, P.D., 1977, Threshold of sediment motion under unidirectional currents: Sedimentology, V. 24, p. 507-527.

Nelson, J.M., and Smith, J.D., 1989 (a), Flow in meandering channels with natural topography, in Ikeda, S., and Parker, G., eds., River meandering: Washington, D.C., Amer. Geophysical Union, p. 69-102.

Nelson, J.M., and Smith, J.D., 1989 (b), Evolution and stability of erodible channel beds, in Ikeda, S., and Parker, G., eds., River meandering: Washington, D.C., Amer. Geophysical Union, p. 321-378.

Neter, J., Wasserman, W., and Kutner, M.H., 1983, Applied Linear Regression Models: Homewood, Ill., Irwin, Inc., 547 p.

Nolan, K.M., and Janda, R.J., 1981, Use of short-term water and suspended sediment discharge observations to assess impacts of logging on stream-sediment discharge in the Redwood Creek basin, northwestern California, U.S.A., in Davies, T.R.H., and Pearce, A.J.,

eds., Erosion and Sedimentation in Pacific Rim Steeplands, Publ. No. 132: Christchurch, N.Z., I.A.H.S., p. 415-437.

Ozaki, V.L., 1988, Geomorphic and hydrologic conditions for cold pool formation on Redwood Creek, California, Tech. Report 24: Arcata, CA, Redwood National Park, 57 p.

Parker, G., and Peterson, A.W., 1980, Bar resistance of gravel-bed streams: J. Hydraul. Div., Am. Soc. Civ. Eng., V. 106, p. 1559-1575.

Parker, G., and Klingeman, P.C., 1982, On why gravel-bed streams are paved: Water Resour. Res., V. 18, p. 1409-1423.

Parker, G., Klingeman, P.C., and McLean, D.G., 1982, Bedload and size distribution in paved gravel-bed streams: J. Hydraul. Div., Am. Soc. Civ. Eng., V. 108, p.544-571.

Pitlick, J., 1982, Sediment routing in tributaries of the Redwood Creek basin: northwestern California, Tech. Report 8: Arcata, CA, Redwood National Park, 67 p.

Prestegaard, K.L., 1983, Bar resistance in gravel-bed streams at bankfull stage: Water Resour. Res., V. 19, p. 472-476.

Reid, I., Frostick, L., and Layman, J.T., 1985, The incidence and nature of bedload transport during flood flows in coarse-grained alluvial channels: Earth Surface Processes and Landforms, V. 10, p.33-44.

Richards, K.S., 1976, The morphology of riffle-pool sequences: Earth Surface Processes and Landforms, V. 1, p. 71-88.

Richards, K.S., 1982, Rivers, form and process in alluvial channels: New York, Methuen, 358 p.

SAS Institute Inc., 1987, SAS/STAT guide for personal computers, Version 6 Edition: Cary, N.C., SAS Institute Inc., 1028 p.

Sedell, J.R., Bisson, P.A., June, J.A., and Speaker, R.W., 1982, Ecology and habitat requirements of fish populations in South Fork Hoh River, Olympic National Park, in Starkey, E.E., Franklin, J.F., and Matthews, J.W., eds., Ecological research in national parks of the Pacific Northwest: Corvallis, OR, Forest Research Laboratory, Oregon State University, p. 47-63.

Shen, H.W., and Komura, S., 1968, Meandering tendencies in straight alluvial channels: J. Hydraul. Div., Am. Soc. Civ. Eng., V. 94, p.997-1016.

Shields, A., 1936, Anwendung der Aehnlichkeitsmechanik und der Turbulenzforschung auf die Geschiebebewegung: Mitteilung der Preussichen Versuchsanstalt fur Wasserbau and Schiffbau, Heft 26, p. 98-109. (Transl.: Ott, W.P. and van Uchelen, J.C., Pub. no. 167: Pasadena, CA., Hydrodynamics Lab., Calif. Inst. of Technol.)

Sidle, R.C., 1988, Bedload transport regime of a small forest stream: Water Resour. Res., V. 24, p. 207-218.

Smith, J.D., and McLean, S.R., 1984, A model for flow in meandering streams: Wat. Res. Res., V.20, p. 1301-1315.

Snedecor, G.W., and Cochran, W.G., 1980, Statistical Methods: Ames, Iowa, Iowa St. Univ. Press, 507 p.

Souter, R.A., 1987, Comparison of regression equations among populations, unpublished report: Portland, OR., U.S.D.A., Forest Service, Pac. Northwest Research Station, 12 p.

Strahler, A.N., 1957, Quantitative analysis of watershed geomorphology: Am. Geophysical Union Trans., V. 38, p. 913-920.

Sullivan, K., 1986, Hydraulics and fish habitat in relation to channel morphology, Ph.D. thesis: Baltimore, Johns Hopkins Univ., 430 p.

Sutherland, A.J., 1967, Proposed mechanism for sediment entrainment by turbulent flows: Journal of Geophysical Research, V. 72, p. 6183-6194.

Swanson, F.J., Lienkaemper, G.W., and Sedell, J.R., 1976, History, physical effects, and management implications of large organic debris in western Oregon streams, USDA, Forest Service, Gen. Tech. Rep. PNW-56: Portland, OR, Pacific Northwest Forest and Range Experiment Stn., 15 p.

Swanson, F.J., and Lienkaemper, G.W., 1978, Physical consequences of large organic debris in Pacific Northwest streams, USDA, Forest Service, Gen. Tech. Rep., PNW-69: Portland, OR, Pac. Northwest Forest and Range Exp. Stn., 12 p.

Swanson, F.J., Benda, L.E., Duncan, S.H., Grant, G.E., Megahan, W.F., Reid, L.M., Ziemer, R.R., 1987, Mass failures and other processes of sediment production in Pacific Northwest forest landscapes, in Salo, E.O., and Cundy, T.W., eds., Streamside management: forestry and fisheries interactions, Contribution no. 57: Seattle, WA, College of Forest Resources, Univ. of Washington, p. 9-38.

Swanston, D.N., and Swanson, F.J., 1976, Timber harvesting, mass erosion, and steepland forest geomorphology in the Pacific Northwest, in Coates, D.R., ed., Geomorphology and engineering: Stroudsburg, PA, Dowden, Hutchinson, and Ross, p. 199-221.

Thompson, S.M., 1985, Transport of gravel by flows up to 500 m^3/s, Ohau River, Otago, N.Z.: J. Hydraul. Res., V. 23, p. 285-303.

Tison, L.J., 1961, Local scour in rivers: J. Geoph. Res., V. 66, p. 4227-4232.

Vanoni, V.A., ed., 1977, Sedimentation Engineering, Manual and report of engineering practice, no. 54: Amer. Soc. Civil Eng., 745 p.

Walkotten, W.H., 1976, An improved technique for freeze sampling stream bed sediments, Research Note PNW-281: Portland, OR, U.S.D.A., Forest Service, Pacific Northwest Research Station, 11 p.

White, W.R., and Day, T.J., 1982, Transport of graded gravel-bed material, in Hey, R.D., Bathurst, J.C., and Thorne, C.R., eds., Gravel-bed rivers: New York, John Wiley & Sons Ltd., p. 181-223.

Wilcock, P.R., 1988, Methods for estimating the critical shear stress of individual fractions in mixed-size sediment: Water Resour. Res., V. 24, p.1127-1135.

Wilcock, P.R., and Southard, J.B., 1988, Experimental studies of incipient motion in mixed-size sediment: Water Resour. Res., V. 24, p. 1137-1151.

Wolman, M.G., 1954, A method of sampling coarse river-bed material: Transactions, Am. Geophysical Union, V. 35, p. 951-956.

APPENDICES

APPENDIX A

Bed Material Grain-size Distribution

TABLE 9. BED MATERIAL GRAIN-SIZE DISTRIBUTION. All pavement and sub-pavement material to a depth of 40 cm is included. All clasts larger than 45 cm are excluded.

DATE	CORE	DEPTH (cm)	D50 (mm)	D84 (mm)	%<4mm	%<1mm
850117	1	0 to 10	16.69	35.23	17.70	3.80
850117	1	10 to 20	10.89	29.36	23.40	5.40
850117	1	20 to 30	11.51	33.94	33.40	16.00
850117	1	30 to 40	6.29	23.96	41.70	18.40
WT. MEAN	1	0 to 40	10.70	29.83	30.38	11.63
850117	2	0 to 10	21.49	38.09	12.10	4.40
850117	2	10 to 20	10.87	30.74	25.80	6.70
850117	2	20 to 30	4.88	23.44	47.20	21.60
850117	2	30 to 40	12.08	37.15	30.80	14.10
WT. MEAN	2	0 to 40	10.91	31.48	30.71	11.94
850117	3	0 to 10	18.96	35.28	17.10	7.30
850117	3	10 to 20	11.95	30.24	29.00	13.10
850117	3	20 to 30	11.26	27.55	29.30	18.20
850117	3	30 to 40	17.11	36.03	23.70	12.10
WT. MEAN	3	0 to 40	14.11	31.58	25.76	13.22
850425	1	0 to 10	11.26	26.90	28.40	10.90
850425	1	10 to 20	14.92	35.19	27.20	16.20
850425	1	20 to 30	19.14	39.54	25.40	14.50
850425	1	30 to 40	9.79	34.75	34.70	16.90
WT. MEAN	1	0 to 40	13.66	34.47	29.23	15.04

TABLE 9 CONTINUED. BED MATERIAL GRAIN-SIZE DISTRIBUTION. All pavement and sub-pavement material to a depth of 40 cm is included. All clasts larger than 45 cm are excluded.

DATE	CORE	DEPTH (cm)	D50	D84	%<4mm	%<1mm
850425	2	0 to 10	12.91	28.50	26.20	9.90
850425	2	10 to 20	19.20	32.32	13.70	3.90
850425	2	20 to 30	15.06	35.00	29.70	18.40
850425	2	30 to 40	10.59	27.07	32.00	16.00
WT. MEAN	2	0 to 40	14.80	31.61	25.69	13.06
850425	3	0 to 10	18.83	35.59	19.40	9.20
850425	3	10 to 20	9.82	28.52	28.20	11.40
850425	3	20 to 30	9.68	30.58	36.60	17.30
850425	3	30 to 40	11.74	35.41	30.90	15.80
WT. MEAN	3	0 to 40	11.95	32.62	29.80	14.06
851231	1	0 to 10	10.50	36.03	34.40	18.70
851231	1	10 to 20	6.48	21.57	40.00	19.60
851231	1	20 to 30	11.16	34.28	35.10	15.40
851231	1	30 to 40	7.12	26.58	38.70	16.90
WT. MEAN	1	0 to 40	8.91	30.10	36.92	17.31
851231	2	0 to 10	13.88	29.41	22.60	9.20
851231	2	10 to 20	14.10	32.32	27.50	15.20
851231	2	20 to 30	10.82	33.57	31.90	14.50
851231	2	30 to 40	10.68	35.37	31.90	13.70
WT. MEAN	2	0 to 40	12.13	33.37	29.75	14.16

TABLE 9 CONTINUED. BED MATERIAL GRAIN-SIZE DISTRIBUTION. All pavement and sub-pavement material to a depth of 40 cm is included. All clasts larger than 45 cm are excluded.

DATE	CORE	DEPTH (cm)	D50	D84	%<4mm	%<1mm
851231	3	0 to 10	14.59	34.28	21.20	9.50
851231	3	10 to 20	21.24	39.60	24.00	12.80
851231	3	20 to 30	7.37	27.00	38.20	20.50
851231	3	30 to 40	12.03	31.88	28.80	14.10
WT. MEAN	3	0 to 40	14.40	33.66	28.28	14.50
860327	1	0 to 10	7.70	35.00	37.80	11.00
860327	1	10 to 20	15.56	37.68	28.70	11.50
860327	1	20 to 30	15.32	36.00	26.60	10.50
860327	1	30 to 40	18.40	38.58	23.10	7.90
WT. MEAN	1	0 to 40	14.06	36.77	29.46	10.51
860327	2	0 to 10	13.69	31.04	24.50	9.70
860327	2	10 to 20	13.14	32.91	31.70	13.20
860327	2	20 to 30	5.72	30.17	43.80	20.20
860327	2	30 to 40	8.69	34.33	35.10	16.50
WT. MEAN	2	0 to 40	10.63	32.27	33.73	14.80
860327	3	0 to 10	15.59	34.55	25.70	9.80
860327	3	10 to 20	10.10	35.76	32.90	13.80
860327	3	20 to 30	6.93	23.54	38.00	11.90
860327	3	30 to 40	7.87	28.72	38.00	17.60
WT. MEAN	3	0 to 40	10.82	31.46	32.69	13.15

TABLE 9 CONTINUED. BED MATERIAL GRAIN-SIZE DISTRIBUTION. All pavement and sub-pavement material to a depth of 40 cm is included. All clasts larger than 45 cm are excluded.

DATE	CORE	DEPTH (cm)	D50	D84	%<4mm	%<1mm
SUMMARY:						
SURFACE (0 cm to 10 cm)						
	850117		18.615	35.848	16.289	5.346
	850425		14.102	30.074	24.950	10.078
	851231		12.528	34.439	27.720	13.866
	860327		12.555	33.937	29.463	10.177
WT. MEAN			14.501	33.578	24.556	9.702
SUBSURFACE (10 cm to 40 cm)						
	850117		7.337	29.995	31.388	13.684
	850425		13.533	33.303	28.540	14.675
	851231		11.825	32.082	32.167	15.539
	860327		11.679	33.444	32.702	13.601
WT. MEAN			11.078	32.101	30.958	14.447
TOTAL (0 cm to 40 cm)						
	850117		11.970	30.975	28.861	12.289
	850425		13.619	32.815	27.998	13.980
	851231		11.931	32.439	31.493	15.286
	860327		11.907	33.572	31.857	12.708
WT. MEAN			12.427	32.361	29.831	13.611

APPENDIX B

Velocity Profiles

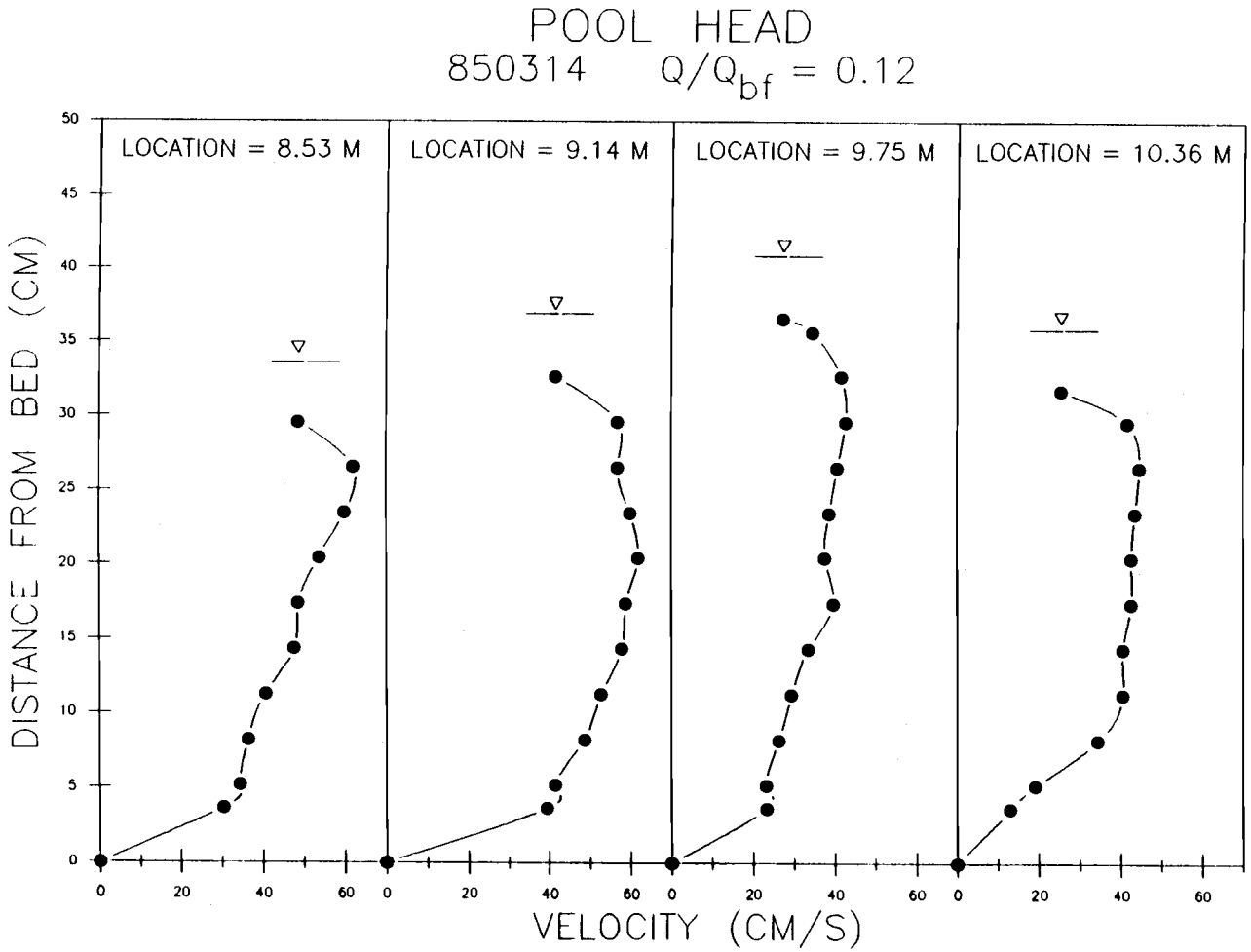

Figure 47. Velocity profiles for the pool head at low discharge. Locations are the distance from the left survey monument (Fig. 2). Q is water discharge. Q_{bf} is bankfull discharge.

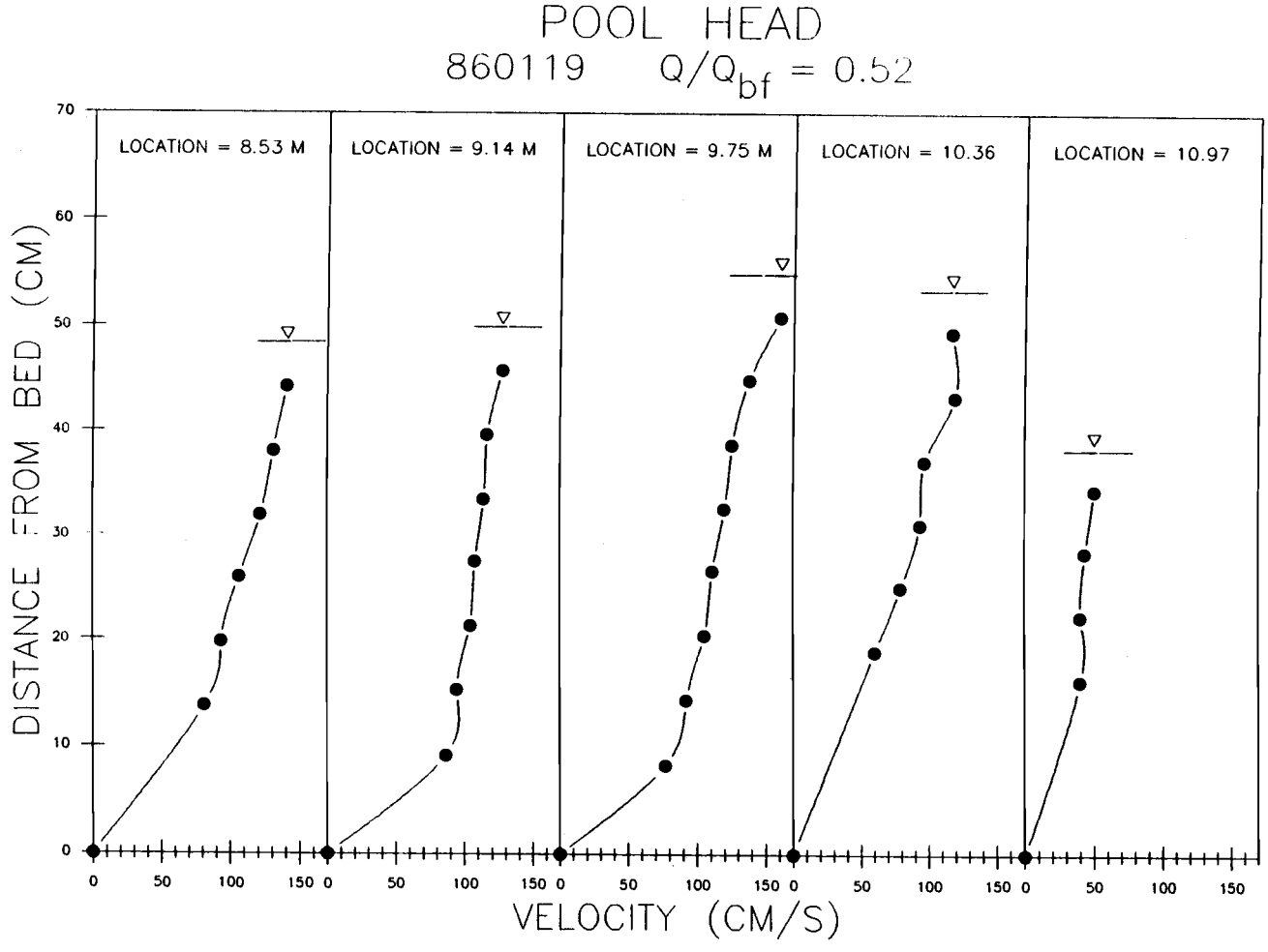

Figure 48. Velocity profiles for the pool head at moderate discharge. Locations are the distance from the left survey monument (Fig. 2). Q is water discharge. Q_{bf} is bankfull discharge.

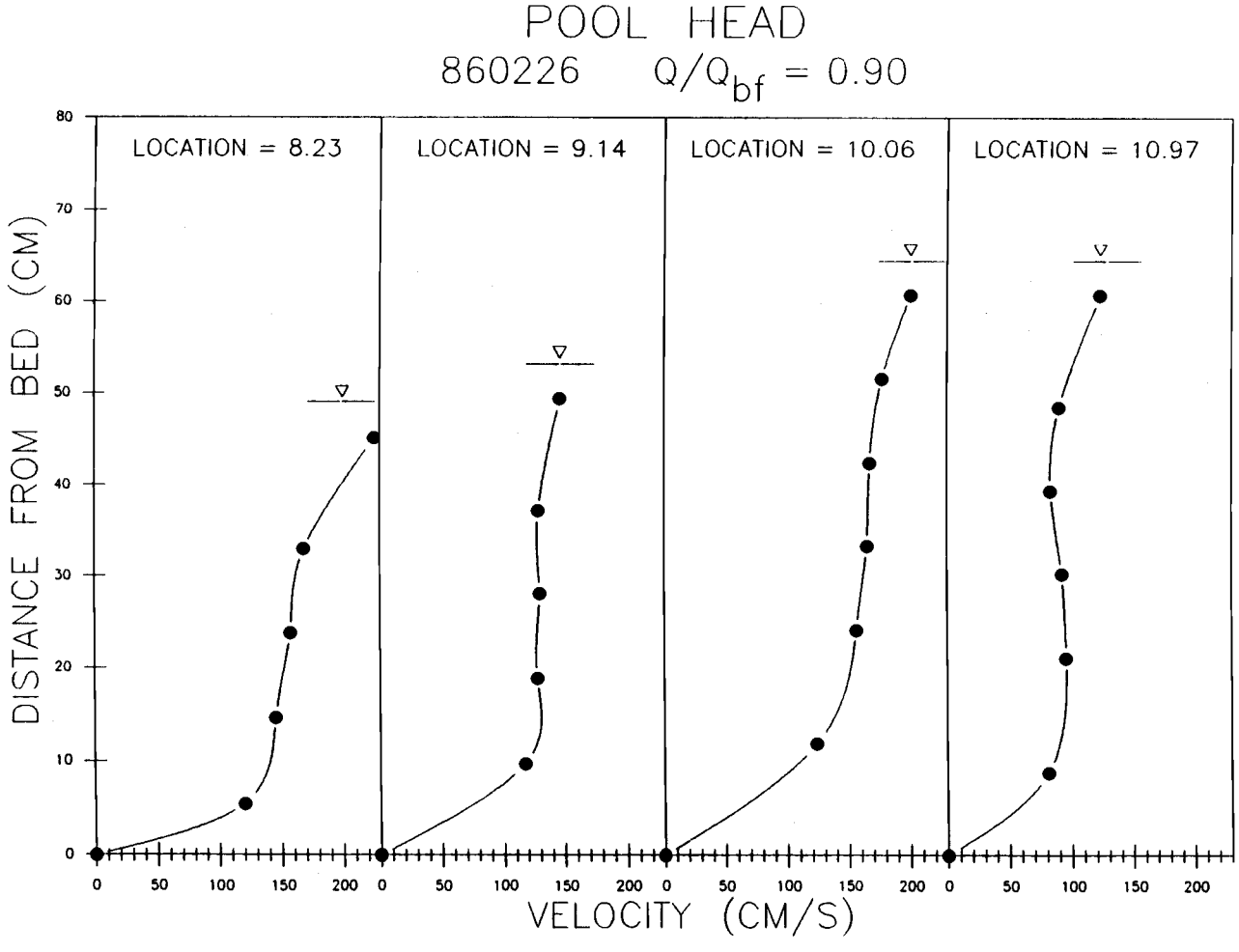

Figure 49. Velocity profiles for the pool head at high discharge. Locations are the distance from the left survey monument (Fig. 2). Q is water discharge. Q_{bf} is bankfull discharge.

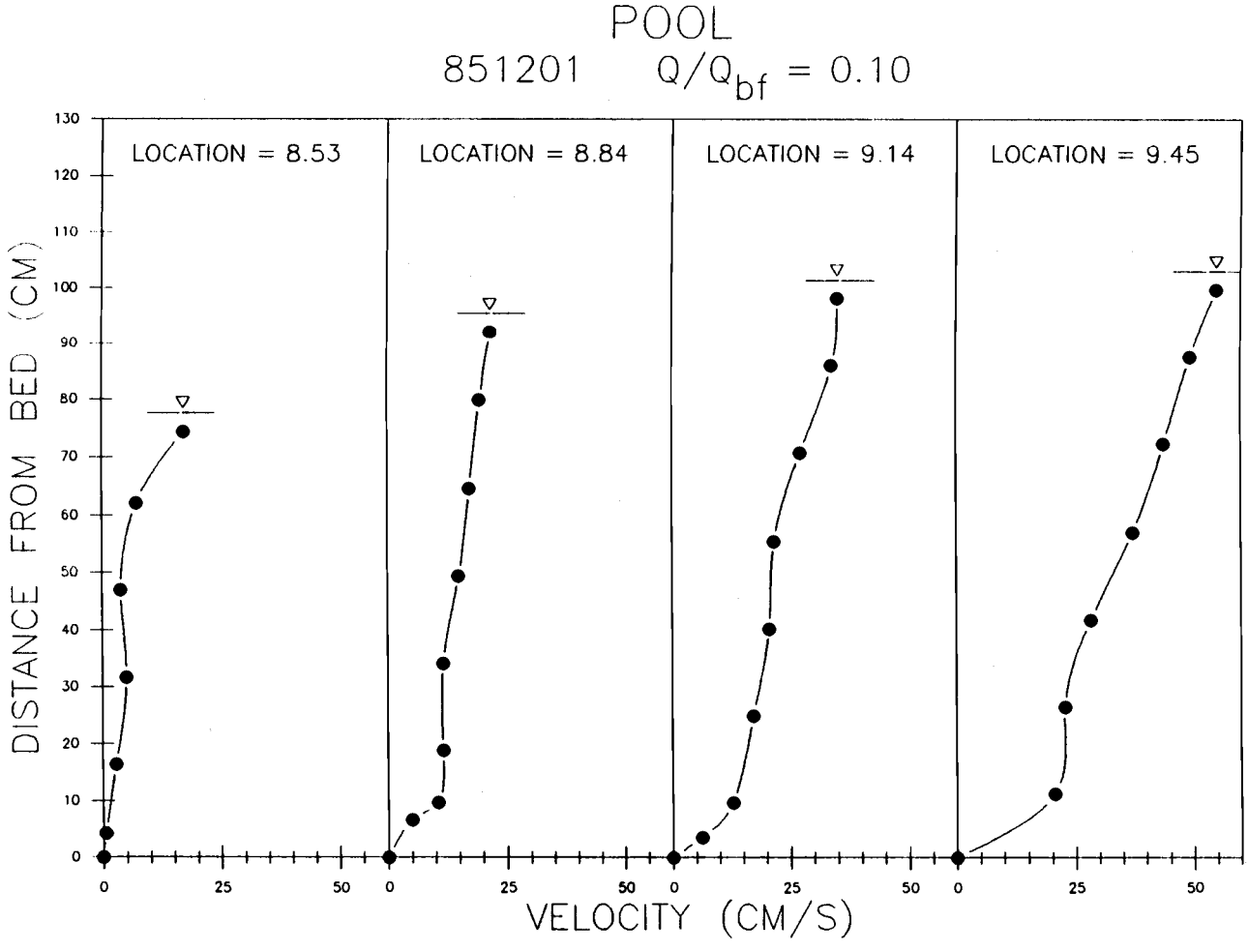

Figure 50. Velocity profiles for the pool at low discharge. Locations are the distance from the left survey monument (Fig. 2). Q is water discharge. Q_{bf} is bankfull discharge.

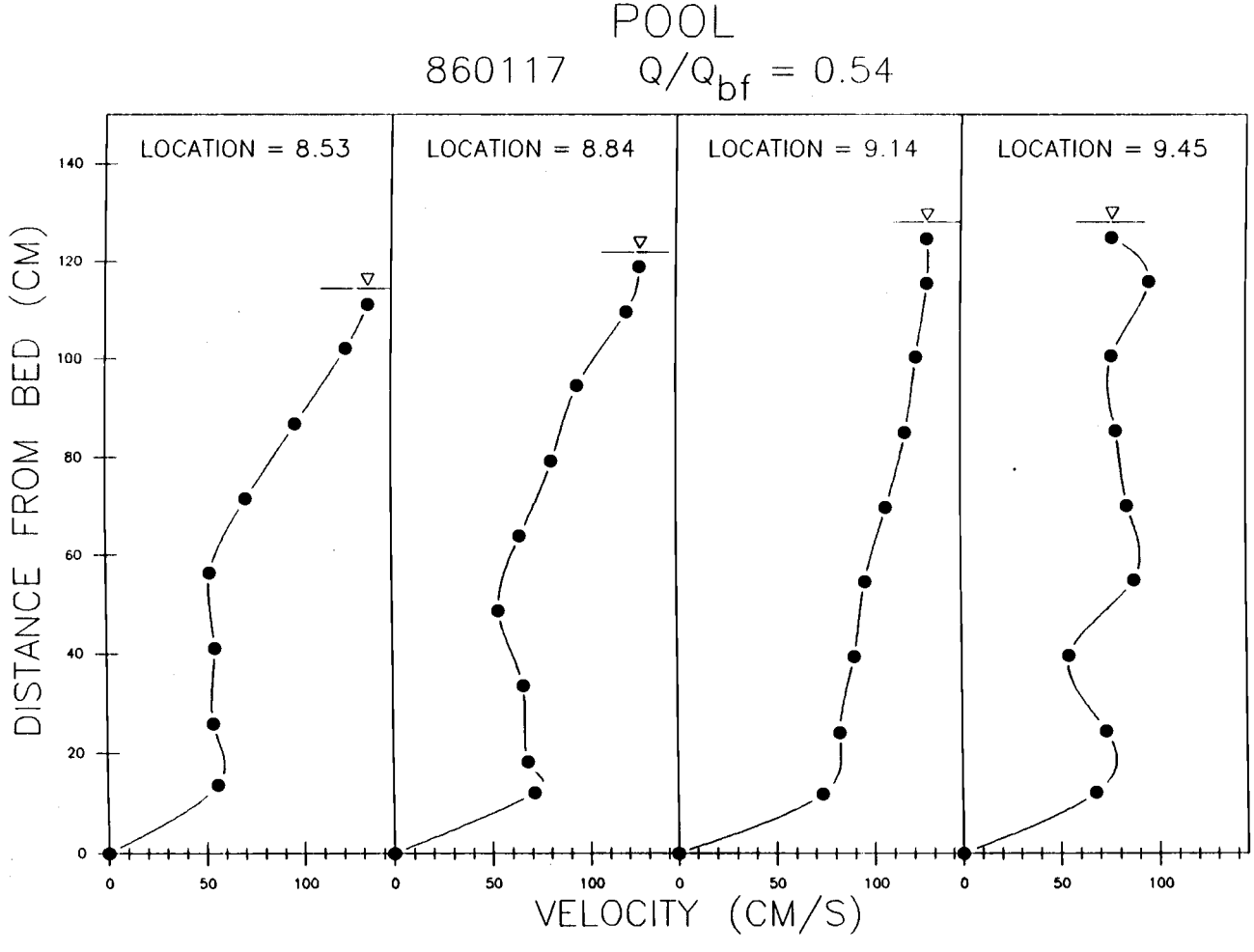

Figure 51. Velocity profiles for the pool at moderate discharge. Locations are the distance from the left survey monument (Fig. 2). Q is water discharge. Q_{bf} is bankfull discharge.

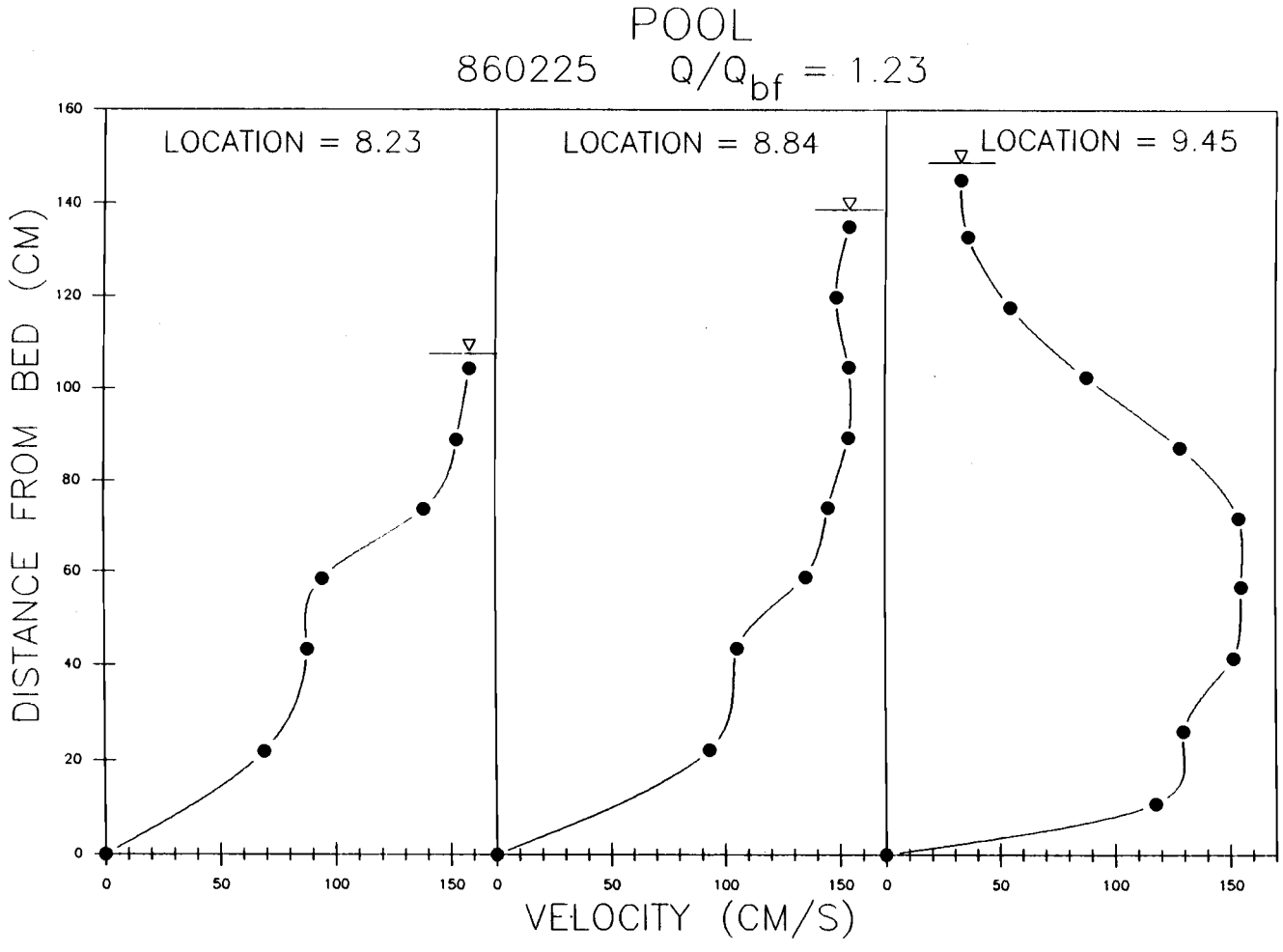

Figure 52. Velocity profiles for the pool at high discharge. Locations are the distance from the left survey monument (Fig. 2). Q is water discharge. Q_{bf} is bankfull discharge.

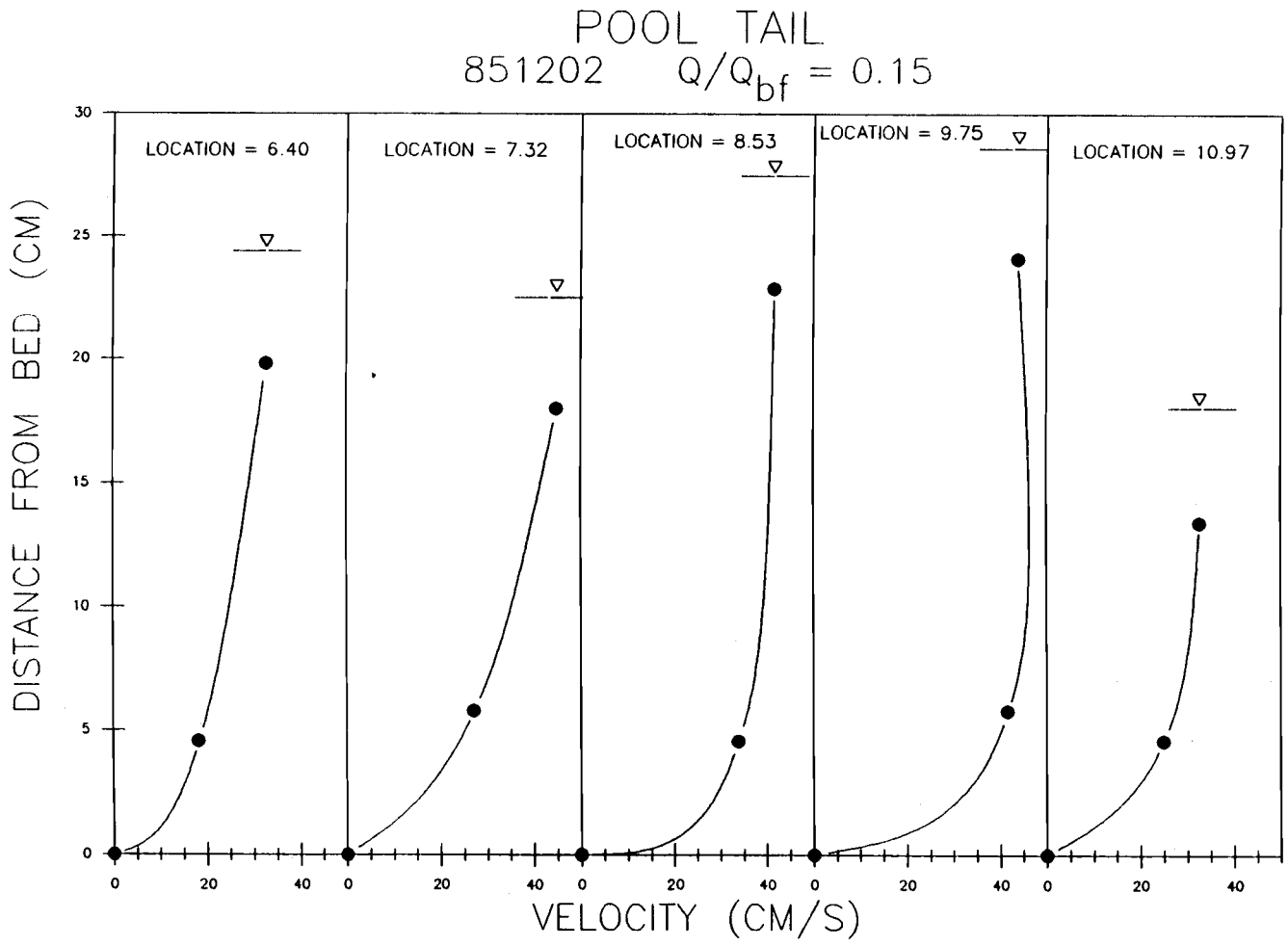

Figure 53. Velocity profiles for the pool tail at low discharge. Locations are the distance from the left survey monument (Fig. 2). Q is water discharge. Q_{bf} is bankfull discharge.

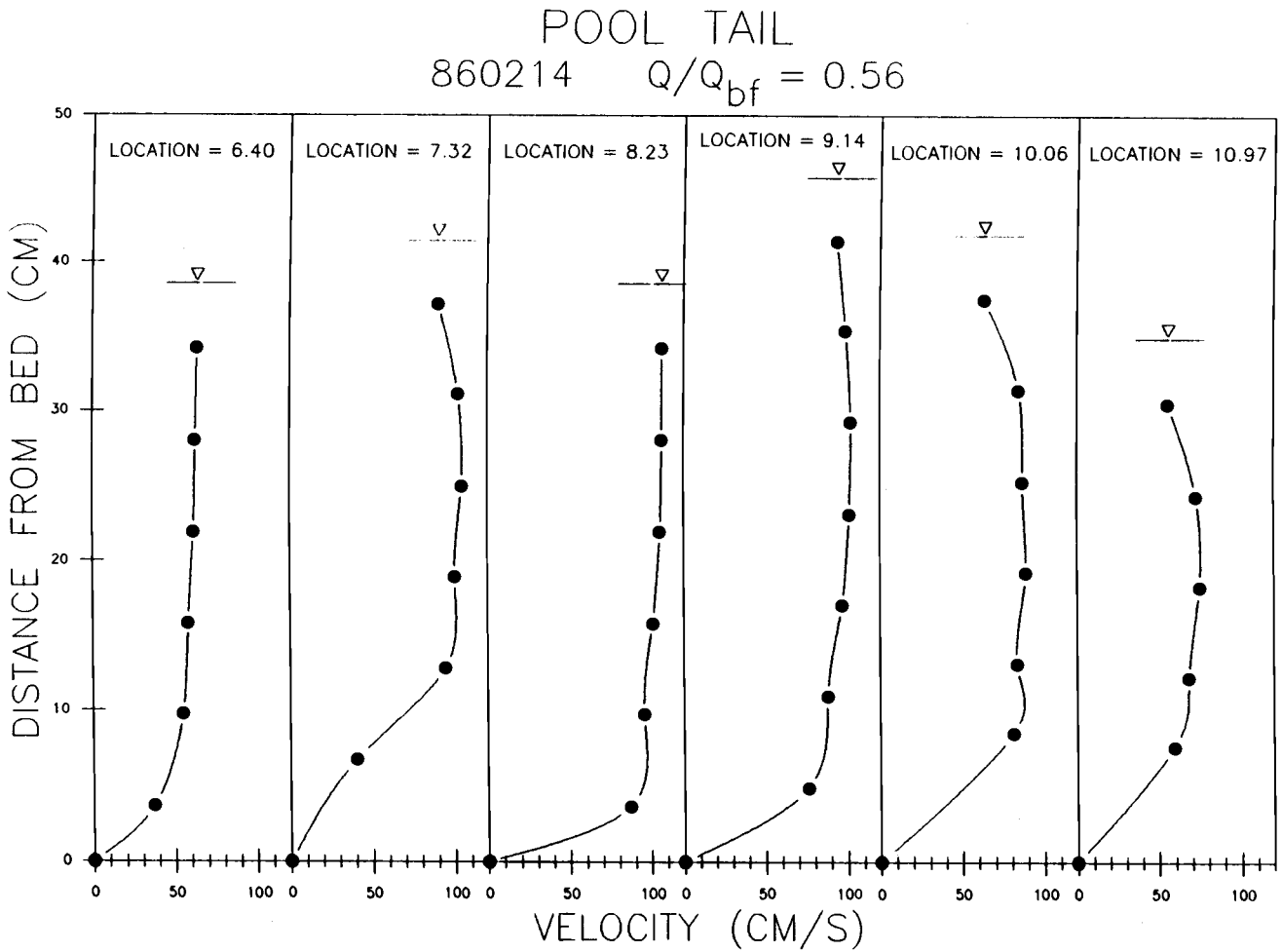

Figure 54. Velocity profiles for the pool tail at moderate discharge. Locations are the distance from the left survey monument (Fig. 2). Q is water discharge. Q_{bf} is bankfull discharge.

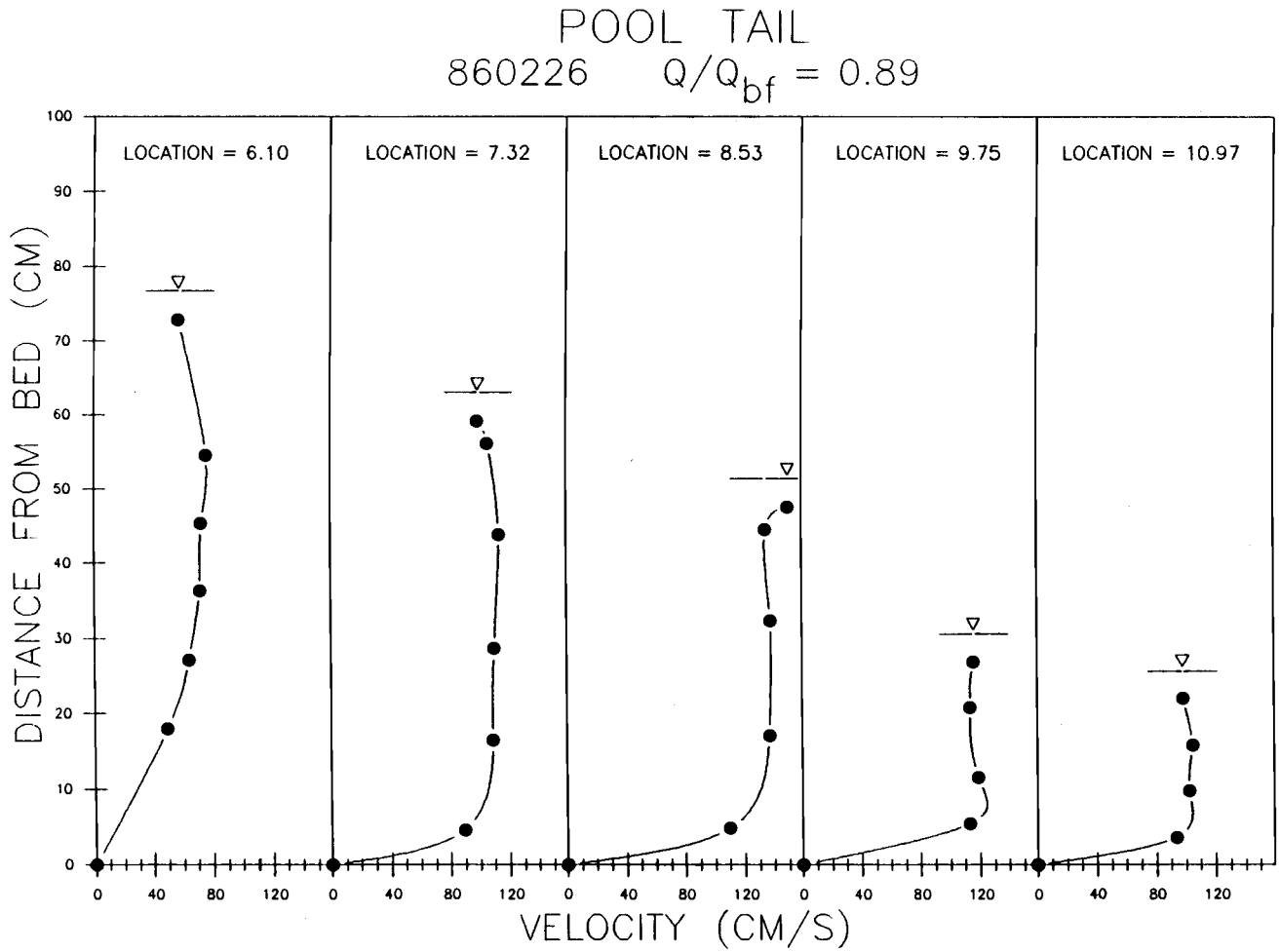

Figure 55. Velocity profiles for the pool tail at high discharge. Locations are the distance from the left survey monument (Fig. 2). Q is water discharge. Q_{bf} is bankfull discharge.

APPENDIX C

Cross-stream Velocity Profiles

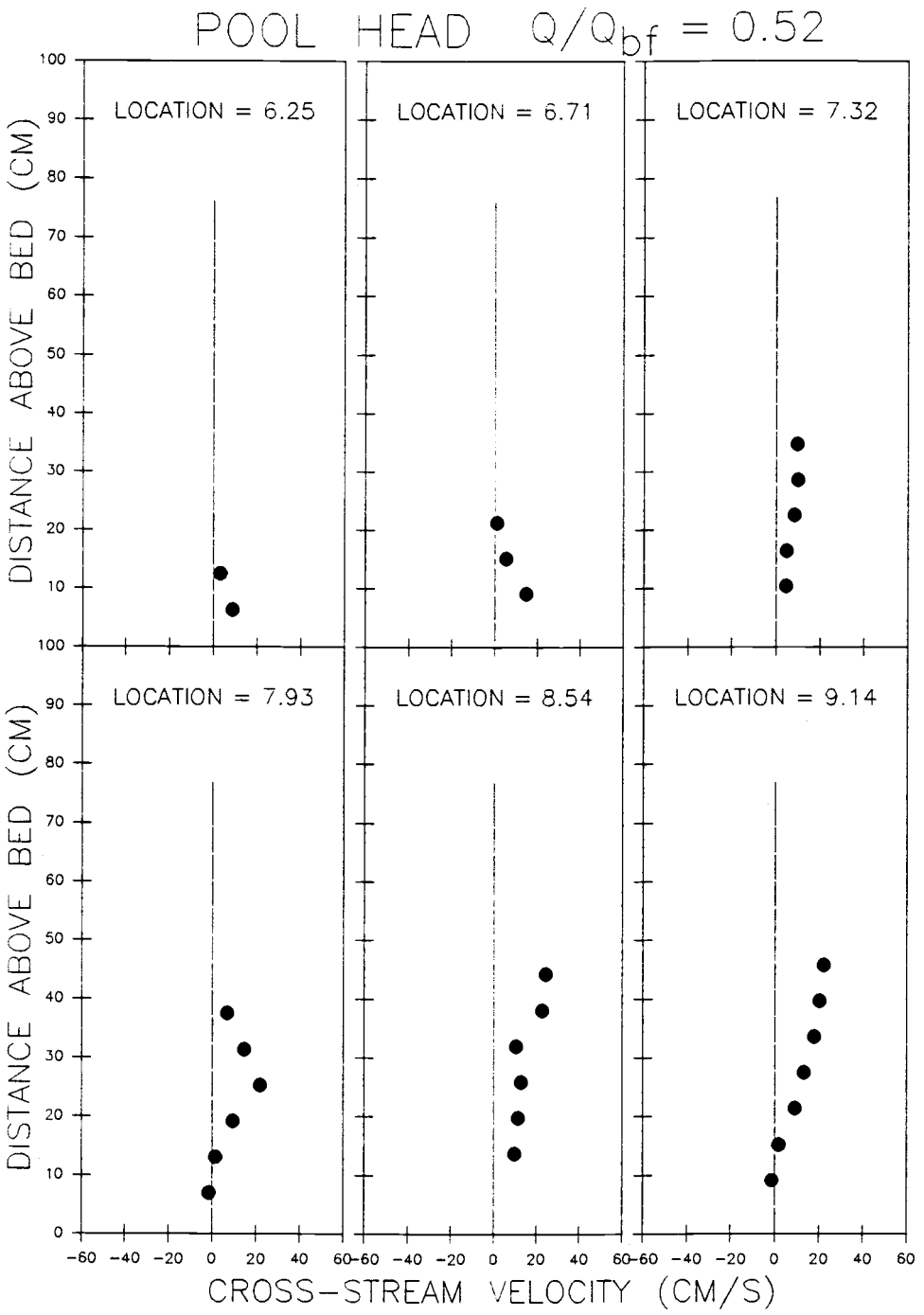

Figure 56. Cross-stream velocity profiles for the pool head at moderate discharge. Locations are the distance from the left survey monument (Fig. 2). Q is water discharge. Q_{bf} is bankfull discharge.

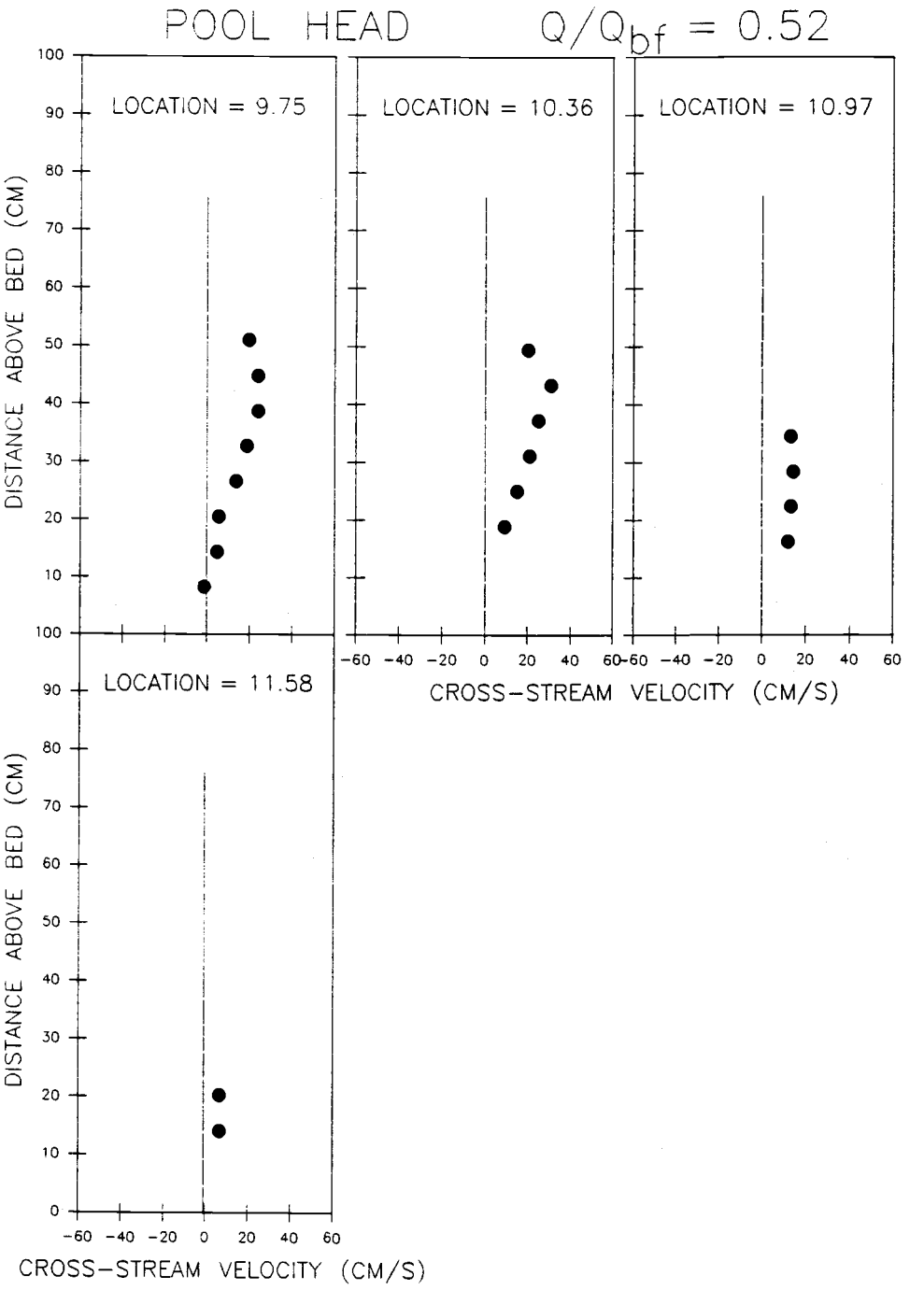

Figure 57. Cross-stream velocity profiles for the pool head at moderate discharge. Locations are the distance from the left survey monument (Fig. 2). Q is water discharge. Q_{bf} is bankfull discharge.

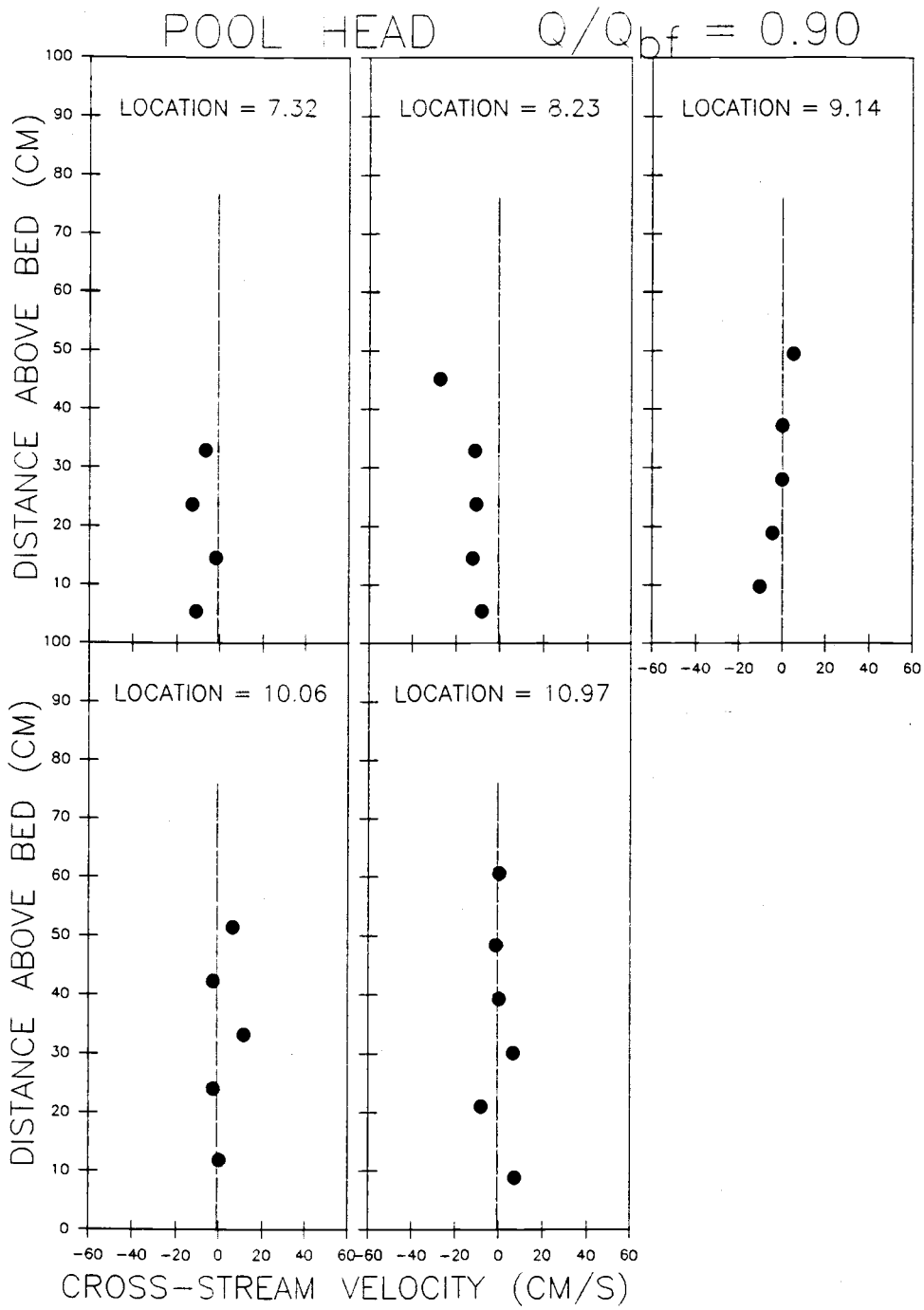

Figure 58. Cross-stream velocity profiles for the pool head at high discharge. Locations are the distance from the left survey monument (Fig. 2). Q is water discharge. Q_{bf} is bankfull discharge.

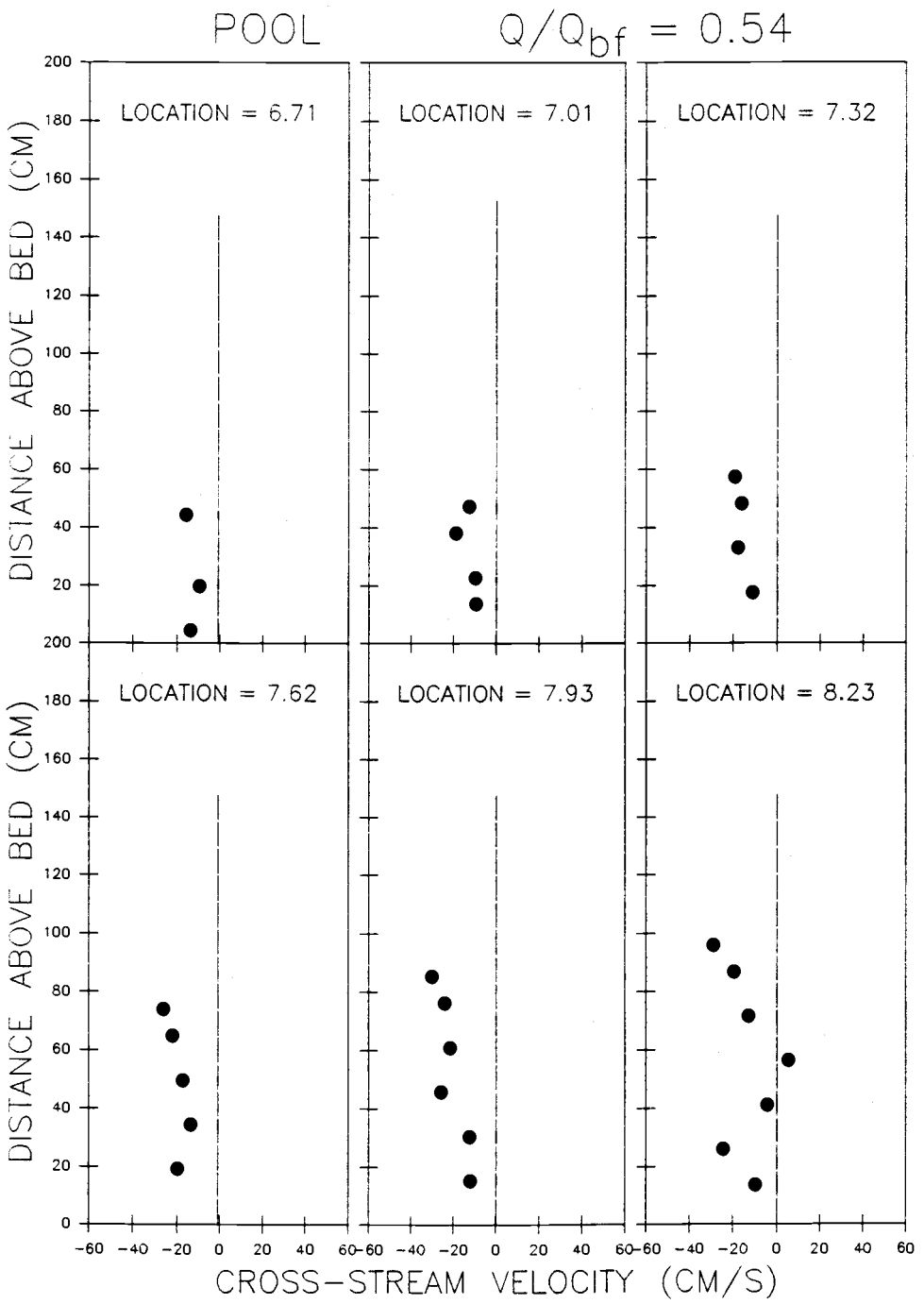

Figure 59. Cross-stream velocity profiles for the pool at moderate discharge. Locations are the distance from the left survey monument (Fig. 2). Q is water discharge. Q_{bf} is bankfull discharge.

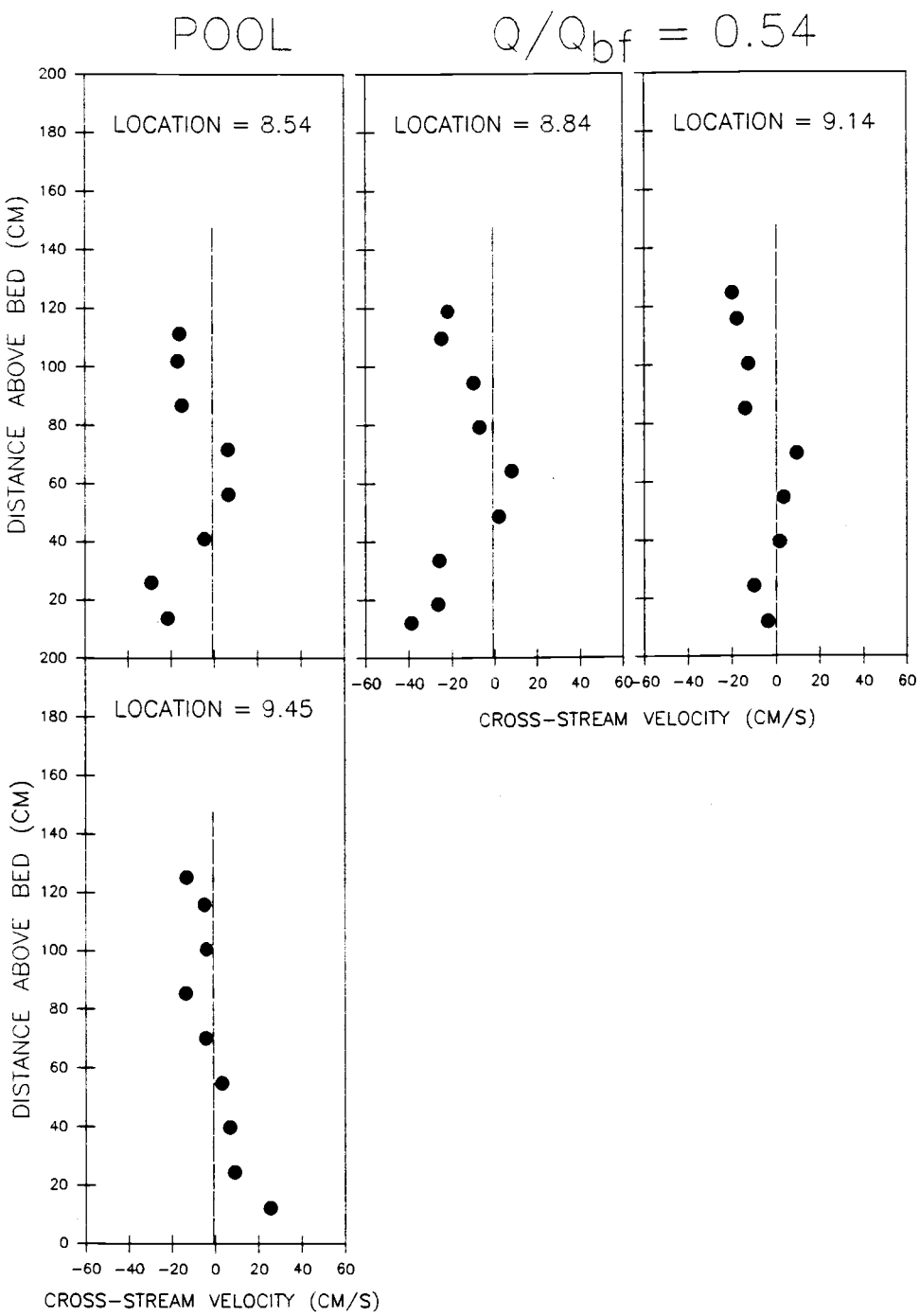

Figure 60. Cross-stream velocity profiles for the pool at moderate discharge. Locations are the distance from the left survey monument (Fig. 2). Q is water discharge. Q_{bf} is bankfull discharge.

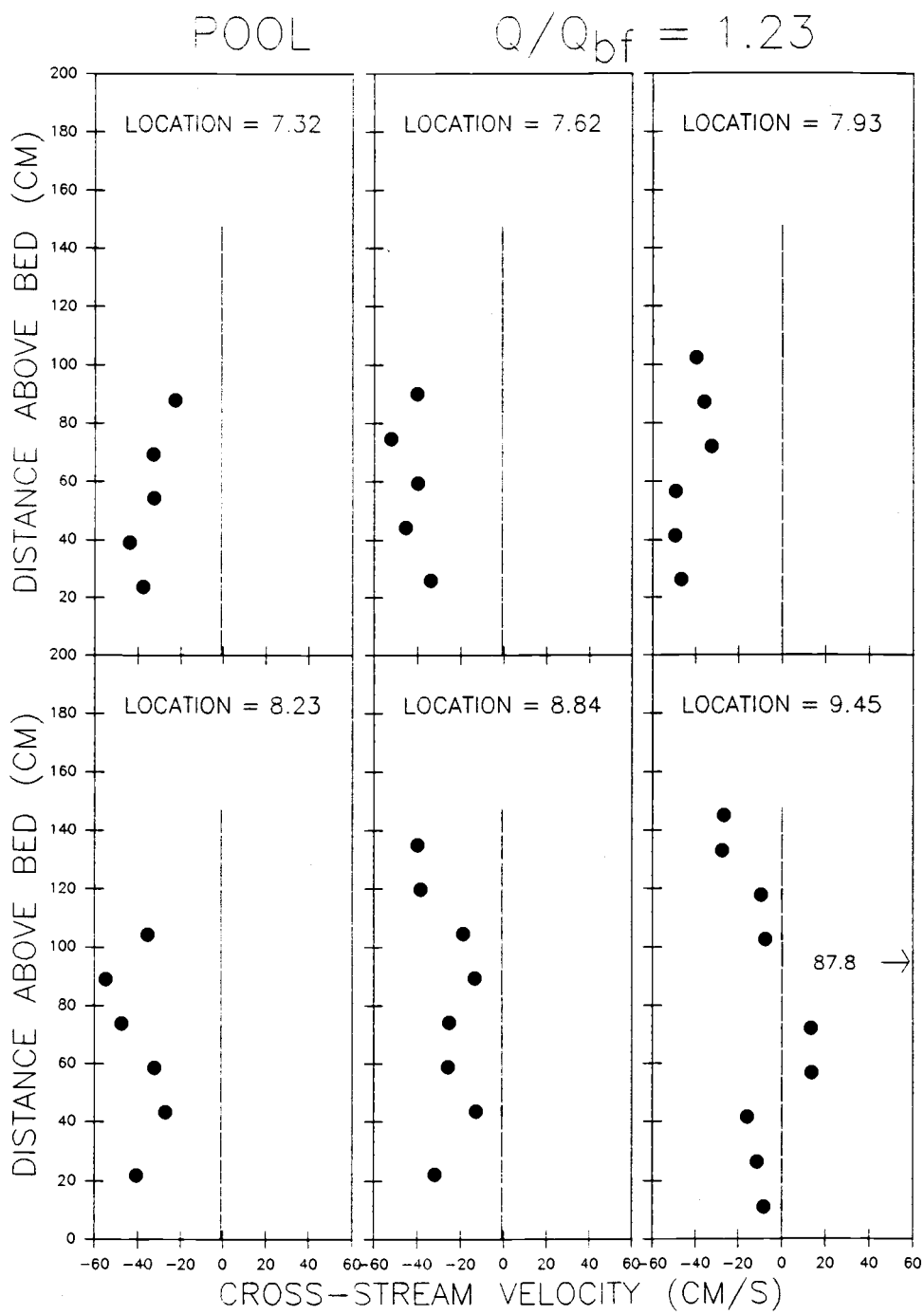

Figure 61. Cross-stream velocity profiles for the pool at high discharge. Locations are the distance from the left survey monument (Fig. 2). Q is water discharge. Q_{bf} is bankfull discharge.

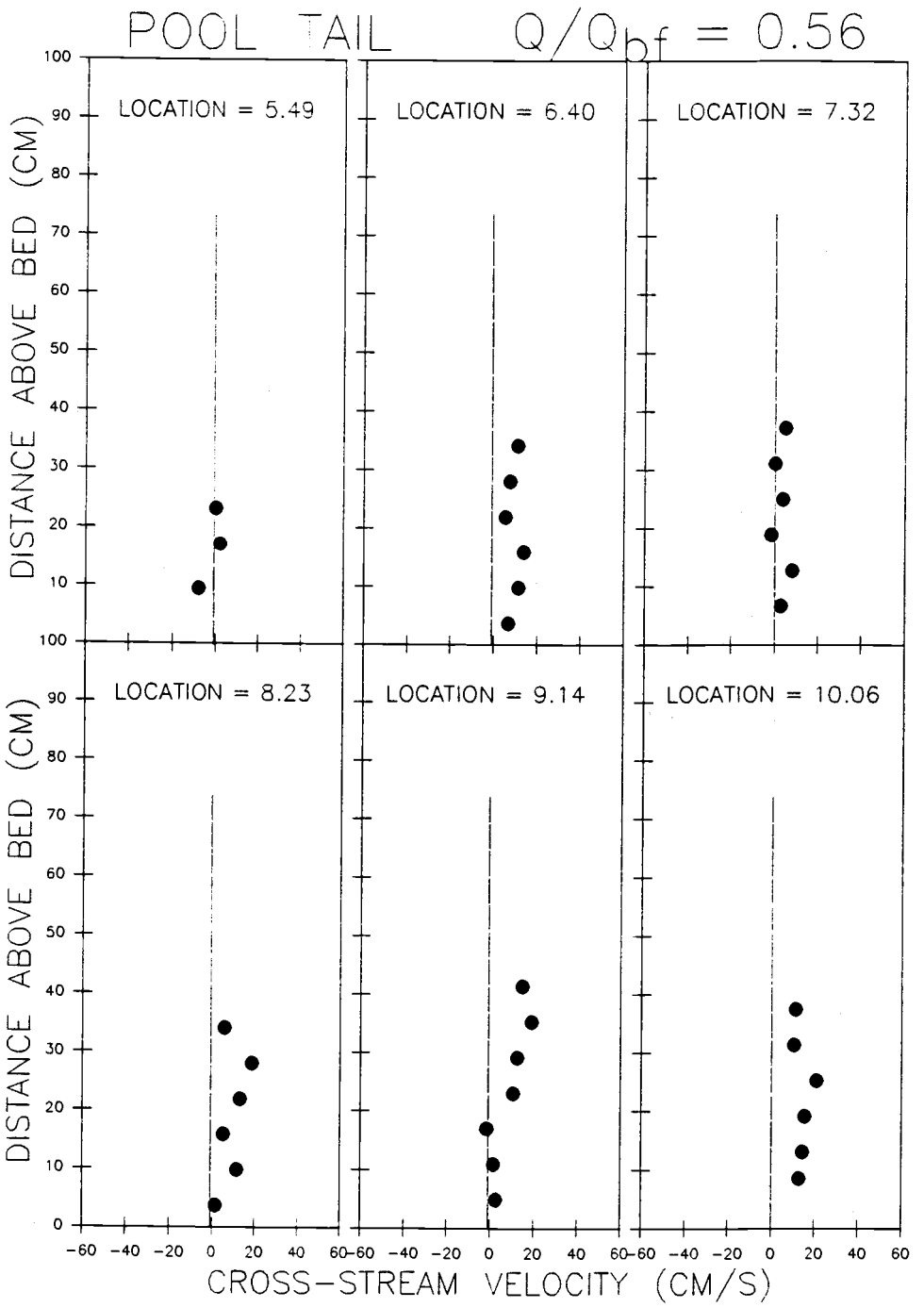

Figure 62. Cross-stream velocity profiles for the pool tail at moderate discharge. Locations are the distance from the left survey monument (Fig. 2). Q is water discharge. Q_{bf} is bankfull discharge.

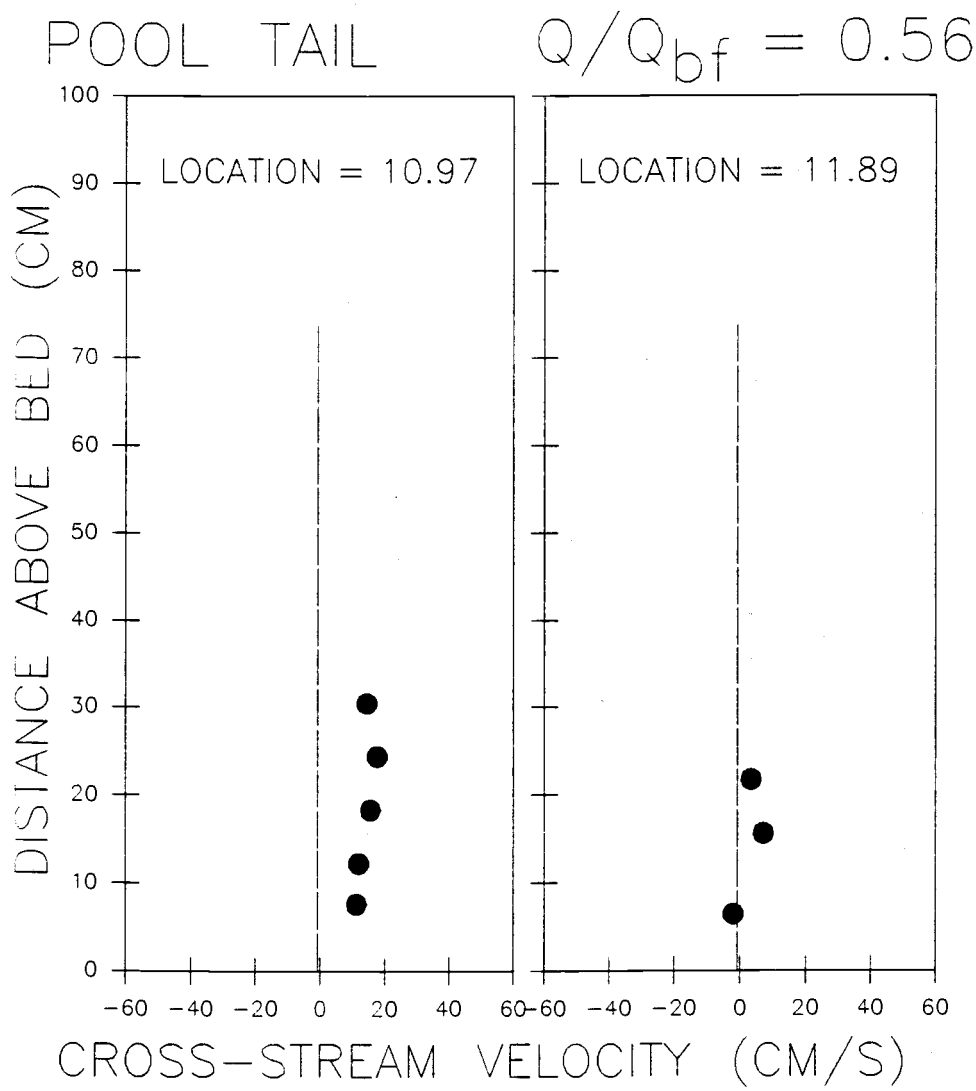

Figure 63. Cross-stream velocity profiles for the pool tail at moderate discharge. Locations are the distance from the left survey monument (Fig. 2). Q is water discharge. Q_{bf} is bankfull discharge.

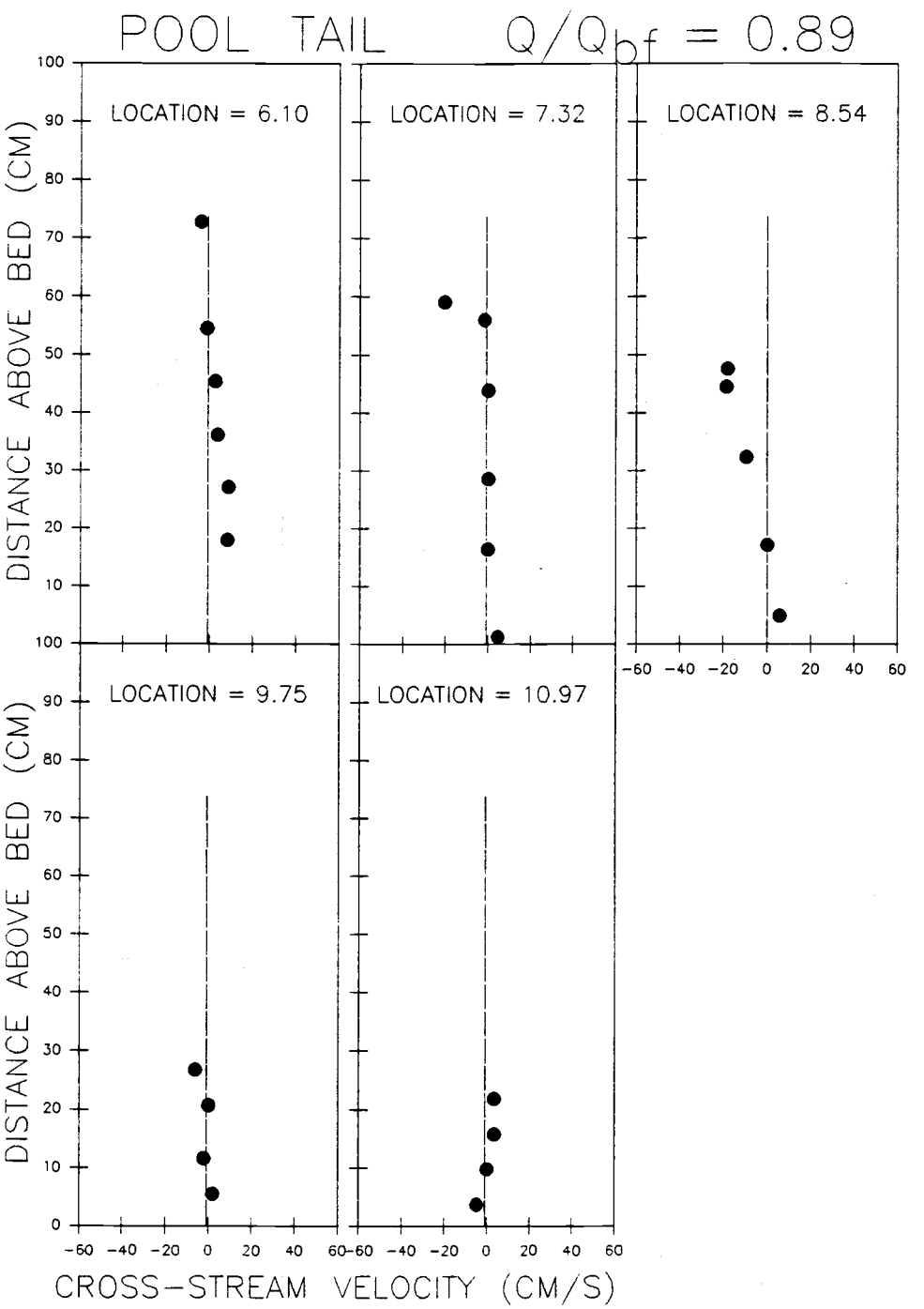

Figure 64. Cross-stream velocity profiles for the pool tail at high discharge. Locations are the distance from the left survey monument (Fig. 2). Q is water discharge. Q_{bf} is bankfull discharge.

APPENDIX D-1

TABLE 10(a). ANALYSIS OF COVARIANCE TESTS FOR COMMON REGRESSION OF NEAR-BED VELOCITY VS DISCHARGE RELATIONSHIP FOR ALL STATIONS. Stations 1, 2, and 3 refer to the pool head, pool, and pool tail respectively. See text for explanation.

STATIONS	REDUCTION OF SS	MODEL MSE	F VALUE	P > F	H_o:
		H_o: SLOPES ARE NOT STATISTICALLY DIFFERENT			
1, 2	39.2	128.8	0.30	0.59	ACCEPT
2, 3	44.3	80.50	0.55	0.47	ACCEPT
1, 3	124	149.5	0.83	0.37	ACCEPT
		H_o: INTERCEPTS ARE NOT STATISTICALLY DIFFERENT			
1, 2	2750	124.7	22.05	0.00	REJECT
2, 3	3740	79.05	47.26	0.00	REJECT
1, 3	16.0	148.3	0.11	0.75	ACCEPT

APPENDIX D-2

TABLE 10(b). ANALYSIS OF COVARIANCE TESTS FOR COMMON REGRESSION OF NEAR-BED VELOCITY VS DISCHARGE RELATIONSHIP FOR A SUBSET OF THE DATA FROM ALL STATIONS. Stations 1, 2, and 3 refer to the pool head, pool, and pool tail respectively. See text for explanation.

STATIONS	REDUCTION OF SS	MODEL MSE	F VALUE	P > F	H_o:
		H_o: SLOPES ARE NOT STATISTICALLY DIFFERENT			
1, 2	5.84	34.60	0.17	0.69	ACCEPT
2, 3	0.16	13.00	0.01	0.91	ACCEPT
1, 3	4.81	26.58	0.18	0.67	ACCEPT
		H_o: INTERCEPTS ARE NOT STATISTICALLY DIFFERENT			
1, 2	883.3	31.72	27.85	0.00	REJECT
2, 3	1398.0	12.01	116.5	0.00	REJECT
1, 3	31.84	25.02	1.27	0.27	ACCEPT

APPENDIX E

TABLE 11. ANALYSIS OF COVARIANCE TESTS FOR COMMON REGRESSION OF SHEAR VELOCITY VS DISCHARGE RELATIONSHIP FOR ALL STATIONS. Stations 1, 2, and 3 refer to the pool head, pool, and pool tail respectively. See text for explanation.

STATIONS	REDUCTION OF SS	MODEL MSE	F VALUE	P > F	H_o:
		H_o: SLOPES ARE NOT STATISTICALLY DIFFERENT			
1, 2	2.39	1.91	1.25	0.29	ACCEPT
2, 3	0.15	0.50	0.30	0.59	ACCEPT
1, 3	1.63	1.47	1.11	0.31	ACCEPT
		H_o: INTERCEPTS ARE NOT STATISTICALLY DIFFERENT			
1, 2	189.2	1.96	96.26	0.00	REJECT
2, 3	94.47	0.48	196.2	0.00	REJECT
1, 3	28.49	1.48	19.22	0.00	REJECT

APPENDIX F

TABLE 12. PEAK FLOWS EXCEEDING 1.82 m^3/s (0.5 Q_{bf}). Q is water discharge. Q_{bf} is bankfull discharge.

DATE	DAY #	TIME	Q (m^3/s)	Q/Q_{bf}	
850212	408	1213	1.99	0.55	
851208	707	1415	1.81	0.50	
860116	746	2100	3.29	0.90	
860119	749	1100	1.95	0.54	
860122	752	1800	2.11	0.58	
860202	763	1545	2.54	0.70	
860203	764	1313	3.37	0.93	
860214	775	1417	2.08	0.57	
860216	777	0000	4.78	1.31	
860216	777	1742	7.63	2.10	
860217	778	2000	26.33	7.23	(1)
860222	783	1230	11.88	3.26	
860222	783	2300	11.92	3.27	
860305	794	0130	2.22	0.61	
860305	794	0600	2.69	0.74	
860306	795	1300	2.45	0.67	
860307	796	2100	2.60	0.71	
860309	798	0500	2.45	0.67	
860309	798	1235	2.45	0.67	
860310	799	0900	2.51	0.69	
860311	800	0400	2.91	0.80	
860311	800	1729	2.36	0.65	
860312	801	0700	3.88	1.07	
860313	802	0000	3.76	1.03	
860313	802	1800	3.18	0.87	
860315	804	1000	2.98	0.82	

(1) EXTRAPOLATED FROM RATING CURVE

APPENDIX G

Cross-sectional Soundings

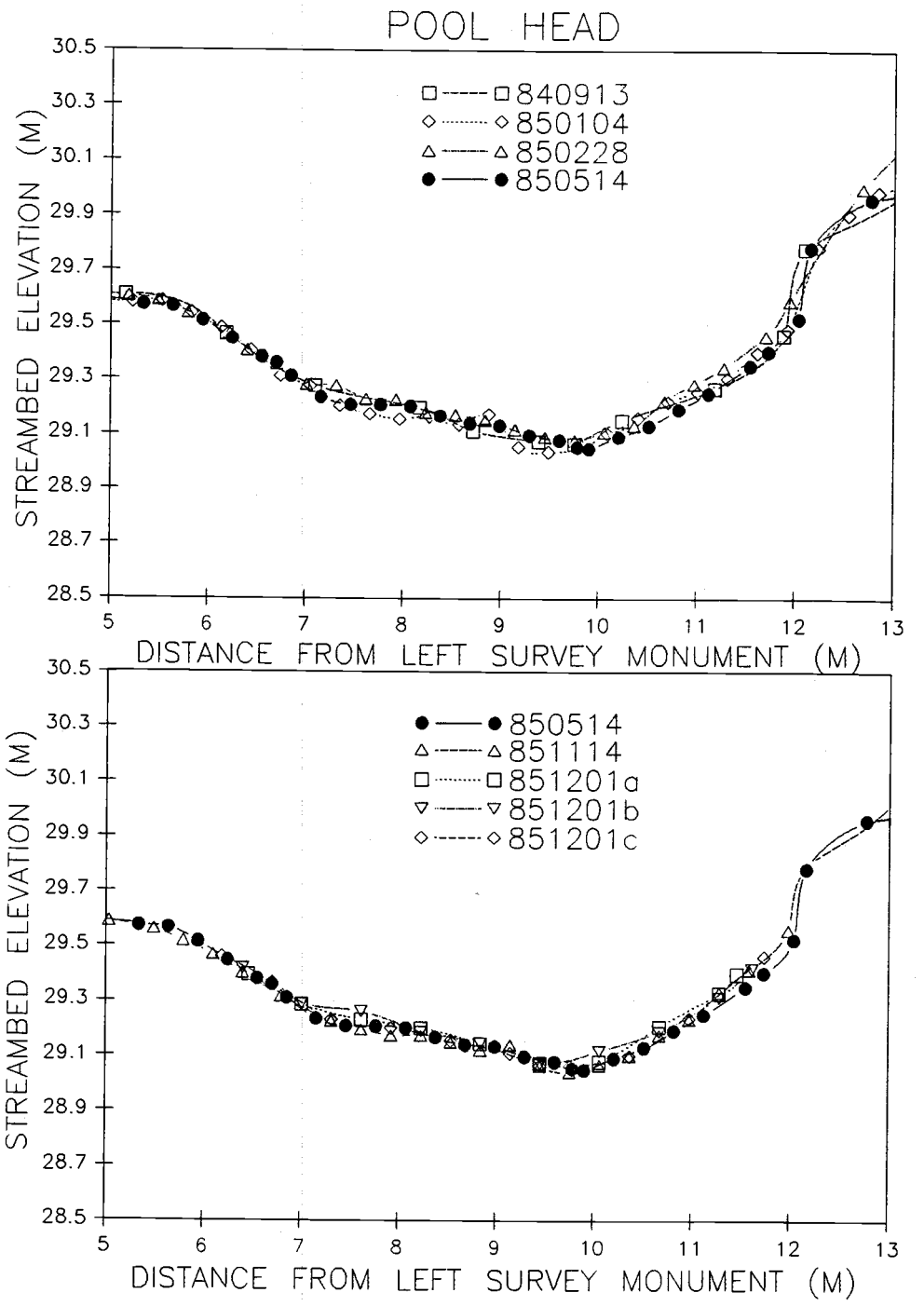

Figure 65. Cross-sectional soundings for the pool head. Elevations are relative to an arbitrary datum.

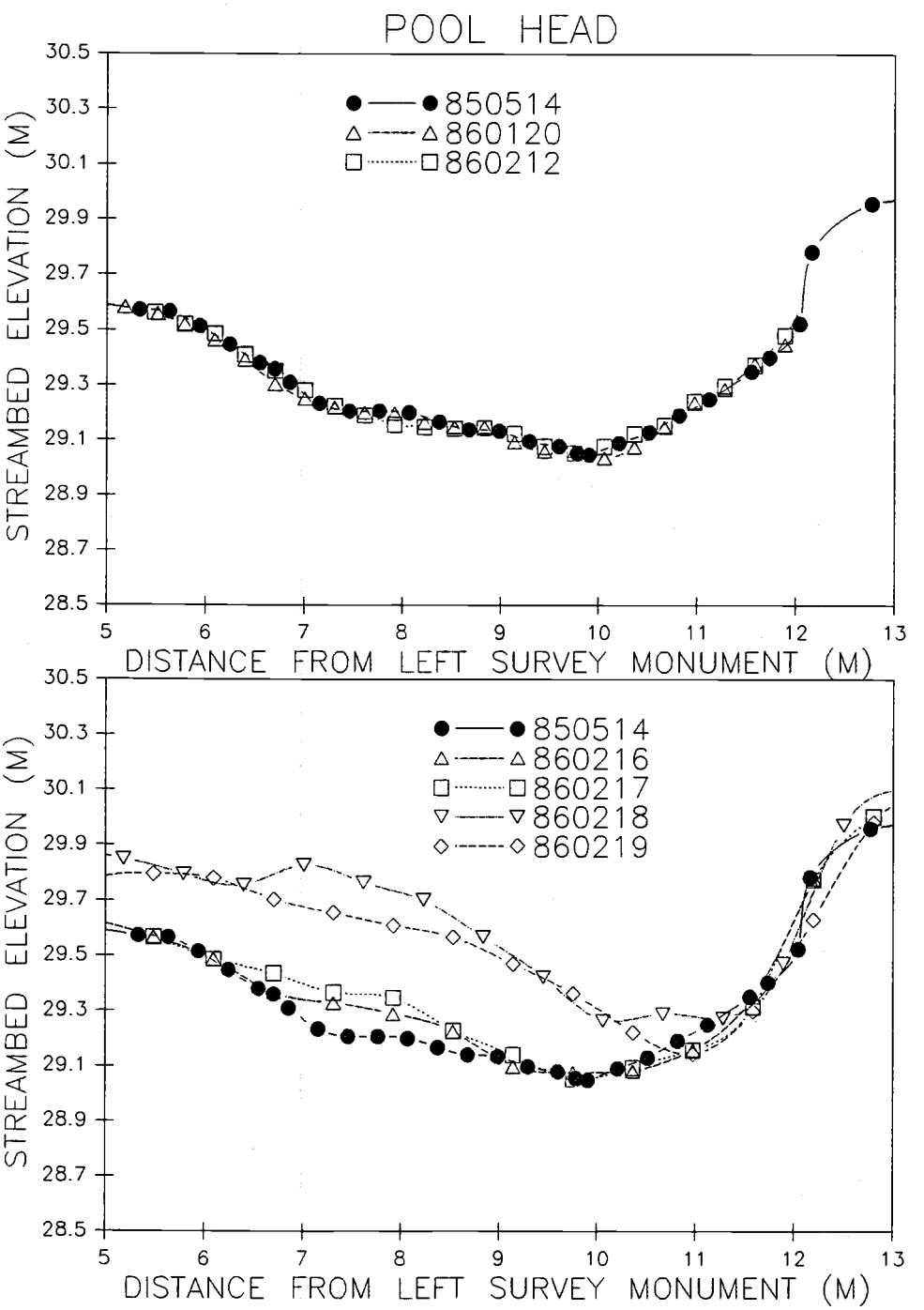

Figure 66. Cross-sectional soundings for the pool head. Elevations are relative to an arbitrary datum.

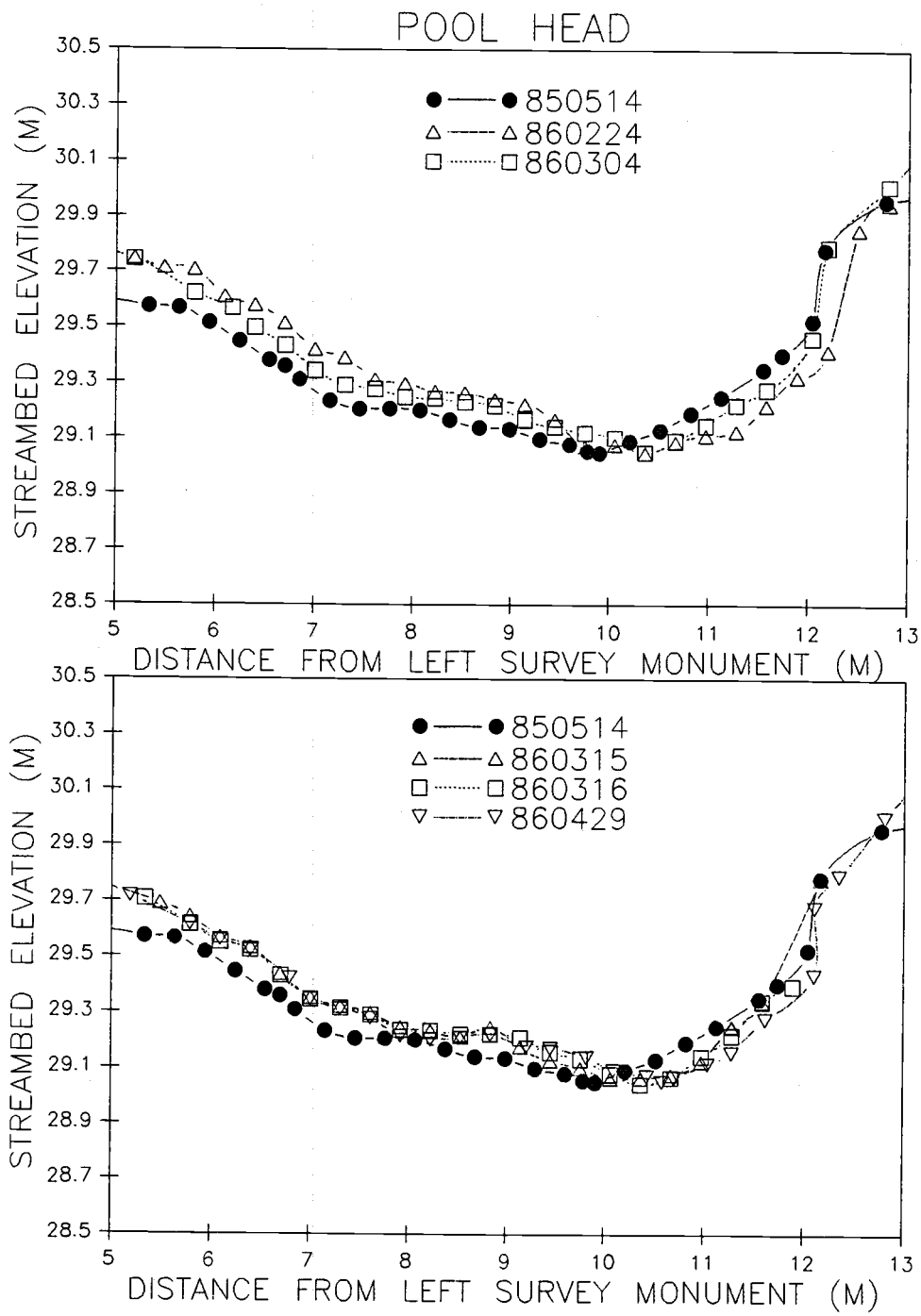

Figure 67. Cross-sectional soundings for the pool head. Elevations are relative to an arbitrary datum.

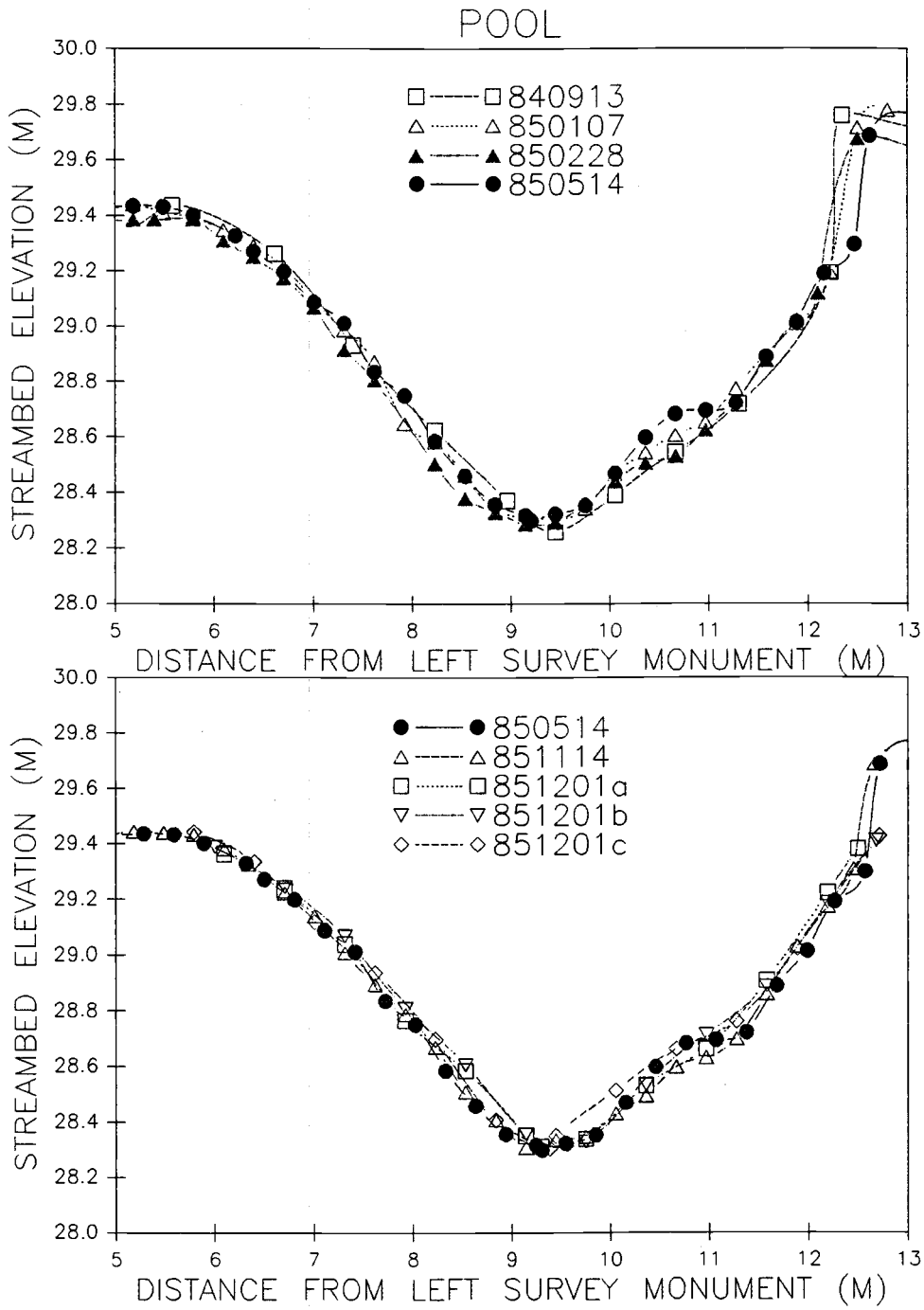

Figure 68. Cross-sectional soundings for the pool. Elevations are relative to an arbitrary datum.

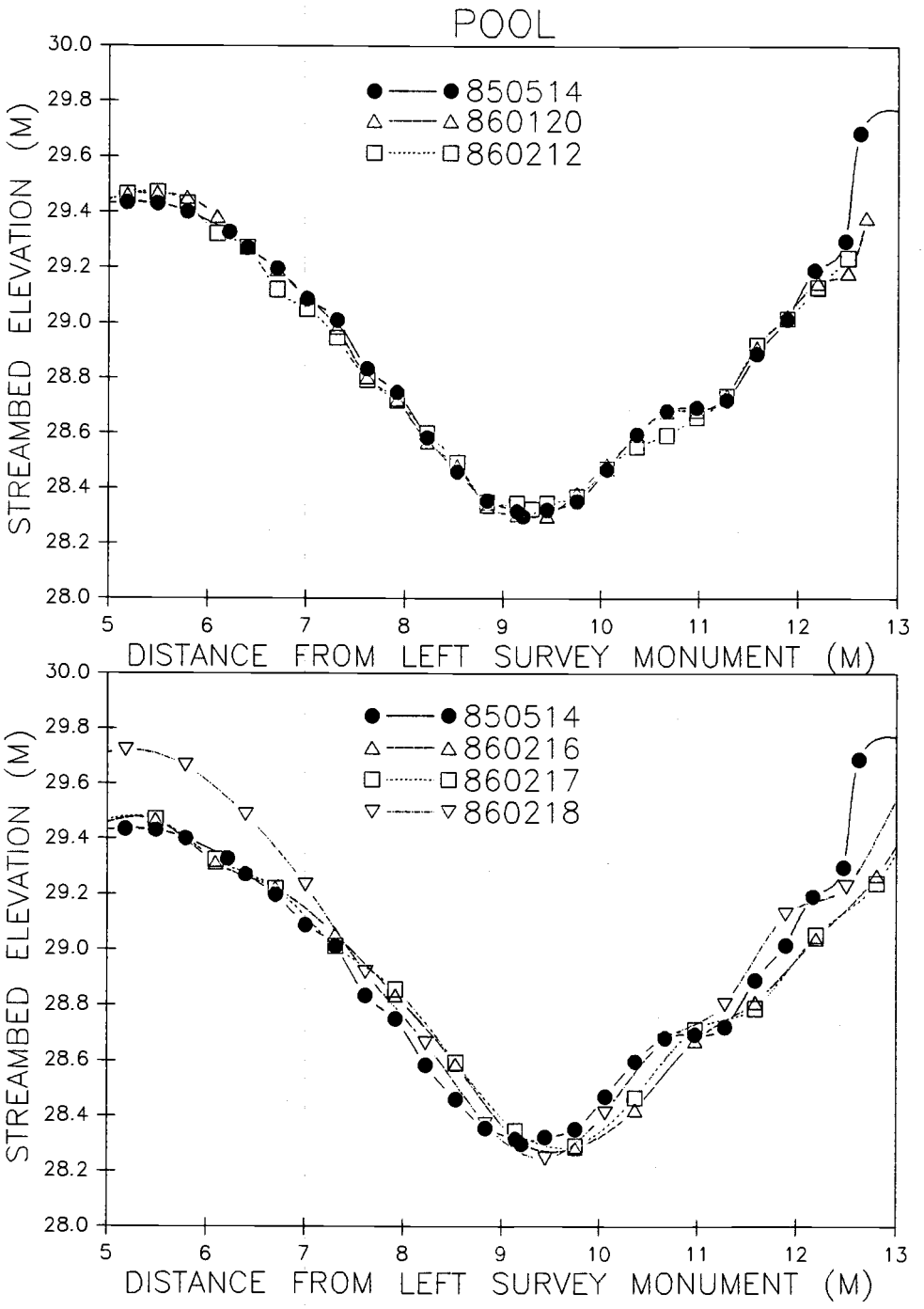

Figure 69. Cross-sectional soundings for the pool. Elevations are relative to an arbitrary datum.

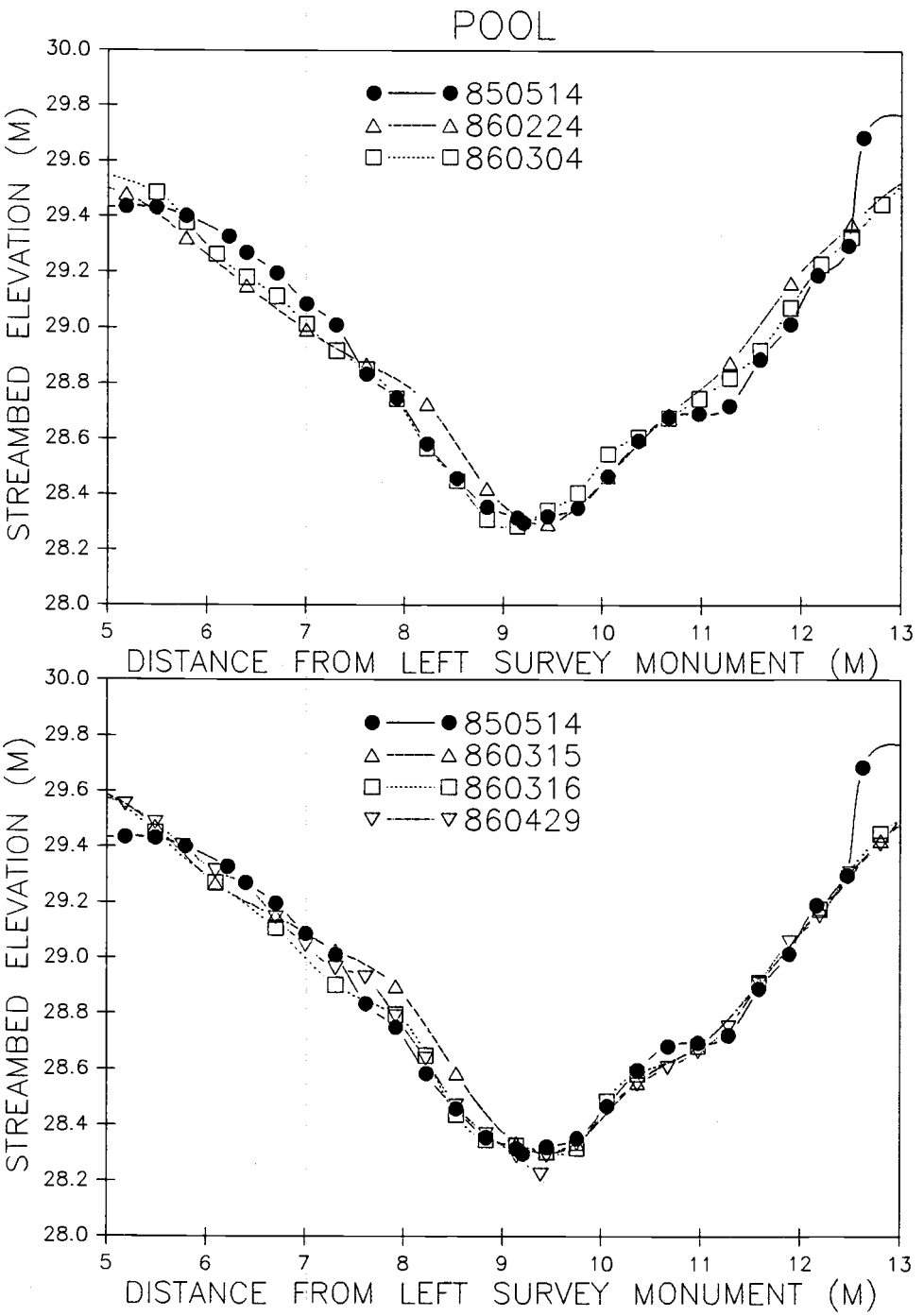

Figure 70. Cross-sectional soundings for the pool. Elevations are relative to an arbitrary datum.

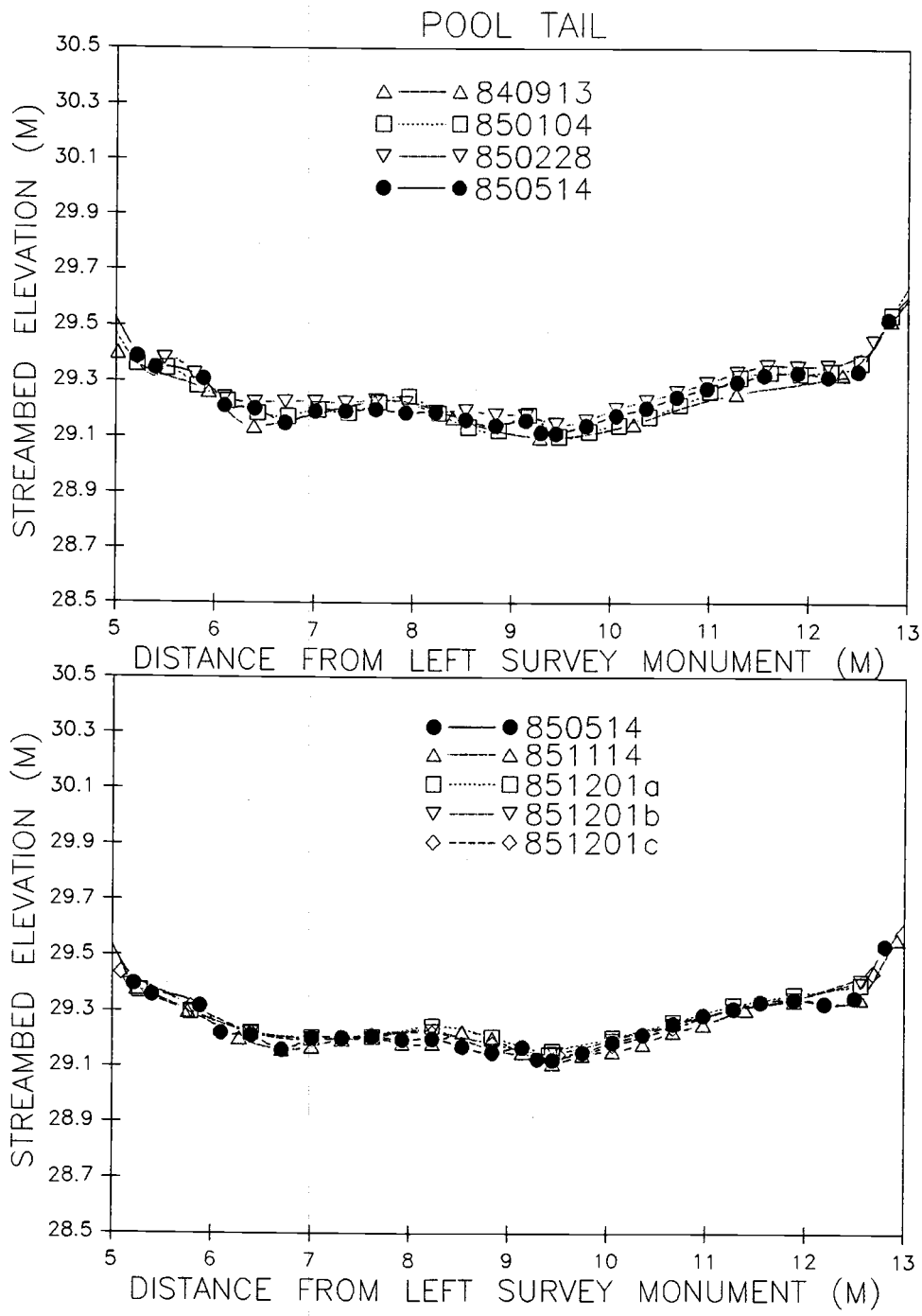

Figure 71. Cross-sectional soundings for the pool tail. Elevations are relative to an arbitrary datum.

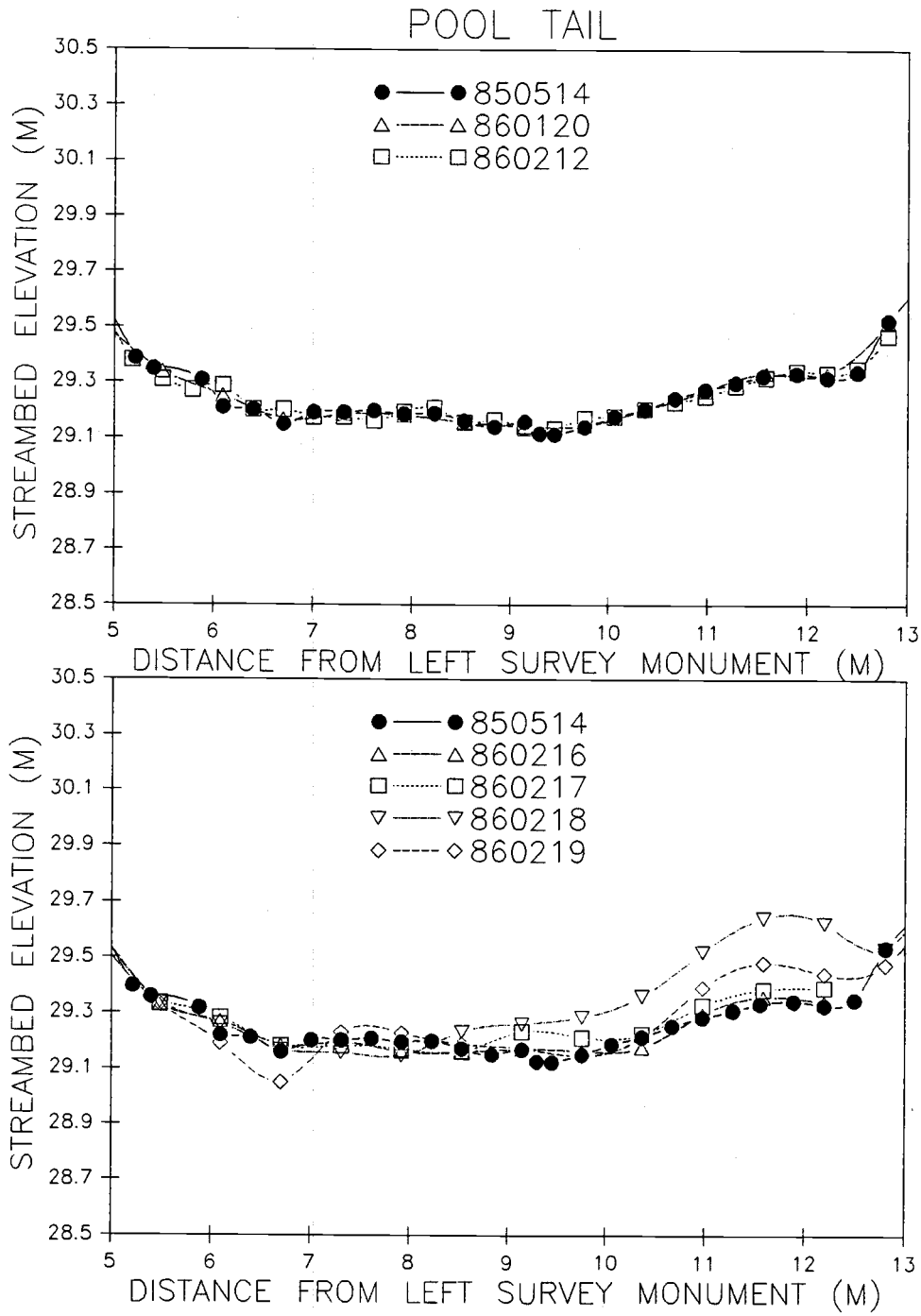

Figure 72. Cross-sectional soundings for the pool tail. Elevations are relative to an arbitrary datum.

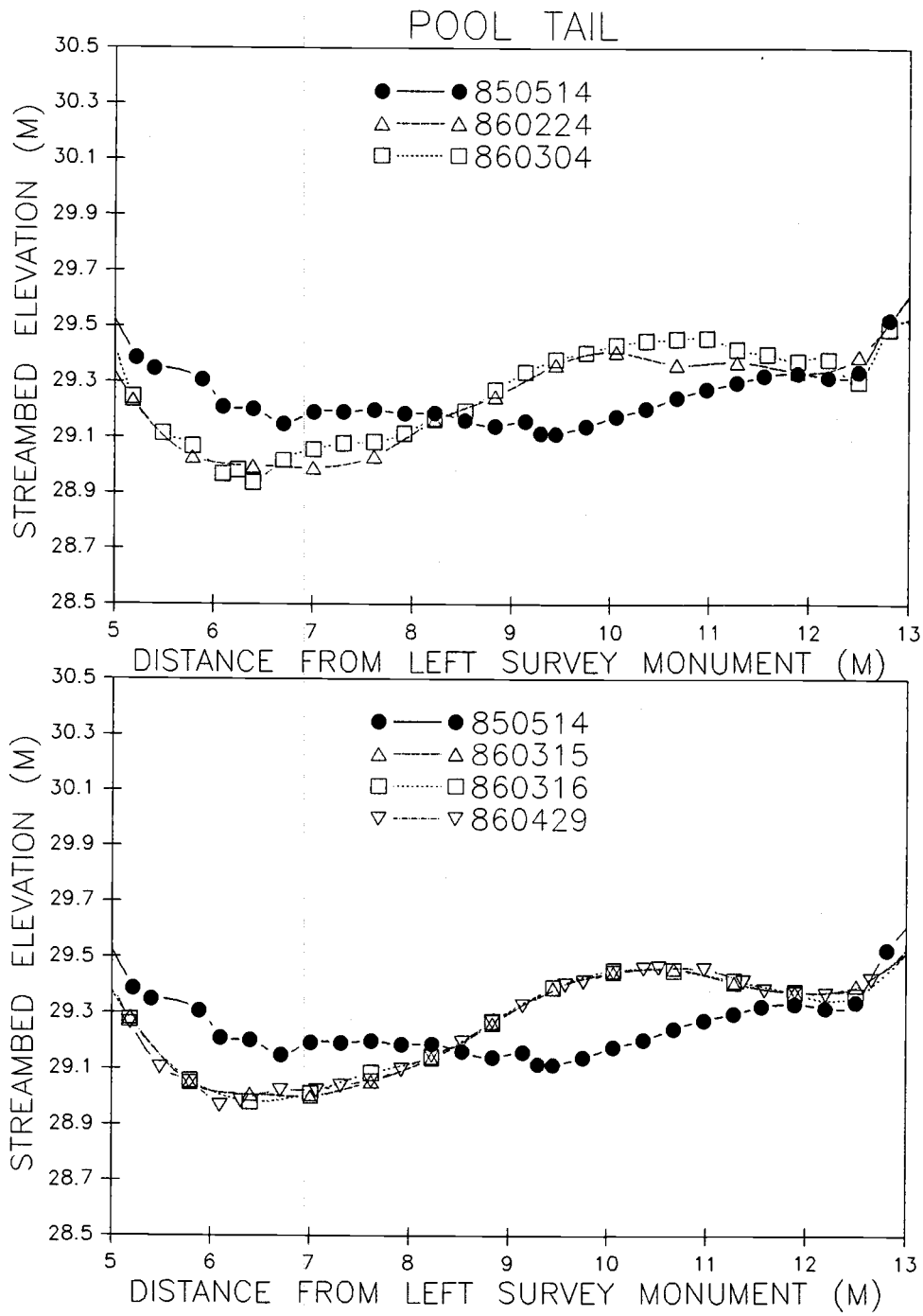

Figure 73. Cross-sectional soundings for the pool tail. Elevations are relative to an arbitrary datum.

APPENDIX H

Bedload Transport Rate (Q_{bl})

TABLE 13. BEDLOAD TRANSPORT RATE (Q_{bl}). Q is water discharge. Dates are also shown as sequential numbers beginning with January 1, 1984 as day 1.

STA	DATE	DAY #	TIME	Q (m^3/s)	Q_{bl} (kg/hr)	Q_{bl} (1) (kg/hr-m)
1	860116	746	1102	1.85	6.9	1.3
2	860116	746	1140	1.75	6.8	1.6
3	860116	746	1221	1.78	5.9	0.80
1	860119	749	1347	1.80	4.9	0.80
2	860119	749	1426	1.76	52	12
2	860120	750	1107	1.32	3.7	0.86
3	860120	750	1340	1.32	4.8	0.65
1	860120	750	1442	1.32	5.0	0.82
1	860122	752	1536	1.38	6.4	1.1
2	860122	752	1620	1.63	5.2	1.2
3	860122	752	1655	1.82	7.1	0.97
1	860202	763	1342	2.40	34	5.6
3	860202	763	1435	2.43	100	13
2	860202	763	1545	2.56	17	3.9
1	860203	764	1217	3.23	46	8.4
3	860203	764	1256	3.23	170	23
2	860203	764	1322	3.22	580	110
1	860204	765	1235	2.87	9.6	1.2
2	860204	765	1307	2.86	16	3.8
3	860204	765	1335	2.85	30	4.1
1	860205	766	1137	2.59	6.2	1.0
2	860205	766	1210	2.59	43	10
3	860205	766	1245	2.59	32.0	4.4
1	860206	767	1142	2.23	11	1.7
2	860206	767	1217	2.18	25	5.7
3	860206	767	1250	2.18	9.2	1.3

TABLE 13 CONTINUED. BEDLOAD TRANSPORT RATE (Q_{bl}). Q is water discharge. Dates are also shown as sequential numbers beginning with January 1, 1984 as day 1.

STA	DATE	DAY #	TIME	Q (m^3/s)	Q_{bl} (kg/hr)	Q_{bl} (1) (kg/hr-m)	
1	860214	775	1417	2.14	17	2.8	
2	860214	775	1435	2.12	32	7.5	
3	860214	775	1545	2.06	9.1	1.2	
1	860216	777	1246	5.29	720	130	
2	860216	777	1301	5.38	1700	390	
3	860216	777	1320	5.55	3200	440	
1	860216	777	1737	7.42	2500	460	
2	860216	777	1748	7.41	2500	580	
3	860216	777	1806	7.41	900	120	
1	860217	778	1258	10.4	3200	580	
2	860217	778	1316	10.6	2500	520	
3	860217	778	1329	10.6	1900	280	
1	860217	778	1708	17.4	12000	2100	(2)
3	860217	778	1725	18.9	2700	400	(2)
1	860219	780	1325	11.7	19000	2300	
3	860219	780	1400	12.1	8900	1300	
1	860219	780	1652	12.8	25000	3000	
3	860219	780	1717	12.9	56000	8330	
1	860221	782	1426	7.87	2400	280	
3	860221	782	1452	7.78	41000	6100	
2	860224	785	1300	6.03	11000	1300	
1	860224	785	1422	5.92	4000	500	
3	860224	785	1513	5.86	4100	610	
1	860226	787	1235	3.31	2500	400	
2	860226	787	1257	3.29	520	85	

TABLE 13 CONTINUED. BEDLOAD TRANSPORT RATE (Q_{bl}). Q is water discharge. Dates are also shown as sequential numbers beginning with January 1, 1984 as day 1.

STA	DATE	DAY #	TIME	Q (m^3/s)	Q_{bl} (kg/hr)	Q_{bl} (1) (kg/hr-m)
3	860226	787	1324	3.29	1300	190
2	860304	793	1300	1.26	1.0	0.24
1	860304	793	1335	1.26	0.97	0.20
3	860304	793	1402	1.26	7.7	1.1
1	860307	796	1135	2.61	260	47
2	860307	796	1206	2.57	320	52
3	860307	796	1241	2.49	1300	180
1	860308	797	1325	2.00	350	71
2	860308	797	1342	2.05	85	20
3	860308	797	1411	2.06	310	46
1	860309	798	1155	1.98	68	14
2	860309	798	1213	1.98	95	22
3	860309	798	1235	1.98	27	4.0
1	860311	800	1228	2.20	37	7.6
2	860311	800	1238	2.20	20	4.8
3	860311	800	1301	2.20	58	8.7
1	860311	800	1648	2.48	32	6.6
2	860311	800	1708	2.48	15	3.5
3	860311	800	1729	2.48	69	10
1	860313	802	1241	3.94	1900	340
2	860313	802	1304	3.96	1200	190
3	860313	802	1329	3.99	1100	160
1	860315	804	0815	2.85	66	14
2	860315	804	0836	2.85	830	200
3	860315	804	0855	2.88	3200	470

TABLE 13 CONTINUED. BEDLOAD TRANSPORT RATE (Q_{bl}). Q is water discharge. Dates are also shown as sequential numbers beginning with January 1, 1984 as day 1.

STA	DATE	DAY #	TIME	Q (m^3/s)	Q_{bl} (kg/hr)	Q_{bl} (1) (kg/hr-m)
1	860316	805	1221	2.39	34	6.9
2	860316	805	1236	2.39	38	8.9
3	860316	805	1253	2.39	46	6.9
1	860318	807	1110	1.84	14	3.4
2	860318	807	1135	1.84	17	3.9
3	860318	807	1205	1.83	21	3.1
1	860320	809	1237	1.45	5.3	1.2
2	860320	809	1300	1.45	8.2	2.2
3	860320	809	1329	1.45	7.5	1.1

(1) Kilograms of bedload per hour per meter of sampled channel width.

(2) Discharge extrapolated from the rating curve.

APPENDIX I

Bedload Grain-size Distribution

TABLE 14. BEDLOAD GRAIN-SIZE DISTRIBUTION. D_{50} and D_{84} are the sizes for which 50% and 84% respectively of the bedload sample is finer.

STA	DATE	TIME	MEAN DIAM. 5 LARGEST CLASTS (mm)	D_{50} (mm)	D_{84} (mm)	%<4mm	%<1mm
1	860116	1102	14.4	0.9	7.0	72	54
2	860116	1140	6.0	0.9	1.7	99	62
3	860116	1221	11.0	0.7	3.5	88	58
1	860119	1347	7.2	0.9	1.8	98	58
2	860119	1426	12.6	1.8	3.7	89	14
2	860120	1107	7.2	1.8	3.6	90	20
3	860120	1340	11.4	1.7	3.7	88	21
1	860120	1442	7.6	1.8	3.6	90	20
1	860122	1536	20.0	1.8	13	70	33
2	860122	1620	7.2	1.6	3.3	94	29
3	860122	1655	13.6	0.8	5.8	78	58
1	860202	1342	18.2	2.4	7.0	69	25
3	860202	1435	20.6	1.7	4.7	83	41
2	860202	1545	14.2	0.9	1.9	94	57
1	860203	1217	33.2	1.5	23	66	44
3	860203	1256	25.8	2.4	8.3	69	30
2	860203	1322	24.4	4.2	9.6	53	13
1	860204	1235	16.0	1.6	18	69	41
2	860204	1307	23.6	5.9	21	45	30
3	860204	1335	23.0	1.9	10	68	35
1	860205	1137	15.0	0.9	2.8	89	54
2	860205	1210	15.0	2.8	6.1	72	17
3	860205	1245	20.2	2.2	6.4	73	21
1	860206	1142	18.4	5.1	11	40	20
2	860206	1217	18.6	3.8	7.5	54	7.6
3	860206	1250	15.0	1.4	4.6	82	40
1	860214	1417	16.8	1.9	6.4	74	27
2	860214	1435	12.2	2.5	5.3	78	14
3	860214	1545	17.0	1.5	7.7	71	41

TABLE 14 CONTINUED. BEDLOAD GRAIN-SIZE DISTRIBUTION. D_{50} and D_{84} are the sizes for which 50% and 84% respectively of the bedload sample is finer.

STA	DATE	TIME	MEAN DIAM. 5 LARGEST CLASTS (mm)	D_{50} (mm)	D_{84} (mm)	%<4mm	%<1mm
1	860216	1246	30.2	4.4	13	50	19
2	860216	1301	32.4	2.0	12	71	31
3	860216	1320	39.0	5.8	12	50	17
1	860216	1737	29.8	3.2	7.1	67	30
2	860216	1748	26.2	2.4	6.1	76	37
3	860216	1806	26.2	3.8	8.9	59	29
1	860217	1258	23.6	2.3	6.3	73	38
2	860217	1316	20.6	2.1	5.0	79	40
3	860217	1329	20.0	2.0	4.5	83	32
1	860217	1708	17.2	1.2	3.0	90	54 (1)
3	860217	1725	26.6	1.0	3.0	90	62 (1)
1	860219	1325	40.4	5.3	17	46	16
3	860219	1400	42.2	4.1	14	55	18
1	860219	1652	49	4.6	13	53	18
3	860219	1717	46.6	6.6	16	42	12
1	860221	1426	29.0	4.8	13	45	15
3	860221	1452	35.6	4.4	11	52	10
2	860224	1300	48.6	4.8	12	51	8.8
1	860224	1422	32.0	3.5	9.0	66	18
3	860224	1513	36.8	6.5	14	40	9.1
1	860226	1235	27.8	2.7	6.8	68	18
2	860226	1257	19.0	3.0	5.8	66	18
3	860226	1324	24.6	2.9	7.3	68	16
2	860304	1300	4.2	0.5	0.9	99	88
1	860304	1335	6.4	0.5	1.2	96	82
3	860304	1402	15.8	1.0	2.6	94	52
1	860307	1135	25.8	1.3	6.4	76	49
2	860307	1206	21.8	2.1	5.0	79	48
3	860307	1241	21.4	1.9	5.8	78	42

TABLE 14 CONTINUED. BEDLOAD GRAIN-SIZE DISTRIBUTION. D_{50} and D_{84} are the sizes for which 50% and 84% respectively of the bedload sample is finer.

STA	DATE	TIME	MEAN DIAM. 5 LARGEST CLASTS (mm)	D_{50} (mm)	D_{84} (mm)	%<4mm	%<1mm
1	860308	1325	22.8	2.2	6.2	75	25
2	860308	1342	12.8	1.9	5.0	80	23
3	860308	1411	14.6	1.9	4.5	85	29
1	860309	1155	25.0	1.9	11	71	31
2	860309	1213	17.2	1.9	3.9	85	16
3	860309	1235	22.2	2.3	12	65	32
1	860311	1228	16.8	1.0	3.9	85	49
2	860311	1238	15.6	1.0	7.3	72	50
3	860311	1301	21.6	1.0	3.9	84	51
1	860311	1648	24.0	1.5	11	72	41
2	860311	1708	12.4	0.9	3.2	88	59
3	860311	1729	29.6	1.9	10	68	33
1	860313	1241	31.4	3.1	7.7	71	29
2	860313	1304	24.4	3.2	8.1	63	19
3	860313	1329	28.2	2.6	7.9	69	21
1	860315	0815	20.8	3.2	8.9	59	21
2	860315	0836	21.6	1.8	5.9	79	32
3	860315	0855	26.6	2.6	6.3	75	17
1	860316	1221	16.6	1.6	10	67	41
2	860316	1236	15.4	1.2	6.0	82	44
3	860316	1253	15.0	1.8	6.9	73	31
1	860318	1110	16.4	1.1	3.5	87	46
2	860318	1135	12.6	0.8	1.7	95	66
3	860318	1205	17.4	1.3	3.9	85	43
1	860320	1237	6.6	0.7	1.4	99	77
2	860320	1300	7.8	1.1	2.0	95	48
3	860320	1329	16.8	1.1	3.7	86	47

(1) Discharge extrapolated from the rating curve.

APPENDIX J

TABLE 15. ANALYSIS OF COVARIANCE TESTS FOR COMMON REGRESSION OF BEDLOAD TRANSPORT RATE VS DISCHARGE RELATIONSHIP FOR ALL STATIONS. Stations 1, 2, and 3 refer to the pool head, pool, and pool tail respectively. See text for explanation.

STATION	REDUCTION OF SS	MODEL MSE	F VALUE	P > F	H_o:
		H_o: SLOPES ARE NOT STATISTICALLY DIFFERENT			
1, 2	0.015	0.282	0.05	0.819	ACCEPT
2, 3	0.058	0.327	0.18	0.676	ACCEPT
1, 3	0.019	0.337	0.06	0.811	ACCEPT
		H_o: INTERCEPTS ARE NOT STATISTICALLY DIFFERENT			
1, 2	0.249	0.277	0.90	0.347	ACCEPT
2, 3	0.129	0.321	0.40	0.530	ACCEPT
1, 3	0.752	0.332	2.27	0.138	ACCEPT

APPENDIX K

TABLE 16. ANALYSIS OF COVARIANCE TESTS FOR COMMON REGRESSION OF BEDLOAD TRANSPORT RATE VS SHEAR STRESS RELATIONSHIP FOR ALL STATIONS. Stations 1, 2, and 3 refer to the pool head, pool, and pool tail respectively. See text for explanation.

STATION	REDUCTION OF SS	MODEL MSE	F VALUE	P > F	H_o:
		H_o: SLOPES ARE NOT STATISTICALLY DIFFERENT			
1, 2	0.005	0.286	0.02	0.899	ACCEPT
2, 3	0.346	0.280	1.24	0.273	ACCEPT
1, 3	0.260	0.340	0.76	0.388	ACCEPT
		H_o: INTERCEPTS ARE NOT STATISTICALLY DIFFERENT			
1, 2	16.562	0.279	59.26	0.0001	REJECT
2, 3	13.197	0.281	46.90	0.0001	REJECT
1, 3	11.225	0.338	33.19	0.0001	REJECT

APPENDIX L

TABLE 17. ANALYSIS OF COVARIANCE TESTS FOR COMMON REGRESSION OF BEDLOAD TRANSPORT RATE VS STREAM POWER RELATIONSHIP FOR ALL STATIONS. Stations 1, 2, and 3 refer to the pool head, pool, and pool tail respectively. See text for explanation.

STATION	REDUCTION OF SS	MODEL MSE	F VALUE	P > F	H_o:
		H_o: SLOPES ARE NOT STATISTICALLY DIFFERENT			
1, 2	0.046	0.293	0.16	0.693	ACCEPT
2, 3	0.481	0.283	1.70	0.200	ACCEPT
1, 3	0.220	0.349	0.63	0.432	ACCEPT
		H_o: INTERCEPTS ARE NOT STATISTICALLY DIFFERENT			
STATION	REDUCTION OF SS	MODEL MSE	F VALUE	P > F	Ho:
1, 2	15.079	0.287	52.48	0.0001	REJECT
2, 3	11.213	0.288	38.93	0.0001	REJECT
1, 3	6.434	0.346	18.62	0.0001	REJECT

APPENDIX M

TABLE 18. ANALYSIS OF COVARIANCE TESTS FOR COMMON REGRESSION OF BEDLOAD TRANSPORT RATE FOR RISING VS FALLING HYDROGRAPH LIMBS FOR ALL STATIONS. Stations 1, 2, and 3 refer to the pool head, pool, and pool tail respectively. See text for explanation.

STATION	REDUCTION OF SS	MODEL MSE	F VALUE	P > F	H_o:
		H_o: SLOPES ARE NOT STATISTICALLY DIFFERENT			
1	NON-HOMOGENEOUS	VARIANCE	----	-----	------
2	0.182	0.236	0.77	0.390	ACCEPT
3	0.966	0.327	2.95	0.099	ACCEPT
		H_o: INTERCEPTS ARE NOT STATISTICALLY DIFFERENT			
1	NON-HOMOGENEOUS	VARIANCE	----	-----	------
2	1.047	0.234	4.48	0.045	REJECT
3	1.082	0.353	3.07	0.092	ACCEPT

APPENDIX N

TABLE 19. ANALYSIS OF COVARIANCE TESTS FOR COMMON REGRESSION OF BEDLOAD TRANSPORT RATE BEFORE VS AFTER A SERIES OF MAJOR STORMS FOR ALL STATIONS. Stations 1, 2, and 3 refer to the pool head, pool, and pool tail respectively. See text for explanation.

STATION	REDUCTION OF SS	MODEL MSE	F VALUE	P > F	H_o:
		H_o: SLOPES ARE NOT STATISTICALLY DIFFERENT			
1	0.708	0.177	4.01	0.063	ACCEPT
2	0.321	0.232	1.38	0.257	ACCEPT
3	0.341	0.262	1.30	0.271	ACCEPT
		H_o: INTERCEPTS ARE NOT STATISTICALLY DIFFERENT			
1	1.267	0.208	6.09	0.025	REJECT
2	0.391	0.237	1.65	0.217	ACCEPT
3	1.943	0.267	7.29	0.016	REJECT

APPENDIX O

TABLE 20. ANALYSIS OF COVARIANCE TESTS FOR COMMON REGRESSION OF COMPETENCE VS DISCHARGE RELATIONSHIP FOR ALL STATIONS. Stations 1, 2, and 3 refer to the pool head, pool, and pool tail respectively. See text for explanation.

STATION	REDUCTION OF SS	MODEL MSE	F VALUE	P > F	H_o:
		H_o: SLOPES ARE NOT STATISTICALLY DIFFERENT			
1, 2	8.330	35.53	0.23	0.630	ACCEPT
2, 3	21.95	34.03	0.64	0.426	ACCEPT
1, 3	4.586	32.02	0.14	0.707	ACCEPT
		H_o: INTERCEPTS ARE NOT STATISTICALLY DIFFERENT			
1, 2	111.0	35.01	3.17	0.081	ACCEPT
2, 3	210.6	33.80	6.23	0.016	REJECT
1, 3	16.04	31.51	0.51	0.479	ACCEPT